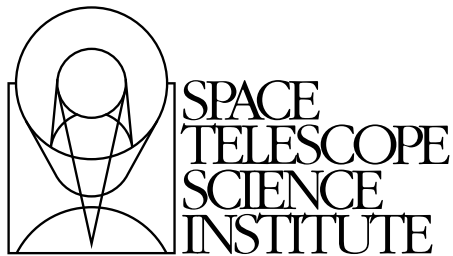


---

Version 5.0  
July 2010

# WFPC2 Data Handbook



Hubble Division  
3700 San Martin Drive  
Baltimore, Maryland 21218  
[help@stsci.edu](mailto:help@stsci.edu)

## User Support

For answers to any question, please contact the STScI Help Desk.

- **E-mail:** [help@stsci.edu](mailto:help@stsci.edu)
- **Phone:** (410) 338-1082  
(800) 544-8125 (U.S. only, toll free)

## World Wide Web

Information, software tools, and other resources are available on the WFPC2 World Wide Web site:

- **URL:** <http://www.stsci.edu/hst/wfpc2>

## WFPC2 Revision History

| Version      | Date          | Editor  |
|--------------|---------------|---|
| 5.0          | July 2010     | S. Gonzaga & J. Biretta   |
| 4.0          | January 2002  | Sylvia Baggett, Matthew McMaster, Editors,<br>WFPC2 Data Handbook<br>Bahram Mobasher, Chief Editor, HST Data Handbook |
| 3.1, Vol. I  | March 1998    | Richard Shaw, Update for V.I., HST Data Handbook  |
| 3.0, Vol., I | October 1997  | Mark Voit, HST Data Handbook  |
| 2.0          | December 1995 | Claus Leitherer, HST Data Handbook  |
| 1.0          | February 1994 | Stefi Baum, HST Data Handbook   |

## Citation

In publications, refer to this document as:

Gonzaga, S., & Biretta, J., et al. 2010, in HST WFPC2 Data Handbook, v. 5.0, ed., Baltimore, STScI

Send comments or corrections to:  
Hubble Division  
Space Telescope Science Institute  
3700 San Martin Drive  
Baltimore, Maryland 21218  
E-mail: [help@stsci.edu](mailto:help@stsci.edu)

# Table of Contents

|   |     |
|---|-----|
| <b>Acknowledgments</b> .....                                  | vii |
| <b>Introduction</b> .....                                     | ix  |
| <i>How to Use this Handbook</i> .....                         | ix  |
| <i>Typographic Conventions</i> .....                          | xi  |
| Visual Cues.....  | xi  |
| Comments .....  | xi  |
| <b>Chapter 1: WFPC2 Instrument Overview</b> ...               | 1   |
| 1.1 WFPC2 Physical Configuration .....                        | 2   |
| 1.2 WFPC2 Quick Reference.....                                | 6   |
| <b>Chapter 2: WFPC2 Data Structures</b> .....                 | 11  |
| 2.1 Historical Data Formats and File Names.....               | 11  |
| 2.2 Header Keywords.....                                      | 15  |
| 2.3 Correlating Phase II Exposures<br>with Data Files .....   | 20  |
| 2.4 WFPC2 Data Products in the Hubble<br>Legacy Archive ..... | 24  |
| <b>Chapter 3: WFPC2 Calibration</b> .....                     | 25  |
| 3.1 Brief History of the WFPC2 Processing<br>Pipeline.....    | 25  |
| 3.2 Data Processing Overview.....                             | 26  |
| 3.2.1 Calibration of WFPC2 Images .....                       | 30  |
| 3.3 Standard Pipeline Calibration.....                        | 34  |
| 3.3.1 Calibration Files.....                                  | 34  |
| 3.3.2 Calibration Steps .....                                 | 35  |

|   |           |
|---|-----------|
| 3.4 Post-calwp2 Processing .....  | 44        |
| 3.4.1 CTE Correction .....  | 44        |
| 3.4.2 PyDrizzle.....  | 44        |
| 3.5 Recalibration .....   | 45        |
| 3.6 Improving the Pipeline Calibration .....                                    | 52        |
| 3.6.1 Warm Pixels.....  | 52        |
| 3.6.2 Alternate Flat fields .....   | 58        |
| 3.6.3 Removing Cosmic Rays from Co-aligned Images ....                          | 60        |
| 3.6.4 Charge Traps.....   | 62        |
| <b>Chapter 4: WFPC2 Error Sources .....</b>                                     | <b>65</b> |
| 4.1 Bias Subtraction Errors.....  | 65        |
| 4.2 Flat Field Correction Errors.....   | 66        |
| 4.2.1 History of Flat Fields .....  | 66        |
| 4.2.2 Flat Fields for Special Observations<br>and Special Purpose Filters ..... | 68        |
| 4.2.3 The Effect of WFPC2 Flat Fields on Point<br>Source Photometry.....        | 69        |
| 4.3 Dark Current Subtraction Errors .....                                       | 69        |
| 4.3.1 Electronic Dark Current .....   | 69        |
| 4.3.2 Dark Glow .....   | 71        |
| 4.4 Pointing Information in Image Headers .....                                 | 72        |
| 4.5 WF4 Background Streaks .....  | 74        |
| 4.6 Image Anomalies.....  | 76        |
| 4.6.1 Bias Jumps .....  | 76        |
| 4.6.2 Residual Images.....  | 77        |
| 4.6.3 PC1 Stray Light .....   | 81        |
| 4.6.4 Other Anomalies .....   | 81        |
| <b>Chapter 5: WFPC2 Data Analysis .....</b>                                     | <b>83</b> |
| 5.1 Photometric Zeropoint.....  | 83        |
| 5.1.1 Photometric Systems Used for WFPC2 Data .....                             | 84        |
| 5.1.2 Determining the Zeropoint .....   | 87        |
| 5.2 Photometric Corrections .....   | 92        |
| 5.2.1 Time-Dependent Corrections.....   | 93        |
| 5.2.2 Position-Dependent Corrections.....                                       | 100       |
| 5.2.3 Other Photometric Corrections .....                                       | 108       |
| 5.2.4 Photometry on Saturated Stars With WFPC2.....                             | 115       |
| 5.2.5 Example: Point Source Aperture Photometry<br>with WFPC2 .....             | 116       |

|  |     |
|--|-----|
| 5.3 Polarimetry .....                                | 125 |
| 5.4 Astrometry .....                                 | 127 |
| 5.4.1 Relative Astrometry Within a Chip .....        | 127 |
| 5.4.2 Relative Astrometry Among the Four Chips ..... | 131 |
| 5.4.3 Absolute Astrometry .....                      | 140 |
| 5.5 Drizzling WFPC2 Data .....                       | 140 |
| 5.6 Deconvolution of WFPC2 Data .....                | 147 |
| 5.7 Accuracy of WFPC2 Results .....                  | 148 |
| <b>References</b> .....                              | 151 |
| <i>WFPC2 Instrument Science Reports (ISRs)</i> ..... | 153 |
| <i>WFPC2 Links</i> .....                             | 158 |
| <b>Index</b> .....                                   | 159 |



# Acknowledgments

The information contained in this Handbook is the summary of the experience gained by members of the STScI ACS-WFPC2 Team (AWT) and their predecessors, and by the WFPC2 Instrument Definition Team (WFPC2 IDT).

Members of the STScI ACS-WFPC2 Team (2010) are L. Smith<sup>1</sup> (lead), A. Armstrong, L. Bedin<sup>1</sup>, J. Biretta (WFPC2 Technical Lead), R. Bohlin, M. Chiaberge<sup>1</sup>, B. Ferguson, A. Fruchter, D. Golimowski (ACS Technical Lead), S. Gonzaga, N. Grogin, P. L. Lim, R. Lucas, A. Maybhat, M. McMaster, and A. Suchkov.

Past members of the STScI WFPC2 team include S. Baggett, G. Ballester, F. Boffi, G. Brammer, C. Burrows, S. Casertano, M. Clampin, C. Cox, T. Desjardins, D. Di Nino, V. D. Dixon, R. Evans, H. Ferguson, R. Gilmozzi, H. Hasan, I. Heyer, A. Koekemoer, D. Peters, V. Kozhurina-Platais, J. Krist, L. Lubin, J. Mack, J. MacKenty, D. Moody, M. Mutchler, K. Noll, C. O’Dea, C. Proffitt, J. Rhoads, M. Richardson, A. Riess, C. Ritchie, K. Rudloff, A. Schultz, P. Scowen, M. Sirianni, W. Sparks, K. Stapelfeldt, M. Stiavelli, J. Surdej, D. Thatte, K. Verner, A. Watson, B. Whitmore, and M. Wiggs.

The WFPC2 IDT members are J. Trauger (PI), C. Burrows, J. Clarke, D. Crisp, J. Gallagher, R. Griffiths, J. Hester, J. Hoessel, J. Holtzman, J. Mould, and J. Westphal.

The contributions of the following people are greatly appreciated: J. Anderson, J. Balleza, P. Bely, I. Dashevsky, A. Dolphin, R. Doxsey, S. Ewald, J. Fitch, W. Hack, A. Holm, R. Hook, J.C. Hsu, E. Karkoschka, I. King, E. Kinney, R. Kutina, M. Lallo, C. Long, R. Makidon, O. Lupie, M. Remy, G. Schneider, A. Welty, T. Wheeler, and our technical editor, S. Rose.

*This document is dedicated to the memory of the contributors who are no longer with us:*

**Rodger Doxsey, Russ Makidon, and James Westphal.**

---

1. European Space Agency (ESA)



# Introduction

---

## How to Use this Handbook

This handbook is designed to help you process and analyze data from the Wide Field and Planetary Camera 2 (WFPC2) instrument which was on-board the Hubble Space Telescope (HST) from December 1993 to May 2009. It is presented as an independent and self-contained document, based on the contents of an earlier edition (version 4.0) released in January 2002. General information about HST data analysis is now available in the [The HST Data Handbook](#).

This (presumably) final edition of the WFPC2 Data Handbook was completed in spring of 2010, a year after the instrument was removed from HST. At the time of this writing, there are still several on-going calibration projects underway, and users are strongly urged to check the [WFPC2 Web site](#) for the latest information and any updated calibrations.

Since the last edition of this document, there have been major changes in the instrument performance, observing strategies, and data analysis.

The aging WFPC2 CCDs have shown significant degradation in Charge Transfer Efficiency (CTE); corrections for this effect, to the extent possible, are provided for both point-source and extended targets.

A failing amplifier in the WF4 signal processing electronics resulted in a temperature-dependent gain reduction that first appeared in March 2002. Among its symptoms are low or zero bias levels, lowered target count levels, and faint horizontal streaks in the images. A series of temperature reductions in the camera electronics were able to alleviate some of the symptoms. New processing steps were added to the WFPC2 calibration pipeline to correct remaining issues with the WF4 data. A new STSDAS task, **wdestreak**, was also created to aid users in removing streaks from their WF4 data.

Since the last edition of this handbook, dithering has become a popular observing strategy for obtaining WFPC2 data, and **multidrizzle** has become the task of choice for combining dithered WFPC2 images to remove cosmic rays and hot pixels.

Now that the WFPC2 mission has been completed, a decision was made to cease On-the-Fly Reprocessing (OTFR), and create a WFPC2 Static Archive populated with reprocessed WFPC2 data, using the best-available and “final” reference files.

The new default format for WFPC2 data from the Static Archive is now Multi-extension FITS (MEF), the same FITS format used by newer HST instruments. All STSDAS tasks are compatible with both the old GEIS and newer MEF formats. Users who prefer working with GEIS format images may continue to request wFITS files from the Archive and then convert them to GEIS format using the STSDAS task **strfits**.

This new and final WFPC2 pipeline processing effort to form the Static Archive included many calibration enhancements. Among these are:

- improved biases, darks, and flats covering various modes and epochs.
- New SYNPHOT tables for time-dependent throughput changes caused by contamination and long-term QE changes.
- More accurate geometric distortion reference files for use in **pydrizzle** and **multidrizzle**.
- Correction of the WF4 CCD amplifier anomaly.
- Improved calibration of linear-ramp filter (LRF) images.
- A new image product in the standard delivery of calibrated data from the Static Archive: a distortion-corrected single-image drizzled mosaic of the entire WFPC2 field of view. This is primarily intended as a “quick-look” image of the entire field, and not to be used for precision photometry.
- New image header keywords:
  - CTE estimates in delta magnitudes for point sources with intensities of 100 e<sup>-</sup>, 1000 e<sup>-</sup>, and 10,000 e<sup>-</sup>.
  - Zeropoint corrections due to UV contamination and QE changes.
  - Estimate of velocity aberration effects.

---

## Typographic Conventions

To help you understand the material in this Data Handbook, we will use a few consistent typographic conventions.

### Visual Cues

The following typographic cues are used:

- **bold** words identify an **STSDAS**, **IRAF**, or **PyRAF** task or package name.
- `typewriter-like` words identify a file name, system command, or response that is typed or displayed as shown.
- *italic* type indicates a new term, an important point, or a mathematical variable, or a task parameter.
- SMALL CAPS identifies a header keyword.
- ALL CAPS identifies a table column.

### Comments

Occasional side comments point out three types of information, each identified by an icon in the left margin.



---

***Warning:** You could corrupt data, produce incorrect results, or create some other kind of severe problem.*

---



---

***Heads Up:** Here is something that is often done incorrectly or that is not obvious.*

---



---

***Tip:** No problems...just another way to do something or a suggestion that might make your life easier.*

---





CHAPTER 1:

# WFPC2 Instrument Overview

In this chapter. . .

|                                      |
|--------------------------------------|
| 1.1 WFPC2 Physical Configuration / 2 |
| 1.2 WFPC2 Quick Reference / 6        |

The Wide Field and Planetary Camera 2 (WFPC2) is a two-dimensional imaging device covering a wavelength range from Lyman- $\alpha$  to about 1  $\mu\text{m}$ . Built at the Jet Propulsion Laboratory by an Instrument Definition Team (IDT) headed by John Trauger, WFPC2 was the replacement for the first Wide Field and Planetary Camera (WF/PC-1); it included built-in corrections for the spherical aberration of the HST Optical Telescope Assembly (OTA). The WFPC2 was installed in HST during the First Servicing Mission in December 1993. After  $\sim 15.5$  years of operation, WFPC2 was removed during Servicing Mission 4 in May 2009, to be replaced by the Wide Field Camera 3.

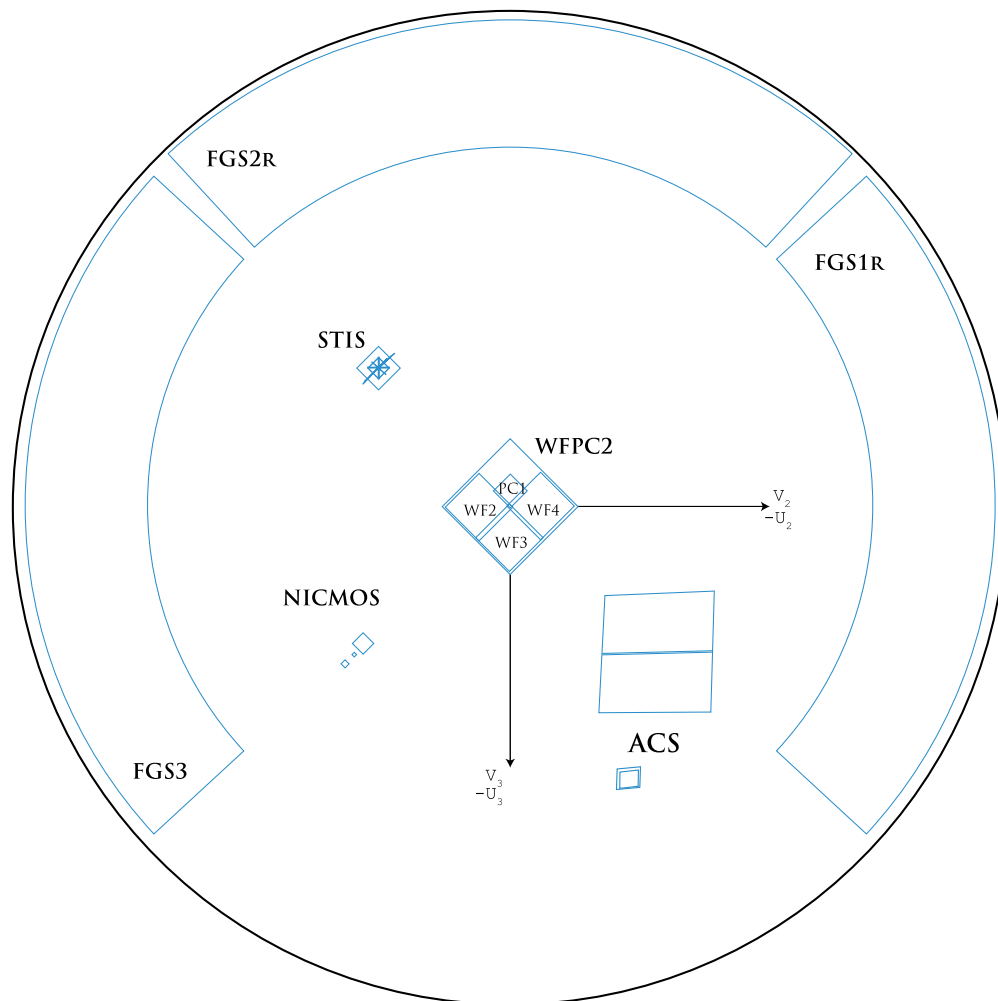
An early IDT report of the WFPC2 on-orbit performance can be found in Trauger et al. (1994, [ApJ](#), 435, L3). A more detailed assessment of its capabilities is available in Holtzman et al. (1995, *PASP*, vol. 107, [page 156](#) and [page 1065](#)). This Data Handbook, along with the [WFPC2 Instrument Handbook \(version 10\)](#), provides information regarding the instrument's performance over its lifetime.

## 1.1 WFPC2 Physical Configuration

The WFPC2 field of view was located at the center of the HST focal plane, as shown in Figure 1.1. Figure 1.2 shows a schematic of its optical arrangement: the central portion of the  $f/24$  beam coming from the OTA is intercepted by a steerable pick-off mirror attached to the WFPC2 and is diverted through an open port entry into the instrument. The beam then passes through a shutter and interposable filters. A total of 48 spectral elements and polarizers are contained in an assembly of 12 filter wheels.

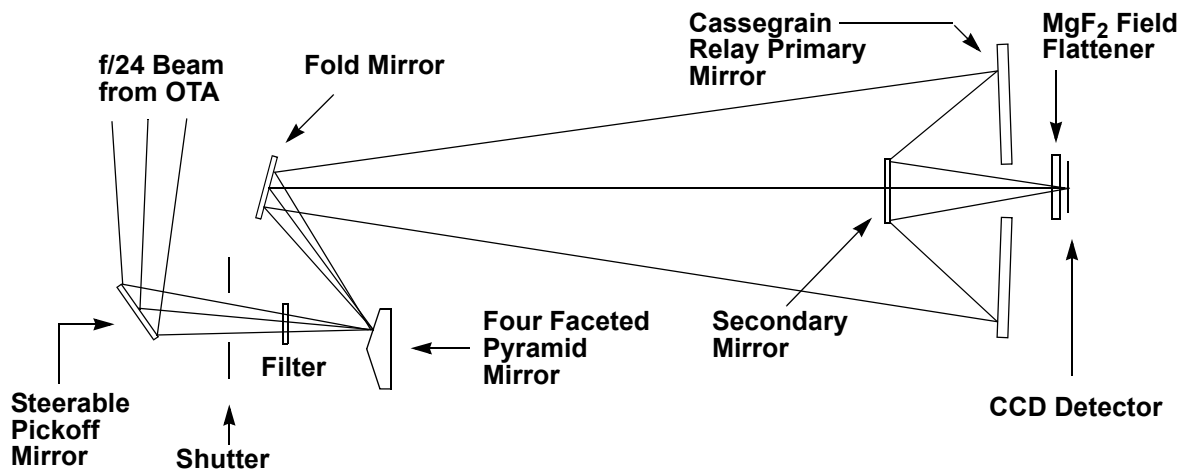
The light falls onto a shallow-angle, four-faceted pyramid, located at the aberrated OTA focus. Each face of the pyramid is a concave spherical surface, dividing the OTA image of the sky into four parts. After leaving the pyramid, each quarter of the full field of view is relayed by an optically-flat mirror to a Cassegrain relay that forms a second field image on a charge-coupled device (CCD) of  $800 \times 800$  pixels. Each of these four detectors is housed in a cell sealed by a  $\text{MgF}_2$  window, which is figured to serve as a field flattener.

**Figure 1.1: WFPC2 Field of View Prior to Servicing Mission 4.**



The aberrated HST wavefront was corrected by introducing an equal but opposite error in each of the four Cassegrain relays. An image of the HST primary mirror was formed on the secondary mirrors in the Cassegrain relays. The spherical aberration from the telescope's primary mirror was corrected on these secondary mirrors, which are extremely aspheric; the resulting point spread function was quite close to that originally expected for WF/PC-1.

**Figure 1.2: WFPC2 Optical Configuration**



**WFPC2 Optical Configuration, showing the light path for one of the four Cassegrain relays after the main beam is split into four parts at the pyramid**

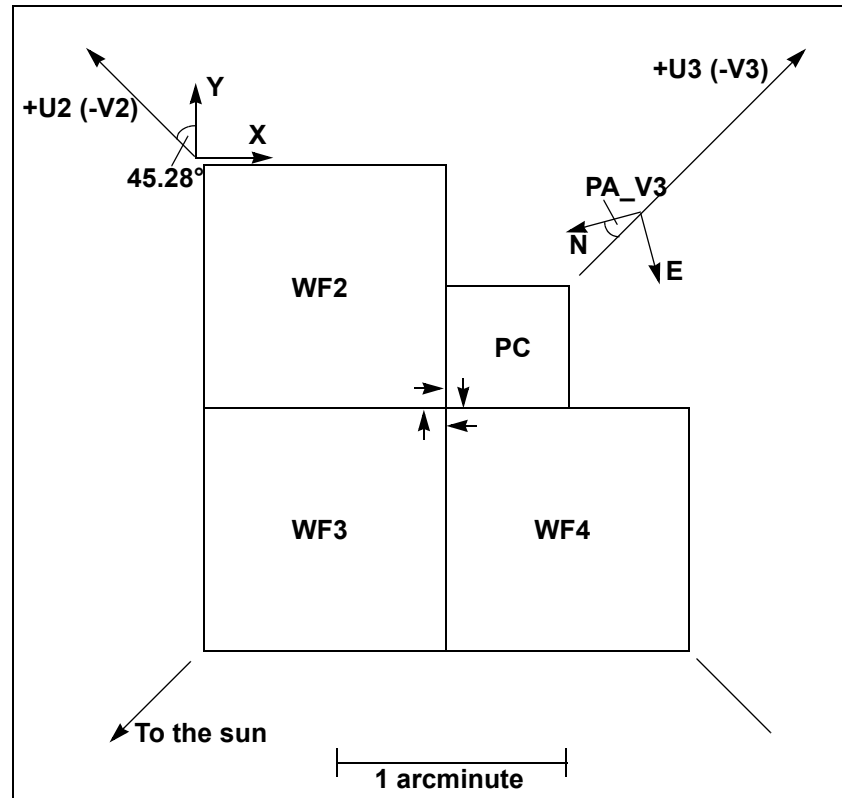
The optics of three of the four cameras, the Wide Field Cameras (WF2, WF3, WF4), are essentially identical, with a final focal ratio of  $f/12.9$ . The fourth camera, known as the Planetary Camera (PC or PC1), has a focal ratio of  $f/28.3$ .

Figure 1.3 shows the field of view of WFPC2 projected on the sky:

- The U2, U3 axes (same as the -V2, -V3 axes) are defined by the nominal Optical Telescope Assembly (OTA) axis, which was near the center of the WFPC2 FOV.
- The readout direction is marked with an arrow near the start of the first row in each CCD. Note that it rotates  $90^\circ$  between successive chips. The readout direction of the four CCDs was defined such that the origin of the CCD was at the corner of the chip pointing towards the apex of the WFPC2 pyramid. (In the STSDAS pixel numbering system, the CCD origin is located at the lower left corner of the CCD image.)

- The  $X$ ,  $Y$  arrows mark the coordinate axes for any POS TARG commands<sup>1</sup> that may have been specified in the proposal; the [HST Phase II Proposal Instructions for Cycle 16](#) elaborates on the use of this requirement.

**Figure 1.3: WFPC2 Field of View Projected on the Sky**



The position angle of V3 on the sky varies with pointing direction and observation epoch, and is recorded in the calibrated science header keyword `PA_V3`. Note that for WFPC2, the `PA_V3` is offset 180° from any `ORIENT` that may have been requested in the HST proposal (the optional special requirement `ORIENT`, if used, is specified in the Phase II proposal but is not recorded in the WFPC2 image headers).

The orientation of each camera on the sky, i.e., position angle of the  $y$ -axis of each detector, is provided by the `ORIENTAT` group keyword in the image headers. (Note: this is not the same as the `ORIENT` special requirement used in Phase II proposals.) The geometry of the cameras and the related image header keywords are explained in greater detail in [Chapter 2](#).

1. POS TARG, an optional special requirement in HST Phase II proposals, places the target in offsets (specified in units of arc seconds) from a specified aperture.

**Table 1.1: Camera Configurations**

| Camera    | Pixels    | Field of View | Scale             | f/ratio |
|-----------|-----------|---------------|-------------------|---------|
| PC        | 800 x 800 | 36" x 36"     | 0".0455 per pixel | 28.3    |
| WF2, 3, 4 | 800 x 800 | 80" x 80"     | 0".0996 per pixel | 12.9    |

The Planetary Camera (PC1) provided a field of view sufficient to obtain full disk images of all planets except Jupiter. The PC1 CCD pixels undersampled the point spread function by a factor of two at 5800 Å. For the WF cameras, their pixel scales were over a factor of two larger than the PC1, and thus undersampled the image by a factor of four at visual wavelengths. Some of the sampling lost to these large pixel scales can be recovered by combining images that were executed with sub-pixel offsets (by using dither patterns or the POS TARG special requirement). Additional information about dithering is provided in [The MultiDrizzle Handbook](#).

As a result of the aberration in the primary beam, the light from sources near the pyramid edges was divided between adjacent chips. Consequently, the lower columns and rows of the PC1 and WF chips are strongly vignetted, as shown in [Table 1.2](#). The CCD  $x, y$  (column, row) numbers given in this table are approximate to the 1 - 2 pixel level due to geometric distortion in the camera.

**Table 1.2: Inner Edges of the WFPC2 Field Projected Onto CCDs**

| Camera | Start Vignetted Field<br>(Zero Illumination) | 50% Illumination      | Start Unvignetted Field<br>(100% Illumination) |
|--------|--|-----------------------|--|
| PC1    | $x > 0$ and $y > 8$                          | $x > 44$ and $y > 52$ | $x > 88$ and $y > 96$                          |
| WF2    | $x > 26$ and $y > 6$                         | $x > 46$ and $y > 26$ | $x > 66$ and $y > 46$                          |
| WF3    | $x > 10$ and $y > 27$                        | $x > 30$ and $y > 47$ | $x > 50$ and $y > 67$                          |
| WF4    | $x > 23$ and $y > 24$                        | $x > 43$ and $y > 44$ | $x > 63$ and $y > 64$                          |

The WFPC2 Static Archive provides a drizzled image product with the four CCDs mosaicked into a single frame at the WF3 pixel scale. This provides a convenient “quick-look” image of the entire field of view. However, this image does not have the full photometric corrections applied, and should generally not be used for detailed analyses. Alternatively, the STSDAS task `wmosaic` provides another way to produce a “quick-look” image with the four CCDs mosaicked together. This task, in its default mode, will combine the four chips into a 1600 x 1600 pixel image at the resolution of the Wide Field cameras. Neither of these “quick-look” products support the full resolution of the Planetary Camera channel.

Finally, a comment about readout modes. There are two observation modes available on WFPC2: FULL and AREA. The mode used for a given observation is recorded in the image header keyword MODE. In FULL mode, each pixel is read out individually, while in AREA mode, pixels are summed in 2 x 2 boxes before they are read out. The advantage of AREA mode is that the readout noise for the “larger” pixels (6 e<sup>-</sup> per pixel) is nearly the same as the readout noise for unsummed pixels (5 e<sup>-</sup> per pixel). Thus, AREA mode can be useful in observations of extended sources when the primary source of noise is readout noise, as is often the case in the far UV.

In practice, observers have made very limited use of the AREA mode capability; less than 0.1% of all WFPC2 images in the Archive were taken in AREA mode. As a result, AREA mode calibration is not supported at the same level as FULL mode. Although reference files such as biases, darks, and flatfields are available for AREA mode images, they may not provide the best calibration as they are not updated and improved as frequently as the FULL mode reference files. Researchers using AREA mode images that require a very high level of calibration should consult the list of best available [reference files](#), and consider generating their own AREA mode reference files. For example, it might be possible to make more accurate reference files by re-binning the FULL mode reference file appropriate for their observation epoch. See [Section 3.5](#) for more information on how to manually recalibrate WFPC2 data. For assistance, questions, or problems, contact the HST helpdesk at [help@stsci.edu](mailto:help@stsci.edu).

---

## 1.2 WFPC2 Quick Reference

**Table 1.3: Main WFPC2 Parameters**

|                          |   |
|--------------------------|---|
| <b>Field of view</b>     | Total L-shaped FOV, 2'.5 x 2'.5.<br>Three wide field chips (WF2, WF3, WF4 at 150" x 150" each).<br>One 34" x 34" chip (PC1).  |
| <b>Plate Scale:</b>      | 0.1 arcsec/pixel for wide field chips: WF2, WF3, and WF4.<br>0.046 arcsec/ pixel for the planetary camera (PC1).  |
| <b>F/ratio</b>           | 12.9 for WF cameras, 28.3 for the PC1 camera.   |
| <b>Image Form</b>        | 4 x 800 x 800 pixels.   |
| <b>Pixel Size</b>        | 15 μm.  |
| <b>Spectral Response</b> | 1,150 Å - 11,000 Å.   |
| <b>Detector</b>          | Thick front side illuminated silicon sensor, multi-pinned phase (MPP) operation to eliminate quantum efficiency hysteresis, lumogen phosphor coating for UV sensitivity. Made by Loral Aerospace. |
| <b>Read noise</b>        | ~5 e <sup>-</sup> for gain 7 (for details, see <a href="#">Table 4.2 of the WFPC2 Instrument Handbook</a> ).  |

---

|                              |  |
|------------------------------|--|
| <b>Dark current</b>          | 0.002 e <sup>-</sup> /sec/pix [WF2] to 0.006 e <sup>-</sup> /sec/pix [PC1].  |
| <b>Gain</b>                  | 7 e <sup>-</sup> /DN, saturates at about 27,000 e <sup>-</sup> .<br>14 e <sup>-</sup> /DN saturates at about 53,000 e <sup>-</sup> . |
| <b>Operating Temperature</b> | -88 °C since Apr. 24, 1994. (Prior to that, -76 °C.)   |

**Table 1.4: WFPC2 Filters, as Described in the WFPC2 Instrument Handbook, Chapter 3**

| Filter | Notes                             | Mean Wavelength $\bar{\lambda}$ (Å) | $\Delta\bar{\lambda}$ (Å) | Peak Transmission (%) | Peak $\lambda$ (Å) |
|--------|-----------------------------------|-------------------------------------|---------------------------|-----------------------|--------------------|
| F122M  | H Ly $\alpha$ - Red Leak          | 1259                                | 224.4                     | 19.3                  | 1240               |
| F130LP | CaF2 Blocker (zero focus)         | 2681                                | 5568.3                    | 94.5                  | 8852               |
| F160AW | Woods A - read leak from pinholes | 1471                                | 457.2                     | 10.1                  | 1403               |
| F160BW | Woods B                           | 1446                                | 457.1                     | 12.1                  | 1400               |
| F165LP | Suprasil Blocker (zero focus)     | 3301                                | 5533.2                    | 95.4                  | 5796               |
| F170W  | -                                 | 1666                                | 434.6                     | 30.7                  | 1655               |
| F185W  | -                                 | 1899                                | 297.4                     | 25.9                  | 1849               |
| F218W  | Interstellar feature              | 2117                                | 367.9                     | 21.1                  | 2092               |
| F255W  | -                                 | 2545                                | 408.2                     | 14.8                  | 2489               |
| F300W  | Wide U                            | 2892                                | 727.6                     | 50.8                  | 2760               |
| F336W  | WFPC2 U, Strömgren u              | 3317                                | 370.5                     | 82.6                  | 3447               |
| F343N  | Ne V                              | 3427                                | 23.5                      | 9.3                   | 3432               |
| F375N  | [OII] 3727 RS                     | 3732                                | 24.4                      | 19.5                  | 3736               |
| F380W  | -                                 | 3912                                | 694.8                     | 65.0                  | 3980               |
| F390N  | CN                                | 3888                                | 45.0                      | 36.5                  | 3886               |
| F410M  | Strömgren v                       | 4086                                | 147.0                     | 70.4                  | 4097               |
| F437N  | [OIII]                            | 4369                                | 25.2                      | 52.0                  | 4368               |
| F439W  | WFPC2 B                           | 4283                                | 464.4                     | 68.2                  | 4176               |
| F450W  | Wide B                            | 4410                                | 925.1                     | 91.4                  | 5060               |
| F467M  | Strömgren b                       | 4663                                | 166.4                     | 75.3                  | 4728               |
| F469N  | He II                             | 4694                                | 25.0                      | 52.4                  | 4697               |
| F487N  | H                                 | 4865                                | 25.9                      | 58.6                  | 4862               |
| F502N  | [OIII]                            | 5012                                | 26.9                      | 63.7                  | 5008               |
| F547M  | Strömgren y (but wider)           | 5446                                | 486.6                     | 91.3                  | 5360               |
| F555W  | WFPC2 V                           | 5202                                | 1222.6                    | 94.6                  | 5148               |

**Table 1.4: WFPC2 Filters, as Described in the [WFPC2 Instrument Handbook, Chapter 3](#)**

| Filter       | Notes                        | Mean Wavelength $\bar{\lambda}$ (Å) | $\Delta\bar{\lambda}$ (Å) | Peak Transmission (%) | Peak $\lambda$ (Å) |
|--------------|------------------------------|-------------------------------------|---------------------------|-----------------------|--------------------|
| F569W        | F555W generally preferred    | 5524                                | 965.7                     | 94.2                  | 5310               |
| F588N        | He I & Na I (NaD)            | 5893                                | 49.0                      | 91.4                  | 5894               |
| F606W        | Wide V                       | 5767                                | 1579.0                    | 96.7                  | 6186               |
| F622W        | -                            | 6131                                | 935.4                     | 95.6                  | 6034               |
| F631N        | [OI]                         | 6306                                | 30.9                      | 85.7                  | 6301               |
| F656N        | H $\alpha$                   | 6564                                | 21.5                      | 77.8                  | 6562               |
| F658N        | [NII]                        | 6591                                | 28.5                      | 79.7                  | 6591               |
| F673N        | [SII]                        | 6732                                | 47.2                      | 87.0                  | 6732               |
| F675W        | WFPC2 R                      | 6714                                | 889.5                     | 97.3                  | 6780               |
| F702W        | Wide R                       | 6940                                | 1480.6                    | 97.1                  | 6538               |
| F785LP       | F814W generally preferred    | 9283                                | 2096.1                    | 91.7                  | 9959               |
| F791W        | F814W generally preferred    | 7969                                | 1304.6                    | 95.9                  | 8082               |
| F814W        | WFPC2 I                      | 8203                                | 1758.0                    | 94.8                  | 8387               |
| F850LP       | -                            | 9650                                | 1672.4                    | 89.2                  | 10028              |
| F953N        | [SIII]                       | 9546                                | 52.5                      | 95.6                  | 9528               |
| F1042M       | -                            | 10437                               | 611.0                     | 81.6                  | 10139              |
| FQUVN-A      | Redshifted [OII] 375         | 3763                                | 73.3                      | 25.9                  | 3769               |
| FQUVN-B      | Redshifted [OII] 383         | 3829                                | 57.3                      | 29.5                  | 3828               |
| FQUVN-C      | Redshifted [OII] 391         | 3912                                | 59.5                      | 34.3                  | 3909               |
| FQUVN-D      | Redshifted [OII] 399         | 3992                                | 63.7                      | 41.0                  | 3989               |
| FQCH4N-A     | CH4 543                      | 5435                                | 34.4                      | 77.0                  | 5442               |
| FQCH4N-B     | CH4 619                      | 6199                                | 33.8                      | 82.7                  | 6202               |
| FQCH4N-C     | CH4 727                      | 7279                                | 38.1                      | 90.9                  | 7278               |
| FQCH4N-D     | CH4 892                      | 8930                                | 54.8                      | 64.8                  | 8930               |
| POLQ_p<br>ar | Pol angle 0°, 45°, 90°, 135° | 4404                                | 5796.8                    | 90.7                  | 11000              |

**Table 1.4: WFPC2 Filters, as Described in the [WFPC2 Instrument Handbook, Chapter 3](#)**

| Filter       | Notes  | Mean Wavelength $\bar{\lambda}$ (Å) | $\Delta\bar{\lambda}$ (Å) | Peak Transmission (%) | Peak $\lambda$ (Å) |
|--------------|--|-------------------------------------|---------------------------|-----------------------|--------------------|
| POLQ_p<br>er | Pol angle $0^\circ, 45^\circ, 90^\circ, 135^\circ$ | 6682                                | 6654.2                    | 89.7                  | 11000              |
| FR418N       | 3700-4720  | W                                   | W/75                      | ~20 - 50              | W                  |
| FR533N       | 4720-6022  | W                                   | W/75                      | ~40 - 50              | W                  |
| FR680N       | 6022-7683  | W                                   | W/75                      | ~60 - 80              | W                  |
| FR868N       | 7683-9802  | W                                   | W/75                      | ~70 - 85              | W                  |

**Segments of the UV and CH4 quads are labeled here by their usual physical designations (A, B, C, and D). The quad polarizer is represented for both parallel and perpendicular polarization to its polarization direction, which is different in each quadrant. Additional information is available at the [WFPC2 Instrument Handbook, Chapter 3](#).**



# WFPC2 Data Structures

In this chapter. . .

2.1 Historical Data Formats and File Names / 11

2.2 Header Keywords / 15

2.3 Correlating Phase II Exposures with Data Files / 20

2.4 WFPC2 Data Products in the Hubble Legacy Archive / 24

---

## 2.1 Historical Data Formats and File Names

HST data files are distributed by the [Archive](#) in FITS (Flexible Image Transport System) format, either electronically via the Internet or on some data storage medium (see Chapter 1 of the [HST Data Handbook](#)).

Historically, WFPC2 files have been provided in the “waiver FITS” (wFITS) format, which is not the same as the “*multi-extension FITS*” (*MEF*) data format of the more recent HST instruments (see chapter 2 of the [HST Data Handbook](#)). **However, starting on August 10, 2009, the default format for WFPC2 data from the [Archive](#) is the multi-extension FITS format.**

### **WFPC2 File Formats: GEIS/Waiver FITS and Multi-extension FITS.**

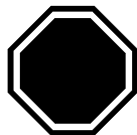
The original data format for WFPC2 images is the Generic Edited Information Sets (GEIS) format. Since the GEIS format is machine-dependent, they were stored in the Archive as waiver FITS (wFITS) files.

At the time WFPC2 image formats were being developed, standard FITS was unable to accommodate files with multiple image extensions. This led to the creation of the non-standard wFITS format for archival

storage. In the past, in order to use WFPC2 data in STSDAS, the wFITS image files had to be converted to the GEIS format using **strfits**.

Several years after the implementation of the wFITS format, new enhancements were developed for the standard FITS format, providing significant flexibility. FITS files can now contain multiple image extensions, each with its own header, size, and data type. This type of FITS is known as multi-extension FITS (MEF) and has been adopted as the standard for current HST instruments' data. *The WFPC2 Static Archive<sup>1</sup> stores data in the multi-extension FITS (MEF) format. The MEF format is also the new default format for all WFPC2 data retrieved from the Archive.* All STSDAS tasks that were previously used with GEIS images are also compatible with MEF images. (Users who prefer working with GEIS images can continue to receive them by specifically requesting wFITS images from the Archive, and converting them to GEIS using **strfits**.)

The differences between GEIS/wFITS and MEF formats are listed in [Table 2.1](#).




---

*Observers who retrieve WFPC2 data in Multi-extension FITS format cannot convert them to the GEIS format. All STSDAS tasks work properly on MEF format files.*

---

### File Naming Conventions

WFPC2 images are usually 4-group images, where group 1 contains data from the Planetary Camera (PC1) and has the DETECTOR keyword value of 1. Similarly, groups 2, 3, and 4 hold data from WF2, WF3, and WF4 cameras, respectively, and have DETECTOR keyword values of 2, 3, and 4, respectively. However, it was also possible to command WFPC2 to read out fewer than four CCDs, which produced a dataset with the same number of requested chip readouts. In those cases, the chip and camera ID for a particular group can be determined from the value of the DETECTOR keyword.

---

1. See [Section 3.1](#) for more information about the WFPC2 Static Archive.

**Table 2.1: Differences Between GEIS and MEF Files**

| Generic Edited Information Set (GEIS) and Waiver FITS (wFITS)   | Multi-extension FITS (MEF)   |                       |          |           |        |        |        |   |               |                   |  |           |      |  |   |       |                       |  |        |  |  |  |      |          |          |       |        |       |        |   |               |                    |  |  |  |    |   |       |     |   |         |     |  |   |       |     |   |         |     |  |   |       |     |   |         |     |  |   |       |     |   |         |     |  |
|---|--|-----------------------|----------|-----------|--------|--------|--------|---|---------------|-------------------|--|-----------|------|--|---|-------|-----------------------|--|--------|--|--|--|------|----------|----------|-------|--------|-------|--------|---|---------------|--------------------|--|--|--|----|---|-------|-----|---|---------|-----|--|---|-------|-----|---|---------|-----|--|---|-------|-----|---|---------|-----|--|---|-------|-----|---|---------|-----|--|
| <p>GEIS data has two components: an ASCII header file (ending with “h”) and a binary data file (ending with “d”). Together, they represent a single WFPC2 image file set. The image file set usually has 4 groups, each containing an image from a CCD.<br/>                     Example: ub080101m.c0h and ub080101m.c0d<br/>                     ub080101m.x0h and ub080101m.x0d</p>  | <p>The entire image is contained in one file.<br/>                     Example: ub080101m_c0m.fits<br/>                     ub080101m_x0m.fits</p>   |                       |          |           |        |        |        |   |               |                   |  |           |      |  |   |       |                       |  |        |  |  |  |      |          |          |       |        |       |        |   |               |                    |  |  |  |    |   |       |     |   |         |     |  |   |       |     |   |         |     |  |   |       |     |   |         |     |  |   |       |     |   |         |     |  |
| <p>GEIS is a machine-dependent format, and is therefore not suitable for archival storage and distribution. A specialized FITS format called waiver FITS (wFITS) was developed to hold a GEIS image file set, the header file and data file, in a single 3-dimensional image file. IRAF/STSDAS can operate on GEIS files, but not on wFITS files; wFITS files must first be converted to the GEIS format using <b>strfits</b>. GEIS files can be converted back to the wFITS format using <b>stwfits</b>. Additional information is available in chapter 2 of the <a href="#">HST Data Handbook</a>.<br/>                     Example: GEIS image file set ub080101m.c0h and ub080101m.c0d were obtained by running <b>strfits</b> on the wFITS file ub080101m_c0f.fits</p> | <p>The MEF format functions as both the archival format and STSDAS image analysis format.<br/>                     Example: ub080101m_c0m.fits</p>   |                       |          |           |        |        |        |   |               |                   |  |           |      |  |   |       |                       |  |        |  |  |  |      |          |          |       |        |       |        |   |               |                    |  |  |  |    |   |       |     |   |         |     |  |   |       |     |   |         |     |  |   |       |     |   |         |     |  |   |       |     |   |         |     |  |
| <p>A GEIS header file (e.g., ub080101m.c0h) contains global keywords and descriptions of group keywords. The data file (e.g., ub080101m.c0d) contains up to 4 groups of image data (where each group represents data from a camera) and values for group keywords.</p>  | <p>Extension zero (e.g., ub080101m_d0m.fits [0]) contains only global keywords. It is also the only location for HISTORY comments. Group data, each representing a chip, are stored in up to four extensions. Each extension contains group keywords and binary image data for a particular group.</p>   |                       |          |           |        |        |        |   |               |                   |  |           |      |  |   |       |                       |  |        |  |  |  |      |          |          |       |        |       |        |   |               |                    |  |  |  |    |   |       |     |   |         |     |  |   |       |     |   |         |     |  |   |       |     |   |         |     |  |   |       |     |   |         |     |  |
| <p>All wFITS data from the Static Archive ends in “f.fits” (e.g., ub080101m_d0f.fits)</p>   | <p>All MEF data from the Static Archive ends in “m.fits” (e.g., ub080101m_d0m.fits)</p>  |                       |          |           |        |        |        |   |               |                   |  |           |      |  |   |       |                       |  |        |  |  |  |      |          |          |       |        |       |        |   |               |                    |  |  |  |    |   |       |     |   |         |     |  |   |       |     |   |         |     |  |   |       |     |   |         |     |  |   |       |     |   |         |     |  |
| <p>The structure of a wFITS file is a 3-dimensional image cube, as shown below when using the STSDAS task <b>catfits</b>. Example:</p> <pre>--&gt; catfits ub080101m_c0f.fits</pre> <table border="1"> <thead> <tr> <th>EXT#</th> <th>FITSNAME</th> <th>FILENAME</th> <th>EXTVE</th> <th>DIMENS</th> <th>BITPI</th> <th>OBJECT</th> </tr> </thead> <tbody> <tr> <td>0</td> <td>ub080101m_c0f</td> <td>ub080101m_cvt.c0h</td> <td></td> <td>800x800x4</td> <td>-32F</td> <td></td> </tr> <tr> <td>1</td> <td>TABLE</td> <td>ub080101m_cvt.c0h.tab</td> <td></td> <td>56Fx4R</td> <td></td> <td></td> </tr> </tbody> </table>   | EXT#   | FITSNAME              | FILENAME | EXTVE     | DIMENS | BITPI  | OBJECT | 0 | ub080101m_c0f | ub080101m_cvt.c0h |  | 800x800x4 | -32F |  | 1 | TABLE | ub080101m_cvt.c0h.tab |  | 56Fx4R |  |  | <p>Running <b>catfits</b> on a Multi-extension FITS file shows:</p> <pre>--&gt; catfits ub080101m_c0m.fits</pre> <table border="1"> <thead> <tr> <th>EXT#</th> <th>FITSNAME</th> <th>FILENAME</th> <th>EXTVE</th> <th>DIMENS</th> <th>BITPI</th> <th>OBJECT</th> </tr> </thead> <tbody> <tr> <td>0</td> <td>ub080101m_c0m</td> <td>ub080101m_c0f.fits</td> <td></td> <td></td> <td></td> <td>16</td> </tr> <tr> <td>1</td> <td>IMAGE</td> <td>SCI</td> <td>1</td> <td>800x800</td> <td>-32</td> <td></td> </tr> <tr> <td>2</td> <td>IMAGE</td> <td>SCI</td> <td>2</td> <td>800x800</td> <td>-32</td> <td></td> </tr> <tr> <td>3</td> <td>IMAGE</td> <td>SCI</td> <td>3</td> <td>800x800</td> <td>-32</td> <td></td> </tr> <tr> <td>4</td> <td>IMAGE</td> <td>SCI</td> <td>4</td> <td>800x800</td> <td>-32</td> <td></td> </tr> </tbody> </table> | EXT# | FITSNAME | FILENAME | EXTVE | DIMENS | BITPI | OBJECT | 0 | ub080101m_c0m | ub080101m_c0f.fits |  |  |  | 16 | 1 | IMAGE | SCI | 1 | 800x800 | -32 |  | 2 | IMAGE | SCI | 2 | 800x800 | -32 |  | 3 | IMAGE | SCI | 3 | 800x800 | -32 |  | 4 | IMAGE | SCI | 4 | 800x800 | -32 |  |
| EXT#  | FITSNAME   | FILENAME              | EXTVE    | DIMENS    | BITPI  | OBJECT |        |   |               |                   |  |           |      |  |   |       |                       |  |        |  |  |  |      |          |          |       |        |       |        |   |               |                    |  |  |  |    |   |       |     |   |         |     |  |   |       |     |   |         |     |  |   |       |     |   |         |     |  |   |       |     |   |         |     |  |
| 0   | ub080101m_c0f  | ub080101m_cvt.c0h     |          | 800x800x4 | -32F   |        |        |   |               |                   |  |           |      |  |   |       |                       |  |        |  |  |  |      |          |          |       |        |       |        |   |               |                    |  |  |  |    |   |       |     |   |         |     |  |   |       |     |   |         |     |  |   |       |     |   |         |     |  |   |       |     |   |         |     |  |
| 1   | TABLE  | ub080101m_cvt.c0h.tab |          | 56Fx4R    |        |        |        |   |               |                   |  |           |      |  |   |       |                       |  |        |  |  |  |      |          |          |       |        |       |        |   |               |                    |  |  |  |    |   |       |     |   |         |     |  |   |       |     |   |         |     |  |   |       |     |   |         |     |  |   |       |     |   |         |     |  |
| EXT#  | FITSNAME   | FILENAME              | EXTVE    | DIMENS    | BITPI  | OBJECT |        |   |               |                   |  |           |      |  |   |       |                       |  |        |  |  |  |      |          |          |       |        |       |        |   |               |                    |  |  |  |    |   |       |     |   |         |     |  |   |       |     |   |         |     |  |   |       |     |   |         |     |  |   |       |     |   |         |     |  |
| 0   | ub080101m_c0m  | ub080101m_c0f.fits    |          |           |        | 16     |        |   |               |                   |  |           |      |  |   |       |                       |  |        |  |  |  |      |          |          |       |        |       |        |   |               |                    |  |  |  |    |   |       |     |   |         |     |  |   |       |     |   |         |     |  |   |       |     |   |         |     |  |   |       |     |   |         |     |  |
| 1   | IMAGE  | SCI                   | 1        | 800x800   | -32    |        |        |   |               |                   |  |           |      |  |   |       |                       |  |        |  |  |  |      |          |          |       |        |       |        |   |               |                    |  |  |  |    |   |       |     |   |         |     |  |   |       |     |   |         |     |  |   |       |     |   |         |     |  |   |       |     |   |         |     |  |
| 2   | IMAGE  | SCI                   | 2        | 800x800   | -32    |        |        |   |               |                   |  |           |      |  |   |       |                       |  |        |  |  |  |      |          |          |       |        |       |        |   |               |                    |  |  |  |    |   |       |     |   |         |     |  |   |       |     |   |         |     |  |   |       |     |   |         |     |  |   |       |     |   |         |     |  |
| 3   | IMAGE  | SCI                   | 3        | 800x800   | -32    |        |        |   |               |                   |  |           |      |  |   |       |                       |  |        |  |  |  |      |          |          |       |        |       |        |   |               |                    |  |  |  |    |   |       |     |   |         |     |  |   |       |     |   |         |     |  |   |       |     |   |         |     |  |   |       |     |   |         |     |  |
| 4   | IMAGE  | SCI                   | 4        | 800x800   | -32    |        |        |   |               |                   |  |           |      |  |   |       |                       |  |        |  |  |  |      |          |          |       |        |       |        |   |               |                    |  |  |  |    |   |       |     |   |         |     |  |   |       |     |   |         |     |  |   |       |     |   |         |     |  |   |       |     |   |         |     |  |
| <p><b>Examples of how to view header keyword values.</b></p> <p><b>hedit</b></p> <pre>--&gt; hedit ub080101m.c0h[2] expstart,detector . ub080101m.c0h[2],EXPSTART = 5.456265019941E+04 ub080101m.c0h[2],DETECTOR = 2</pre> <p><b>hselect</b></p> <pre>--&gt; hsel ub080101m.c0h[2] expstart,detector yes 5.456265019941E+04      2</pre> <p><b>imheader</b></p> <pre>--&gt; imhead ub080101m.c0h[2] long+   match EXPSTART EXPSTART= 5.456265019941E+04 / exposure start time (Modified Julian Date)</pre> <pre>--&gt; imhead ub080101m.c0h[2] long+   match DETECTOR DETECTOR=                2</pre>  | <p><b>Examples of how to view header keyword values.</b></p> <p><b>hedit</b></p> <pre>--&gt; hedit ub080101m_c0m.fits[2] expstart,detector . ub080101m_c0m.fits[2],EXPSTART = 5.456265019941E+04 ub080101m_c0m.fits[2],DETECTOR = 2</pre> <p><b>hselect</b></p> <pre>--&gt; hsel ub080101m_c0m.fits[2] expstart,detector yes 5.456265019941E+04      2</pre> <p><b>imheader</b></p> <pre>--&gt; imhead ub080101m_c0m.fits[2] long+   match EXPSTART EXPSTART= 5.456265019941E+04 / exposure start time (Modified Julian Date)</pre> <pre>--&gt; imhead ub080101m_c0m.fits[2] long+   match DETECTOR DETECTOR=                2 / CCD number of the detector: PC 1, WFC 2-4</pre> |                       |          |           |        |        |        |   |               |                   |  |           |      |  |   |       |                       |  |        |  |  |  |      |          |          |       |        |       |        |   |               |                    |  |  |  |    |   |       |     |   |         |     |  |   |       |     |   |         |     |  |   |       |     |   |         |     |  |   |       |     |   |         |     |  |

WFPC2 files have a nine-character rootname (e.g., u2850303p) and a three-character suffix (also called the extension). All files for a single exposure, called a dataset, will have the same rootname. A detailed explanation of the rootname nomenclature can be found in [Section 2.3](#). For each instrument, the suffix uniquely identifies the file contents. The WFPC2 suffixes are listed in [Table 2.2](#).

**Table 2.2: WFPC2 Dataset Suffixes and File Sizes**

| GEIS Format Suffix           | Waiver FITS <sup>1</sup> Format Suffix | Multi-extension FITS Format Suffix | File Contents  | Approximate Size |
|------------------------------|--|------------------------------------|--|------------------|
| <b>Raw Data Files</b>        |  |                                    |  |                  |
| .d0h/.d0d                    | _d0f.fits                              | _d0m.fits                          | Raw science data.  | 5 MB             |
| .q0h/.q0d                    | _q0f.fits                              | _q0m.fits                          | Data quality for raw science data.   | 5 MB             |
| .x0h/.x0d                    | _x0f.fits                              | _x0m.fits                          | Extracted engineering data (CCD overscan image).   | 1 MB             |
| .q1h/.q1d                    | _q1f.fits                              | _q1m.fits                          | Data quality for extracted engineering data.   | 0.1 MB           |
| .shh/.shd <sup>2</sup>       | _shf.fits                              | _shm.fits                          | Standard header packet containing observation parameters.  | 0.03 MB          |
| .dgr <sup>2, 3</sup>         | _dgr.fits                              | _dgr.fits                          | Text file listing the values of the group header keywords in the raw image.  | 0.03 MB          |
| <b>Calibrated Data Files</b> |  |                                    |  |                  |
| .c0h/.c0d                    | _c0f.fits                              | _c0m.fits                          | Calibrated science data.   | 10 MB            |
| .c1h/.c1d                    | _c1f.fits                              | _c1m.fits                          | Data quality for calibrated science data.  | 5 MB             |
| .c2h/.c2d <sup>4</sup>       | -                                      | -                                  | Histogram of science data pixel values (not included in the standard delivery of calibrated data).   | 0.2 MB           |
| .c3t                         | _c3t.fits                              | _c3m.fits                          | The throughput table for the observation mode, as specified in the PHOTMODE group header keyword.  | 0.2 MB           |
| .cgr <sup>3</sup>            | _cgr.fits                              | _cgr.fits                          | Text file listing the values of the group header keywords in the calibrated image.   | 0.03 MB          |
| .trl                         | _trl.fits                              | _trl.fits                          | Trailer file, see <a href="#">Figure 3.1</a> .   | 0.03 MB          |
| -                            | -                                      | _drz.fits                          | Quick-look drizzled mosaic of all four groups, only in the MEF format. This file is created by the OPUS pipeline, and cannot be produced using the stand-alone <b>calwp2</b> task in STSDAS. | 25 MB            |

1. wFITS files must be converted to the GEIS format using the STSDAS task **strfits**; most IRAF/STSDAS tasks do not work properly when directly used on wFITS files.

2. This file is not required for manual recalibration.

3. This file is not included in the standard delivery of raw or calibrated data files, and must be requested by specifying its extension in the Archive retrieval form.

4. This file is only created when a user recalibrates the image with the switch DOHISTOS=PERFORM. See [Section 3.3.2, Histogram Creation](#) for details.

## 2.2 Header Keywords

WFPC2 header keywords include items such as integration time (EXPTIME), filters (FILTNAM1 and FILTNAM2), the software version used in the pipeline (OPUS\_VER and CAL\_VER), reference files used for calibration, the calibration steps, and properties of the data itself (e.g., number of groups, NEXTEND<sup>2</sup>). Some additional calibration information is given at the end of the header in the HISTORY<sup>3</sup> keywords.

Group keywords (i.e. keywords associated with each separate CCD) include observing mode (PHOTMODE), reference pixels (CRPIX1, CRPIX2), coordinates of the reference pixel (CRVAL1, CRVAL2), scale (IDCSCALE<sup>2</sup>), flux units (PHOTFLAM), properties of data in the group (e.g., dimensions in pixels, NAXIS1<sup>2</sup>, NAXIS2<sup>2</sup>) and image statistics for each chip (MEDIAN, HISTWIDE, MEANC100, BACKGRND, etc.).

Observers new to WFPC2 data should peruse the header keywords and comments in their image headers. Some keywords can occasionally be misleading. For example, DATE refers to the date the file was written while DATE-OBS refers to the date of the observation. PROCTIME refers to the date and time an image was processed in the pipeline. FILTER1 and FILTER2 keywords record the numerical designations of the filter(s) while the filter names are stored in FILTNAM1 and FILTNAM2. Also, PHOTZPT is not the photometric zeropoint (in the ST magnitude system) as normally understood, but rather the zeropoint in the ST magnitude system to be used after the conversion of counts to FLAM units (see [Section 5.1](#)).

Astrometry keywords can also be confusing. The orientation of the image is specified by a global keyword, PA\_V3, and a group keyword, ORIENTAT. The keyword, PA\_V3, gives the position angle (in degrees) of the telescope's V3 axis on the sky, measured from North through East (see [Figure 1.3](#)). The V3 axis is roughly 225° from the x axis of PC1. The V3 axis differs by exactly 180° from the ORIENT value defined in the [Phase II Proposal Instructions](#). The group keyword, ORIENTAT, records, for each detector, the position angle of the y axis in the plane of the sky, measured from North through East. This angle differs from PA\_V3 by roughly -135°, -45°, +45°, and +135°, for PC1, WF2, WF3, and WF4, respectively. See [Figure 1.3](#) for a graphical representation of the geometric relationship between the four detectors. Accurate values of the positions and rotations between chips can be obtained from the [Science Instrument Aperture File \(SIAF\)](#) at:

<http://www.stsci.edu/hst/observatory/apertures/siaf.html>.

---

2. Only available in MEF format files

3. History keywords in MEF images can only be viewed in group 0 (e.g., `ub080101m_c0m.fits[0]`)

Some of the more commonly-used WFPC2 header keywords are listed in Table 2.3 and Table 2.4. A list of most header keywords, with brief explanations, can be found in the [HST Keyword Dictionary](http://www.dpt.stsci.edu/keyword/) at

<http://www.dpt.stsci.edu/keyword/>

**Table 2.3: Important WFPC2 Global<sup>1</sup> Header Keywords**

| Keyword                                  | Description  |
|--|--|
| <b>Information about the groups</b>      |  |
| GCOUNT                                   | Number of groups per observation (1 to 4). GEIS files only.  |
| NEXTEND                                  | Number of standard extensions per observation (1 to 4). MEF files only.  |
| <b>Image keywords</b>                    |  |
| FILETYPE                                 | SHP - standard header packet.<br>EXT - extracted engineering file.<br>EDQ - EED data quality file.<br>SDQ - science data quality file.<br>SCI - science data file. |
| INSTRUME                                 | Instrument used; always WFPC2.   |
| ROOTNAME                                 | Rootname of the observation set.   |
| PROCTIME                                 | Date and time of pipeline processing (Modified Julian Date).   |
| MODE                                     | Mode: FULL (full resolution) or AREA (2 x 2 pixel binning).  |
| SERIALS                                  | Serial clocks: ON, OFF.  |
| <b>Data type keywords</b>                |  |
| IMAGETYP                                 | Image type: DARK/BIAS/IFLAT/UFLAT/VFLAT/KSPOT/EXT/ECAL.  |
| CDBSFILE                                 | GENERIC/BIAS/DARK/FLAT/MASK/ATOD/NO. If the image is a reference file, the type of reference file is specified by this keyword.                                    |
| <b>Reference file selection keywords</b> |  |
| FILTNAM1                                 | First filter name.   |
| FILTNAM2                                 | Second filter name; blank if none used.  |
| FILTER1                                  | First filter number (0–48). (Used in SOGS - Science Operations Ground System).   |
| FILTER2                                  | Second filter number (0–48).   |
| FILTROT                                  | Partial filter rotation angle (degrees).   |
| ATODGAIN                                 | Analog to digital gain (e <sup>-</sup> /DN). Either 7 or 15.   |
| <b>Calibration switches</b>              |  |
| MASKCORR                                 | Do mask correction: PERFORM, OMIT, COMPLETE.   |
| ATODCORR                                 | Do A-to-D correction: PERFORM, OMIT, COMPLETE.   |
| WF4TCORR                                 | Correct the WF4 data for temperature-dependent errors: PERFORM, OMIT, COMPLETE.  |
| BLEVCORR                                 | Do bias level correction: PERFORM, OMIT, COMPLETE.   |
| BIASCORR                                 | Do bias correction: PERFORM, OMIT, COMPLETE.   |
| DARKCORR                                 | Do dark correction: PERFORM, OMIT, COMPLETE.   |
| FLATCORR                                 | Do flat field correction: PERFORM, OMIT, COMPLETE.   |
| SHADCORR                                 | Do shutter shading correction: PERFORM, OMIT, COMPLETE.  |

**Table 2.3: Important WFPC2 Global<sup>1</sup> Header Keywords**

| <b>Keyword</b>                                      | <b>Description</b>  |
|---|---|
| DOSATMAP  | Output saturated pixel map: PERFORM, OMIT, COMPLETE.                                    |
| DOPHOTOM  | Fill photometry keywords: PERFORM, OMIT, COMPLETE.                                      |
| DOHISTOS  | Make histograms: PERFORM, OMIT, COMPLETE.   |
| DRIZCORR  | Drizzle processing pipeline switch (used in the OPUS pipeline, not <b>calwp2</b> ).     |
| OUTDTYPE  | Output image datatype: REAL, LONG, SHORT.   |
| <b>Calibration reference files used<sup>2</sup></b> |   |
| MASKFILE  | Name of the input static mask containing known bad pixels and charge traps.             |
| ATODFILE  | Name of the A-to-D conversion file.   |
| WF4TFILE  | Name of the WF4 correction reference file.  |
| BLEVFILE  | Name of engineering file with extended register data.                                   |
| BLEVDFIL  | Name of data quality file (DQF) for the engineering file.                               |
| BIASFILE  | Name of the superbias reference file.   |
| BIASDFIL  | Name of the superbias reference DQF.  |
| DARKFILE  | Name of the dark reference file.  |
| DARKDFIL  | Name of the dark reference DQF.   |
| FLATFILE  | Name of the flat field reference file.  |
| FLATDFIL  | Name of the flat field reference DQF.   |
| SHADFILE  | Name of the reference file for shutter shading.   |
| PHOTTAB   | Name of the photometry calibration table.   |
| SATURATE  | Data value at which saturation occurs (always 4095 for WFPC2, which includes the bias). |
| GRAPHTAB  | the HST graph table.  |
| COMPTAB   | the HST components table.   |
| IDCTAB  | Geometric distortion correction table.  |
| OFFTAB  | CCD drift correction table.   |
| DGEOFILE  | 34th row distortion correction image.   |
| <b>Ephemeris data</b>                               |   |
| PA_V3   | Position angle of V3 axis of HST.   |
| RA_SUN  | Right ascension of the sun (degrees).   |
| DEC_SUN   | Declination of the sun (degrees).   |
| EQNX_SUN  | Equinox of the sun.   |
| <b>Fill values</b>                                  |   |
| PODPSFF   | 0 (no fill), 1 (fill present).  |
| RSDPFILL  | Bad data fill value set in pipeline for calibrated image.                               |
| <b>Exposure Information</b>                         |   |
| DARKTIME  | Estimate of darktime (in seconds).  |
| EQUINOX   | Equinox of the celestial coordinate system.   |
| SUNANGLE  | Angle between sun and V1 axis (degrees).  |
| MOONANGL  | Angle between moon and V1 axis (degrees).   |

**Table 2.3: Important WFPC2 Global<sup>1</sup> Header Keywords**

| Keyword                     | Description   |
|-----------------------------|---|
| SUN_ALT                     | Altitude of the sun above Earth's limb (degrees).   |
| FGSLOCK                     | Commanded FGS lock (FINE, COARSE, GYROS, UNKNOWN).  |
| <b>Timing information</b>   |   |
| DATE-OBS                    | UT date of start of observation.  |
| TIME-OBS                    | UT time of start of observation (hh:mm:ss).   |
| EXPSTART                    | Exposure start time (Modified Julian Date).   |
| EXPEND                      | Exposure end time (Modified Julian Date).   |
| EXPTIME                     | Exposure duration (seconds).  |
| EXPFLAG                     | Exposure interruption indicator (NORMAL, INTERRUPTED, INCOMPLETE, EXTENDED, UNCERTAIN, INDETERMINATE, PREDICTED). |
| <b>Proposal information</b> |   |
| TARGNAME                    | Target name.  |
| RA_TARG                     | Right ascension of the target (degrees) (J2000).  |
| DEC_TARG                    | Declination of the target (degrees) (J2000).  |
| PROPOSID                    | Phase II proposal identifier number.  |

1. *Global* header keywords contain values that apply to the entire image dataset, regardless of image group.
2. Calibration reference file keywords are populated even if unused.

**Table 2.4: Important WFPC2 Group<sup>1</sup> Header Keywords**

| Keyword                        | Description  |
|--------------------------------|--|
| <b>Position</b>                |  |
| CRPIX1 <sup>2</sup>            | <i>X</i> coordinate of reference pixel.                                    |
| CRPIX2 <sup>2</sup>            | <i>Y</i> coordinate of reference pixel.                                    |
| CRVAL1 <sup>2</sup>            | RA of reference pixel (degrees).   |
| CRVAL2 <sup>2</sup>            | Dec. of reference pixel (degrees).   |
| CD1_1 <sup>2</sup>             | Partial derivative of RA with respect to <i>x</i> .                        |
| CD1_2 <sup>2</sup>             | Partial derivative of RA with respect to <i>y</i> .                        |
| CD2_1 <sup>2</sup>             | Partial derivative of Dec. with respect to <i>x</i> .                      |
| CD2_2 <sup>2</sup>             | Partial derivative of Dec. with respect to <i>y</i> .                      |
| VAFactor                       | Velocity aberration plate scale factor.                                    |
| DETECTOR                       | CCD detector used for the group data (1, 2, 3, or 4).                      |
| NAXIS1,<br>NAXIS2 <sup>3</sup> | the <i>x</i> and <i>y</i> dimensions of the image, in pixels.              |
| A_ORDER,<br>B_ORDER            | Order of the polynomial used to describe geometric distortion corrections. |

**Table 2.4: Important WFPC2 Group<sup>1</sup> Header Keywords**

| Keyword   | Description  |
|---|--|
| A_0_2,<br>B_0_2,<br>A_1_1,<br>B_1_1,<br>A_2_0,<br>B_2_0,<br>A_0_3,<br>B_0_3,<br>A_1_2,<br>B_1_2,<br>A_2_1,<br>B_2_1,<br>A_3_0,<br>B_3_0 | Non-linear or high-order polynomial coefficients, in the SIP convention, describe the geometric distortion model for each image group. They are present for use by SIP-enabled code such as DS9 and may be used by future versions of the pipeline software, <b>multidrizzle</b> and other STSDAS tasks. |
| <b>Orientation</b>  |  |
| MIR_REVR  | Is image mirror reversed?  |
| ORIENTAT <sup>2</sup>   | Orientation of <i>y</i> axis (degrees) - a different value for each group.   |
| <b>Bias Information</b>   |  |
| DEZERO  | Mean bias level from engineering data.   |
| BIASEVEN  | Bias value for even-numbered columns in the science image.   |
| BIASODD   | Bias value for odd-numbered columns in the science image.  |
| BIASEVNU  | BIASEVEN value prior to the <a href="#">WF4 Anomaly Correction</a> .   |
| BIASODDU  | BIASODD value prior to the <a href="#">WF4 Anomaly Correction</a> .  |
| <b>Pixel statistics</b>   |  |
| GOODMIN   | Minimum value of the “good” <sup>4</sup> pixels.   |
| GOODMAX   | Maximum value of the “good” <sup>4</sup> pixels.   |
| DATAMEAN  | Mean value of the “good” <sup>4</sup> pixels.  |
| GPIXELS   | Number of “good” <sup>4</sup> pixels (out of 640,000).   |
| ATODSAT   | Number of saturated pixels.  |
| <b>Image statistics keywords</b>  |  |
| MEDIAN  | Middle data value of sorted good quality pixels.   |
| HISTWIDE  | Width of the image histogram.  |
| SKEWNESS  | Skewness of the image histogram.   |
| MEANC10   | Mean of a 10 x 10 pixel region at the center of the chip.  |
| MEANC100  | Mean of a 100 x 100 pixel region at the center of the chip.  |
| MEANC300  | Mean of a 300 x 300 pixel region at the center of the chip.  |
| BACKGRND  | Estimated background level.  |
| CTE_1E2 <sup>5</sup>  | Expected worst-case delta magnitude from CTE, 100 e <sup>-</sup> point source.   |
| CTE_1E3 <sup>5</sup>  | Expected worst-case delta magnitude from CTE, 1,000 e <sup>-</sup> point source.   |
| CTE_1E4 <sup>5</sup>  | Expected worst-case delta magnitude from CTE, 10,000 e <sup>-</sup> point source.  |

**Table 2.4: Important WFPC2 Group<sup>1</sup> Header Keywords**

| Keyword   | Description   |
|---|---|
| <b>Photometry keywords (populated if header keyword DOPHOTOM=YES)</b> |   |
| PHOTMODE  | Photometry mode.  |
| PHOTFLAM  | Inverse sensitivity (units of erg/sec/cm <sup>2</sup> /Å for 1 DN/sec).                 |
| PHOTZPT   | Zeropoint in the ST Magnitude system after conversion to FLAM units (currently -21.10). |
| PHOTPLAM  | Pivot wavelength (in Å).  |
| PHOTBW  | RMS bandwidth of filter (in Å).   |
| ZP_CORR   | Time-dependent sensitivity correction (in delta magnitude).                             |

1. *Group* header keywords contain values that are unique to a specific image group.
2. This keyword also appears in the header preceded by "O" (i.e. OCRVAL1). These are the original values produced during generic conversion. The current value (i.e. CRVAL1) was updated during pipeline processing to make it compatible with the IDCTAB reference file (geometric distortion correction table).
3. The keywords NAXIS1 and NAXIS2 are only visible when using **hedit** or **hselect** to retrieve keyword values from an image. It will not appear in an image header listing generated by **imheader**.
4. “good” refers to pixels not flagged in the Data Quality File (DQF).
5. CTE\_1E2, CTE\_1E3, and CTE\_1E4 are estimates of the charge-transfer losses (in units of delta mag) for a star at x = 400, y = 400 with brightness of 100 e<sup>-</sup>, 1000 e<sup>-</sup>, and 10,000 e<sup>-</sup> (respectively). CTE (Charge Transfer Efficiency) is computed using [Andrew Dolphin’s \(2004\)](#) recipe, which is a function of star brightness, observation date, and background level.

## 2.3 Correlating Phase II Exposures with Data Files

In this section, we discuss how to correlate the image data with the exposures specified in the Phase II proposal submission. The Phase II proposal submitted by the investigator can be viewed at:

[http://www.stsci.edu/hst/scheduling/program\\_information](http://www.stsci.edu/hst/scheduling/program_information)

For each Phase II program, there are three types of files:

- “Phase 2 File” is the xml file that can be directly read by the [Astronomers Proposal Tool \(APT\)](#).
- “Phase 2 PDF” is similar to the PDF-formatted proposal file obtained from APT’s “PDF Preview” menu button.
- “Formatted Listing” is an ASCII version of the proposal (that pre-dates APT), formatted so it’s easy to read. See [Figure 2.1](#) for an example.

**Figure 2.1: Excerpt of the exposure logsheet (ASCII formatted listing) associated with observation u9ps8507m**

```

Visit: 85
  Visit Priority:      <none>
  Visit Requirements: GROUP 85, 86, 87, 88 WITHIN 3.6 Orbits
  On Hold Comments:  <none>
  Additional Comments: <none>

Exposures
-----
Exp | Target | Instr | Oper. | Aper | Spectral | Central |           | Num | Time |           |
Num | Name   | Config | Mode  | or FOV | Element | Waveln. | Optional | Exp |      | Special |
           |         |        |       |         |         |         | Parameters |    |      | Requirements |
-----
1 | HD-130819 | WFPC2 | IMAGE | PC1-FIX | F606W |         |         | 1 | 2 S | POS TARG -14.1,-14.3 |
2 | HD-130819 | WFPC2 | IMAGE | PC1-FIX | F606W |         | CLOCKS=YES | 3 | 40 S | POS TARG -14.1,-14.3 |
3 | HD-130819 | WFPC2 | IMAGE | PC1-FIX | F606W |         | CLOCKS=YES | 3 | 590 S | POS TARG -14.1,-14.3 |
-----

Sub Exposures
-----
Target | Exp | Instr | Oper. | Aper | Spectral | Cent. | Primary | Secondary | Iteration | CR-SPLIT | Orbit | Duration |
Name   | Num | Config | Mode  | or FOV | Element | Wave. | Pattern Pos | Pattern Pos | Num      | Num      | Number |          |
-----
HD-130819 | 1 | WFPC2 | IMAGE | PC1-FIX | F606W |         | none | none | none | none | 1 | N/A |
HD-130819 | 2 | WFPC2 | IMAGE | PC1-FIX | F606W |         | none | none | 1 | none | 1 | N/A |
HD-130819 | 2 | WFPC2 | IMAGE | PC1-FIX | F606W |         | none | none | 2 | none | 1 | N/A |
HD-130819 | 2 | WFPC2 | IMAGE | PC1-FIX | F606W |         | none | none | 3 | none | 1 | N/A |
HD-130819 | 3 | WFPC2 | IMAGE | PC1-FIX | F606W |         | none | none | 1 | none | 1 | N/A |
HD-130819 | 3 | WFPC2 | IMAGE | PC1-FIX | F606W |         | none | none | 2 | none | 1 | N/A |
HD-130819 | 3 | WFPC2 | IMAGE | PC1-FIX | F606W |         | none | none | 3 | none | 1 | N/A |

```

Specific image header keywords that correspond to entries in the Phase II proposal are provided in [Table 2.5](#).

**Table 2.5: Comparing Phase II Proposal Keywords to Image Header Keywords**

| Image Header Keyword  | Phase II Formatted ASCII File                 | Phase II PDF File   |
|-----------------------|---|---|
| PROPOSID              | Proposal ID<br>(see “Cover Page”)             | The proposal ID is part of the document title in the “Overview” and all page headers. |
| TARGNAME              | Target_Name<br>(see “Target List”)            | In each visit summary:<br>Name in the “Fixed Targets” section.                        |
| RA_TARG,<br>DEC_TARG  | Target Position<br>(see “Target List”)        | In each visit summary:<br>Target Coordinates in the “Fixed Targets” section.          |
| FILTNAM1,<br>FILTNAM2 | Spectral Element<br>(see “Exposure Logsheet”) | In each visit summary:<br>Spectral Els. in the “Exposures” section.                   |
| EXPTIME               | Time<br>(see “Exposure Logsheet”)             | In each visit summary:<br>Exp. Time/ [Actual Dur.] in the “Exposures” section.        |

The STSDAS task `iminfo` provides a brief overview of the observation, as seen in this example for `u9ps8507m_c0m.fits`.

```
--> iminfo u9ps8507m_c0m.fits[3]

-----
Rootname          Instrument          Target Name
u9ps8507m        WFPC2              HD-130819

Program           = 9ps              Obs Date          = 2007-05-01
Observation set   = 85              Proposal ID       = 10896
Observation       = 07              Exposure ID       = 85-003#003
Source            = Unknown         Right ascension   = 14:50:41.1
File Type         = SCI           Declination       = -15:59:51
                                           Equinox          = J2000

First filtername  = F606W          Number of groups  = 1
Second filtername =                    Data type         = real

Image type        = EXT           Exposure time (sec) = 500.
Mode              = FULL         Dark time (sec)    = 500.
Serials           = ON
Shutter           = A             Calibration steps done:
Kelsall spot lamp = OFF          MASK ATOD BLEV BIAS DARK FLAT
```

Note: in the example above for the MEF image (`c0m.fits`), “Number of groups” refers to the number of sub-groups *within* group 3 only (i.e.,

u9ps8507m\_c0m.fits[3]). It does not tell you the number of groups within the entire image file, u9ps8507m\_c0m.fits<sup>4</sup>. To find out the number of groups within the entire MEF image file, check the header keyword NEXTEND.

```
--> hsel u9ps8507m_c0m.fits[3] NEXTEND yes
4
```

The proposal ID for this observation is found in the **iminfo** listing, or it can be found using **hedit** or **hselect** on the image to get the value of the PROPOSID header keyword. The proposal can then be viewed by entering the proposal ID in the field “Proposal ID” under “Program Status” at:

<http://www.stsci.edu/hst/>

or at:

[http://www.stsci.edu/hst/scheduling/program\\_information](http://www.stsci.edu/hst/scheduling/program_information)

The example of running **iminfo** on u9ps8507m\_c0m.fits also shows the origins of the observation’s rootname, u9ps8507m.

- u All WFPC2 rootnames start with "U".
- 9ps This is the program ID; it’s assigned to all exposures in a proposal during the scheduling process.
- 85 “Observation set” in the **iminfo** listing corresponds to the visit number in the Phase II proposal, in this case, visit 85.
- 07 “Observation” in the **iminfo** listing corresponds to, in this example, the 7th exposure taken in that visit. In [Figure 2.1](#), exposure line 1 shows one 2 second exposure. Exposure line 2 shows three exposures, each 40 seconds long because the Phase II exposure logsheet “num exp” field was set to 3. Similarly, exposure line 3 shows three exposures, each with an exposure time of 590 seconds. The image in u9ps8507m was the 7th and last exposure taken in visit 85.
- m The last letter in the rootname indicates how the data was transferred to the ground from HST. "m" means that real time and tape recorded data for this observation were merged to create the dataset. Other designations for data transmission type can be found in [Table B.1](#) in the [HST Data Handbook](#).

There were times when the requested exposure times in the proposal did not match that of the executed observations. One reason was due to a recommendation that WFPC2 exposures longer than 600 seconds be split into two shorter exposures to facilitate the removal of cosmic rays. If the optional parameters CR-SPLIT and CR-TOLERANCE were omitted in the Phase II submission, and the exposure was longer than 600 seconds, the default setting was to split it into two exposures of approximate equal lengths; a default CR-TOLERANCE value of 0.2 meant that the split

---

4. For a 4-group GEIS image (.c0h/.c0d), **iminfo** would have returned the value "4" for “Number of groups” because of the different image file structure.

exposure times could each range from 30% to 70% of the total exposure, with their sum equal to the original total exposure time.

Another reason for the occurrence of mismatches between requested and executed exposure times was because exposure times were occasionally shortened or lengthened by up to 20% without the approval of the PI, provided that the resulting S/N was 90% of that with the original exposure time. Such changes may have been required to fit observations into specific orbital time slots.

---

## 2.4 WFPC2 Data Products in the Hubble Legacy Archive

The Hubble Legacy Archive (HLA), at:

<http://hla.stsci.edu>,

is a useful source of WFPC2 data, offering enhanced data products as well as multiple ways to search through HST data to find observations from WFPC2 and other instruments. For most public WFPC2 data, the HLA provides both single-exposure and visit-level combined images, rotated to have North up and corrected for geometric distortion. Two different flavors are provided: full images that include both WF and PC1 data, at a scale of 0.1 arcsec/pixel, as well as PC1-only images, with a scale of 0.05 arcsec/pixel.

The images are produced by the [Canadian Astronomical Data Center \(CADC\)](#) using a pipeline based on **multidrizzle**. The HLA also provides source lists obtained with DAOPHOT (optimized for point sources) and **SExtractor** (more suited to extended objects), including an approximate correction for CTE following the prescriptions of [Dolphin \(2008\)](#). All images and catalogs, as well as the calibrated data and many intermediate products, can be downloaded directly via a shopping cart feature.

Through the HLA site, users can search for HST data on the basis of location in the sky, program name, and instrument. The location of the data can be seen at a glance in the “footprint” view. Data properties can be inspected and saved in tabular form, and multiple images can be previewed simultaneously through either thumbnails or cutouts. Each image can be fully displayed through an interactive FITS viewer. If multiple filters are available, color images can be generated on-the-fly and adjusted to the user’s preferences. Source lists and external catalogs (currently SDSS, GSC2, 2MASS, FIRST, and GALEX) can be superimposed on the WFPC2 image data; whenever possible, the astrometry of the images has been adjusted to match one of these reference catalogs.

The properties of the HLA as of August 2009 are described in detail in a forthcoming paper (Whitmore et al. 2009, in prep.). However, the HLA is still evolving, frequently including more data and improved interfaces every few months. Users are encouraged to visit the [HLA Web page](#) for the most up-to-date information and description of the data holdings and interfaces.

# WFPC2 Calibration

In this chapter. . .

3.1 Brief History of the WFPC2 Processing Pipeline / 25

3.2 Data Processing Overview / 26

3.3 Standard Pipeline Calibration / 34

3.4 Post-calwp2 Processing / 44

3.5 Recalibration / 45

3.6 Improving the Pipeline Calibration / 52

---

## 3.1 Brief History of the WFPC2 Processing Pipeline

Until 1999, HST data products from the Archive were the result of pipeline processing, using calibration reference files available *at the time the image was taken*. In December 1999, the “On-The-Fly Calibration” (OTFC) system was released to the public. When a user requested data from the Archive, OTFC retrieved raw files (d0h/d0d, q0h/q0d, x0h/x0d, q1h/q1d) from the Archive, calibrated each dataset using the best-available calibration reference files at the time of the user’s request, and shipped the data to the user. The primary advantages of OTFC included:

- Automatic application of improved calibration files and switches,
- Use of the most recent calibration software (allowing for rapid access to improved algorithms, new capabilities, and software fixes),
- Correction of header keywords, if needed.

In May 2001, OTFC was replaced by the “On-The-Fly-Reprocessing” (OTFR) system. The primary difference between the two systems was that OTFR began processing earlier in the data path, starting with the telemetry files (“POD” files) originally received from the Goddard Space Flight Center. It performed all the pipeline processing steps: data partitioning, repairing data dropouts, converting the partitioned data packets into raw

science files, and calibrating the newly-created raw files. (OTFC had only performed the last pipeline processing step, calibration of raw files stored in the Archive.)

With the end of WFPC2 observations in May 2009 came the end of periodic updates to the calibration pipeline and associated reference files. In order to speed up deliveries and reduce costs, a decision was made to reprocess the entire archive of WFPC2 POD files using the best associated reference files, and place the resulting raw and calibrated data in a “*Static Archive*.” When all WFPC2 data have been reprocessed one final time, OTFR will be turned off; all subsequent data requests will be fulfilled from this new Static Archive. Raw data and calibration reference files will continue to be available in the Static Archive for users who wish to perform their own calibrations.

---

## 3.2 Data Processing Overview

During pipeline calibration, raw WFPC2 data files were passed through the “OPUS<sup>1</sup> pipeline;” all calibration steps were recorded in the trailer file<sup>2</sup> (`tr1` file) for each dataset. Figure 3.1 shows an example of a trailer file that identifies the major pipeline steps as described below:

- (A) The data was partitioned; the POD file was separated into individual files representing the engineering and science data sections.
- (B) Any missing pixel values were replaced with dummy values (an arbitrary assigned value given in the header keyword `STDCFFP`).
- (C) The data was evaluated to determine discrepancies between planned and executed observation parameters.
- (D) The data was converted to a format necessary for further processing, a step known as “generic conversion.” Header keywords were also populated at this stage.
- (E) The data was calibrated using a standard WFPC2-specific calibration algorithm, `calwp2`, and the best-available reference files.
- (F) A series of new Python routines were run to populate various header keywords and generate a drizzled quick-look image mosaic of all the chips.
- (G) After processing, many of the header keyword values were also written to Archive databases (these steps are not shown in Figure 3.1)

---

1. OPUS is the name of the pipeline software that controls the processing and archiving of data at STScI: converting telemetry into FITS data products, populating the Archive catalog, and performing housekeeping on the pipelines.

2. A few trailer files may show error messages near the beginning of the file. This may be a residual artifact from a previous processing run. The correct processing comments should be appended to it. If you suspect a problem with your data, please contact us at [help@stsci.edu](mailto:help@stsci.edu).

**Figure 3.1: Sample Trailer File for u5k10101r**

```

(A) 2009010181506-I-INFO ----- Data Partitioning Starts ----- (1)3
    2009010181506-I-INFO POD file name:
    /info/sthubbins/otfr/clark/dat/dct//lz_a22c_303_0000213465_u5k10101r.pod_proc (1)
    2009010181506-I-INFO Observation name: u5k10101r (1)
    2009010181506-I-INFO Finished partitioning obs u5k10101r (1)
    2009010181506-I-INFO Expected 3201 packets, Received 3201 packets (1)
    2009010181506-I-INFO (1 SHP, 0 UDL, 0 BAD, 3200 SCI). (1)
    2009010181506-I-INFO ----- Data Partitioning ends ----- (1)
(B) 2009010181510-I-INFO ----- Data Quality Editing Started: u5k10101r ----- (1)
    2009010181510-I-INFO ----- Data Quality Editing Completed: u5k10101r ----- (1)
(C) 2009010181526-I-INFO ----- Data Validation Started: u5k10101r ----- (1)
    2009010181526-W-WARNING PMDB-PDB comparison will NOT be done (1)
    2009010181528-I-INFO ----- Data Validation Completed: u5k10101r ----- (1)
    2009010181532-I-INFO ----- World Coordinate System Started: u5k10101r ----- (1)
    2009010181532-I-INFO ----- World Coordinate System Ended: u5k10101r ----- (1)
(D) 2009010181548-I-INFO ----- Generic Conversion Started: u5k10101r ----- (1)
    2009010181551-I-INFO ----- Generic Conversion Completed: u5k10101r ----- (1)
    2009010181558-I-INFO----- REF started for: u5k10101r -----
    2009010181558-I-INFO-GRAPHTAB value changed: => mtab$scf1549pm_tmg.fits
    2009010181558-I-INFO-COMPTAB value changed: => mtab$scg1705am_tmc.fits
    2009010181558-I-INFO-BIASFILE value changed: => uref$kc1557lu.r2h
    2009010181558-I-INFO-DARKFILE value changed: => uref$ja614574u.r3h
    2009010181558-I-INFO-FLATFILE value changed: => uref$m3c1004au.r4h
    2009010181558-I-INFO-ATODFILE value changed: => uref$dbu1405iu.r1h
    2009010181559-I-INFO-SHADFILE value changed: => uref$e371355iu.r5h
    2009010181559-I-INFO-IDCTAB value changed: => uref$sad1946fu_idc.fits
    2009010181559-I-INFO-OFFTAB value changed: => uref$s9518396u_off.fits
    2009010181559-I-INFO-WF4TFILE value changed: => N/A
    2009010181559-I-INFO-DGEOFILE value changed: N/A => uref$s8f1222cu_dxy.fits
    2009010181559-I-INFO----- REF ended for: u5k10101r -----
(E) CALBEG ----- Sat Jan 10 18:35:41 GMT 2009-----
    --- WFPC2 Calibration Starting: CALWP2 Version 2.5.3 (Sep 4, 2008)
    --- Starting CALWP2: Input = u5k10101r Output = u5k10101r
    *** WARNING From: CALWP-2 While Processing: u5k10101r
    *** No WF4TFILE specified. Skipping WF4TCORR.
    MASKFILE=uref$f8213081u.r0h MASKCORR=COMPLETED
    PEDIGREE=INFLIGHT 01/01/1994 - 15/05/1995
    DESCRIP=STATIC MASK - INCLUDES CHARGE TRANSFER TRAPS
    uref$dbu1405iu.r1h has no PEDIGREE keyword
    BIASFILE=uref$kc1557lu.r2h BIASCORR=COMPLETED
    PEDIGREE=INFLIGHT 26/08/99 - 29/08/00
    DESCRIP=not significantly different from j9a1612mu.
    DARKFILE=uref$ja614574u.r3h DARKCORR=COMPLETED
    PEDIGREE=INFLIGHT 27/09/1999 - 27/09/1999
    DESCRIP=Pipeline dark: 120 frame superdark with hotpixels from 27/09/99
    FLATFILE=uref$m3c1004au.r4h FLATCORR=COMPLETED
    PEDIGREE=INFLIGHT 30/10/1996 - 30/04/2001
    DESCRIP=Improved Cyc6-9 flat, rms errors < 0.2-0.3% - see ISR 2002-02
    --- Starting processing of element 1
    photmode = WFPC2,1,A2D7,F439W,,CAL

```

3. The text "----- (1)" is part of the trailer file content.

```

photmode(cont) = WFPC2,1,A2D7,F439W,,cont#51454.191,CAL
--- Starting processing of element 2
photmode = WFPC2,2,A2D7,F439W,,CAL
photmode(cont) = WFPC2,2,A2D7,F439W,,cont#51454.191,CAL
--- Starting processing of element 3
photmode = WFPC2,3,A2D7,F439W,,CAL
photmode(cont) = WFPC2,3,A2D7,F439W,,cont#51454.191,CAL
--- Starting processing of element 4
photmode = WFPC2,4,A2D7,F439W,,CAL
photmode(cont) = WFPC2,4,A2D7,F439W,,cont#51454.191,CAL
--- Computing image statistics of element 1
--- Computing image statistics of element 2
--- Computing image statistics of element 3
--- Computing image statistics of element 4
--- WFPC2 Calibration Completed
CALEND ----- Sat Jan 10 18:36:41 GMT 2009-----

```

(F) Filename: u5k10101r\_c0f.fits

| No. | Name    | Type       | Cards | Dimensions | Format  |
|-----|---------|------------|-------|------------|---------|
| 0   | PRIMARY | PrimaryHDU | 251   | ()         | int16   |
| 1   | SCI     | ImageHDU   | 143   | (800, 800) | float32 |
| 2   | SCI     | ImageHDU   | 107   | (800, 800) | float32 |
| 3   | SCI     | ImageHDU   | 107   | (800, 800) | float32 |
| 4   | SCI     | ImageHDU   | 107   | (800, 800) | float32 |

Background computed to be: 7.0

CTE\_1E2 = 0.278727

CTE\_1E3 = 0.114256

CTE\_1E4 = 0.056283

Background computed to be: 7.56305964487

CTE\_1E2 = 0.273426

CTE\_1E3 = 0.111878

CTE\_1E4 = 0.0549846

Background computed to be: 7.0

CTE\_1E2 = 0.278727

CTE\_1E3 = 0.114256

CTE\_1E4 = 0.056283

Background computed to be: 7.0

CTE\_1E2 = 0.278727

CTE\_1E3 = 0.114256

CTE\_1E4 = 0.056283

Updating keywords in: u5k10101r\_c0f.fits

+ MAKEWCS Version 1.1.0 (2 Sept 2008)

-Updating image u5k10101r\_c0f.fits[sci,1]

- IDCTAB: Distortion model from row 18 for chip 1 : F439W and CLEAR

- OFFTAB: Offset interpolated from rows 17 and 21

- IDCTAB: Distortion model from row 158 for chip 3 : F439W and CLEAR

- OFFTAB: Offset interpolated from rows 19 and 23

-Updating image u5k10101r\_c0f.fits[sci,2]

- IDCTAB: Distortion model from row 88 for chip 2 : F439W and CLEAR

- OFFTAB: Offset interpolated from rows 18 and 22

- IDCTAB: Distortion model from row 158 for chip 3 : F439W and CLEAR

- OFFTAB: Offset interpolated from rows 19 and 23

-Updating image u5k10101r\_c0f.fits[sci,3]

- IDCTAB: Distortion model from row 158 for chip 3 : F439W and CLEAR

```

- OFFTAB: Offset interpolated from rows 19 and 23- IDCTAB: Distortion model from row 158 for
chip 3 : F439W and CLEAR
- OFFTAB: Offset interpolated from rows 19 and 23
-Updating image u5k10101r_c0f.fits[sci,4]
- IDCTAB: Distortion model from row 228 for chip 4 : F439W and CLEAR
- OFFTAB: Offset interpolated from rows 20 and 24
- IDCTAB: Distortion model from row 158 for chip 3 : F439W and CLEAR
- OFFTAB: Offset interpolated from rows 19 and 23
Setting up output name: u5k10101r_drz.fits
Starting PyDrizzle Version 6.3.0 (15-Oct-2008) at 18:37:03 (10/01/2009)
- IDCTAB: Distortion model from row 18 for chip 1 : F439W and CLEAR
- OFFTAB: Offset interpolated from rows 17 and 21
- IDCTAB: Distortion model from row 88 for chip 2 : F439W and CLEAR
- OFFTAB: Offset interpolated from rows 18 and 22
- IDCTAB: Distortion model from row 158 for chip 3 : F439W and CLEAR
- OFFTAB: Offset interpolated from rows 19 and 23
- IDCTAB: Distortion model from row 228 for chip 4 : F439W and CLEAR
- OFFTAB: Offset interpolated from rows 20 and 24
Drizzle parameters have been calculated. Ready to .run()...
Finished calculating parameters at 18:37:10 (10/01/2009)
PyDrizzle: drizzle task started at 18:37:11 (10/01/2009)
Callable DRIZZLE Version 0.7 (4th Apr 2005)
-Opening coefficients file: u5k10101r_c0f_coeffs1.dat
-Using distortion reference point: [ 425.0000, 425.0000]
Callable DRIZZLE Version 0.7 (4th Apr 2005)
-Opening coefficients file: u5k10101r_c0f_coeffs2.dat
-Using distortion reference point: [ 425.0000, 425.0000]
Callable DRIZZLE Version 0.7 (4th Apr 2005)
-Opening coefficients file: u5k10101r_c0f_coeffs3.dat
-Using distortion reference point: [ 425.0000, 425.0000]
Callable DRIZZLE Version 0.7 (4th Apr 2005)
-Opening coefficients file: u5k10101r_c0f_coeffs4.dat
-Using distortion reference point: [ 425.0000, 425.0000]
! Warning, 253 points were outside the output image.
card is too long, comment is truncated.
-Generating multi-extension output file: u5k10101r_drz.fits
PyDrizzle drizzling completed at 18:37:33 (10/01/2009)

```

### 3.2.1 Calibration of WFPC2 Images

**calwp2** is the software used to calibrate WFPC2 images. It contains the steps used in standard astronomical CCD data reduction such as removing the effects of bias, dark current, and pixel response (flat-fielding). In the OPUS pipeline, **calwp2** is run after raw science data are extracted from telemetry (POD) files, processed, and formatted. A version of **calwp2** identical to that in the pipeline is available in STSDAS for users who wish to recalibrate their images.

For final reprocessing to create the WFPC2 Static Archive, the best reference files from the “Calibration Data Base” (CDBS) at STScI were used in the final OPUS pipeline calibration. These reference files are available at the [WFPC2 CDBS](http://www.stsci.edu/hst/observatory/cdbS/SIfileInfo/WFPC2/reftablequeryindex_wfpc2) reference files Web page at:

[http://www.stsci.edu/hst/observatory/cdbS/SIfileInfo/WFPC2/reftablequeryindex\\_wfpc2](http://www.stsci.edu/hst/observatory/cdbS/SIfileInfo/WFPC2/reftablequeryindex_wfpc2).

The processing steps for the data through **calwp2** is presented in schematic form in [Figure 3.2](#), and discussed in further detail in [Section 3.3](#). The software takes as input the raw WFPC2 data files and any necessary calibration reference images and tables.

The calibration steps are determined by the values of the calibration switches (e.g., MASKCORR, BIASCORR, etc.) in the image headers. In raw image files (`d0m.fits`), calibration switches will indicate whether a specific calibration step will be performed or not:

PERFORM - calibration step to be applied by **calwp2**.

OMIT - correction is not performed by **calwp2**.

In calibrated images, the switches will indicate if a particular calibration step was done or not:

COMPLETE - calibration step has been completed.

SKIPPED - step was skipped because the reference file was a dummy or placeholder (i.e., had no effect on the data). Or it was specified by the user during recalibration.

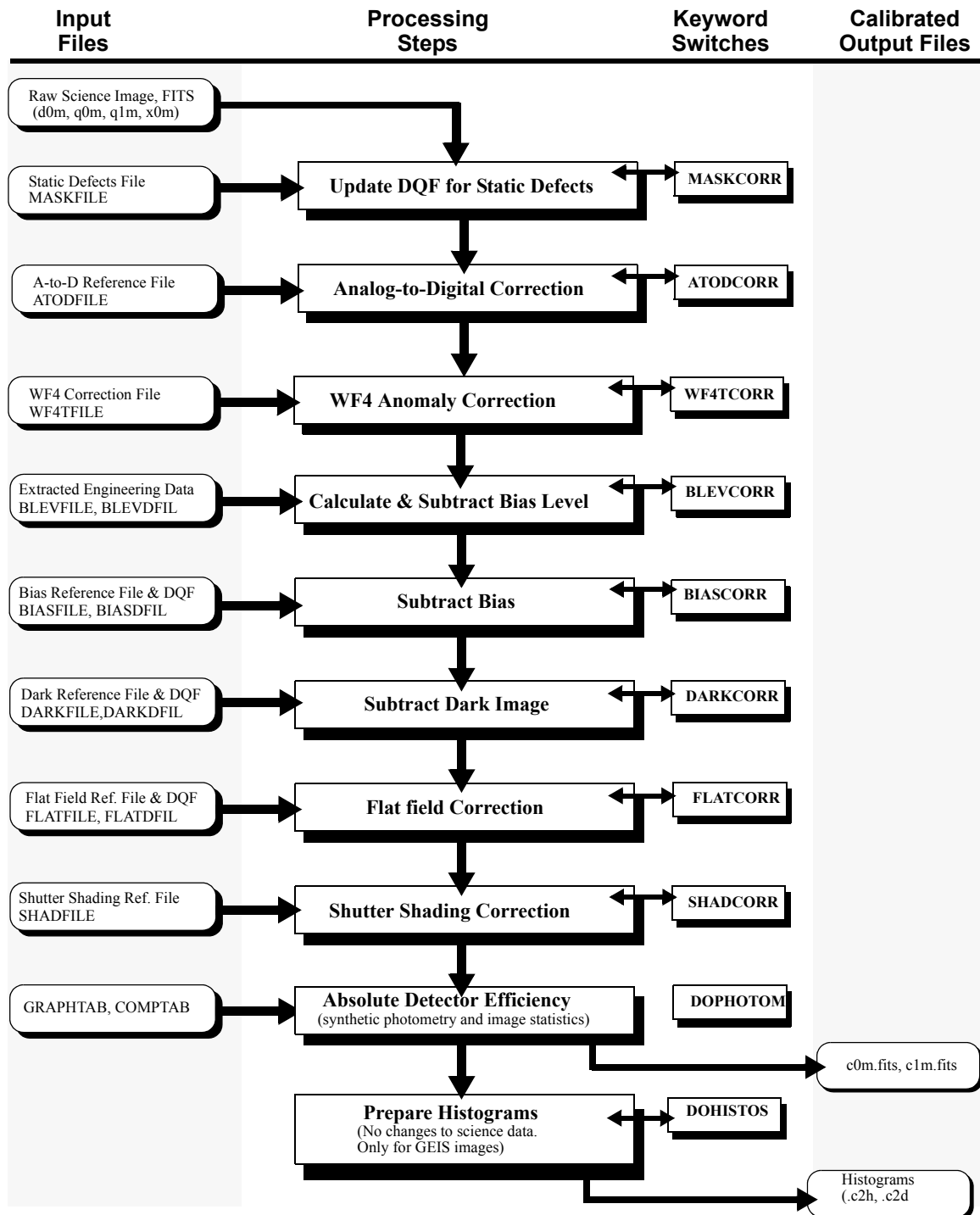
An excerpt from the header of `ub080101m_d0m.fits[0]` showing the calibration switches:

```

/ RSDP CONTROL KEYWORDS
MASKCORR= 'PERFORM ' / Do mask correction: PERFORM, OMIT, COMPLETE
ATODCORR= 'PERFORM ' / Do A-to-D correction: PERFORM, OMIT, COMPLETE
WF4TCORR= 'PERFORM ' / correct WF4 data for temp-dependent amp error
BLEVCORR= 'PERFORM ' / Do bias level correction
BIASCORR= 'PERFORM ' / Do bias correction: PERFORM, OMIT, COMPLETE
DARKCORR= 'OMIT ' / Do dark correction: PERFORM, OMIT, COMPLETE
FLATCORR= 'PERFORM ' / Do flat field correction
SHADCORR= 'PERFORM ' / Do shaded shutter correction
DOSATMAP= 'OMIT ' / Output saturated pixel map
DOPHOTOM= 'PERFORM ' / Fill photometry keywords
DOHISTOS= 'OMIT ' / Make histograms: PERFORM, OMIT, COMPLETE
DRIZCORR= 'PERFORM ' / drizzle processing
OUTDTYPE= 'REAL ' / Output image datatype: REAL, LONG, SHORT

```

**Figure 3.2: Pipeline Processing by calwp2**



Likewise, the reference files to be used in the calibration of the data are set by the values in the reference file keywords. The appropriate settings of the calibration switches and reference file keywords depend on the instrument configuration used (such as gain, exposure time, readout mode, filters), the date of observation, and any special pre-specified observing constraints. They are initially set in the header of the raw data file during the generic conversion step (Figure 3.1, step D); if manual calibration with different calibration settings is necessary, the reference filenames and calibration switches can be changed by editing the raw header file (`d0m.fits`) using the STSDAS tasks **hedit** or **chcalpar** and then running **calwp2** on the modified raw files.

An excerpt of the raw image header showing calibration reference files for dataset `ub080101m_d0m.fits[0]`:

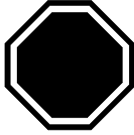
```

/ CALIBRATION REFERENCE FILES

MASKFILE= 'uref$f8213081u.r0h' / name of the input DQF of known bad pixels
ATODFILE= 'uref$dbu1405fu.r1h' / name of the A-to-D conversion file
WF4TFILE= 'uref$t721550cu.r7h' / name of the WF4 correction reference file
BLEVFILE= 'ucal$ub080101m.x0h' / Engineering file with extended register da
BLEVDFIL= 'ucal$ub080101m.q1h' / Engineering file DQF
BIASFILE= 'uref$t7d1506ou.r2h' / name of the bias frame reference file
BIASDFIL= 'uref$t7d1506ou.b2h' / name of the bias frame reference DQF
DARKFILE= 'uref$t6h10308u.r3h' / name of the dark reference file
DARKDFIL= 'uref$t6h10308u.b3h' / name of the dark reference DQF
FLATFILE= 'uref$m3c10041u.r4h' / name of the flat field reference file
FLATDFIL= 'uref$m3c10041u.b4h' / name of the flat field reference DQF
SHADFILE= 'uref$e371355eu.r5h' / name of the reference file for shutter sha
PHOTTAB = ' / name of the photometry calibration table
GRAPHTAB= 'mtab$t2605492m_tmg.fits' / the HST graph table
COMPTAB = 'mtab$t6i1714pm_tmc.fits' / the HST components table
IDCTAB = 'uref$sad1946fu_idc.fits' / Distortion correction table
OFFTAB = 'uref$s9518396u_off.fits' / Drift correction table
DGEOfILE= 'uref$s8f1222cu_dxy.fits' / Distortion correction image

```

For convenience, the calibration keywords that hold the switches and reference file names are also reported in the trailer files (Figure 3.1), and in the HISTORY keywords at the end of the calibrated science data header (`.c0h` or `c0m.fits[0]`).



*A note about recalibration: calwp2 can operate on GEIS or MEF raw datasets. However, image reference files used by calwp2 must always be converted from wFITS to GEIS regardless of whether the raw datasets are in GEIS or MEF formats. The format of calwp2 output files will always be the same as that of the input files. We recommend that you use MEF format raw datasets for recalibration; MEF files have additional keywords that may be useful for future data analysis.*

As with other header keywords, the calibration keywords can be viewed using the STSDAS tasks **imhead**, **hselect**, or **hedit**. Alternatively, the **chcalpar** task in the STSDAS **tools** package can be used to view and change group calibration keyword values directly.

Figure 3.2 shows a flow chart that summarizes the sequence of calibration steps performed by **calwp2**, including the type of input calibration reference files and tables, and type of the output data files from each step. The purpose of each calibration step is briefly described in Table 3.1, and a more detailed explanation is provided in Section 3.3.

**Table 3.1: Calibration Steps and Reference Files used for WFPC2 Pipeline Processing**

| Switch   | Processing Step  | Reference File (GEIS suffix)               |
|----------|--|--|
| MASKCORR | Update the science data quality file using the static bad pixel mask reference file (MASKFILE), which flags defects in the CCD that degrade pixel performance. These are defects that are stable over time. (No changes are made to the science image.)                      | maskfile (r0h, r0d)                        |
| ATODCORR | Correct the value of each science data pixel for the analog-to-digital conversion error using information in the A/D lookup reference file (ATODFILE).   | atodfile (r1h, r1d)                        |
| WF4TCORR | Correct the value of each science data pixel on the WF4 chip using information in the WF4 anomaly reference file (WF4TFILE).   | wf4tfile (r7h, r7d)                        |
| BLEVCORR | Subtract the mean bias level from each pixel in the science data. Mean values are determined separately for even column pixels (group keyword value BIASSEVEN) and odd column pixels (BIASODD) because the bias level exhibits a column-wise pattern that changes over time. | blevfile (x0h, x0d)<br>blevdfil (q1h, q1d) |
| BIASCORR | Subtract the bias image reference file (BIASFILE) from the science image and update the science data quality file with bias image data quality (BIASDFIL).   | biasfile (r2h, r2d)<br>biasdfil (b2h, b2d) |
| DARKCORR | Correct for dark current: scale the normalized dark image reference file to the value in the header keyword DARKTIME, the total dark accumulation time. Then, subtract it from the science image.  | darkfile (r3h, r3d)<br>darkdfil (b3h, b3d) |
| FLATCORR | Correct for pixel-to-pixel gain variations by multiplying with the flat-field image.   | flatfile (r4h, r4d)<br>flatdfil (b4h, b4d) |

| Switch   | Processing Step   | Reference File<br>(GEIS suffix)           |
|----------|---|---|
| SHADCORR | Remove shading due to finite shutter velocity for exposures less than 10 seconds.   | shadfile (r5h, .r5d)                      |
| DOPHOTOM | Determine absolute sensitivity using SYNPHOT throughput tables identified in the GRAPHTAB and COMPTAB reference tables. Science data are not changed.   | graphtab (tmg.fits)<br>comptab (tmc.fits) |
| DOHISTOS | An optional recalibration processing step: create a 3-row image (c2h, c2d) for each group. Row 1 is a histogram of raw science values, row 2 has the A/D correction histogram, and row 3 contains the calibrated image histogram. The default value for DOHISTOS is OMIT. | -   |

### 3.3 Standard Pipeline Calibration

Each calibration step, and the keyword switch used to turn that step on or off, is described in detail in [Section 3.3.2](#). These steps are performed in the following order:

1. Flag static bad pixels in the science data quality file.
2. Perform the analog-to-digital (A/D) correction.
3. Correct for the WF4 anomaly (in data taken on, and after, March 1, 2002).
4. Subtract the bias level.
5. Subtract the bias image.
6. Scale and subtract the dark image for exposures longer than 10 seconds.
7. Multiply by the flat field image.
8. Apply the shutter shading correction to exposures of less than 10 seconds.
9. Calculate photometry keywords and update the calibrated science image header accordingly (*this does not affect image pixel values*).
10. Generate the final science data quality file.

#### 3.3.1 Calibration Files

[Table 3.2](#) lists the types and related suffixes of the GEIS format WFPC2 reference files used in **calwp2**. Most suffixes have the form “rN<sub>h</sub>, rN<sub>d</sub>” where *N* is a number that, most of the time, identifies the calibration step order for which the file is used. Its associated data quality file, if it exists, has the suffix “bN<sub>h</sub>, bN<sub>d</sub>.” The rootname of a reference file is based on the [date and time](#) that the file was generated.

**Table 3.2: WFPC2 Calibration Reference Files**

| GEIS Header and Data Files Suffix | Reference File   |
|-----------------------------------|--|
| r0h, r0d                          | Static mask  |
| r1h, r1d                          | Analog-to-digital look-up table  |
| r7h, r7d <sup>1</sup>             | WF4 anomaly  |
| x0h, x0d<br>or x0m.fits           | Bias level reference file, which is actually part of the raw image dataset. It should be in the same format as the other raw data files being processed by <b>calwp2</b> . |
| r2h, r2d<br>b2h, b2d              | Bias reference and data quality images   |
| r3h, r3d<br>b3h, b3d              | Dark frame reference and data quality images   |
| r4h, r4d<br>b4h, b4d              | Flat field reference and data quality images   |
| r5h, r5d                          | Shutter shading  |

1. The suffix for calibration files are numbered to reflect their steps in the calibration process. However, the WF4 anomaly was discovered fairly late in WFPC2's operational life; even though the correction is performed as the third step in **calwp2** (for data taken on and after March 1, 2002), the suffix is r7h, r7d.

The file names and history of all WFPC2 reference files are listed in the [CDBS WFPC2 Reference Files](#) Web page,

[http://www.stsci.edu/hst/observatory/cdbS/SIfileInfo/WFPC2/reftablequeryindex\\_wfpc2](http://www.stsci.edu/hst/observatory/cdbS/SIfileInfo/WFPC2/reftablequeryindex_wfpc2)

Some older, alternative reference files generated by the WFPC2 IDT are listed in the [IDT Reference File Memo](#), at:

[http://www.stsci.edu/hst/wfpc2/analysis/wfpc2\\_idtrefs.html](http://www.stsci.edu/hst/wfpc2/analysis/wfpc2_idtrefs.html)

These files can be downloaded from the “Non-pipeline Reference Files” table at the [CDBS WFPC2 Reference Files](#) Web page.

All reference files contain HISTORY keywords at the end of the header that can be viewed using the **imhead** task. These HISTORY keywords provide detailed information about how the reference file was generated and when it was installed in the database.

### 3.3.2 Calibration Steps

#### Static Mask Application

Header Switch: MASKCORR

Header Keywords Updated: MASKCORR

Reference File: MASKFILE (r0h, r0d)

The static mask reference file (r0h, r0d) contains a map of the known bad pixels and columns; the mask reference filename is recorded in the

MASKFILE header keyword in the science header images (`d0m.fits` and `c0m.fits`). If this correction is requested (`MASKCORR = PERFORM` in the raw image file), the mask is included in the calibration output data quality file (`c1m.fits`); the science data are *not* changed in any way. The STSDAS task **wfixup** can be used to make cosmetic touch-ups on the final calibrated science image (`c0m.fits`) by interpolating across pixels flagged as bad in the final calibrated data quality file (`c1m.fits`).

### A/D Correction

Header Switch: ATODCORR

Header Keywords Updated: ATODCORR

Reference File: ATODFILE (`r1h`, `r1d`)

The analog-to-digital (A/D) converter takes the observed charge in each pixel in the CCD and converts it to a digital number. Two settings, or gains, are used on WFPC2. The first converts a charge of approximately seven electrons to a single count (called a “Data Number” or “DN”), and the second converts a charge of approximately 14 electrons to a DN, also referred to as “gain 15” for historical reasons. The precise gain conversion values for each chip are listed in Table 4.2 in [Section 4.4](#) of the [WFPC2 Instrument Handbook](#).

Depending on the Bay 3 temperature and the gain setting (gain 7 or gain 15), the A/D converter compares the charge detected in each pixel with a reference number that translates the charge (in electrons) to a count value (DN). A/D converters work by comparing the observed charge with a reference and act mathematically as a “floor” function (i.e. rounding down to the next lower integer value). However, these devices are not perfect; some values are reported more (or less) frequently than they would from a theoretically perfect device. Although the “true” DN values can never be recovered, their known systematic errors allow for statistical adjustments to reflect more realistic DN values. Fortunately, the WFPC2 A/D converters are relatively well-behaved and the correction is small (the largest correction is about 1.8 to 2.0 DN for bit 12 [2048]).

The A/D fix-up is applied when the ATODCORR keyword is set to PERFORM in the raw image. The A-to-D calibration file (a lookup table) has four groups, one for each detector. Each group has 4096 columns (i.e., all possible DN values for a 12 bit detector, from 0 to 4095). The first row contains -1 in the first column, followed by Bay 3 temperature values in subsequent columns. The second row contains A/D conversion corrections for each DN value corresponding to the first temperature in row 1. The third row would have A/D conversion corrections for the second temperature in row 1, and so on. On-orbit tests have shown that the conversion values have remained constant in WFPC2; therefore, the A-to-D reference file contains only one temperature and one set of conversion values. The example below illustrates how to get the corrected DN value, in WF2, using the gain 7 A-to-D reference file (`dbu1405iu.r1h`), for an initial DN count of 450. Note that the

corrected DN value in row 2 is found in the DN+1'th column because the correction value in the first column of row 2 is for DN=0.

```
-->listpix dbu1405iu.r1h[2] [451,2]
1. 450.1722
```

### WF4 Anomaly Correction

Header Switch: WF4TCORR

Header Keywords Updated: WF4TCORR

Group Header Keywords Updated: BIASEVNU, BIASODDU

Reference File: WF4TFILE (r7h, r7d)

Since 2002, a temperature-dependent reduction in the gain has plagued images obtained with the WF4 detector. Characterized by low or zero bias levels, faint horizontal streaks, and low photometry, the WF4 anomaly is thought to be caused by a failing amplifier in the WF4 signal-processing electronics.

The WF4 gain correction performs a number of tasks: first, it uses the contents of the `x0m.fits` file (overscan columns) to compute the bias levels of the uncorrected WF4 image, storing them in the new header keywords BIASEVNU and BIASODDU. (The computation of those keyword values is identical in method to the calculation of the BIASEVEN and BIASODD values described in the next subsection.) Next, it rescales the counts in each WF4 detector pixel by a correction factor from the WF4 anomaly correction reference file; this correction depends on both the BIASEVNU value and the observed counts in the image pixel. Then, it sets a data-quality flag (2048 or bit number 11) for all pixels in the image with bias values that are so low that they're unlikely to be properly corrected.

The error contributed to the corrected photometry by the WF4 anomaly correction is 1% to 2%. As this is close to the size of all the other error sources, its effect on the total error is not large. Additional information about how this correction is implemented can be found in [WFPC2 ISR 09-03](#), Pipeline Correction of Images Impacted by the WF4 Anomaly.

### Bias Level Removal

Header Switch: BLEVCORR

Header Keywords Updated: BLEVCORR

Group Header Keywords Updated: DEZERO, BIASEVEN, BIASODD

Reference File: BLEVFILE, BLEVDFIL

(`x0m.fits` and `q1m.fits`,

which are part of the raw image dataset)

The charge in each pixel sits on an electronic pedestal, or "bias" which keeps the A/D levels consistently above zero. The mean level of the bias, or "global" bias, is determined empirically using the extended register (overscan) pixels which are not exposed to the sky. The values of these

pixels are placed in the extracted engineering files (`x0m.fits`). For each group, a [9:14,10:790] subsection of the overscan image is used to calculate the mean bias levels; `BIASODD` is determined from columns 10, 12, and 14, and `BIASEVEN` from columns 9, 11, and 13. This counter-intuitive nomenclature is due to an offset in the `x0m.fits` file.

For images affected by the WF4 anomaly, the bias subtraction routine is modified as follows: if `WF4TCORR = PERFORM`, the WF4 gain correction, as computed in the previous subsection, is applied to the contents of the `x0m.fits` file. This modified overscan image is then used to compute the values for `BIASEVEN` and `BIASODD`, which are written to the image header.

If the `BLEVCORR` keyword is set to `PERFORM` in the raw image header, the `BIASODD` keyword value is subtracted from odd-numbered columns in the science image, and the `BIASEVEN` value is subtracted from the even columns.

Note: for PC1, WF2, and WF3, the `BIASEVEN` and `BIASODD` values are, as expected, identical to the `BIASEVNU` and `BIASODDU` values, respectively.

### Bias Image Subtraction

Header Switch: `BIASCORR`

Header Keywords Updated: `BIASCORR`

Reference File: `BIASFILE`, `BIASDFIL` (`r2h`, `r2d` and `b2h`, `b2d`)

The value of the bias pedestal varies slightly with position across the CCD. After the mean bias level correction has been applied, the pipeline checks the keyword `BIASCORR` in the raw image. If it is set to `PERFORM`, then a bias image reference file is subtracted from the data to remove any position-dependent bias patterns.

The bias image reference file is generated by stacking a large set of good quality individual bias images (zero-length exposures) that were calibrated for A-to-D conversion and global bias removal. Bad pixels flagged in the bias reference image data quality file (`b2h`, `b2d`) are also flagged in the science image data quality file (`c1m.fits`).

### Dark Image Subtraction

Header Switch: `DARKCORR`

Header Keywords Updated: `DARKCORR`

Reference File: `DARKFILE`, `DARKDFIL` (`r3h`, `r3d` and `b3h`, `b3d`)

There are two primary sources of dark current; a dominant component is strongly correlated with cosmic ray flux in the image, probably due to scintillation in the  $\text{MgF}_2$  CCD windows. There is also a smaller thermal dark current in the CCD itself. The dark reference file, used to remove the effects of dark current, is generated from two components: a superdark image (created from a stack of typically 120 good quality dark frames taken over one to two years<sup>4</sup>) and warm pixels identified from a smaller

stack of individual dark frames, typically five individual darks taken during the week of the observation.

If a dark correction is requested (`DARKCORR = PERFORM` in the raw science image), the dark reference file, which was normalized to one second, is scaled by the image's `DARKTIME` keyword value, and then subtracted from the observation. By default, `DARKCORR` is set to `PERFORM` for all exposures longer than 10 seconds, and set to `OMIT` for exposures less than 10 seconds (due to noise considerations).

### Flat Field Multiplication

Header Switch: `FLATCORR`

Header Keywords Updated: `FLATCORR`

Reference File: `FLATFILE`, `FLATDFIL` (`r4h`, `r4d` and `b4h`, `b4d`)

The number of electrons generated in a pixel due to a star of a given magnitude depends upon the quantum efficiency of that individual pixel as well as any large scale vignetting of the field of view caused by the telescope and camera optics. To correct for these variations, the science image is multiplied by an inverse flat field file. WFPC2 flat fields are generated from a combination of on-orbit data (so-called “Earthflats” which are images of the bright Earth) and pre-launch ground data. The on-orbit data allow a determination of the large-scale illumination pattern while the pre-launch data are used to determine the pixel-to-pixel response function. The application of the flat field file is controlled by the keyword `FLATCORR`.

### Shutter Shading Correction

Header Switch: `SHADCORR`

Header Keywords Updated: `SHADCORR`

Reference File: `SHADFILE` (`r5h`, `r5d`)

The finite velocity of the shutter produces uneven illumination across the field of view (thus the term “shutter shading”), resulting in a position-dependent exposure time. The shutter shading calibration is applied by default to all exposures less than ten seconds. It has the form of an additive correction, scaled to the appropriate exposure time, that varies spatially across the detectors. The keyword switch is `SHADCORR`, and the shutter shading file name is stored in the keyword, `SHADFILE`.

### Creation of Photometry Keywords

Header Switch: `DOPHOTOM`

Header Keywords Updated: `DOPHOTOM`, `PHOTTAB`

Group Header Keywords Updated: `PHOTMODE`, `PHOTFLAM`,  
`PHOTZPT`, `PHOTPLAM`, `PHOTBW`, `ZP_CORR`

Reference File: `GRAPHTAB`, `COMPTAB` (`tmg.fits`, `tmc.fits`)

---

4. A dark frame is a long exposure taken with the shutter closed; each individual dark has the standard calibration corrections applied (`ATODCORR`, `BLEVCORR`, and `BIASCORR`).

Photometry keywords, which provide the conversion from calibrated counts (DN) to an astronomical magnitude, are computed by **calwp2** using the STSDAS package **synphot**. (More information on SYNPHOT can be found in the [Synphot User's Guide](#)) at:

[http://www.stsci.edu/resources/software\\_hardware/stsdas/synphot/SynphotManual.pdf](http://www.stsci.edu/resources/software_hardware/stsdas/synphot/SynphotManual.pdf).

The keyword switch for this step is DOPHOTOM, and the reference file keywords are GRAPHTAB and COMPTAB. Note that the science data (`c0m.fits`) pixel values are not changed as a result of performing the DOPHOTOM step; the data remain in units of DN (Data Number); **calwp2** only computes the photometric parameters and populates the appropriate header keywords.

The photometric keywords that are computed are listed in [Figure 3.3](#) below; the first two, DOPHOTOM and PHOTTAB, are global keywords in the raw and calibrated image headers (`d0m.fits` and `c0m.fits`). The last six keywords, PHOTMODE, PHOTFLAM, PHOTZPT, PHOTPLAM, PHOTBW, and ZP\_CORR are group header keywords that are only populated in calibrated image headers. (Use the IRAF tasks **imheader**, **hselect**, or **hedit** to view group keywords.) PHOTZPT is not the photometric zeropoint (in the ST magnitude system) as normally understood, but rather the zeropoint in the ST magnitude system to be used after conversion to FLAM units (see [Section 5.1](#)).

**Figure 3.3: Photometry keyword descriptions, taken from `ub080101m_c0m.fits[1]`**

|                   |           |                             |  |
|-------------------|-----------|-----------------------------|--|
| Header parameters | DOPHOTOM= | 'COMPLETE'                  | / Fill photometry keywords                     |
|                   | PHOTTAB = | 'ub080101m_c3t.fits'        | / name of the photometry calibration table     |
| Group parameters  | PHOTMODE= | 'WFPC2,1,A2D15,F1042M,,CAL' |  |
|                   | PHOTFLAM= | 3.943637E-16                | / Inverse Sensitivity                          |
|                   | PHOTZPT = | -21.1                       | / Zero point                                   |
|                   | PHOTPLAM= | 10220.96                    | / Pivot wavelength                             |
|                   | PHOTBW =  | 276.148                     | / RMS bandwidth of the filter                  |
|                   | ZP_CORR = | 0.0352478                   | / Delta magnitude correction for contamination |

**calwp2** constructs the PHOTMODE keyword value using the INSTRUMENT, DETECTOR, ATODGAIN, FILTNAM1, FILTNAM2, EXPSTART, and LRFWAVE header keyword values. A throughput table for that observing mode, as expressed by the PHOTMODE keyword value, is generated using individual SYNPHOT throughput tables for the instrument optics, detector, gain, time-dependent throughput changes, and filters. The mapping of the observation parameters to their respective SYNPHOT throughput files is done using throughput reference look-up tables specified by the GRAPHTAB and COMPTAB header keywords. **calwp2** writes the total throughput for the observing mode to a table with extension `c3m.fits`, then uses that throughput table to calculate values for calibrated image header photometric keywords such as PHOTFLAM and PHOTZPT.

The individual SYNPHOT throughput files used to determine total throughput for an observing mode (as specified by PHOTMODE) can be

obtained using the STSDAS **showfiles** task in the **synphot** package. Information about this and other tasks in the **synphot** package can be found in the [Synphot Users Guide](#), at:

[http://www.stsci.edu/resources/software\\_hardware/stsdas/synphot/SynphotManual.pdf](http://www.stsci.edu/resources/software_hardware/stsdas/synphot/SynphotManual.pdf).

The most recent SYNPHOT tables can be downloaded from CDBS, at <ftp://ftp.stsci.edu/cdb/comp/wfpc2>

Examples:

What are the observing parameters for WF2 in calibrated dataset ua3f0603m?

```
-->hsl ua3f0603m_c0m.fits[2]
$I,instrume,detector,atodgain,filtnam1,filtnam2 yes
ua3f0603m_c0m.fits[2]   WFPC2   2       7.0   F218W
```

What are the photometry keyword values for WF3 in calibrated image ua3f0603m?

```
-->hsl ua3f0603m_c0m.fits[3]
$I,photmode,photflam,photplam,photbw,photzpt,zp_corr yes
ua3f0603m_c0m.fits[3]  WFPC2,3,A2D7,F218W, ,CAL 1.069375E-15
2205.658              172.1904      -0.06953716      -21.1
```

## Histogram Creation

Header Switch: DOHISTOS

Header Keywords Updated: DOHISTOS

Reference File: none

**Note: this step is not performed in the standard pipeline, but users may use this feature during recalibration of their data.**

This step will create a multigroup image (c2h, c2d) with one group for each chip in the calibrated dataset. Each group contains a three-line image where the first row is a histogram of the raw data values, the second row is a histogram of the A/D corrected data, and the third row is a histogram of the final calibrated science data. This operation is controlled by setting the keyword DOHISTOS to PERFORM in the raw image; the default is to skip this step. *Note: If you really need this histogram image, you have to recalibrate your data with GEIS raw science images because **calwp2** does not work for the setting DOHISTOS=PERFORM with MEF raw science images.*

## Data Quality File Creation

By performing a “bitwise logical OR,” the **calwp2** software combines the raw data quality file (q0m.fits) with the static pixel mask (r0h, r0d) and the data quality files for bias, dark, and flat field reference files (b2h, b2d; b3h, b3d; b4h, b4d) in order to generate the calibrated science data quality file (c1m.fits). This step is always performed, even when calibration switch keywords are set to OMIT. A c1m.fits file

would still be generated, though it would not contain much useful information. The flag values used are defined in Table 3.3. By convention, DQF pixel values of zero (0) are designated as good pixels. The final calibrated data quality file (`c1m.fits`) may be examined, for example, using FITS image display software such as **SAOimage** and **ximtool**, and can be blinked with the calibrated science image to directly identify areas of bad and questionable pixels on the science image.

**Table 3.3: Data Quality File Flags**

| Flag Value | Description   |
|------------|---|
| 0          | Good pixel.   |
| 1          | Reed-Solomon decoding error. This pixel is part of a packet of data in which one or more pixels may have been corrupted during transmission.  |
| 2          | Calibration file defect—set if the pixel is flagged in any of the reference data quality files. This includes charge transfer traps identified in the static pixel mask file ( <code>r0h, r0d</code> ). |
| 4          | Permanent camera defect. Static defects are maintained in the CDBS database, used to flag problems such as blocked columns and dead pixels. (Not used.)   |
| 8          | A/D converter saturation. The actual signal is unrecoverable but known to exceed the A/D full-scale signal (4095). <sup>1</sup>   |
| 16         | Missing data. The pixel was lost during readout or transmission. (Not used.)  |
| 32         | Bad pixel that does not fall into any of the other categories.  |
| 128        | Permanent charge trap. (Not used.)  |
| 256        | Questionable pixel. A pixel lying above a charge trap which may be affected by the trap.  |
| 512        | Unrepaired warm pixel.  |
| 1024       | Repaired warm pixel.  |
| 2048       | Uncorrected bias level is less than 100 DN.   |

1. Calibrated saturated pixels may have values significantly lower than 4095 due to bias subtraction and flat-fielding. In general, data values above 3500 DN are likely saturated.



*There are history records at the bottom of calibrated image headers. For MEF files, the HISTORY keyword can be read using the STSDAS task imheader on the group zero header (i.e., `c0m.fits[0]`) where all global keywords are stored. For GEIS-calibrated images, the HISTORY keywords can be read by paging through the ASCII header file (`.c0h`) or using imheader with any of the groups (i.e., `.c0h[3]`). HISTORY records are also available in the GEIS calibration reference file headers; these history comments contain important information about the reference files used to calibrate the data.*

Example of how to view the HISTORY values for calibrated image ua3f0603m.

```
-->imhead ua3f0603m_c0m.fits[0] long+ | match HISTORY
HISTORY MASKFILE=uref$f8213081u.r0h MASKCORR=COMPLETED
HISTORY PEDIGREE=INFLIGHT 01/01/1994 - 15/05/1995
HISTORY DESCRIP=STATIC MASK - INCLUDES CHARGE TRANSFER TRAPS
HISTORY WF4TFILE=uref$s8q14446u.r7h WF4TCORR=COMPLETED
HISTORY PEDIGREE=INFLIGHT 09/01/2002 10/03/2008
HISTORY DESCRIP=Corrects reduction in temperature dependent gain for WF4.
HISTORY BIASFILE=uref$r6c1454eu.r2h BIASCORR=COMPLETED
HISTORY PEDIGREE=INFLIGHT 21/02/06 - 14/05/2007
HISTORY DESCRIP=Feb 2006-May 2007 yearly superbias
HISTORY DARKFILE=uref$s931030su.r3h DARKCORR=COMPLETED
HISTORY PEDIGREE=INFLIGHT 24/12/2007
HISTORY DESCRIP=Pipeline dark: 120 frame superdark with hotpixels from
HISTORY 24/12/2007
HISTORY FLATFILE=uref$s9n15363u.r4h FLATCORR=COMPLETED
HISTORY PEDIGREE=INFLIGHT 01/01/1994 - 01/03/1994
HISTORY DESCRIP=Thermal vac data + onorbit OTA illumination pattern (cycle 4
HISTORY data)
HISTORY PC1: bias jump level ~0.114 DN.
HISTORY The following throughput tables were used:
HISTORY crotacomp$hst_ota_007_syn.fits, crwfpc2comp$wfpc2_optics_006_syn.fits,
HISTORY crwfpc2comp$wfpc2_f218w_006_syn.fits,
HISTORY crwfpc2comp$wfpc2_dqepc1_005_syn.fits,
HISTORY crwfpc2comp$wfpc2_a2d7pc1_004_syn.fits,
HISTORY crwfpc2comp$wfpc2_flatpc1_003_syn.fits
HISTORY WF2: bias jump level ~0.095 DN.
HISTORY The following throughput tables were used:
HISTORY crotacomp$hst_ota_007_syn.fits, crwfpc2comp$wfpc2_optics_006_syn.fits,
HISTORY crwfpc2comp$wfpc2_f218w_006_syn.fits,
HISTORY crwfpc2comp$wfpc2_dqewfc2_005_syn.fits,
HISTORY crwfpc2comp$wfpc2_a2d7wf2_004_syn.fits,
HISTORY crwfpc2comp$wfpc2_flatwf2_003_syn.fits
HISTORY The following throughput tables were used:
HISTORY crotacomp$hst_ota_007_syn.fits, crwfpc2comp$wfpc2_optics_006_syn.fits,
HISTORY crwfpc2comp$wfpc2_f218w_006_syn.fits,
HISTORY crwfpc2comp$wfpc2_dqewfc3_005_syn.fits,
HISTORY crwfpc2comp$wfpc2_a2d7wf3_004_syn.fits,
HISTORY crwfpc2comp$wfpc2_flatwf3_003_syn.fits
HISTORY WF4: bias jump level ~0.129 DN.
HISTORY The following throughput tables were used:
HISTORY crotacomp$hst_ota_007_syn.fits, crwfpc2comp$wfpc2_optics_006_syn.fits,
HISTORY crwfpc2comp$wfpc2_f218w_006_syn.fits,
HISTORY crwfpc2comp$wfpc2_dqewfc4_005_syn.fits,
HISTORY crwfpc2comp$wfpc2_a2d7wf4_004_syn.fits,
HISTORY crwfpc2comp$wfpc2_flatwf4_003_syn.fits
HISTORY WFPC2CTE version 1.2.4 (2-July-2008)
```

## 3.4 Post-calwp2 Processing

A number of new calibration routines were developed as part of the final close-out activities for WFPC2. Some were incorporated into **calwp2**, but the others were written as stand-alone Python routines. These routines are described below.

### 3.4.1 CTE Correction

Group Header Keywords Updated: CTE\_1E2, CTE\_1E3, CTE\_1E4

An internal Python routine (called “wfp2cte”) in the OPUS pipeline uses [Andrew Dolphin’s \(2004\) recipe](#), which is a function of star brightness, observation date, and background level, to estimate the charge-transfer losses (in units of delta magnitude) for a star at  $x = 400$ ,  $y = 400$  with intensities of  $100 e^-$ ,  $1000 e^-$ , and  $10,000 e^-$ . The program only populates these header keywords. It makes no changes to image pixel values.

Note that “wfp2cte” calculates its own background values, which are recorded in the trailer files distributed with each dataset. It does not read the BACKGRND keywords from the image headers. (This task is not available in STSDAS.)

### 3.4.2 PyDrizzle

Header Switch: DRIZCORR

Header Keywords Updated: various

Group Header Keywords Updated: various

Reference Files: OFFTAB, IDCTAB, DGEOFILE (off.fits, idc.fits, dxy.fits)

The pipeline uses PyDrizzle to construct a quick-look mosaic of the images from all four detectors. The new files, labeled *\*drz.fits*, contain geometrically-corrected images with a plate scale of 0.1 arcsec / pixel. (If the exposure consists of a single PC image, the native plate scale of the PC1, 0".045 is used.) **pydrizzle** is run on one WFPC2 exposure at a time (it should not be confused with **multidrizzle** which can combine several images at a time with sub-pixel sampling and cosmic-ray rejection.) The resulting *drz.fits* files, which are generated in the MEF format, are thus intended as quick-look images rather than as science data products.

The units for drizzled WFPC2 images retrieved from the Archive are counts per second (or DN per second). Note that all other WFPC2 image products, like the *c0m.fits* calibrated science data, are in units of counts, not countrate. (Always check the value of the *drz.fits* keyword BUNIT to verify the units.) Note that the keyword PHOTFLAM<sup>5</sup> in the *drz.fits* file is taken from the first extension (usually the PC1 chip) of the calibrated data file.

## 3.5 Recalibration

Calibrated data from the WFPC2 Static Archive have been processed using the best-available reference files and are ready for analysis. However, there may be occasions where a user may need calibrated data that's processed with non-default reference files or calibration switches; in these instances, the raw datasets can be recalibrated with the desired reference files and switches using the WFPC2 calibration task, **calwp2**.

### File formats for running calwp2

Users who wish to run **calwp2** using different reference files have the option of using either GEIS or MEF raw science images. The default data format for science images retrieved from the WFPC2 Static Archive is the Multi-extension FITS (MEF) format. If you prefer to use Generic Edited Information Set (GEIS) science images, you need to specifically request waiver FITS (wFITS) images from the Archive and convert them to GEIS using the STSDAS task **strfits**.

For users who have recalibrated GEIS format images in the past, there are no changes to the procedures. *But for recalibrating MEF format images, please note the slightly different steps outlined further down in this section.*

The recalibration examples in this section use the raw dataset `ub080101m`, in both GEIS and MEF formats.

This is the MEF format raw dataset for `ub080101m`:

```
ub080101m_d0m.fits
ub080101m_q0m.fits
ub080101m_q1m.fits
ub080101m_x0m.fits
```

This is the wFITS format raw dataset for `ub080101m`:

```
ub080101m_d0f.fits
ub080101m_q0f.fits
ub080101m_q1f.fits
ub080101m_x0f.fits
```

---

5. Due to a software bug, most `drz.fits` images from the WFPC2 Static Archive have the incorrect `PHOTFLAM` value. This should have little impact on users since `drz.fits` images are not meant for data analysis. Please see the [WFPC2 Web page](#) for additional details. The `PHOTFLAM` values in the calibrated headers, `c0m.fits`, are correct.

Those wFITS files need to be converted, using **strfits**, to the GEIS format for recalibration. Be sure to move the wFITS files to another location (“wfits\_dir” in the example below), so as to not confuse **calwp2**.

```
-->unlearn strfits
-->strfits *f.fits "" ""
-->ls *h *d
ub080102m.d0d  ub080102m.q0d  ub080102m.q1d  ub080102m.x0d
ub080102m.d0h  ub080102m.q0h  ub080102m.q1h  ub080102m.x0h
-->!mkdir wfits_dir
-->!mv *fits wfits_dir/
```

### Retrieve necessary files

In order to recalibrate a WFPC2 observation, you need to retrieve the raw dataset (`d0m.fits`, `q0m.fits`, `x0m.fits`, `q1m.fits`) as well as *all* the reference files and tables needed for calibration. An overview of retrieving data from the HST Archive is available in Chapter 1 of the [HST Data Handbook](#). We suggest that you make backup copies of the raw data files and the required reference files and tables to a subdirectory in your working directory. Before running **calwp2**, any calibrated files for the dataset you’re about to process should be removed from the working directory—**calwp2** does not overwrite pre-existing calibrated products and will therefore abort the calibration.

### Dealing with wFITS WFPC2 Reference Files

---

*For historical reasons, most WFPC2 reference files are only available from the Archive as wFITS files. Therefore, even if your science image data are in the MEF format, **calwp2** can only use GEIS format reference files.*

---



This is an example of how the reference files are specified in the science image header (excerpted from image `ub080101m_d0m.fits`).

```

                                / CALIBRATION REFERENCE FILES
MASKFILE= 'uref$f8213081u.r0h      ' / name of the input DQF of known bad pixels
ATODFILE= 'uref$dbu1405fu.r1h' / name of the A-to-D conversion file
WF4TFILE= 'uref$t721550cu.r7h' / name of the WF4 correction reference file
BLEVFILE= 'ucal$sub080101m.x0h      ' / Engineering file with extended register da
BLEVDFIL= 'ucal$sub080101m.q1h      ' / Engineering file DQF
BIASFILE= 'uref$t7d1506ou.r2h' / name of the bias frame reference file
BIASDFIL= 'uref$t7d1506ou.b2h' / name of the bias frame reference DQF
DARKFILE= 'uref$t6h10308u.r3h' / name of the dark reference file
DARKDFIL= 'uref$t6h10308u.b3h' / name of the dark reference DQF
FLATFILE= 'uref$m3c10041u.r4h' / name of the flat field reference file
FLATDFIL= 'uref$m3c10041u.b4h' / name of the flat field reference DQF
SHADFILE= 'uref$e371355eu.r5h' / name of the reference file for shutter sha
PHOTTAB = '                        ' / name of the photometry calibration table
GRAPHTAB= 'mtab$t2605492m_tmg.fits' / the HST graph table
COMPTAB = 'mtab$t6i1714pm_tmc.fits' / the HST components table
IDCTAB  = 'uref$sad1946fu_idc.fits' / Distortion correction table
OFFTAB  = 'uref$s9518396u_off.fits' / Drift correction table
DGEOFILE= 'uref$s8f1222cu_dxy.fits' / Distortion correction image

```

In that calibration reference file list, *filenames ending with \*h are only available from the Archive in the wFITS format, and need to be converted to the GEIS format using **strfits***. The GRAPHTAB, COMPTAB, IDCTAB, OFFTAB, and DGEOFILE reference files are STSDAS FITS tables, and do not require any conversions.

- Create a separate directory for your reference files (“ref/” in the example below). Convert all the wFITS reference file images (\*f.fits) that were retrieved from the Archive to the GEIS format using **strfits**. After that, move those wFITS reference files to a separate sub-directory (“ref/ref\_fits” in the example below); keeping them in the same directory as the GEIS reference files will just confuse **calwp2**, causing it to crash.) Use **strfits** to convert those reference files in wFITS format to GEIS format:

```

-->unlearn strfits
-->strfits *r?f.fits "" ""
-->strfits *b?f.fits "" ""
-->!mkdir ref
-->!mkdir ref/ref_fits
-->!mv *r?f.fits *b?f.fits ref/ref_fits/
-->!mv *r?h *r?d *fits ref/

```

- Reference files listed in the image header have a prefix, either `uref$`, `ucal$` or `mtab$`. These are IRAF pointers that tell **calwp2** where the files are located. For the purpose of this example, the refer-

ence files and tables from the previous step are located in `/user/myname/data/ref/`, so the pointers for `uref$` and `mtab$` are set as follows:

```
-->set uref = /user/myname/data/ref/
-->set mtab = /user/myname/data/ref/
```

The `ucal$` pointer is the prefix for the bias level reference file (`x0m.fits` or `.x0h`), which is the overscan image for that observation. It is also considered part of the raw image dataset, and has the same rootname as the raw image. Therefore, the pointer for `ucal$` should be directed to the working directory where the raw science dataset is located, in this example,

```
-->set ucal = /user/myname/data/
```

### Making Changes to Calibration Switches or Reference Files

If you're recalibrating the raw science data using different reference files and/or calibration switches, the relevant keywords have to be changed in the raw image header. For the purpose of the example below, a different dark reference file is being used, and the shutter shading correction step is being turned off:

- the `DARKFILE` keyword value will be changed from `uref$t6h10308u.r3h` to `uref$t6p1135gu.r3h`
- Its data quality file, specified in `DARKDFIL` will be changed from `uref$t6h10308u.b3h` to `uref$t6p1135gu.b3h`.
- The shutter shading correction switch, specified by `SHADCORR` will be changed from `PERFORM` to `OMIT`.

#### *For MEF format raw science datasets:*

The IRAF task **hedit** can be used to change the header reference file and calibration switch keyword values in the raw science image. Since these are global keywords, the change can be made in group 0 of the image file.

```
-->unlearn hedit
-->hedit ub080101m_d0m.fits[0] DARKFILE uref$t6p1135gu.r3h verify=no
-->hedit ub080101m_d0m.fits[0] DARKDFIL uref$t6p1135gu.b3h verify=no
-->hedit ub080101m_d0m.fits[0] SHADCORR OMIT verify=no
```

*For GEIS format raw science datasets:*

**hedit** is unable to properly change header keywords for GEIS format images. Therefore, another task, called **chcalpar**, is used.

```
-->unlearn chcalpar
-->chcalpar ub080101m.d0h
```

This command, when run in **pyraf**, opens a GUI interface for editing the keyword values (you can adjust the size of the window by dragging on the lower right corner). Enter the new names for the dark reference file and its data quality file in their respective header keyword fields, **DARKFILE** and **DARKDFIL**, respectively, then change the **SHADCORR** switch from **PERFORM** to **OMIT**. When you're done, click on the "Save & Quit" button. The GUI screen reappears, but this time, it's blank except for the changes you just made. After verifying that the entries are correct, click on "Save & Quit" again, then confirm your actions at the prompt in your **pyraf** working window. (**chcalpar** can be run using a wildcard in the image name field [e.g., `chcalpar u*.d0h`] as long as the same keywords are being updated with the same values.)

## Running calwp2

*For GEIS format raw science datasets:*

The **calwp2** command is run as follows:

```
-->unlearn calwp2
-->calwp2 ub080101m ""
```

The resulting calibrated files are:

```
ub080102m.c0d  ub080102m.c1d  ub080102m.c3t
ub080102m.c0h  ub080102m.c1h  ub080102m.cgr
```

*For MEF format raw science datasets:*

**Please note these special instructions for recalibrating MEF format datasets.**

Before **calwp2** is run on MEF format files, which have the suffix "m.fits," the files need to be renamed. For historical reasons, **calwp2** is only able to recognize FITS files with the suffix "f.fits." Therefore, the raw MEF format dataset has to be temporarily renamed from "m.fits" to

“f.fits.” After making a backup copy of the original raw data, rename the files, then run **calwp2**:

```
-->!mv ub080101m_d0m.fits ub080101m_d0f.fits
-->!mv ub080101m_q0m.fits ub080101m_q0f.fits
-->!mv ub080101m_x0m.fits ub080101m_x0f.fits
-->!mv ub080101m_q1m.fits ub080101m_q1f.fits
-->unlearn calwp2
-->calwp2 ub080101m ""
```

For MEF format input files that were renamed to change the suffix from “m.fits” to “f.fits,” the calibrated files produced by **calwp2** are:

```
ub080102m.cgr          ub080102m_c1f.fits
ub080102m_c0f.fits    ub080102m_c3t.fits
```

To maintain the naming convention for MEF format files (and to avoid confusion!), rename those “\*f.fits” image files back to “\*m.fits.”

```
-->!mv ub080101m_c0f.fits ub080101m_c0m.fits
-->!mv ub080101m_c1f.fits ub080101m_c1m.fits
-->!mv ub080101m_x0f.fits ub080101m_x0m.fits
-->!mv ub080101m_q1f.fits ub080101m_q1m.fits
-->!mv ub080101m_c3t.fits ub080101m_c3m.fits
-->!mv ub080101m_d0f.fits ub080101m_d0m.fits
-->!mv ub080101m_q0f.fits ub080101m_q0m.fits
```

### Determining the absolute sensitivity for WFPC2

If the keyword switch `DOPHOTOM = PERFORM` is specified in the raw image header before running **calwp2**, the following keyword values are written to the calibrated image header:

- PHOTFLAM, inverse sensitivity
- PHOTPLAM, pivot wavelength
- PHOTBW, RMS bandwidth
- PHOTZPT, zeropoint
- PHOTMODE, observation mode
- ZP\_CORR, time dependent sensitivity correction

Remember that the `DOPHOTOM` calibration step does not alter the values of image data (which are always in units of counts or data numbers [DN] in the calibrated file), but only writes the information necessary to convert counts to flux units in the image header file.

The absolute sensitivity can also be determined using `SYNPHOT`. Additional information about this can be found in [Section 3.4.4 of HST Data Handbook, version 7](#), as well as the [SYNPHOT Users Guide](#).

For example, to calculate the absolute sensitivity for an observation taken in the PC1, at gain=7, in F658N, use the **synphot** task **bandpar**:

```
-->bandpar WFPC2,1,A2D7,F658N
```

|                    |            |            |          |
|--------------------|------------|------------|----------|
| # OBSMODE          | URESP      | PIVWV      | BANDW    |
| WFPC2,1,A2D7,F658N | 1.0356E-16 | 6590.8     | 29.383   |
| # OBSMODE          | FWHM       | WPEAK      | TPEAK    |
| WFPC2,1,A2D7,F658N | 69.191     | 6592.      | 0.016399 |
| # OBSMODE          | AVGWV      | QTLAM      | EQUVW    |
| WFPC2,1,A2D7,F658N | 6590.9     | 9.7613E-5  | 0.64335  |
| # OBSMODE          | RECTW      | EMFLX      | REFWAVE  |
| WFPC2,1,A2D7,F658N | 39.231     | 4.0638E-15 | 6590.9   |
| # OBSMODE          | TLAMBDA    |            |          |
| WFPC2,1,A2D7,F658N | 0.016395   |            |          |

According to the online help file for **bandpar** (which can be accessed by typing “help bandpar” in STSDAS), we find that the output parameter “URESP” is the same as PHOTFLAM since both are defined as “Flux (in FLAM) of a star that produces a response of one photon<sup>6</sup> per second in this passband.”

**calwp2** and **synphot** use a series of component lookup and throughput tables to calculate absolute sensitivity. These tables are not part of STSDAS itself but belong to the set of SYNPHOT data files which can easily be installed on your computer (see [Appendix A.5 of the HST Data Handbook, version 7](#) for further information). A more detailed discussion of photometric calibration can be found in [Section 5.2](#).




---

*The most recent SYNPHOT tables must be in place to recalculate absolute sensitivity for WFPC2 data using either calwp2 or tasks in the synphot package (see [Chapter 3 of the HST Data Handbook](#)).*

---

6. For WFPC2, substitute “photon” with “DN.”

## 3.6 Improving the Pipeline Calibration

The individual calibrated images produced by the standard pipeline processing are, in most respects, as good as our knowledge of the instrument can make them. The usefulness of post-pipeline calibration is, in general, limited to three areas:

- Improving the correction of pixels with elevated dark current, also known as warm pixels, which are known to vary with time. (Calibrated images retrieved from the Static Archive were processed with the best-available dark reference file; therefore, in most cases, running **warmpix** on them may be unnecessary.)
- Employing a correction flat field or alternate flat field.
- Removing cosmic rays by comparing multiple images of the same field.




---

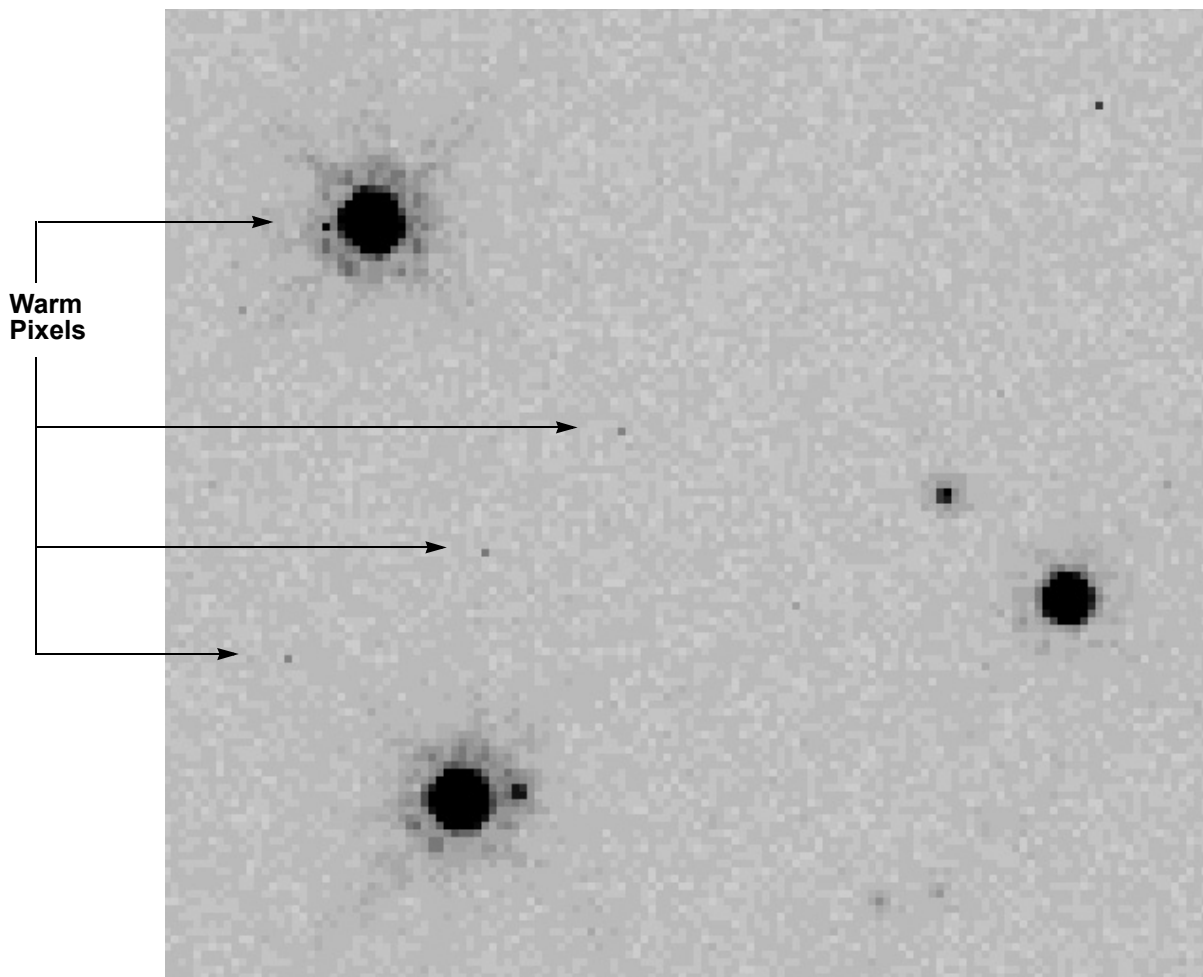
*The treatment of warm pixels and cosmic rays is quite different in the case of dithered data. This case is discussed in [Section 5.5](#); the present discussion refers to co-aligned data only.*

---

### 3.6.1 Warm Pixels

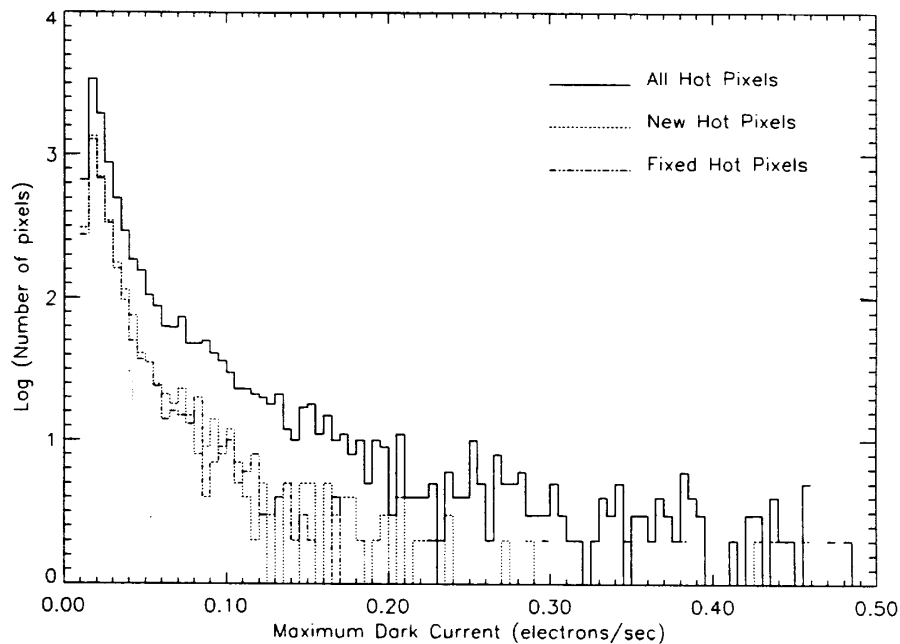
[Figure 3.4](#) shows a section of a stellar field in PC1 where cosmic rays were removed through comparison of successive images. Nonetheless, individual bright pixels remain clearly visible throughout the field.

These bright pixels are *warm (or hot)* pixels, i.e., pixels with an elevated dark current. The vast majority of WFPC2 pixels have a total dark current of about  $0.005 \text{ e}^-/\text{s}$  (including the *dark glow* discussed in [Section 4.3.2](#)). However, at any given time, there are a few thousand pixels in each CCD, called warm pixels, with a dark current greater than  $0.02 \text{ e}^-/\text{s}$ , up to several  $\text{e}^-/\text{s}$  in a few cases (see [Figure 3.5](#)). Some of these pixels are permanently warm but most other warm pixels become warm over time, probably as a consequence of on-orbit bombardment by heavy nuclei. The other CCD instruments aboard HST show similar behavior. For WFPC2, most warm pixels returned to normal after the CCDs were brought to  $+22^\circ\text{C}$  during WFPC2 decontaminations.

**Figure 3.4: PC Image of Stellar Field Showing Warm Pixels**

### Will Warm Pixels Hurt my Science?

The impact of warm pixels on the scientific results obtained from WFPC2 images depends on a number of factors: the exposure length, the number of objects, and the science goals. If the principal goal of the program is to acquire morphological information on well-resolved targets, warm pixels are usually not a serious concern since they are easily recognizable. If the goal is accurate photometry of point sources, the probability that uncorrected warm pixels will influence the measurement at a given level can be determined from the distribution of warm pixels shown in [Figure 3.5](#). In general, warm pixels are a concern in two cases: (1) accurate photometry of faint sources in crowded fields where some warm pixels can easily be confused with cores of faint sources, and (2) aperture photometry using very large apertures and/or of extended objects; warm pixels cause a positive tail in the count distribution that is not included in the background determination, but—depending on the software used—could be included in the integrated source flux, resulting in positively biased photometric measurements.

**Figure 3.5: Distribution of Dark Current for Warm Pixels**

### Repairing warm pixels

A decontamination (“decon” for short) is a procedure that increases the CCD operating temperature from  $-88^{\circ}\text{C}$  to  $+22^{\circ}\text{C}$  for 6 hours. This is done to dissipate accumulated contaminants that affect UV throughput and to repair most hot pixels. In the early years of WFPC2 operations, decons were done every 30 days but as the camera proved to be more stable, the decon interval was increased to 49 days.

Warm pixels, with dark current levels of  $0.02\text{ e}^{-}/\text{s}$  or higher, generally appear at a rate of about 30 pixels per detector per day. A decontamination procedure typically anneals about 80% of the new warm pixels that arise during the decon intervals. Of those pixels that are not fixed, about half are fixed after two or three additional decontamination procedures. After that, the rate of correction decreases. Longer decontaminations do not appear to improve the fraction of pixels fixed. For more detailed information, see the [WFPC2 Instrument Handbook](#).

Because of the time variability of warm pixels, the standard pipeline dark correction may not deal with them adequately. Even dark frames taken within a day of the observation will contain some warm pixels that vary significantly from those in the science observation. There are several ways to improve the correction for pixels which are known to be warm or which have varied near the time of the observations: flag the pixels in some way, use the STSDAS task **warmpix**, or generate a custom dark reference file and recalibrate manually. These methods will be outlined in the following sections.

### *Identifying and flagging warm pixels*

The first method to treat warm pixels is to identify and flag them. Depending on the software used, the flagged pixels can either be ignored (PSF fitting software generally allows this) or be interpolated from nearby pixels (for software that requires a valid value for all pixels, such as most aperture photometry tasks).

The identification of warm pixels can be accomplished by taking advantage of the fact that they are the only WFPC2 feature where most of the flux is concentrated in one pixel (followed by a faint tail along the y-axis due to CTE); both cosmic rays and photons from point sources involve more than one pixel. The IRAF task **cosmicrays**, written originally to remove single-pixel cosmic rays in ground-based data, has been used with some success to identify warm pixels in WFPC2 data. Identification of warm pixels is also possible using information from dark frames taken before and after the observations were executed, as described below.

### *Subtracting warm pixels via **warmpix***

Note: All calibrated images from the WFPC2 Static Archive were processed with the best available darks. *In most cases, running **warmpix** on your images will not yield significant improvements. This material on **warmpix** is provided primarily for historical purposes.*

The second option is to attempt subtraction of the warm pixel dark current that existed at the time of the observations. This has the advantage of retaining the measured signal from a source but adjusting the dark current to the value it used to be before the pixel became “warm.” WFPC2 takes about five 30 minute-long dark frames every week, thus information on warm pixels is available with a time resolution of about one week. The STSDAS task **warmpix** will flag and/or correct warm pixels in calibrated science data using warm pixel tables available at:

<http://www.stsci.edu/hst/wfpc2/analysis/warmpix.html>

These tables contains the locations and dark count rates for warm pixels that existed around the time of the science observation. Each table typically spans the time interval between decontamination procedures, with information derived from dark files taken at several epochs (roughly once per week) within that period. This procedure will generally fix 90% to 95% of the warm pixels found in typical user data, though there are some uncertainties in the results due to the intrinsic variability of warm pixels and the time span between darks.

The steps necessary to run **warmpix** are summarized below.

1. Obtain the relevant [warm pixel tables](#) from the Web. Each table name reflects its applicability dates; for example, the table named `vary_080313_080430_1.dat` applies to all PC1 observations between March 13, 2008 and April 30, 2008 (both are decon dates).




---

*These tables are stored in Unix-compressed format (e.g. vary\_080313\_080430\_1.dat.Z). On some systems, the retrieved table will not have the .Z extension, but they still need to be renamed to add the .Z extension and uncompressed by the Unix task `uncompress`. Please contact the Help Desk at [help@stsci.edu](mailto:help@stsci.edu) if you have a non-Unix system or if you encounter difficulties in retrieving the tables.*

---

2. Retrieve the calibration reference files used for dark subtraction and flat-fielding from the Archive. The filenames are recorded in the science header keywords `DARKFILE` and `FLATFILE`, respectively.
3. Redefine the IRAF variable `uref$` to point to the directory where those dark and flat field files are stored. This step is required for **warmpix** to undo the dark current subtraction performed in the pipeline and substitute its own. If **warmpix** cannot find these reference files, it will not be able to correct the dark current subtraction and will flag all pixels as being uncorrectable.
4. Run **warmpix** to correct and/or flag warm pixels. There are a number of user-adjustable parameters to decide which pixels should be fixed and which should be flagged as uncorrectable. Please see the online **warmpix** STSDAS help file for more details (type “`help warmpix`” in STSDAS.)

At the end of this process, pixels that exceed the user-defined thresholds will either be corrected for the dark current measured in the darks, linearly interpolated to the date of the observation, or flagged as uncorrectable. Specifically, if the pixel has a high or extremely variable dark count rate, **warmpix** will not change the pixel value in the science image but the data quality file will have its 10th least significant bit set to indicate that it is a “bad” or irreparable pixel (i.e. value of 512, logically OR’ed with the other reference files’ data quality flags for that pixel). If the pixel has a moderate dark count rate, **warmpix** will fix the science image pixel: first, it will determine the new dark value by interpolating between dark values from epochs immediately before and after the observation. Then, the old dark value will be removed from the science image pixel, and the new dark value will be applied in its place. In addition, the science data quality file will have the value 1024 logically OR’ed with the flags from the other reference data quality files. Pixels with low dark count rates are not modified by **warmpix**.

The example below shows how the task **warmpix** is run on image `ub080105m_c0m.fits`.

First, obtain the names of the dark and flat-field reference files that were used to calibrate the image. (Be sure to keep a backup copy of the image in another directory because **warmpix** will change the image file.)

```
-->hssel ub080105m_c0m.fits[1] date-obs,darkfile,flatfile yes
2008-04-06      uref$t6h10308u.r3h      uref$m3c10041u.r4h
```

Retrieve the reference files and their data quality files, place them in a directory (e.g., /user/myname/data/ref/), then create an IRAF pointer to that directory.

```
-->set uref = /user/myname/data/ref/
```

Copy the warm pixel tables suitable for this observation from:

[http://www.stsci.edu/hst/wfpc2/analysis/wfpc2\\_hotpix.html#List](http://www.stsci.edu/hst/wfpc2/analysis/wfpc2_hotpix.html#List)

and uncompress them (on a unix machine, run the `uncompress` command). There is one warm pixel table per chip.

```
vary_080313_080430_1.dat      vary_080313_080430_3.dat
vary_080313_080430_2.dat      vary_080313_080430_4.dat
```

Run **warmpix** with the default values (more information about the threshold values for fixing warm pixels are available in the **warmpix** help file.)

```
-->unlearn warmpix
-->warmpix ub080105m_c0m.fits ub080105m_c1m.fits
vary_080313_080430_?.dat rej_thresh=0.1 fix_thresh=0.003
var_thresh=0.003
```




---

*Non-STSDAS tasks generally ignore the data quality files, and thus may not properly use the information indicating which pixels need to be rejected. Users should propagate this information using the appropriate method suited for their tasks.*

---

### *Generating a custom dark reference file using “daily darks”*

Between July 1997 and September 2004, calibration programs were run to obtain up to three dark frames every day, to allow for better warm pixel corrections. These darks, also referred to as “refer daily darks,” were relatively short (1000 seconds) so that they could fit into almost any occultation period, making automatic scheduling feasible. The scheduling

priority of the daily darks were low, taken only when there were no other requirements for the specific occultation period. Observers should be aware that only the standard (1800 seconds) darks, taken at the rate of five per week, were used in generating the pipeline darks, superdarks, and warm pixel tables. The daily darks were taken as an additional calibration resource for users that may find them useful, and are available from the Archive.

These daily darks should be used if very accurate identification of warm pixels is needed. Some observers have developed their own software to make use of daily darks to improve warm pixel correction. [WFPC2 ISR 01-01](#) and [Addendum 01-08](#)) document IRAF scripts that can be used as a guide for developing procedures to create a custom dark reference file for use in recalibrating science data.

### 3.6.2 Alternate Flat fields

#### *Correction Flat fields*

As of December 2001, the noise characteristics of the WF chips in the standard WFPC2 pipeline flat field reference files are such that the signal-to-noise achievable in the final calibrated science images is *not* limited by the flat field. However, all PC1 flat fields (and some WF flat fields in the UV) have less than ideal noise properties; improving these flat fields can improve the resulting signal-to-noise in the calibrated images.

A set of “correction” flat fields, designed to be applied after normal pipeline processing have been developed in order to help reduce the flat field noise. In particular, highly-exposed science images ( $> 20,000$  e<sup>-</sup>/pixel, that’s 2860 and 1335 DN/pixel for gains 7 and 15, respectively) will show significant noise reduction, especially in PC1, if the new correction flat fields are used. Science images in some of the UV filters will show significant improvement as well, even at lower exposure levels. The correction flats have been generated so that they merely need to be multiplied into the calibrated (including flat-fielded) science images. They can be retrieved from the [CDBS WFPC2 Reference Files](#) Web page, in the “Non-pipeline Reference Files” table. Please see [WFPC2 ISR 01-07](#) for the details and names of these correction flats, as well as some caveats regarding their application to science images.

#### **Flat-fielding Linear Ramp Filter Images**

During final reprocessing to populate the WFPC2 Static Archive, Linear Ramp Filter (LRF) images were flat-fielded using a narrow-band filter flat chosen to be close in wavelength range to the image’s LRF wavelength setting. Additional information about LRF data is available at:

[http://www.stsci.edu/hst/wfpc2/analysis/lrf\\_calibration.html](http://www.stsci.edu/hst/wfpc2/analysis/lrf_calibration.html)

For instance, the raw science image `u9w1010fm_d0m.fits` uses LRF filter `FR680N`, and has been assigned flat field reference file `m3c1004nu.r4h`. Using **hedit** to find out more about this reference file, we learn that it is a flat field (header keyword `FILETYPE=FLT`) for filter `F656N` (`FILTNAM1=F656N`). This flat field should be used for data taken after October 30, 1996 (`USEAFTER='Oct 30 1996 00:00:00'`), and the reference file description provides a brief description of the reference file (`DESCRIP='Improved Cyc6-9 flat, rms errors < 0.2-0.3% - see ISR 2002-02'`).

```
-->hsel u9w1010fm_d0m.fits[0]
$I,filtnam1,filtnam2,flatcorr,flatfile,flatdfile yes
u9w1010fm_d0m.fits[0]   FR680N           PERFORM
uref$m3c1004nu.r4h

-->hsel m3c1004nu.r4h[0]
filetype,filtnam1,pedigree,descrip yes
FLT   F656N   "INFLIGHT 30/10/1996 - 30/04/2001"
"Improved Cyc6-9 flat, rms errors < 0.2-0.3% - see ISR
2002-02"
```

*A note about LRF data retrieved from the OTFR Archive before its availability in the Static Archive:*

Prior to the WFPC2 Static Archive, calibrated LRF images from the Archive were, by design, not flat-fielded; the calibrated science headers and trailers would indicate that the flat field used was a “dummy” (i.e., 1’s everywhere) and that the correction was effectively skipped.

The initial justification for using dummy flats (values of 1) for LRF images was because pipeline flat fields were difficult to generate for the LRFs, primarily due to the lack of an accurate spectrum for the external and internal flat field light sources (i.e., observations of the bright Earth or images taken with the internal WFPC2 VISFLAT lamp). The color of the Earth varies considerably, depending upon the feature observed (land, sea, or clouds). The color of the internal VISFLAT lamp was known to vary as a function of the position in the field of view, the total lamp “on” time, and the total number of times the lamp had been cycled on and off.

Furthermore, since the linear ramp filters were far from the focal plane (the OTA beam has a diameter of approximately 33 arcseconds at the filter), any dust spots and other small imperfections in the filter had essentially no effect on the data. Any large-scale variations in the filter were contained in the filter transmission curves and were corrected during photometric calibration. Moreover, some of the ramps had pinholes and if LRF flats were to be made, they would have unnecessarily degraded the science data. Therefore, observers with LRF data had been advised to manually recalibrate their data using **calwp2** with a narrow band flat field reference file close in wavelength to their LRF science observation (the

wavelength of the image is recorded in the header keyword `LRFWAVE`). Since there were no narrow band filters near 8000 Å, the best alternative at those wavelengths was to use the F791W flat field reference file.

### 3.6.3 Removing Cosmic Rays from Co-aligned Images

WFPC2 images typically contain a large number of *cosmic ray* events which are caused by the interaction of galactic cosmic rays and protons from the Earth's radiation belt with the CCD. Hits occur at an average rate of about 1.8 events  $s^{-1}$  per CCD ( $1.2 s^{-1}cm^{-2}$ ), with an overall variation in rate of 60% (peak-to-peak) depending upon geomagnetic latitude and position with respect to the South Atlantic Anomaly (also see the [WFPC2 Instrument Handbook for Cycle 17, Section 4.10](#)).

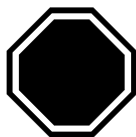
Unlike events seen on the ground, most WFPC2 cosmic ray events deposit a significant amount of charge in several pixels; the average number of pixels affected per strike is 6, with a peak signal of 1500  $e^{-}$  per pixel and a few tens of electrons per pixel at the edges. About 3% of the pixels, or 20,000 pixels per CCD, would be affected by cosmic rays in a long exposure (1800 seconds). [Figure 3.6](#) shows the impact of cosmic rays in an 800 second exposure with WFPC2. The area shown is about 1/16th of one chip (a 200 x 200 region); pixels affected by cosmic rays are shown in black and unaffected pixels are shown in white. A typical long WFPC2 exposure (2000 seconds) would have about 2.5 times as many pixels affected by cosmic rays.

Cosmic rays are noticeable even in short exposures. The WFPC2 electronics allowed instrument activities to be started at one-minute intervals. Therefore, a minimum-length exposure would collect at least one minute's worth (the interval between camera reset and readout) of cosmic rays, about a hundred strikes per CCD.

As a result of the undersampling of the WFPC2 PSF by the WF and PC1 pixels, it is sometimes difficult to differentiate stars from cosmic rays using a single exposure. If multiple co-aligned images are available, cosmic rays can be removed simply and reliably by comparing the flux in the same pixel in different images, assuming that any differences well above the noise are positive deviations due to cosmic rays. For exposures taken at the same pointing, STSDAS tasks such as `crrej` and `gcombine` can identify and correct WFPC2 image pixels affected by cosmic rays. (The task `crrej` is recommended.) If the images are shifted by an integral number of pixels, they can be realigned using a task such as `imshift` (one chip at a time) or `multidrizzle`.

Another consequence of the undersampling of WFPC2 pixels is that small pointing shifts will cause measurable differences between images at the same nominal pointing. These differences are especially noticeable in PC1 data, where offsets of only 10 mas can cause a difference between successive images of 10% or more near the edges of stellar PSFs. We

recommend that users allow for such differences by using the multiplicative noise term included in the noise model of the cosmic ray rejection task (**scalenoise** for **crrej** and **snoise** for **gcombine**). For typical pointing uncertainties, a multiplicative noise of 10% is adequate (note, this is specified as 10 for **crrej.scalenoise** and 0.1 for **gcombine.snoise**). It is also strongly recommended that an image mask be generated for each image, in order to determine if an undue concentration of cosmic rays are identified near point sources—usually an indication that the cores of point sources are mistaken for cosmic rays. Detailed explanations of the **crrej** and **gcombine** tasks can be found in their on-line help files in STSDAS.



---

*If your observation employed sub-pixel dithering, use the **multidrizzle** task in the **drizzle** package (see [Section 5.5](#)) to create combined images free of most cosmic rays and hot pixels.*

---

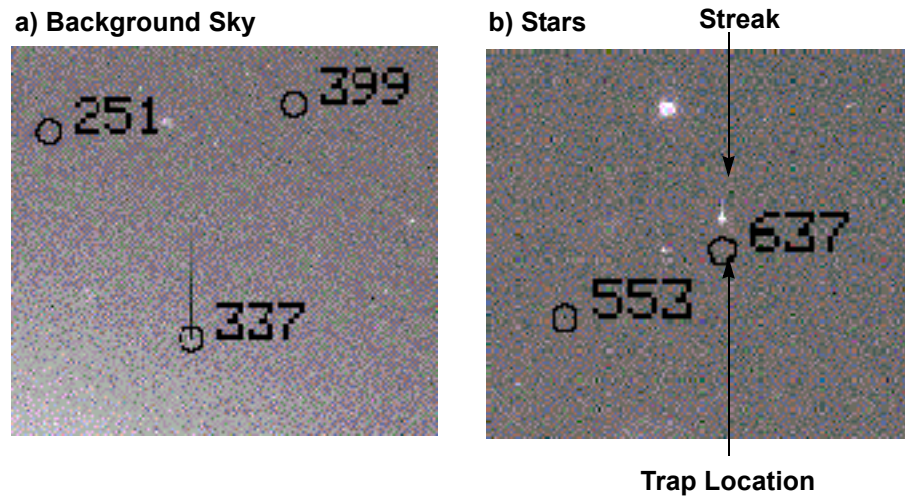
Cosmic rays are so numerous in WFPC2 data that double hits are not uncommon. For example, the combination of two 2000 second images will typically contain about 500 pixels per CCD that are affected by cosmic rays in both images; in most of these cases, the hit will be marginal in one of the two images. If the science goals require a high level of cosmic ray rejection, it is desirable to conduct a more stringent test in pixels adjacent to detected cosmic rays (see the task parameter **radius** in **crrej**).

**Figure 3.6: WF Exposure Showing Pixels Affected by Cosmic Rays**

### 3.6.4 Charge Traps

There are about 30 pixels in WFPC2 which do not transfer charge efficiently during readout, producing artifacts that are often quite noticeable. Typically, charge is delayed into successive pixels, producing a streak above the defective pixel. In the worst cases, the entire column above the pixel can be rendered useless. On blank sky, these traps will tend to produce a *dark* streak. However, when a bright object or cosmic ray is read through them, a bright streak will be produced. [Figure 3.7](#) shows examples of both effects. (Note that these “macroscopic” charge traps are different from the much smaller traps believed to be responsible for the charge transfer effect discussed in [Section 5.2.2](#).)

The images in [Figure 3.7](#) show streaks (a) in the background sky, and (b) stellar images produced by charge traps in the WFPC2. Individual traps have been cataloged and their identifying numbers are shown.

**Figure 3.7: Streaks in a) Background Sky, and b) Stars**

Bright tails have been measured on images taken both before and after the April 23, 1994 cool down and indicate that the behavior of the traps has been quite constant with time. Fortunately, there is no evidence for the formation of new traps since the ground system testing in May 1993. The charge delay in each of the traps is well characterized by a simple exponential decay which varies in strength and spatial scale from trap to trap.

The positions of the traps, as well as those of pixels immediately above the traps, are marked in the science data quality files (`c1m.fits`) with the flag value of 2, indicating a chip defect. Obviously, these pixels will be defective in images of sources with uniform surface brightness. However, after August 1995, the entire column above traps has been flagged with the value of 256, which indicates a “Questionable Pixel.” An object with sharp features (such as a star) will leave a trail should it fall on any of these pixels.

In cases where a bright streak is produced by a cosmic ray, standard cosmic ray removal techniques will usually remove both the streak and the cosmic ray. However, in cases where an object of interest has been affected, the user must be more careful. While standard techniques such as **wfixup** will interpolate across affected pixels and produce an acceptable cosmetic result, interpolation can bias both photometry and astrometry. In cases where accurate reconstruction of the true image is important, modelling of the charge transfer is required. For further information on charge traps, including the measured parameters of the larger traps, users should consult [WFPC2 ISR 95-03](#).



# WFPC2 Error Sources

In this chapter. . .

|  |
|--|
| 4.1 Bias Subtraction Errors / 65               |
| 4.2 Flat Field Correction Errors / 66          |
| 4.3 Dark Current Subtraction Errors / 69       |
| 4.4 Pointing Information in Image Headers / 72 |
| 4.5 WF4 Background Streaks / 74                |
| 4.6 Image Anomalies / 76                       |

---

## 4.1 Bias Subtraction Errors

*Note: all WFPC2 data retrieved from the HST Archive after May 16, 2001 are not affected by the bias subtraction errors discussed in this section.*

Very early in the WFPC2 mission (January 1994), it was discovered that the first few columns of the overscan region of the WFPC2 CCDs can be positively offset if a strong signal is present in the image itself. These columns were used for the bias level correction (BLEV CORR); the result was an oversubtraction of the bias level, which caused the sky background level in calibrated images to be incorrect. In a few cases, a significant part of the image had negative pixel values. The improvement was implemented in **calwp2** version 1.3.0.5 (March 1994) and was automatically performed on any image processed through On-The-Fly Reprocessing at the time.

Somewhat later in 1994, it was also realized that an improved bias level (BLEV CORR) subtraction could be obtained by using separate bias values for odd and even columns. WFPC2 data processed through the pipeline before May 4, 1994 used only a single average value for the bias level subtraction and as a result, a striated pattern with a typical amplitude of a few electrons (a fraction of a DN) remained. Observers working with versions of these images that were calibrated prior to May 1994 (e.g., from

data tapes) should therefore consider re-requesting these data from the Archive. Alternatively, the images could be reprocessed manually using **calwp2**, version 1.3.0.6 or later, unless the signal of the observation is so large that the noise statistics are dominated by Poisson noise. A detailed study of the on-orbit characteristics of bias frames, the overscan region, and superbias used in the pipeline can be found in [WFPC2 ISR 97-04](#).

---

## 4.2 Flat Field Correction Errors

This section summarizes the history of the WFPC2 flats field and the various versions that are available. Also included are some comments about point source photometry.

### 4.2.1 History of Flat Fields

While the flats were generally quite stable, some changes were noted in 1995 and 1996, and new versions were produced to correct these changes. There are also several special purpose versions for certain filters and situations. Note that the most recently-produced flat for a given filter will not necessarily be the optimum one.

One can easily determine which flat was used for a calibrated science image by inspecting the `FLATFILE` keyword in the headers, and by also checking that the `FLATCORR` keyword is set to `COMPLETED` (indicating the data were flat-fielded) as opposed to `SKIPPED` or `OMITTED`. Cursory information about the flat that was used can be found in the `PEDIGREE` and `DESCRIP` keywords which are copied from the flat to the calibrated data `HISTORY` records at the end of the image header. For example, the header for a calibrated image would contain a description like:

```
HISTORY  FLATFILE=uref$m3c10050u.r4h  FLATCORR=COMPLETED
HISTORY  PEDIGREE=INFLIGHT 30/10/1996 - 30/04/2001
HISTORY  DESCRIP=Improved Cyc6-9 flat, rms errors < 0.2-0.3% - see ISR 2002-02
```

Further information about a flat reference file can usually be found in the `HISTORY` records attached to the flat file's header (e.g., a full description of how it was made), or in reports referenced therein.

#### Pre-1995 Flat Fields

WFPC2 data processed during the first few months of the mission were calibrated using flat fields created from pre-launch ground test data, which did not take into account the large-scale structure of the flat field. These flats have rootnames<sup>1</sup> that begin with “d” or “e1” and if they have the

keyword, PEDIGREE (many predated the existence of this keyword), it has been set to GROUND. Flat fields installed in CDBS prior to launch were obtained purely from data taken during the pre-launch Thermal Vacuum test, and thus do not properly reflect the illumination function typical of the HST OTA; in this case, zonal errors of several percent can be encountered.

In March 1994, the WFPC2 IDT (Instrument Definition Team) delivered an updated set of flat fields. These flats have rootnames beginning with “e3” and are a combination of pre-launch calibration data and early on-orbit EARTH-CALIB images (observations of the bright Earth). These on-orbit images were flat-fielded with the pre-launch data, then stacked and smoothed so that a map of the OTA illumination pattern could be developed. This map, which included the chip-to-chip normalization, was then applied to the ground flat fields and the resulting flats installed in CDBS. Though they are a combination of ground and on-orbit data, the PEDIGREE of these early flat fields is also set to GROUND. The HISTORY comments at the bottom of the flat field reference files (.r4h) provide more details about how they were generated.

### Flat Fields Produced in Late 1995 and Early 1996

A completely new set of flat fields were delivered between late 1995 (for the filters used in [Hubble Deep Field](#) observations) and early 1996 (for the remaining filters). These flat fields are more accurate than the previous ones. The new flats, with rootnames beginning with “g” and having a PEDIGREE of “INFLIGHT,” are effectively the preflight ground data flat fields that include an improved on-orbit illumination pattern correction applied to scales larger than 7 pixels. In the optical (400 nm to 700 nm), the new flats differ from the old by 1% or less over the vast majority of the chip, with differences growing to about 8% at all wavelengths in the outer 50 pixels of the chip. Longward of 850 nm, differences of up to 1.5% are seen across the main body of the chips. Shortward of 300 nm, the differences between the old and new flat fields are less than 3%. As always, the HISTORY comments at the bottom of the flat field reference files (.r4h) provide more details on their creation.

### Flat Fields Produced in 2001 - 2002

In 2001 a major effort was made to study and update the flats ([WFPC2 ISR 02-02](#)). As a result of this study, it was recognized that large scale flat field gradients appeared across all the CCDs with amplitude about  $\pm 1\%$  during 1994 - 1996, after which the flats were relatively stable. In addition, several strong dust spots appeared in October 1996. To address these issues, new flats were generated for all filters (F300W and longwards) to

---

1. The rootname of a reference file is based on the year, date, and time that the file was delivered to the Calibration Data Base System (CDBS). The first character in the rootname denotes the year, in base 36, since 1980 (i.e., files installed in CDBS in 1993 start with “d”, those from 1994 start with “e”) while the second and third characters are the month and day, respectively, in base 36.

cover two time ranges: September 1995 through October 1996, and from November 1996 onwards. Flat field files for these two time periods begin with “m34” and “m3c,” respectively.

The new flats generally differ by less than 1% - 2% from the previous generation in terms of large-scale structure variations across the chips; However, the time-dependence is more pronounced for small-scale features and will allow these to be removed more effectively than with the old flats. In addition, the new flat fields offer improved pixel-to-pixel rms fluctuations of around 0.3% or less. The previous series of flats—the “g” series discussed in the previous section—remain appropriate for data taken before September 1995.

For most filters the “m3c” series of flats remain the optimum choice from November 1996 through the end of the WFPC2 mission in May 2009. While a detailed study has not been performed, cursory checks on the flats during this time indicate little or no change. A study by Bohlin, Mack, and Biretta (WFPC2 ISR 08-01) of two flats, the F606W and F814W flats, found that any low-frequency changes in the flat during this time were < 1%, though a new 10% feature was noted in the outermost corner of the WF4 CCD. The raw materials for producing improved flats for epochs late in the WFPC2 mission do exist (i.e., thousands of “EARTH-CALIB”<sup>2</sup> exposures) and could be used in the future to generate new flats.

## 4.2.2 Flat Fields for Special Observations and Special Purpose Filters

### Flat Fields for Special Observation Cases

Prior to the final reprocessing of the WFPC2 archive, in 2008 and 2009, numerous flats were generated to cover a wide range of special cases. These have file names starting with the letters “s” or “t.” Some of these flats cover the period between the installation of WFPC2 in December 1993 and the CCD temperature reduction on April 24, 1994. While the “e” series IDT flats had previously been used for these epochs, we found that the “g” series gave better results (even though they were derived at a different temperature). Therefore, these “g” series flats were copied into a new series covering the earlier time period. Other flats created during this time are for AREA mode data (i.e., data binned 2 x 2) and are usually re-binned copies of the appropriate FULL mode (unbinned) flat. Still others cover situations where pairs of filters were crossed (i.e., F122M x F130LP or F555W x F606W). These cross-filter flats are not derived from cross-filter data, but instead are single filter flats that are chosen as a best approximation, and then copied and re-labeled for use with

---

2. Calibration target designation for the bright Earth; observations are used for creating flat fields.

that filter pair. The intent here was to provide at least some level of flat-fielding for all the data in the WFPC2 Static Archive, even if high-accuracy flats were not available for all situations. Further details of the flat fields can be found in the PEDIGREE, DESCRIP, and HISTORY keywords attached to each flat header.

### Flat Fields for Special Purpose Filters

Flat fields for infrequently-used filters, such as the polarizers, have generally been available since late 1996 and have rootnames beginning with “g.” Other filters, such as the Woods filter (F160BW) and some of the other UV filters, have flat fields with significant noise and other errors; in these cases, the application of a post-pipeline correction flat can provide significant improvement (see [Section 3.6.2](#) and [WFPC2 ISR 01-07](#)). Finally, note that the linear ramp filters do not have exact flats available, but instead have been flattened using the flat for a normal narrow band filter at a nearby wavelength (see [Flat-fielding Linear Ramp Filter Images](#)). The [WFPC2 Reference File](#) web page can be used to peruse the available flat fields.

## 4.2.3 The Effect of WFPC2 Flat Fields on Point Source Photometry

WFPC2 flat fields are defined such that a source of uniform brightness produces the same count rate per pixel across the image. However, due to geometric distortion of the image by the optics, the area of WFPC2 pixels on the sky depends on the location on the chip; the total variation across the chip is a few percent, with the largest changes occurring deep in the CCD corners. Therefore, the photometry of point sources is slightly corrupted by the standard flattening procedure. This effect and its correction, as well as the effect of the 34th row defect on photometry and astrometry of point sources, are discussed in [Section 5.2.2](#).

---

## 4.3 Dark Current Subtraction Errors

### 4.3.1 Electronic Dark Current

At the operating temperature of  $-88^{\circ}\text{C}$ , maintained after April 23, 1994, the WFPC2 CCDs have a low dark background, ranging between 0.002 and  $0.01\text{ e}^{-}/\text{s}/\text{pixel}$ . A relatively small number of pixels have dark currents many times this value. These *warm pixels* are discussed in great detail in [Section 3.6.1](#).

To remove the dark current, the standard pipeline procedure takes a dark reference file (which contains the average dark background in DN/s), multiplies it by the “dark time” (determined by the header keyword `DARKTIME`), and subtracts this from the bias subtracted image. Prior to April 23, 1994, the CCDs were operated at  $-76^{\circ}\text{C}$ . The correction procedure is the same for these early data, but the average dark current was about an order of magnitude larger due to the higher temperature. Hence, the dark current correction is both more important and less accurate for these images than for later data.

The dark time is usually close to the exposure time, but it can exceed the latter substantially if the exposure was interrupted and the shutter closed temporarily, as in the case of a loss of lock. Such instances are rare; they are identified in the `EXPFLAG` header keyword and in the data quality comments for each observation. It is also indicated when the difference between the predicted exposure start (header keyword `PSTRTIME`<sup>3</sup>) and end (`PSTPTIME`<sup>3</sup>) times is greater than the total exposure time (header keyword `EXPTIME`); that is,  $\text{PSTPTIME} - \text{PSTRTIME} > \text{EXPTIME}$ . Also, the commanded exposure time in the header, `UEXPDUR`, will be different from the actual exposure time, `EXPTIME`.

The true dark time differs slightly from pixel to pixel because of the time elapsed between reset and readout (even after the first pixel is read out, the last pixel is still accumulating dark counts). To the extent that dark current is constant with time, this small differential is present both in the bias image and in the observation itself, and therefore is automatically corrected by the bias subtraction.

During WFPC2 operation, dark reference files were generated each week for use in pipeline calibrations of data taken that week. However, it usually took about two to four weeks for the dark reference files to be available. Therefore, data calibrated before those best dark reference files became available contained uncorrected warm pixels. (The primary difference between successive darks is in the location and value of warm pixels, and is most noticeable when comparing darks taken before and after a decontamination.) When the appropriate dark reference file became available, instead of having to recalibrate the image with that new dark file, users could make the necessary warm pixel corrections using the **warmpix** task, as outlined in [Section 3.6.1](#).

All science data in the WFPC2 Static Archive have been calibrated using the best possible reference files available for each dataset, including dark reference files that were created during the week of the observation. Therefore, it’s not necessary to run **warmpix** on any calibrated data from the Static Archive. In some cases, users may wish to create custom dark reference files for recalibrating their data; the procedure for doing it is described in [Section 3.6.1](#).

---

3. The predicted start and stop times are not accurate but the difference between them is accurate. Start times are based on predicted timelines that may slightly change during implementation.

Prior to August 1996, weekly dark reference files for tracking variable warm pixels were created from a small number of dark exposures, typically around ten, taken over a two week period. However, darks created that way can be a significant component of the total noise in deep images. Therefore, users working with observations totalling more than five orbits, taken before August 1996, may wish to recalibrate their data by creating their own custom “superdarks” which are generated from about 120 individual good quality dark exposures taken over a one or two year period. Two sample superdark calibration files, with rootnames `s1n1124cu` (created in 2007) and `t5i2039ku` (2008), are available from the Archive for use as a comparison with your own custom darks.

Since August 1996, weekly dark reference files had been produced by combining the relevant superdark with warm pixel information obtained from dark frames taken on a given week. A weekly dark reference file was created using the superdark value for all pixels that appeared normal in the weekly darks, that is, if the mean dark current pixel value in a set of weekly darks did not differ from the superdark pixel value by more than  $5\sigma$ , the superdark pixel value was adopted for the weekly dark reference file. Otherwise, the mean value of the weekly dark exposure was used in the weekly dark reference file. This compromise allowed for a timely tracking of warm pixels while maintaining the low noise properties of the superdark for stable pixels.

### 4.3.2 Dark Glow

While the electronic dark current was relatively stable between observations, a variable component was also seen; the intensity of this *dark glow* was correlated with the observed cosmic ray rate, and is believed to be due to luminescence in the  $\text{MgF}_2$  CCD windows from cosmic ray bombardment. As a result of the geometry of the windows, the dark glow was not constant across the chip, but showed a characteristic edge drop of about 50%. The dark glow was significantly stronger in the PC1, where it dominated the total dark background, and weakest in WF2. The average *total* signal at the center of each camera was  $0.006 \text{ e}^-/\text{s}$  in the PC1,  $0.004 \text{ e}^-/\text{s}$  in WF3 and WF4, and  $0.0025 \text{ e}^-/\text{s}$  in WF2; of this, the true dark current was approximately  $0.0015 \text{ e}^-/\text{s}$ . For more details, see the [WFPC2 Instrument Handbook \(v.10\), Section 4.8.1, Sources of Dark Current](#).

Because of the variability in the dark glow contribution, the standard dark correction may leave a slight curvature in the background. For the vast majority of observations, this is not a significant problem since the level of the error is very low (worst-case center-to-edge difference of  $2 \text{ e}^-/\text{pixel}$ ) and because it varies slowly across the chips. Some programs, however, may require a careful determination of the absolute background level; observers may wish to consider employing techniques developed by other groups (e.g., Bernstein et al., 2001) or contact the Help Desk ([help@stsci.edu](mailto:help@stsci.edu)).

## 4.4 Pointing Information in Image Headers

### Precision of Commanded Pointing

The commanded target position values in the header are located in several header keywords. The target position as specified in the Phase II proposal is contained in the global header keywords RA\_TARG and DEC\_TARG.

For each chip in each exposure, the RA and Dec of a reference pixel (CRPIX1, CRPIX2) is specified in the group keywords CRVAL1 and CRVAL2. If the observation was part of a dither set, CRVAL1 and CRVAL2 are the commanded positions that included the offset.

The observed pointing depends on several factors. Thermal variations in each orbit cause “breathing” that changes the Optical Telescope Assembly (OTA) and affects guide star tracking by the Fine Guidance Sensors (FGS). Many WFPC2 observations were taken with FINE LOCK using two FGSs, and in such cases, uncertainties were usually due to thermal variations and spacecraft jitter. Some observations taken with FINE LOCK on a single guide star (perhaps due to loss of lock in one FGS or specifically requested for very short exposures) could be affected by a roll drift,  $\sim 1 - 5$  mas/sec about the guide star.

Preliminary information about the pointing can be obtained by checking the FGSLOCK and EXPFLAG global keywords. FGSLOCK specifies the type of guiding used during the observation. The four possible values for WFPC2 are FINE, FINE/GYRO, GYRO, and UNKNOWN.

|           |   |
|-----------|---|
| FINE      | Fine lock on guide stars using two FGSs. This is the most accurate pointing option, within 0.2 to 1 arcsec.   |
| FINE/GYRO | Fine lock on a guide star using one FGS to control the pitch/yaw of the spacecraft while roll control is handled by the gyros. Absolute accuracies can range from 0.5 - 5 arcseconds, while error due to roll drift about the guide star would be $\sim 1 - 2$ mas/sec. |
| GYRO      | Rate gyro assembly controls the pitch, yaw, and roll of the spacecraft. This mode produces the least accurate absolute and relative pointing. Absolute pointing accuracy is about 2 - 50 arcsec and drift would be 1 - 5 mas/sec  |
| UNKNOWN   | Check the jitter files to find out what happened during the observation.  |

Additional information about these tracking modes can be found at:

[http://www.stsci.edu/hst/observatory/pointing/obslog/OL\\_7.html#HEADING55](http://www.stsci.edu/hst/observatory/pointing/obslog/OL_7.html#HEADING55)

The EXPFLAG keyword indicates whether or not the observation executed successfully, with values NORMAL and INTERRUPTED:

|             |   |
|-------------|---|
| NORMAL      | The observation completed as requested.   |
| INTERRUPTED | The observation was not completed; the reason for this is documented in the header keyword QUALITY. |

Additional information about pointing precision can be found in the [MultiDrizzle Handbook](#), Chapter 4; reproduced below is Table 4.1 from that chapter which provides typical pointing stability values for commonly-used observing scenarios in fine lock with both FGSs. Specific information for each observation can be found in its associated jitter files; details about this are available in the [HST Data Handbook, Appendix C: Observation Logs](#) and at:

[http://www.stsci.edu/hst/observatory/pointing/obslog/OL\\_1.html](http://www.stsci.edu/hst/observatory/pointing/obslog/OL_1.html)

**Table 4.1: Typical HST Pointing and Stability Characteristics.**

| Observing Scenario (with Fine lock on Two guide Stars)                | Type of Program   | Typical RMS Precision |
|---|---|-----------------------|
| Multiple exposures at same pointing within an orbit.                  | Small programs (no dithering).  | < 2 to 5 mas          |
| Offsets within an orbit (recommend < 1 arcsec).                       | Small programs (with dithering).  | ~2 to 5 mas           |
| Re-acquisition for contiguous orbits in the same visit.               | Medium-sized programs (e.g., < 5 orbits per target).                    | 5 to 20 mas           |
| Repeatability for different visits, same guide stars and same ORIENT. | Large/deep programs (e.g., > 5 orbits per target).                      | ~50 to 100 mas        |
| Pointing repeatability with different guide stars.                    | Not recommended unless unavoidable, e.g., due to scheduling constraints | 0.2 to 0.5 arcsec     |

*The paragraph below only pertains to data from the HST Archive retrieved prior to May 16, 2001:*

Improved knowledge of the detector plate scales and chip rotations, as well as changes in reference pixel locations, have resulted in periodic changes to the pointing parameters, especially early in the instrument's lifetime. These header parameters, which define the mapping between the pixel and world coordinate systems, can be updated using the STSDAS task **uchcoord**. The keywords affected include the reference pixel locations (CRPIX\*), the values of the world coordinate system at the reference location (CRVAL\*), the partial derivatives of the world coordinate system with respect to the pixel coordinates (CD\*), and the orientation of the chip (ORIENTAT). Prior to OTFR (which was released on May 16, 2001), observers requiring the most up-to-date pointing information in their science image headers ran **uchcoord** on their calibrated images. The new OTFR system, however, automatically calculates the best values for these parameters at the time the data are requested so there is no need to run **uchcoord** on freshly-processed OTFR data. OTFR data that have not been recently retrieved (i.e. have been sitting on disk or tape for some time) or pre-OTFR data may benefit from an update; any version of **uchcoord** may be used to update pre-OTFR data, but note that only the June 2001 or later version of **uchcoord** should be run on data processed through OTFR.

---

## 4.5 WF4 Background Streaks

Images obtained with the WF4 detector after March 2002 suffer from low or zero bias levels, faint horizontal streaks, and low photometry. These are manifestations of a temperature-dependent gain reduction that is thought to be caused by a failing amplifier in the WF4 signal processing electronics. These anomalies were more severe during temperature peaks caused by the WFPC2 Replacement Heaters ([WFPC2 ISR 2005-02](#)). Images taken during these episodes often show horizontal streaks in the background (See [Figure 4.1](#)) with the streak amplitude reaching as much as ~1 DN RMS for very low bias values (bias less than 200 DN).

The WF4 anomaly can be obvious, as in [Figure 4.1](#), or subtle, especially if the gain reduction is slight. If the uncorrected image bias is less than 300 DN, then OPUS<sup>4</sup> automatically writes the following warning to the QUALCOM1 keyword in the image file header: “WF4 anomaly. Gain error & streaks. Check keywords & documentation.”

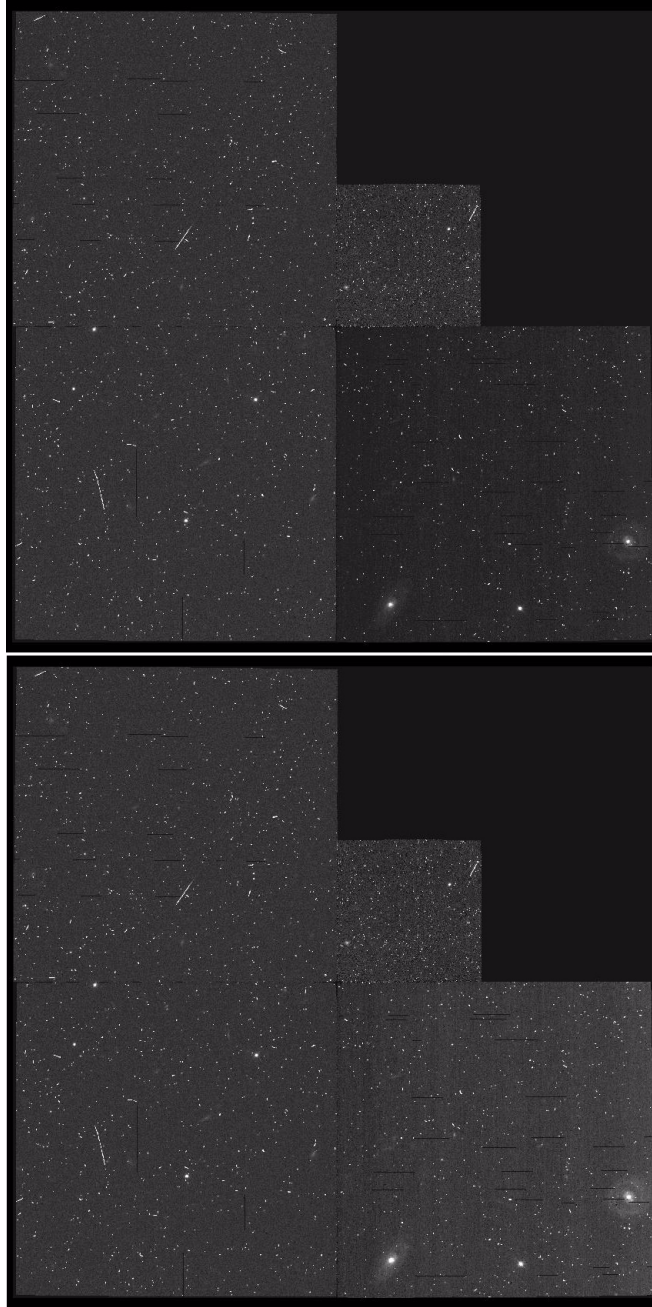
Calibrated WFPC2 images taken after 1 March 2002 and retrieved from the Static Archive are corrected for the WF4 anomaly. The algorithm rescales each pixel by a correction factor that depends on both the bias level of the entire image and the observed counts in the individual pixel. The old uncorrected values of BIASEVEN and BIASODD ([Section 3.3.2](#)) are stored in the header keywords BIASEVNU and BIASODDU. If BIASEVNU is less than 100, then all pixels in the data-quality array are flagged.

The faint horizontal streaks remaining after the WF4 anomaly correction can be removed with the task **wdestreak**. For more information please see Chapter 5, [WF4 Anomaly and Correcting Background Streaks](#) and [WFPC2 ISR 2008-03](#).

---

4. OPUS is the name of the software that controls the processing and archiving of data at STScI: converting telemetry into FITS data products, populating the Archive catalog, and performing housekeeping on the pipelines.

**Figure 4.1: Effect of the Pipeline WF4 Anomaly Correction on Calibrated Images**



Two versions of the calibrated image `u8zq0104m`, displayed at the same stretch, were mosaicked using `pydrizzle` to show the appearance of the WF4 chip in comparison to WF2 and WF3; the top image, processed in `calwp2` without the WF4 anomaly correction (header keyword switch `WF4TCORR=OMIT`), shows a considerably lower count rate in WF4 due to a lower bias level. The bottom image was calibrated with the WF4 bias anomaly correction (`WF4TCORR=COMPLETE`) and shows the WF4 image restored to a similar count level as the other chips. The "horizontal streaks" due to the WF4 anomaly are faintly visible as vertical streaks (due to image rotation). The calibration pipeline corrects the gain level of the WF4 CCD, but does not correct the faint streaks. The dark black lines in the image are blocked columns and unrelated to the WF4 anomaly.

## 4.6 Image Anomalies

In this section we present a number of features which occasionally affect WFPC2 data.

### 4.6.1 Bias Jumps

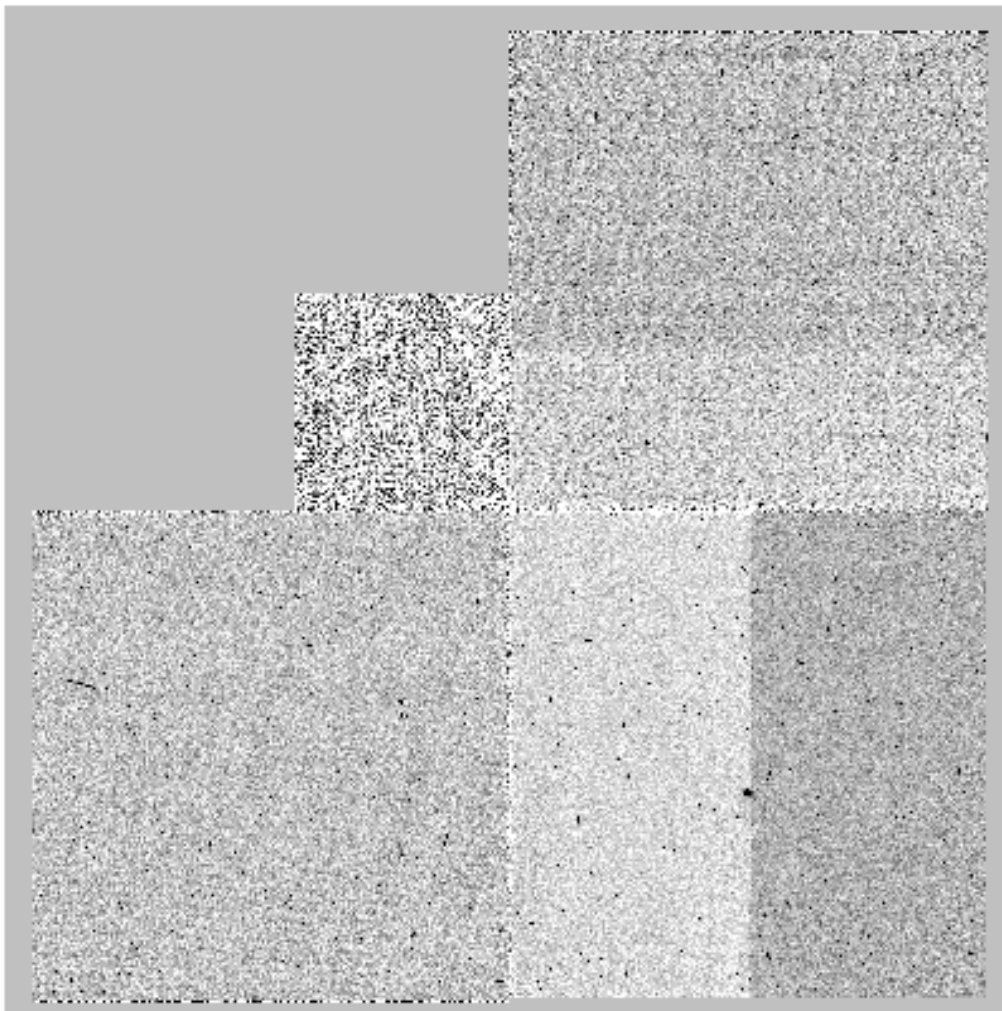
The average bias level for each image is obtained from the engineering data file (`x0m.fits`). However, WFPC2 is subject to *bias jumps*, changes in the bias level during the readout. Large bias jumps ( $> 0.5$  DN) are relatively rare, but small bias jumps, at the 0.1 DN level, affect about 15% of all images. [Figure 4.2](#) shows a very unusual event where the bias has jumped twice in the same image.

Bias jumps are fairly obvious from a cursory inspection of the image. Users are also alerted to their presence by comments in the HISTORY global keywords documented in group 0 of the calibrated image file (`c0m.fits[0]`) and trailer file (`tr1.fits`). Bias jumps are identified by an automatic procedure in **calwp2** that searches the overscan data for possible anomalies (for details see [WFPC2 ISR 97-04](#)) and only jumps larger than 0.09 DN are reported. Some bias jumps found by **calwp2** may be false positives caused by image features such as strongly saturated stars which affect the overscan data.

There is no standard procedure to remove bias jumps but it can be corrected by measuring the jump in the extracted engineering file (`x0m.fits`), or directly in the image provided the image is clean enough. Standard IRAF procedures such as **imexamine** or **imstat** are sufficient to obtain a good estimate of the offset. The offset can then be removed, for instance, using the STSDAS task **imcalc** as shown below:

```
im>imcalc image_in image_out "if (y.lt.YJUMP) then im1 else (im1 - BJUMP)"
```

where *YJUMP* is the line at which the jump occurs, and *BJUMP* is its amplitude.

**Figure 4.2: Bias Jump in Two Chips**

#### 4.6.2 Residual Images

Observations of relatively bright sources can leave behind a residual image. This residual is caused by two distinct effects.

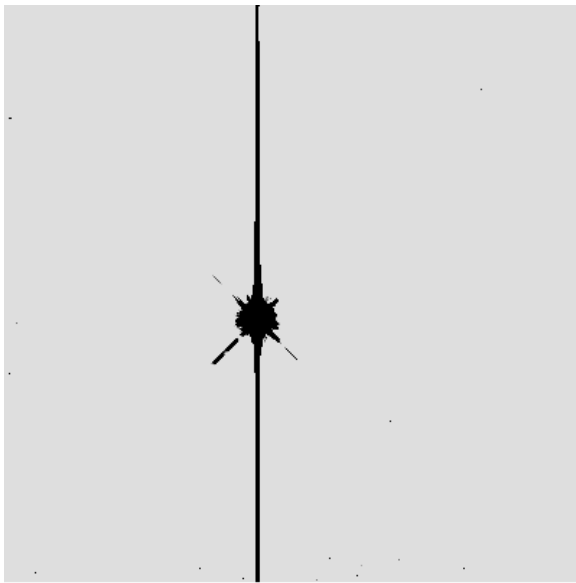
1. Charge in heavily saturated pixels is forced into deeper layers of the CCD, which are not normally cleared by readout. This charge slowly leaks back into the imaging layers and appears in subsequent images. The time scale for leakage back into the imaging region depends on the amount of over-exposure. Strongly saturated images can require several hours to clear completely.
2. Charge transfer inefficiencies also leave a residual image. At all exposure levels, some charge becomes bound temporarily to impurities in the silicon of the CCD. The effect is most noticeable in images with high exposure levels (high counts) probably because electrons

become exposed to more impurities as the wells are filled. This effect leaves behind some of the charge from bright regions of the image, the columns which first clocked out the charge to the readout register, and in the part of the chip from which the bright objects were read out.

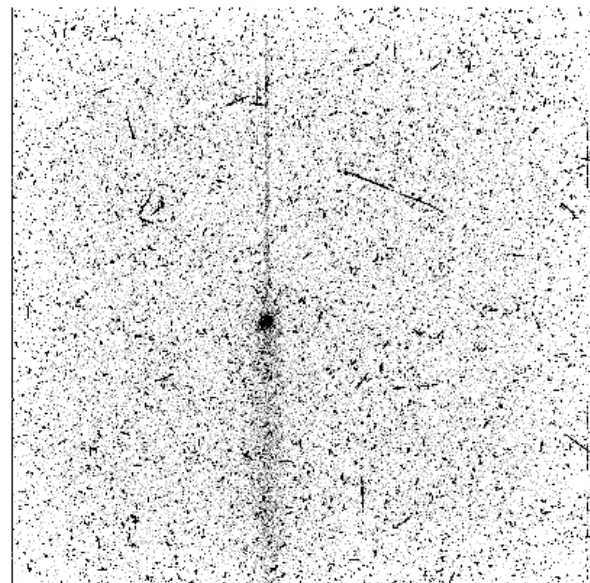
Figure 4.3(a) shows a saturated star on PC1. Figure 4.3(b) is an 1800 second dark calibration frame that was started six minutes later, showing residual charge from that saturated star released during the dark frame. Note that the residual image is bright not only where the star's PSF was overexposed (the first effect), but also in a wide swath below the star due to the second effect, and a narrower swath above the star due to bleeding during the exposure.

**Figure 4.3: Saturated Star and Residual Image**

a) Saturated Star on PC1



b) Residual Image on Dark Frame 6 Minutes Later



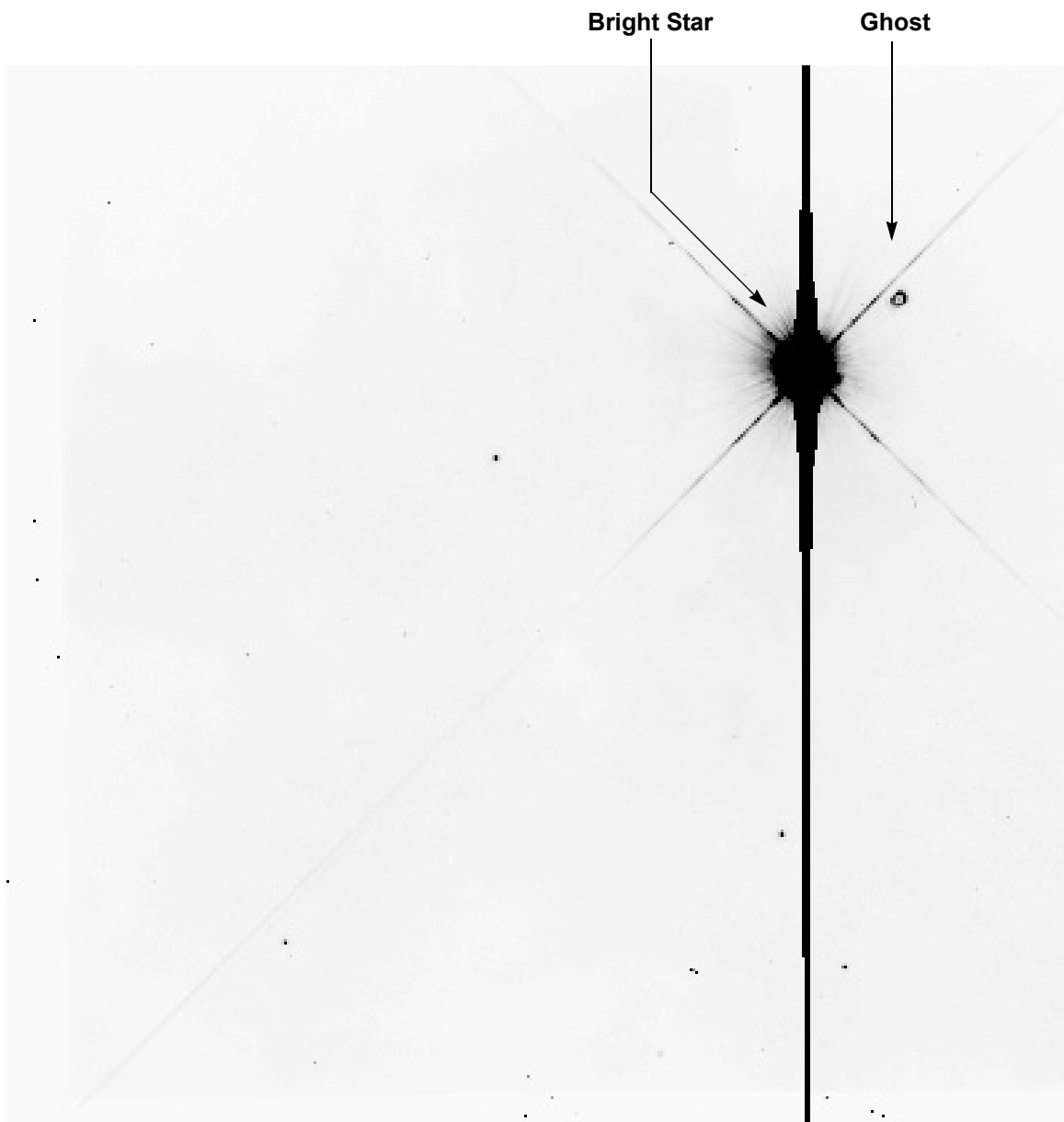
### Ghosts

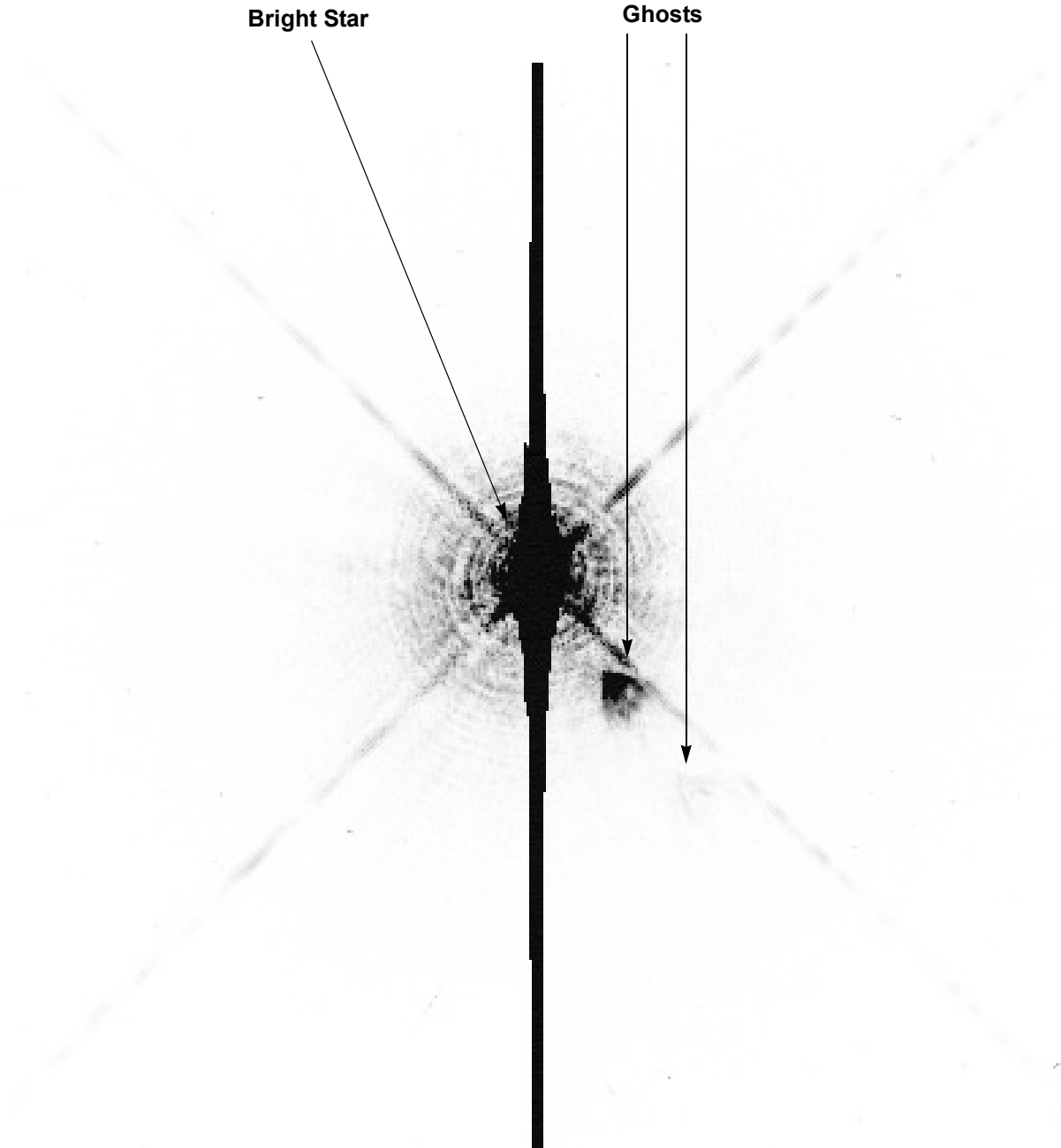
Ghost images may occur in exposures of bright objects due to internal reflections in the WFPC2 camera. The most common ghosts are caused by internal reflections in the  $\text{MgF}_2$  field flatteners. In these ghosts, the line connecting the ghost and the primary image passes through the optical center of the chip. The ghost always lies further away from the center than the primary image. Figure 4.4 gives an example of one of these ghosts.

Reflections on the internal surfaces of a filter may also result in ghost images. The position of these ghosts vary from filter to filter, and chip to chip. For any given filter-chip combination, the direction of the offset of

the ghost from the primary image will be constant, although the size of the offset may vary as a function of the position of the primary image. Filter ghosts can be easily recognized by their comatic (fan-shaped) structure. Particularly bright objects may produce multiple ghosts due to repeated internal reflections. [Figure 4.5](#) shows an example of filter ghosts.

**Figure 4.4: Field-Flattener Ghost in WF2—Image Shows Entire CCD**

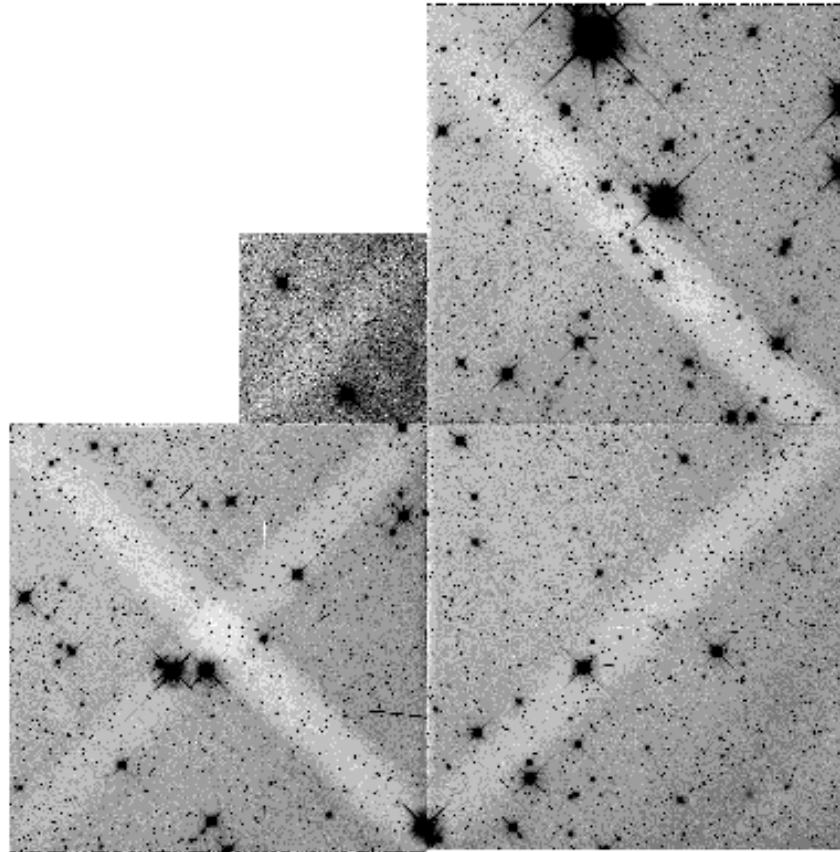


**Figure 4.5: Detail of Filter Ghosts on WF4****Earth Reflections**

Light from the bright sun-lit Earth is, on rare occasion, reflected off the Optical Telescope Assembly (OTA) baffles and secondary support structures into the WFPC2. These reflections occur when the bright Earth is less than  $\sim 40^\circ$  from the OTA axis. (The default bright Earth limb avoidance for science observations is  $20^\circ$ . Science observations are not scheduled at smaller limb angles to the sunlit Earth.) The scattered bright Earth light raises the overall background level of the field but vignetting by WFPC2 camera mirror supports can create either X-shaped or diagonal depressions against the background level. [Figure 4.6](#) shows a typical

example of the pattern formed by the scattered light; in this image, the background is about 100 electrons but in the darkest portion of the “X,” the counts are about 40 electrons below the average background level.

**Figure 4.6: Scattered Light Pattern (inverse image showing lower counts as bright areas)**



### 4.6.3 PC1 Stray Light

The WFPC2 was originally intended to contain two separate pyramids—one for four PC cameras and the other for four WF cameras. Budget reductions caused the PC pyramid to be abandoned and the first WF camera to be replaced by a PC camera. However, the pyramid mirror corresponding to the PC camera was not reduced in size. As a result, baffling for the PC1 chip is not optimal; a bright star falling just outside the PC1 field of view can produce an obvious artifact, typically shaped like a broad, segmented arc. A star bright enough to produce a total count rate of 1 DN/s on the chip will produce an arc with a count rate of about  $1 \times 10^{-7}$  DN/pixel/s over the affected region.

### 4.6.4 Other Anomalies

Other image anomalies, such as bright streaks from other spacecraft, scattered light from bright stars near the field of view, and missing image sections due to dropped data have occurred on rare occasion. These anomalies are documented in [WFPC2 ISR 95-06](#).



# WFPC2 Data Analysis

In this chapter. . .

|                                       |
|---------------------------------------|
| 5.1 Photometric Zeropoint / 83        |
| 5.2 Photometric Corrections / 92      |
| 5.3 Polarimetry / 125                 |
| 5.4 Astrometry / 127                  |
| 5.5 Drizzling WFPC2 Data / 140        |
| 5.6 Deconvolution of WFPC2 Data / 147 |
| 5.7 Accuracy of WFPC2 Results / 148   |

---

## 5.1 Photometric Zeropoint

The zeropoint of an instrument, by definition, is the magnitude of an object that produces one count (or data number, DN) per second. The magnitude of an arbitrary object producing DN counts in an observation of length EXPTIME is therefore:

$$m = -2.5 \times \log_{10}(\text{DN} / \text{EXPTIME}) + \text{ZEROPOINT}$$

It is the setting of the zeropoint that determines the connection between observed counts and a standard photometric system (such as Cousins RI), or between counts and astrophysically interesting measurement units such as the flux incident on the telescope.

### Zeropoints and Apertures

Historically, each zeropoint refers to a countrate measured in an infinite aperture. Since it's almost never practical to measure counts in a very large aperture, a definition of zeropoint linked to a smaller aperture is often more convenient.

*Holtzman et al. (1995b) published a list of zeropoints that refers to counts measured within a standard aperture of radius 0".5 for point source targets. The photometric calibrations defined by STScI and returned by*

*SYNPHOT* are for infinite apertures. In the case of WFPC2, the nominal infinite aperture is defined as having 1.096 times the flux in a 0".5 radius aperture. This is equivalent to setting the aperture correction between a 0".5 radius aperture and an infinite aperture to 0.1 magnitudes.

### 5.1.1 Photometric Systems Used for WFPC2 Data

There are several photometric systems commonly used for WFPC2 data, often causing some confusion about the interpretation of the photometric zeropoint used, and the subsequent photometry results. Before continuing with the discussion, it is worthwhile to define these photometric systems more precisely.

The WFPC2 filters do not have exact counterparts in any standard filter sets. For example, while F555W and F814W are reasonable approximations of Johnson V and Cousins I respectively, neither match is exact, and the differences can amount to 0.1 magnitudes, clearly significant in precise photometric work. Other commonly used filters, such as F336W and F606W, have much poorer matches in the Johnson-Cousins system. **We recommend that, whenever practical, WFPC2 photometric results be referred to a system based on its own filters.**

It is possible to define “photometric transformations” which convert WFPC2 photometry to another photometric system (see Holtzman et al. [1995b] for some examples). However, such transformations have limited precision, and depend on the color range, metallicity, and surface gravity of the stars considered; they can easily have errors of 0.2 magnitudes or more, depending on the filter and on how much the spectral energy distribution differs from that of the objects on which the transformation is defined, which happens frequently for galaxies at high redshift.

There are several photometric systems defined for WFPC2 observations. Two of them, the **WFPC2 Flight System**<sup>1</sup> and the **WFPC2 Synthetic System**<sup>1</sup>, have zeropoints tied to observed standards. A modified version of the WFPC2 Synthetic System was subsequently implemented in SYNPHOT as the **VEGAMAG**<sup>2</sup> System.

In recent years, it has become increasingly common to use photometric systems in which the zeropoint is defined directly in terms of a reference flux in physical units. The **STMAG system** is a flux-based system similar to the AB system. [Figure 5.1](#), taken from the SYNPHOT Users Manual, shows the relationship between Johnson V, STMAG, and AB MAG systems, superposed on the spectrum of Vega. Flux-based systems make the conversion of magnitudes to fluxes much simpler and cleaner, but have the side effect that any new determination of the absolute efficiency of the instrumental setup results in revised magnitudes. The choice between

1. Developed by the WFPC2 IDT and detailed in Holtzman et al.(1995b).

2. For additional details, see [WFPC2 ISR 96-04](#) and the SYNPHOT User’s Guide.

standard-based and flux-based systems is mostly a matter of personal preference.

Additional details about these systems are outlined below:

### 1. WFPC2 Flight System

This system is defined such that:

- stars of color zero in the Johnson-Cousins UBVRI system have color zero between any pair of WFPC2 standard photometric filters (F336W, F439W, F555W, F675W, F814W), and
- those stars have the same magnitude in V and F555W.

This system was established by Holtzman et al. (1995b) by observing two globular cluster fields ( $\omega$  Cen and NGC 6752) with HST and from the ground. The ground-based observations were taken with WFPC2 flight-spare filters and standard UBVRI filters. In practice, the system was defined by least-squares optimization of the transformation matrix. The observed stars near color zero were primarily white dwarfs, so the WFPC2 zeropoints defined in this system match the UBVRI zeropoints for stars with high surface gravity; the zeropoints for main sequence stars would differ by 0.02–0.05 magnitudes, depending on the filter

### 2. WFPC2 Synthetic System

These zeropoints were determined such that the magnitude of Vega, when observed through the WFPC2 photometric filter set in a 0".5 aperture radius, is identical to the magnitude of Vega in their counterpart Johnson-Cousins filters. For the filters in the WFPC2 photometric filter set, F336W, F439W, F555W, F675W, and F814W, these magnitudes are 0.02, 0.02, 0.03, 0.039, and 0.035, respectively. The calculations were done via synthetic photometry.

### 3. WFPC2 VEGAMAG System

This is a modified version of the WFPC2 synthetic system used in SYNPHOT. The zeropoints were defined by the magnitude of Vega being exactly zero in all filters and therefore differ from the synthetic zeropoints published by Holtzman et al. (1995b). VEGAMAG for a star of flux  $F$  is

$$\text{VEGAMAG} = -2.5 * \log_{10}(F/F_{\text{Vega}})$$

where  $F_{\text{Vega}}$  is the calibrated spectrum of Vega in SYNPHOT constructed from observed and synthetic spectra (Bohlin & Gilliland, 2004, AJ). SYNPHOT zeropoints refer to the nominal infinite aperture (and therefore differ from the WFPC2 Synthetic System zeropoints by  $\sim 0.1$  magnitudes).

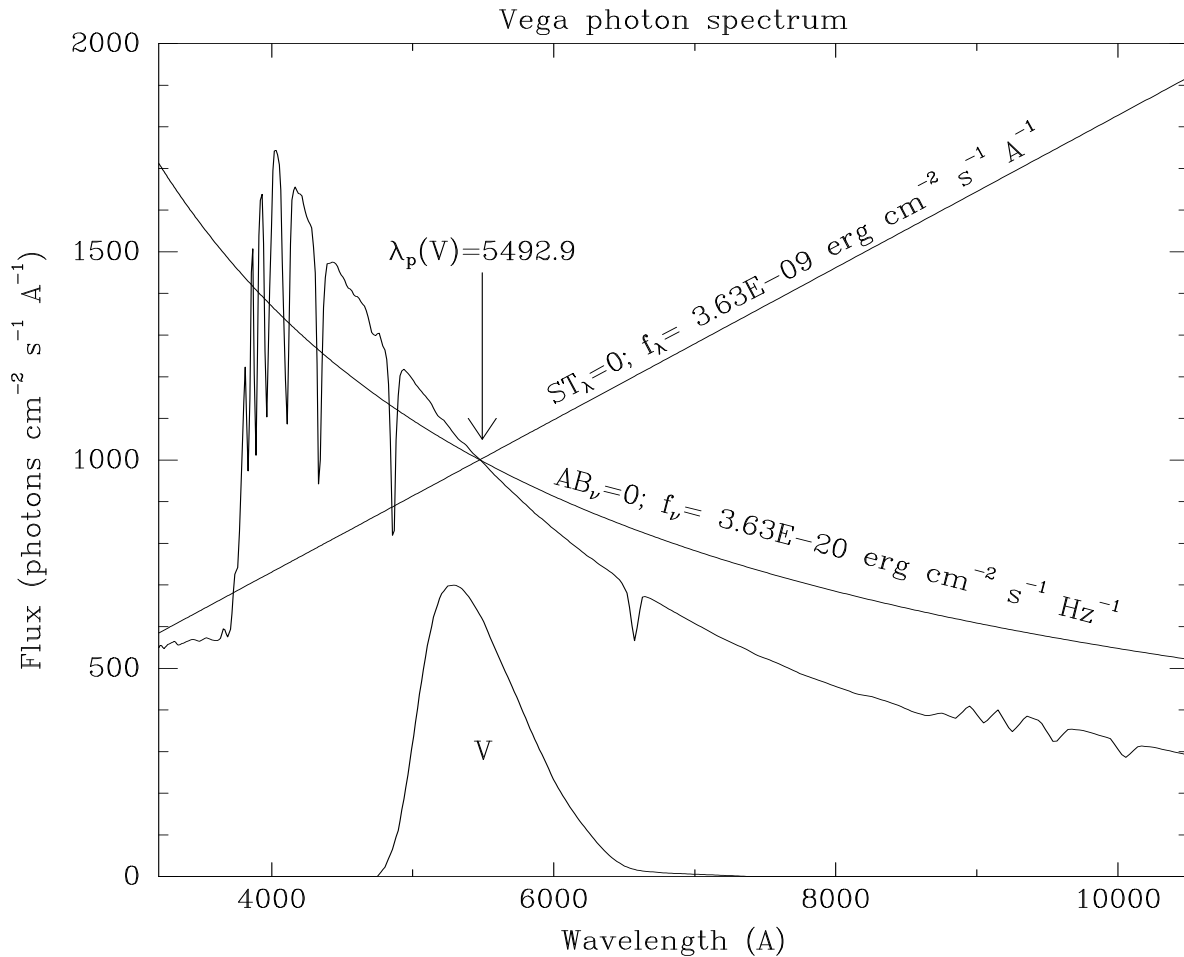
## 4. STMAG System

This system, along with the AB System (Oke 1974), are the most commonly-used flux-based systems at UV and visible wavelengths. The STMAG system is based on a spectrum with constant flux density per unit wavelength. The AB system is based on a spectrum with constant flux density per unit frequency. (In other words, the reference spectrum flux density,  $f_\lambda$ , and reference spectrum flux density,  $f_\nu$ , for the STMAG and AB systems, respectively, are flat.) Their zeropoint values, 21.10 and 48.6, respectively, are set such that the magnitude of Vega is close to zero in  $m_{AB}$ ,  $m_{ST}$ , and Johnson V. The magnitudes can be expressed as

$$m_{AB} = -48.60 - 2.5 \log f_\nu$$

$$m_{ST} = -21.10 - 2.5 \log f_\lambda$$

where  $f_\nu$  is expressed in  $\text{erg cm}^{-2} \text{s}^{-1} \text{Hz}^{-1}$ , and  $f_\lambda$  in  $\text{erg cm}^{-2} \text{s}^{-1} \text{\AA}^{-1}$ . Another way to express these zeropoints is to say that an object with  $f_\nu = 3.63 \times 10^{-20} \text{ erg cm}^{-2} \text{s}^{-1} \text{Hz}^{-1}$  will have  $m_{AB} = 0$  in every filter, and an object with  $f_\lambda = 3.63 \times 10^{-9} \text{ erg cm}^{-2} \text{s}^{-1} \text{\AA}^{-1}$  will have  $m_{ST} = 0$  in every filter. For more information, please refer to the [SYNPHOT User's Guide](#).

**Figure 5.1: Comparison of  $AB_V$  and  $ST_\lambda$  Systems**

**Standard photometric systems generally use the spectrum of Vega to define magnitude zero. The spectrophotometric magnitudes  $AB_V$  and  $ST_\lambda$  refer instead to spectra of constant  $f_\nu$  and  $f_\lambda$ , respectively. Magnitude zero in both systems is defined to be the mean flux density of Vega in the Johnson V passband. Thus all three of the spectra shown here produce the same count rate in the Johnson V passband. The pivot wavelength of Johnson V is defined to be the crossing point of the  $AB_V = 0$  and  $ST_\lambda = 0$  spectra. (Same as Figure 3.1 in the [SYNPHOT Users Guide, version 5](#)).**

### 5.1.2 Determining the Zeropoint

Several ways to determine the zeropoint, depending on the photometric system being used, are listed below. Note: adjustments to zeropoints, based on time-dependent UV contamination and QE changes are covered in [Section 5.2](#).

1. **Do it yourself:** over the operational life of WFPC2, a substantial amount of effort has gone into obtaining accurate zeropoints for all of the filters used. Nonetheless, if good ground-based photometry is available for objects in your WFPC2 field, it can be used to determine a zeropoint for these observations. This approach may be par-

ticularly useful in converting magnitudes to a standard photometric system, provided all targets have similar spectral energy distribution; in this case, the conversions are likely to be more reliable than those determined by Holtzman et al. (1995b), which are only valid for stars within a limited range of color, metallicity, and surface gravity.

2. **Use a summary list:** lists of zeropoints have been published<sup>3</sup> by Holtzman et al. (1995b), [WFPC2 ISR 96-04](#), and [WFPC2 ISR 97-10](#). **A list of zeropoints derived from observations done in the final years of WFPC2 operation may be posted to the WFPC2 Web site in the near future.** The Holtzman et al. (1995b) zeropoints essentially define the WFPC2 flight photometric system as discussed earlier; they are based on observations of  $\omega$  Cen and NGC 6752 for the five main broad band colors (i.e., F336W, F439W, F555W, F675W, F814W), as well as synthetic photometry for most other filters. Transformations from the WFPC2 filter set to UBVRI are included, although these should be used with caution, as stated above. Holtzman et al. (1995b) also includes a cookbook section describing in detail how to do photometry with WFPC2. Zeropoints in [WFPC2 ISRs 96-04, 97-10](#) and in [Table 5.1](#)<sup>3</sup> are based on the VEGAMAG system and do not include new conversions to UBVRI.
3. **Use the PHOTFLAM keyword in the header of your data:** the zeropoint of your data in the STMAG system can be determined using the PHOTFLAM keyword in the header of your calibrated science image. PHOTFLAM is defined as the flux of a source with constant flux per unit wavelength (in  $\text{erg s}^{-1} \text{cm}^{-2} \text{\AA}^{-1}$ ) which produces a count rate of 1 DN per second for the observing mode specified in the keyword PHOTMODE. The PHOTFLAM value is generated by the STSDAS synthetic photometry package, **synphot**, which you may also find useful for a wide range of photometric and spectroscopic analyses. PHOTFLAM can be used to convert an exposure-normalized image from counts per second to flux units in  $\text{erg s}^{-1} \text{cm}^{-2} \text{\AA}^{-1}$  simply by multiplying the exposure-normalized image by the value of PHOTFLAM. For point-source photometry, STMAG magnitudes can be obtained by adding the STMAG zeropoint for an image's observing mode to the measured instrumental magnitudes (after correction to an infinite aperture). The STMAG zeropoint is defined as

$$\begin{aligned} \text{STMAG\_ZPT} &= -2.5 \text{Log}(\text{PHOTFLAM}) - \text{PHOTZPT} \\ &= -2.5 \text{Log}(\text{PHOTFLAM}) - 21.10 \end{aligned}$$

---

3. [Table 5.1](#) gives approximate values of PHOTFLAM and zeropoints in the VEGAMAG system as of 2002. Observers requiring accurate results are advised to use the PHOTFLAM values in their image headers, as those have the latest calibrations and updates. Alternatively, the latest version of SYNPHOT can be used to compute updated parameters (see the end of [Section 3.5](#) for details about **bandpar** and URESP/PHOTFLAM).

**Table 5.1: Values, From 2002, of PHOTFLAM and Zeropoint in the VEGAMAG System<sup>3</sup>**

| Filter <sup>1</sup> | PC           |         | WF2          |         | WF3          |         | WF4          |         |
|---------------------|--------------|---------|--------------|---------|--------------|---------|--------------|---------|
|                     | New photflam | Vega ZP |
| f122m               | 8.088e-15    | 13.768  | 7.381e-15    | 13.868  | 8.204e-15    | 13.752  | 8.003e-15    | 13.778  |
| f160bw              | 5.212e-15    | 14.985  | 4.563e-15    | 15.126  | 5.418e-15    | 14.946  | 5.133e-15    | 15.002  |
| f170w               | 1.551e-15    | 16.335  | 1.398e-15    | 16.454  | 1.578e-15    | 16.313  | 1.531e-15    | 16.350  |
| f185w               | 2.063e-15    | 16.025  | 1.872e-15    | 16.132  | 2.083e-15    | 16.014  | 2.036e-15    | 16.040  |
| f218w               | 1.071e-15    | 16.557  | 9.887e-16    | 16.646  | 1.069e-15    | 16.558  | 1.059e-15    | 16.570  |
| f255w               | 5.736e-16    | 17.019  | 5.414e-16    | 17.082  | 5.640e-16    | 17.037  | 5.681e-16    | 17.029  |
| f300w               | 6.137e-17    | 19.406  | 5.891e-17    | 19.451  | 5.985e-17    | 19.433  | 6.097e-17    | 19.413  |
| f336w               | 5.613e-17    | 19.429  | 5.445e-17    | 19.462  | 5.451e-17    | 19.460  | 5.590e-17    | 19.433  |
| f343n               | 8.285e-15    | 13.990  | 8.052e-15    | 14.021  | 8.040e-15    | 14.023  | 8.255e-15    | 13.994  |
| f375n               | 2.860e-15    | 15.204  | 2.796e-15    | 15.229  | 2.772e-15    | 15.238  | 2.855e-15    | 15.206  |
| f380w               | 2.558e-17    | 20.939  | 2.508e-17    | 20.959  | 2.481e-17    | 20.972  | 2.558e-17    | 20.938  |
| f390n               | 6.764e-16    | 17.503  | 6.630e-16    | 17.524  | 6.553e-16    | 17.537  | 6.759e-16    | 17.504  |
| f410m               | 1.031e-16    | 19.635  | 1.013e-16    | 19.654  | 9.990e-17    | 19.669  | 1.031e-16    | 19.634  |
| f437n               | 7.400e-16    | 17.266  | 7.276e-16    | 17.284  | 7.188e-16    | 17.297  | 7.416e-16    | 17.263  |
| f439w               | 2.945e-17    | 20.884  | 2.895e-17    | 20.903  | 2.860e-17    | 20.916  | 2.951e-17    | 20.882  |
| f450w               | 9.022e-18    | 21.987  | 8.856e-18    | 22.007  | 8.797e-18    | 22.016  | 9.053e-18    | 21.984  |
| f467m               | 5.763e-17    | 19.985  | 5.660e-17    | 20.004  | 5.621e-17    | 20.012  | 5.786e-17    | 19.980  |
| f469n               | 5.340e-16    | 17.547  | 5.244e-16    | 17.566  | 5.211e-16    | 17.573  | 5.362e-16    | 17.542  |
| f487n               | 3.945e-16    | 17.356  | 3.871e-16    | 17.377  | 3.858e-16    | 17.380  | 3.964e-16    | 17.351  |
| f502n               | 3.005e-16    | 17.965  | 2.947e-16    | 17.987  | 2.944e-16    | 17.988  | 3.022e-16    | 17.959  |
| f547m               | 7.691e-18    | 21.662  | 7.502e-18    | 21.689  | 7.595e-18    | 21.676  | 7.747e-18    | 21.654  |
| f555w               | 3.483e-18    | 22.545  | 3.396e-18    | 22.571  | 3.439e-18    | 22.561  | 3.507e-18    | 22.538  |
| f569w               | 4.150e-18    | 22.241  | 4.040e-18    | 22.269  | 4.108e-18    | 22.253  | 4.181e-18    | 22.233  |
| f588n               | 6.125e-17    | 19.172  | 5.949e-17    | 19.204  | 6.083e-17    | 19.179  | 6.175e-17    | 19.163  |
| f606w               | 1.900e-18    | 22.887  | 1.842e-18    | 22.919  | 1.888e-18    | 22.896  | 1.914e-18    | 22.880  |
| f622w               | 2.789e-18    | 22.363  | 2.700e-18    | 22.397  | 2.778e-18    | 22.368  | 2.811e-18    | 22.354  |
| f631n               | 9.148e-17    | 18.514  | 8.848e-17    | 18.550  | 9.129e-17    | 18.516  | 9.223e-17    | 18.505  |
| f656n               | 1.461e-16    | 17.564  | 1.410e-16    | 17.603  | 1.461e-16    | 17.564  | 1.473e-16    | 17.556  |
| f658n               | 1.036e-16    | 18.115  | 9.992e-17    | 18.154  | 1.036e-16    | 18.115  | 1.044e-16    | 18.107  |
| f673n               | 5.999e-17    | 18.753  | 5.785e-17    | 18.793  | 6.003e-17    | 18.753  | 6.043e-17    | 18.745  |
| f675w               | 2.899e-18    | 22.042  | 2.797e-18    | 22.080  | 2.898e-18    | 22.042  | 2.919e-18    | 22.034  |
| f702w               | 1.872e-18    | 22.428  | 1.809e-18    | 22.466  | 1.867e-18    | 22.431  | 1.883e-18    | 22.422  |
| f785lp              | 4.727e-18    | 20.688  | 4.737e-18    | 20.692  | 4.492e-18    | 20.738  | 4.666e-18    | 20.701  |
| f791w               | 2.960e-18    | 21.498  | 2.883e-18    | 21.529  | 2.913e-18    | 21.512  | 2.956e-18    | 21.498  |
| f814w               | 2.508e-18    | 21.639  | 2.458e-18    | 21.665  | 2.449e-18    | 21.659  | 2.498e-18    | 21.641  |
| f850lp              | 8.357e-18    | 19.943  | 8.533e-18    | 19.924  | 7.771e-18    | 20.018  | 8.194e-18    | 19.964  |
| f953n               | 2.333e-16    | 16.076  | 2.448e-16    | 16.024  | 2.107e-16    | 16.186  | 2.268e-16    | 16.107  |
| f1042m              | 1.985e-16    | 16.148  | 2.228e-16    | 16.024  | 1.683e-16    | 16.326  | 1.897e-16    | 16.197  |

1. Values are for the gain 7 setting. The PHOTFLAM values for gain 14 can be obtained by multiplying by the gain ratio: 1.987 (PC1), 2.003 (WF2), 2.006 (WF3), and 1.955 (WF4) (values from Holtzman et al. 1995b). For the zeropoints, add  $-2.5 \log(\text{gain ratio})$ , or  $-0.745$ ,  $-0.754$ ,  $-0.756$ , and  $-0.728$ , respectively. The above values should be applied to the counts referenced to a nominal “infinite aperture,” defined by an aperture correction of 0.10 mag with respect to the standard aperture with  $0''.5$  radius. *Note: these values are out of date and only approximate. See Footnote 3, page 88.*

Most of the tables used by the **synphot** package were updated in August 1995 and May 1997; an additional update for QE variations and contamination was provided in 2009. With these updates, SYNPHOT now provides absolute photometric accuracy of 2% rms for broad-band and intermediate-width filters between F300W and F814W, and of about 5% in the UV. Narrow-band filters are calibrated using continuum sources, but checks on line sources indicate that their photometric accuracy is also determined to 5% or better (the limit appears to be in the quality of the ground-based spectrophotometry). Prior to the May 1997 update, some far UV and narrow-band filters were in error by 10% or more; additional details are provided in [WFPC2 ISR 97-10](#).

The **synphot** package can also be used to determine the transformation between magnitudes in different filters, subject to the uncertainties related to how well the spectrum chosen to do the determination matches the spectrum of the actual source. The transformation is relatively simple using SYNPHOT, and the actual correction factors are small when converting from the WFPC2 photometric filter set to Johnson-Cousins magnitudes. A variety of [spectral atlases](#) are available on the Web and in SYNPHOT.

In the examples below, the **synphot** command **calcphot** is used to determine the difference in zeropoint between the F814W filter and the Cousins I band for a K0 III star on WF3 using the gain = 7 setting. The Bruzual stellar atlas is being used to provide the spectrum for the K0 III star (file `crgridbz77$bz_54.fits`).

(1) Determine the STMAG value for the F814W passband:

```
-->calcphot "band(wfpc2,3,a2d7,f814W)" crgridbz77$bz_54.fits stmag
Mode = band(wfpc2,3,a2d7,f814W)
  Pivot      Equiv Gaussian
Wavelength      FWHM
  8012.206      1539.682   band(wfpc2,3,a2d7,f814W)
Spectrum:  crgridbz77$bz_54.fits
  VZERO      STMAG      Mode: band(wfpc2,3,a2d7,f814W)
    0.        -15.099
```

## (2) Determine the VEGAMAG value in Cousins I passband

```

-->calcpht "band(cousins,I)" crgridbz77$bz_54.fits vegamag
Mode = band(cousins,I)
      Pivot      Equiv Gaussian
Wavelength      FWHM
      7874.842      897.6061      band(cousins,I)
Spectrum: crgridbz77$bz_54.fits
      VZERO      VEGAMAG      Mode: band(cousins,I)
      0.      -16.336

```

The correction for the KO III star is the difference between its STMAG and VEGAMAG values, which is 1.24 magnitudes.

Nearly all of this offset is due to the definition of STMAG; the F814W filter is a very close approximation to the Cousins I, and color terms between these filters are very small. This is evident in [Figure 5.2](#), which was created using the following **synphot** commands:

```

-->plband "band(cousins,I)" normalize=yes left=6000 right=9500
-->plband "band(wfpc2,3,a2d7,f814W)" normalize=yes append=yes ltype=dotted

```

The Johnson UBVRI throughput data in SYNPHOT are the U3, B2, and V synthetic passbands given in Buser and Kurucz (1978) and the R,I are from Johnson (1965), Table A1. The Cousins R,I throughputs are from Bessell (1983), Table AII, the Strömgren passbands from Matsushima (1969), and the Walraven bands are from Lub and Pel (1977), Table 6. For more details, please see the [SYNPHOT User's Guide](#).

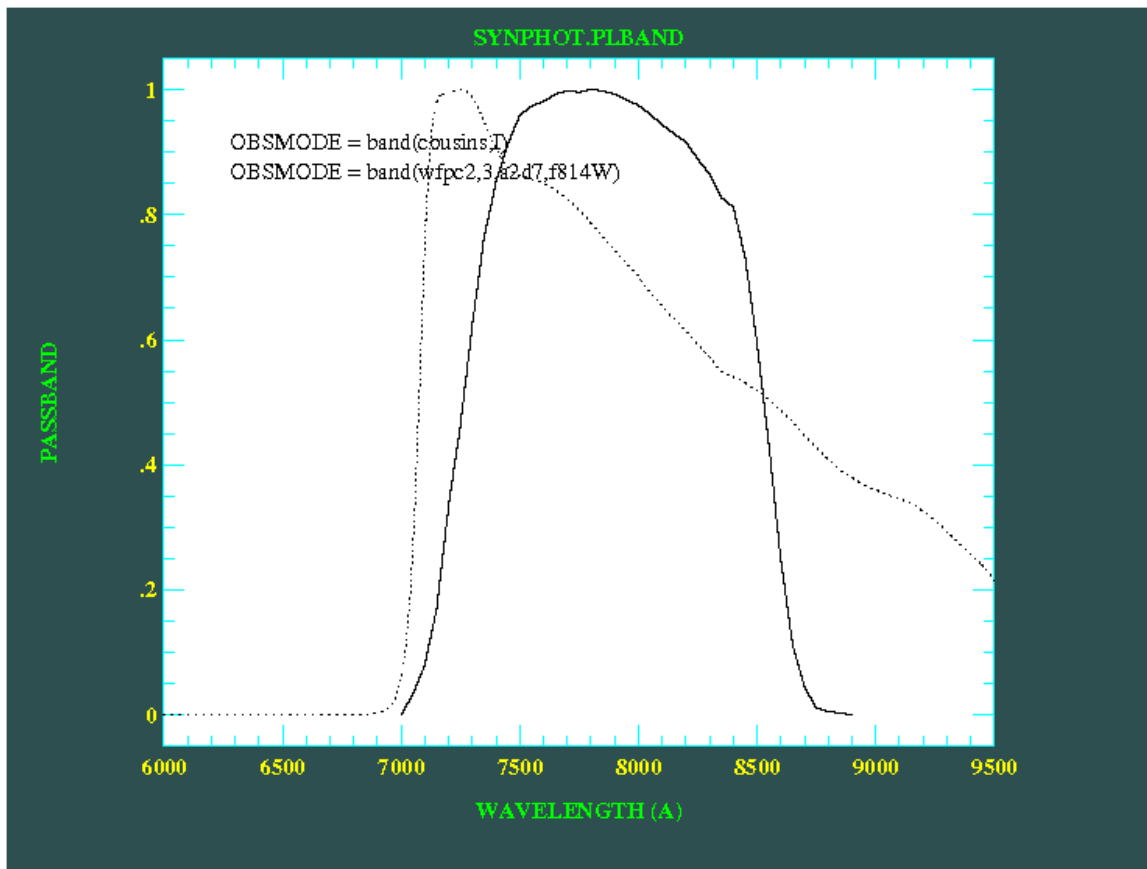
---

*Note that the zeropoints listed by Holtzman et al. (1995b) differ systematically by 0.85 mag from the SYNPHOT zeropoints in [WFPC2 ISR 97-10](#). Most of the difference, 0.75 mag, is due to the fact that the Holtzman zeropoints are given for gain 14, while the SYNPHOT zeropoints are reported for gain 7, which is generally used for science observations. An additional 0.1 mag is due to the aperture correction; the Holtzman zeropoint refers to an aperture of 0".5, while the SYNPHOT zeropoint refers to a nominal infinite aperture, defined as 0.10 mag brighter than the 0".5 aperture*

---



**Figure 5.2: Plot of Passbands "wfpc2,3,a2d7,f814w" (dotted plot) and Cousins I (solid plot)**



## 5.2 Photometric Corrections

A number of corrections must be made to WFPC2 data to obtain the best possible photometry. Some of these, such as the corrections for UV throughput variability and CTE, are time dependent, and others, such as the correction for the geometric distortion of WFPC2 optics, are position dependent. Finally, some general corrections, such as the aperture correction, are needed as part of the analysis process.

## 5.2.1 Time-Dependent Corrections

A major time-dependent correction for UV observations is that for the contamination of the CCD windows which affects UV throughput shortward of about 3500 Å. Other time-dependent corrections covered in this sub-section are due to the change in operating temperature in April 1994 and the variations in PSF shape as a function of focus position due to “breathing” and the PSF’s location on the chip. The effects of CTE, also a time-dependent effect, is covered in [Section 5.2.2](#).

### UV Contamination

Contaminants that accumulated on the WFPC2 CCD windows had characteristics that reduced the UV throughput. Periodic decontaminations (decons) were conducted by warming the CCD enclosures from the -88°C operating temperature to +22°C for about 6 hours which removed the contaminants. However, contaminants would gradually re-accumulate on the windows, eventually requiring another decon to restore UV throughput.

Early in the mission, decons were done about every 30 days. Later in the mission contaminants were seen to accumulate more slowly, and the interval between decons was increased to about 49 days. A list of decon times can be found at:

[http://www.stsci.edu/hst/wfpc2/analysis/wfpc2\\_decon\\_dates.html](http://www.stsci.edu/hst/wfpc2/analysis/wfpc2_decon_dates.html)

Standard star data spanning the WFPC2 mission have been used to characterize the time-dependence of the photometric variations related to contamination. Four parameters were used to characterize the variations:

1. the daily throughput loss in magnitudes due to short-term contamination buildup,
2. the long-term rate of change of (1) due to these contaminants slowly dissipating,
3. the QE in the “clean” state immediately following decontaminations,
4. the long-term rate of change of the “clean” QE due to genuine QE changes, semi-permanent contaminants dissipating or building-up, or other long-term effects.

Data from April 1994<sup>4</sup> to April 2008 were used to obtain linear fits for these parameters for each of the primary UV filters as well as F555W and F814W. Details will be provided in an upcoming ISR, “The Contamination History of the WFPC2.” For the convenience of the user, the fit coefficients for QE changes and daily contamination rate changes are available in [Table 5.2](#) and [Table 5.3](#).

---

4. Date when CCD operating temperature was reduced from -76 °C to -88 °C

**Table 5.2: Linear Fit Coefficients for UV Contamination Rate Changes (Normalized to 1996.12, in Units of Fractional Change per Day)**

| Filter Chip | Intercept (1996.12) | Intercept Uncertainty | Slope (yr <sup>-1</sup> ) | Slope Uncertainty |
|-------------|---------------------|-----------------------|---------------------------|-------------------|
| F160BW PC1  | -0.007650           | 0.000703              | 0.000318                  | 0.000134          |
| F160BW WF2  | -0.012713           | 0.001391              | 0.000789                  | 0.000263          |
| F160BW WF3  | -0.011955           | 0.000882              | 0.000703                  | 0.000238          |
| F160BW WF4  | -0.011137           | 0.002283              | 0.000697                  | 0.000435          |
| F170W PC1   | -0.005252           | 0.000225              | 0.000283                  | 3.3e-05           |
| F170W WF2   | -0.009173           | 0.000457              | 0.000550                  | 5.5e-05           |
| F170W WF3   | -0.009355           | 0.000363              | 0.000581                  | 4.5e-05           |
| F170W WF4   | -0.007457           | 0.000322              | 0.000404                  | 4.0e-05           |
| F218W PC1   | -0.004467           | 0.000417              | 0.000221                  | 7.9e-05           |
| F218W WF2   | -0.008014           | 0.000740              | 0.000462                  | 0.000103          |
| F218W WF3   | -0.007817           | 0.000440              | 0.000445                  | 7.0e-05           |
| F218W WF4   | -0.006286           | 0.000831              | 0.000309                  | 0.000100          |
| F255W PC1   | -0.002183           | 0.000365              | 0.000136                  | 7.7e-05           |
| F255W WF2   | -0.004065           | 0.000603              | 0.000224                  | 8.6e-05           |
| F255W WF3   | -0.004253           | 0.000374              | 0.000219                  | 6.0e-05           |
| F255W WF4   | -0.003105           | 0.000683              | 0.000152                  | 8.3e-05           |
| F336W PC1   | -0.000459           | 0.000191              | 1.1e-06                   | 3.4e-05           |
| F336W WF2   | -0.001869           | 0.000296              | 0.000133                  | 4.2e-05           |
| F336W WF3   | -0.001950           | 0.000195              | 0.000101                  | 3.2e-05           |
| F336W WF4   | -0.001823           | 0.000342              | 9.3e-05                   | 4.1e-05           |
| F555W PC1   | -0.000161           | 0.000127              | 2.0e-05                   | 2.4e-05           |
| F555W WF2   | -0.000638           | 0.000283              | 3.1e-05                   | 3.8e-05           |
| F555W WF3   | -0.000418           | 0.000198              | 1.8e-06                   | 3.2e-05           |
| F555W WF4   | -0.000110           | 0.000295              | 7.3e-06                   | 3.3e-05           |
| F814W PC1   | 1.3e-05             | 0.000130              | 3.2e-05                   | 4.3e-05           |
| F814W WF2   | -0.000716           | 0.000374              | 0.000103                  | 6.5e-05           |
| F814W WF3   | 4.4e-05             | 0.000229              | -6.4e-05                  | 5.1e-05           |
| F814W WF4   | -8.7e-05            | 0.000422              | 4.0e-05                   | 7.8e-05           |

**Table 5.3: Linear Fit Coefficients for Changes in Post-decon Throughput (QE), in Fractional Units**

| Filter Chip | Intercept (1996.12)                              | Intercept Uncertainty                             | Slope (1996.12)                                    | Slope Uncertainty                                 |
|-------------|--|---|--|---|
| F160BW PC1  | 1.000000<br>(1999.8194,<br>1.14728) <sup>1</sup> | 0.017293<br>(1999.8194,<br>0.067235) <sup>1</sup> | 0.042517<br>(1999.8194,<br>0.000511) <sup>1</sup>  | 0.009851<br>(1999.8194,<br>0.009956) <sup>1</sup> |
| F160BW WF2  | 1.000000   | 0.037359  | -0.004914  | 0.008729  |
| F160BW WF3  | 1.000000   | 0.019691  | 0.005260   | 0.005171  |
| F160BW WF4  | 1.000000   | 0.057365  | 0.009284   | 0.011350  |
| F170W PC1   | 1.000000<br>(1998.8194<br>1.10166) <sup>1</sup>  | 0.005675<br>(1998.8194,<br>0.013020) <sup>1</sup> | 0.035748<br>(1998.8194,<br>-0.001311) <sup>1</sup> | 0.003795<br>(1998.8194,<br>0.001923) <sup>1</sup> |
| F170W WF2   | 1.000000   | 0.017683  | 0.001875   | 0.002454  |
| F170W WF3   | 1.000000   | 0.008168  | -0.001585  | 0.001255  |
| F170W WF4   | 1.000000   | 0.007293  | -0.002741  | 0.001381  |
| F218W PC1   | 1.000000   | 0.009651  | -0.002159  | 0.002042  |
| F218W WF2   | 1.000000   | 0.017942  | -0.003490  | 0.002894  |
| F218W WF3   | 1.000000   | 0.009781  | -0.002681  | 0.001829  |
| F218W WF4   | 1.000000   | 0.023587  | -0.001738  | 0.004017  |
| F255W PC1   | 1.000000   | 0.008243  | -0.006123  | 0.001837  |
| F255W WF2   | 1.000000   | 0.014614  | -0.005511  | 0.002501  |
| F255W WF3   | 1.000000   | 0.008322  | -0.005457  | 0.001560  |
| F255W WF4   | 1.000000   | 0.016897  | -0.007234  | 0.003161  |
| F336W PC1   | 1.000000   | 0.004496  | -0.001204  | 0.000910  |
| F336W WF2   | 1.000000   | 0.007370  | -0.002931  | 0.001262  |
| F336W WF3   | 1.000000   | 0.004660  | -0.002069  | 0.000906  |
| F336W WF4   | 1.000000   | 0.008690  | -0.002316  | 0.001602  |
| F555W PC1   | 1.000000   | 0.003536  | 0.002200   | 0.000653  |
| F555W WF2   | 1.000000   | 0.006988  | 0.001361   | 0.001143  |
| F555W WF3   | 1.000000   | 0.004354  | 0.001980   | 0.000886  |
| F555W WF4   | 1.000000   | 0.009861  | 0.002352   | 0.001913  |
| F814W PC1   | 1.000000   | 0.003947  | 0.002717   | 0.001253  |
| F814W WF2   | 1.000000   | 0.008780  | 0.000510   | 0.001927  |
| F814W WF3   | 1.000000   | 0.005444  | 0.004390   | 0.001334  |
| F814W WF4   | 1.000000   | 0.012221  | 0.004652   | 0.002609  |

1. For F160BW/PC1 and F170W/PC1, separate linear fits were done for data taken after 1999.8194 and 1998.8194 respectively, because the trend for increasing QE seen earlier in the mission appeared to be slowing. Data taken after those dates were normalized to their respective “break” dates.

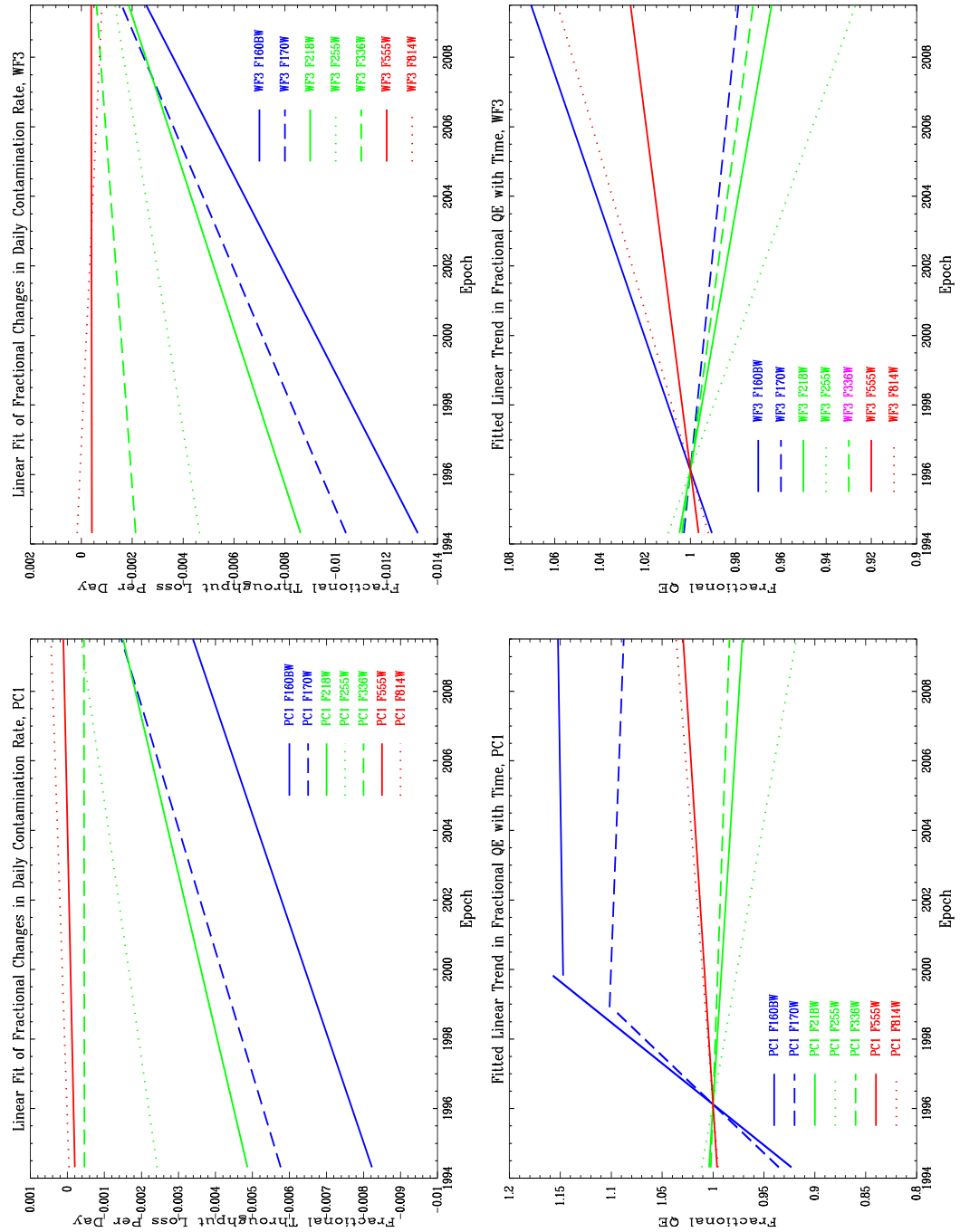
Figure 5.3 is a graphical representation of the linear fits applied to standard star (GRW+70D5824) photometry, in PC1 and WF3, showing the changes in QE and daily UV contamination rate.

The results of this analysis were used to update the SYNPHOT “contamination” tables which were also used for computing the value of a new header keyword, ZP\_CORR (added as part of the photometry group header keywords). The value of ZP\_CORR provides the throughput changes due to contamination and long-term QE changes, in delta magnitudes, for the date of the observation.

Several trends were noted:

- The largest daily contamination values were seen in all chips for F160BW, F170W, and F218W.
- Over the lifetime of WFPC2, some contaminants gradually dissipated. The largest declines in contamination rates were seen in the WF chips for F160BW and F170W, followed by F160BW/PC1 and F170W/PC1, and all chips in F218W. There was negligible change in contamination rate for all chips in F255W, F336W, F555W and F814W.
- The post-decon QE over the WFPC2 lifetime, in F160BW/PC1, showed an increase till late 1999 then appeared to leveled off to a constant value until the instrument was decommissioned. A similar trend was seen in F170W/PC1, except that the transition to stable QE value occurred in late 1998. This may have been due to long-term dissipation of semi-permanent contaminants from the CCD faceplate.
- The largest declines in UV post-decon QE were seen in all chips for the F255W filters. This could be due to the accumulation of a different contaminant on the CCD faceplate with absorption properties in that passband.
- With the exception of F160BW/PC1, F170W/PC1, and F255W/all chips, most filter/chip configurations showed no significant long-term change in QE (due either to a level slope or slope values that were within the slope uncertainty range).

**Figure 5.3: Linear Fits to Observed Photometric Changes for Standard Star GRW+70D5824 for the PC1 and WF3 Detectors in Selected Filters<sup>5</sup>**



*Calculating Fractional Total UV Throughput Loss for an Observation*

For the convenience of observers, the correction, in delta magnitude, for the effects of UV contamination and QE changes on an image are stored in

the group header keyword, ZP\_CORR. To apply the correction for throughput loss due to UV contamination and QE changes, the user simply adds the value of ZP\_CORR, available for each chip, from the measured magnitudes.

This value can also be obtained using **synphot**. The example below shows how ZP\_CORR is calculated for an observation taken on June 23, 2008 (MJD 54640.0828), in the PC1, at gain 7, with filter F170W. (The header keyword value ZP\_CORR was given as 0.06701469 mag.)

(1) First, determine the STMAG value for the bandpass, using a constant value spectrum renormalized to 1. This magnitude has no time-dependent corrections applied to it, and is only based on the instrument throughput tables<sup>6</sup>.

```
--> calcphot WFPC2,1,A2D7,F170W
"rn(unit(1,flam),band(WFPC2,1,A2D7,F170W),1,counts)" stmag
Mode = band(WFPC2,1,A2D7,F170W)
      Pivot      Equiv Gaussian
Wavelength      FWHM
      1831.198      686.7557      band(WFPC2,1,A2D7,F170W)
Spectrum:
rn(unit(1,flam),band(WFPC2,1,A2D7,F170W),1,counts)
      VZERO      STMAG      Mode: band(WFPC2,1,A2D7,F170W)
      0.          15.92322
```

(2) Next, determine the STMAG value on the date of the observation, for the passband, using the same constant value spectrum renormalized to 1. The observation date, in MJD, is inserted in the bandpass so

5. The figures on the left show the fractional throughput loss per day (due to contaminants) vs. year. On the right, the figures show fractional changes in QE vs. year. Here, QE is defined as the throughput immediately after a decontamination. QE values were normalized to year = 1996.12, which corresponds to the mean epoch of the WFPC2 SYNPHOT QE throughput tables. For F160BW and F170W, the QE increased for several years after launch, and then stabilized to a constant value; those trends necessitated breaks in 1999.8 and 1998.8, respectively.

6. The STSDAS **showfiles** task lists throughput tables for a bandpass. Here, the observation date is added to the bandpass to include the time-dependent UV contamination and QE changes table.

```
--> showfiles WFPC2,1,A2D7,F170W,cont#54640.0828
#Throughput table names:
crotacomp$hst_ota_007_syn.fits      (Optical telescope assembly)
crwfp2comp$wfp2_optics_006_syn.fits (WFPC2 optics)
crwfp2comp$wfp2_f170w_006_syn.fits  (F170W filter)
crwfp2comp$wfp2_dqepc1_005_syn.fits (PC1 QE as of 1996.12)
crwfp2comp$wfp2_a2d7pc1_004_syn.fits (PC1 AtoD gain)
crwfp2comp$wfp2_contpc1_011_syn.fits[cont#] (UV contamination
& QE changes)
```

time-dependent changes due to UV contamination as well as QE changes, are included in the computation.

```
--> calcphot WFPC2,1,A2D7,F170W,cont#54640.0828
"rn(unit(1,flam),band(WFPC2,1,A2D7,F170W,cont#54640.0828),1,counts)" stmag
Mode = band(WFPC2,1,A2D7,F170W,cont#54640.0828)

Pivot      Equiv Gaussian
Wavelength      FWHM
1817.068      669.5286      band(WFPC2,1,A2D7,F170W,cont#54640.0828)

Spectrum:
rn(unit(1,flam),band(WFPC2,1,A2D7,F170W,cont#54640.0828),1,counts)

VZERO      STMAG      Mode: band(WFPC2,1,A2D7,F170W,cont#54640.0828)
0.          15.99025
```

ZP\_CORR is the magnitude difference for STMAG with and without the time-dependent UV contamination and QE corrections:

$$15.99025 - 15.92322 = 0.067030.$$

### Cool Down on April 23,1994

The temperature of the WFPC2 was lowered from  $-76^{\circ}\text{C}$  to  $-88^{\circ}\text{C}$  on April 23, 1994, in order to minimize the CTE problem. While this change increased the contamination rates, it also improved the photometric throughput, especially in the UV, reduced the CTE losses, and greatly reduced the impact of warm pixels. Table 5.4 shows, as an example, a partial list of corrections to obtain the pre-cooldown throughput. Including the MJD in a `synphot` calculation and using up-to-date SYNPHOT contamination tables will automatically correct PHOTFLAM for this change.

**Table 5.4: Ratio Between Pre- and Post-Cool Down Throughput**

| Filter | PC    | PC (mag) | WF    | WF (mag) |
|--------|-------|----------|-------|----------|
| F160BW | 0.865 | -0.157   | 0.895 | -0.120   |
| F170W  | 0.910 | -0.102   | 0.899 | -0.116   |
| F218W  | 0.931 | -0.078   | 0.895 | -0.120   |
| F255W  | 0.920 | -0.091   | 0.915 | -0.096   |
| F336W  | 0.969 | -0.034   | 0.952 | -0.053   |
| F439W  | 0.923 | -0.087   | 0.948 | -0.058   |
| F555W  | 0.943 | -0.064   | 0.959 | -0.045   |
| F675W  | 0.976 | -0.026   | 0.962 | -0.042   |
| F814W  | 0.996 | -0.004   | 0.994 | -0.007   |

### PSF Variations

The point spread function (PSF) of the telescope varies with time, and for some filters, these variations can affect photometry that relies on very small apertures and PSF fitting. Changes in focus are observed on an orbital timescale (about 90 minutes) due to thermal *breathing* of the telescope. On a longer timescale, moisture desorption of the graphite epoxy OTA structures has resulted in secondary mirror movement relative to the primary mirror, requiring periodic adjustments to maintain acceptable focus for all the science instruments. Additional information is available at the HST Focus History Web site at

<http://www.stsci.edu/hst/observatory/focus/focushistory.html>

The effect of focus position on aperture photometry is described in [WFPC2 ISR 97-01](#).

In addition, *jitter*, or pointing motion, can occasionally alter the effective PSF. The Engineering Data Processing System (EDPS) provides information on telescope pointing during observations in the jitter files; these files can be retrieved from the Archive with your data and instructions on how to use them can be found in Appendix C of the HST Data Handbook at

[http://www.stsci.edu/hst/HST\\_overview/documents/datahandbook/v7/intro\\_cover.html](http://www.stsci.edu/hst/HST_overview/documents/datahandbook/v7/intro_cover.html)

and the HST Pointing Web page at

<http://www.stsci.edu/hst/observatory/pointing>

Remy et al. (1997) have been able to obtain high-quality photometry of well-exposed point sources by modeling the point spread function with TinyTim ([Krist, 1995](#)), and taking into account focus and jitter terms via a chi-squared minimization method. Similar results have been obtained using observed PSFs ([Surdej et al., 1997](#)), provided that the PSF used is less than 10" from the observed star and corresponds to a spectral energy distribution similar to that of the target. The [WFPC2 PSF library](#) was established to help users find suitable PSFs, if they exist, or carry out experiments with what is available.

### 5.2.2 Position-Dependent Corrections

In this Section we discuss the Charge Transfer Efficiency (CTE) correction and the possibly-related long vs. short anomaly, the geometric distortion, the gain differences between different chips, and the effect of pixel centering.

## Charge Transfer Efficiency

Shortly after the installation of WFPC2 in December 1993, the WFPC2 Investigation Definition Team noticed that the CCDs had unexpectedly poor Charge Transfer Efficiency (CTE, Holtzman et al. 1995). Approximately 10% to 15% of the detected signal from point sources was lost as the charge was transferred across 800 rows of pixels toward the CCD output node. To mitigate these losses, the operating temperature of the CCDs was lowered from  $-76^{\circ}\text{C}$  to  $-88^{\circ}\text{C}$  in April 1994. This action reduced the charge losses across 800 vertical transfers to approximately 3% to 4%.

In subsequent years additional CTE losses appeared which were caused by radiation damage to the CCD detectors. These losses grew throughout the WFPC2 mission, and became an important source of photometric error. By the end of the WFPC2 mission, these effects were so strong that, in some situations, a faint target could lose over half its counts during the readout process. Various photometric corrections for CTE were devised and are summarized below.

This long-term CTE degradation resulted from continuous exposure to trapped ions in the van Allen radiation belts. This radiation progressively damaged the CCD's silicon lattice, creating more electrical traps that inhibited the transfer of photoelectrons during a pixel clocking cycle. Consequently, the amount of charge lost from an imaged WFPC2 target became a function of WFPC2's time in orbit, the brightness of the target, its location on the detector, and the background illumination.

### *Effect on Point Sources*

Several assessments of WFPC2's time-dependent CTE were made over the course of the WFPC2 mission (Whitmore et al. 1999; Dolphin 2000a, 2002, 2009). These studies provided effective formulae for correcting the errors in point-source aperture photometry caused by degrading CTE. Dolphin's latest study provides the most comprehensive correction for WFPC2 stellar aperture photometry to date (Dolphin 2009). It is based on images of the globular cluster Omega Cen spanning 13 years which were taken primarily with the WF2 and WF4 cameras, and utilizes his own WFPC2 photometry package (HSTphot; Dolphin 2000b). Dolphin documents the updates and revisions to his CTE correction formula on a Web site hosted at the University of Arizona:

[http://purcell.as.arizona.edu/wfpc2\\_calib/](http://purcell.as.arizona.edu/wfpc2_calib/)

For convenience, the latest version of this correction (dated 13 May 2009) is reproduced here. WFPC2 users are strongly encouraged to check Dolphin's Web site for updates and revisions of the formula which may appear at later dates, as well as the [WFPC2 Web site](#).

Dolphin's formula is more complex than other CTE-correction formulae because it accounts for changing source brightness as the charge packet is

read out (i.e., the signal loss per pixel changes during readout). Calculation of the correction begins by computing the following parameters:

$$\begin{aligned} \text{lb}_g &= \ln(\sqrt{(BKG^2+1)}) - 1 \\ \text{yr} &= (\text{MJD} - \text{MJD}_0) / 365.25 \end{aligned}$$

where  $BKG$  is the true background signal in electrons around the source (i.e., excluding any star light in the sky annulus),  $\text{MJD}$  is the Mean Julian Date of the observation, and  $\text{MJD}_0 = 49461.9 \pm 0.1$

Second, compute the correction for CTE losses during the horizontal (i.e., X direction) transfers of the charge packet on the detector:

$$\text{XCTE (mags)} = A * \exp(B*\text{lb}_g) * (1 + C*\text{yr}) * X/800$$

where  $X$  is the abscissa of the source coordinate on the CCD. The coefficients  $A$ ,  $B$ , and  $C$  are provided below.

Third, calculate the following parameters related to CTE losses during the vertical transfers (i.e. Y direction) of the charge packet on the detector:

$$\begin{aligned} \text{lct} &= \ln(\text{CTS}) + 0.921*\text{XCTE} - 7 \\ \text{c1} &= \text{maximum of } (1 - D*\text{lb}_g + E*\text{lb}_g*\text{lct} + F*\text{lct}) \text{ or } G \\ \text{c2} &= H * (\text{yr} - I*\text{yr}^2) * \exp(J*\text{lct}) \end{aligned}$$

where  $\text{CTS}$  is the point-source signal in electrons measured within a circular aperture of radius  $0''.5$ , and the coefficients  $D$  to  $J$  are given below. Note that  $\text{CTS}$  is, by definition, an aperture-corrected value computed by `HSTPhot` based on a photometric aperture of radius 3 pixels (for the PC1) or 2 pixels (for the WF cameras).

Finally, compute the correction for CTE losses during the vertical transfers:

$$\text{YCTE (mags)} = K * \ln(\exp(L * \text{c1} * Y/800) * (1 + \text{c2}) - \text{c2})$$

where  $Y$  is the ordinate of the source coordinates, and  $K$  and  $L$  are given below.

The coefficients have values and uncertainties:

$$\begin{aligned} A &= 0.0077 \pm 0.0008 \\ B &= -0.50 \pm 0.06 \\ C &= 0.10 \pm 0.3 \\ D &= 0.201 \pm 0.002 \\ E &= 0.039 \pm 0.002 \\ F &= 0.002 \pm 0.003 \\ G &= 0.15 \pm 0.03 \end{aligned}$$

$$\begin{aligned}
 H &= 0.96 \pm 0.02 \\
 I &= 0.0255 \pm 0.0004 \\
 J &= -0.450 \pm 0.004 \\
 K &= 2.41 \pm 0.02 \\
 L &= 0.02239 \pm 0.00001
 \end{aligned}$$

Dolphin reports residual photometric errors of  $< 0.05$  mag regardless of star brightness, background level, or observation date (Dolphin 2009).

These correction formulae assume CTE effects are identical in all four WFPC2 cameras, but this has not been well established. Manufacturing differences and shielding effects within WFPC2 may have resulted in small CTE differences among the CCDs. There is some evidence that CTE is better in the WF4 camera than in the other cameras (WFPC2 ISR 2005-01, Biretta & Kozhurina-Platais; Golimowski & Biretta 2010, in prep.).

Dolphin’s formulae exclude WF4 data obtained after March 2002, when WF4’s amplifier gain anomaly was first observed (WFPC2 ISR 2005-02, Biretta & Gonzaga). Consequently, Dolphin’s CTE correction may be more accurate for sources imaged in WF2 and WF3 than for sources imaged in WF4, especially after 2002.

Finally, correction of photometry in the PC1 camera may be less reliable than that of the other cameras due to the relative paucity of calibrator stars in the smaller PC1 field of view. More detailed information about the performance of Dolphin’s CTE correction on photometry obtained near WFPC2’s end-of-mission is provided by Golimowski & Biretta (2010, in prep.).

### *Effect on Extended Sources*

Extended sources will suffer CTE losses in much the same way as point sources. One difference, however, is that the broader leading (amplifier-side) edge of extended targets can fill additional traps in the CCD during readout (similar to a higher sky background) and thus reduce the fraction of counts lost to CTE effects, as compared to point sources.

We have quantified the photometric CTE of extended sources using galaxies in the long-term monitor observations of the Hubble Deep Field North (HDFN; Williams et al. 1995) in F606W from Programs 6337 (epoch 1995), 8389 (epoch 2000), and 11032 (epoch 2007 to 2008). An early ACS/WFC image of the same region was used as a “truth” image. Because of the WF4 Anomaly (WFPC2 ISRs 05-02; 08-03), and the low number of sources in the PC1, we limited our investigation to WF2 and WF3.

Typically the galaxies had low fluence ( $< 100 e^-$ ) relative to the moderate to high backgrounds ( $55 e^-$  to  $150 e^-$ ) of individual exposures. The counts for the galaxies were derived from dual-image mode SExtractor (Bertin & Arnouts 1996) using the ACS “truth image” as the detection image for determining matched-aperture FLUX AUTO values of resolved sources in the WFPC2 mosaics.

We adopt the same functional form for CTE loss as derived by Dolphin (2009) for point sources, and re-fitted the free parameters using our HDFN galaxy data. The resulting best fit parameters for the galaxies are as follows:

$$\begin{aligned} \text{MJD}_0 &= 49478.1 \\ A &= 0.4690 \\ B &= 2.20 \\ C &= 2.88 \\ D &= 0.0594 \\ E &= 1.080 \\ F &= 0.684 \\ G &= 0.022 \\ H &= 0.0000482 \\ I &= -0.0603 \\ J &= -0.673 \\ K &= 0.000100 \\ L &= 0.1288 \end{aligned}$$

The difference between these corrections for extended sources, and those for point sources, is a complicated function of the input variables, but is generally less than 0.10 mag and is greatest (in the sense of lower CTE loss for extended sources) for the brightest sources ( $> 2000 e^-$ ) at the latest epochs. The full details of our extended source CTE study will appear in a future WFPC2 ISR (Grogin et al., in prep.).

In addition to these photometric effects, CTE can also impact the shape and structure of extended sources (c.f. [WFPC2 ISR 00-04](#)). During read-out, charge is primarily lost from the leading (amplifier-side) edge of the galaxy image. The side of the galaxy away from the amplifier suffers little charge loss because the charge traps encountered during the read-out have already been filled (by the leading edge), and also because some trapped charge is being released. Hence CTE will produce asymmetries in images of otherwise symmetric targets. Additional studies of these morphological effects are underway and will appear in future WFPC2 ISRs.

### *First Exposure CTE Effect*

During observations, it was fairly common practice to take consecutive frames of a target without moving the telescope (e.g. this was often done to aid in cosmic ray removal, or to image in different filters). There is evidence that in these situations, the first exposure of the sequence will have greater CTE effects than the subsequent ones.

The evidence comes from standard star observations taken near the end of the WFPC2 mission where the first exposure typically had 4% to 5% fewer counts than the later exposures, when the star was placed at high Y pixel positions on the detector ( $Y > 700$ ; McMaster and Biretta, 2010, in prep.).

The effect is presumably caused by electrons from the first exposure filling traps in the CCD, which reduce CTE effects in subsequent exposures. At this writing, very little else is known about the effect—its dependencies on target brightness and image background counts have not been evaluated. Presumably the effect would grow over time in proportion to the normal CTE effects (though this hypothesis has not been tested). For example, for bright targets observed at the middle of the WFPC2 mission near the center of the detector, the effect might be estimated at only 1%.

A common practice, especially towards the end of the WFPC2 mission, was to make small pointing offsets between consecutive exposures (i.e. pointing dithers) and in this situation it seems likely that each exposure would behave as a “first exposure” unless the dither was precisely in the Y (or possibly X) direction. This “first exposure” effect could also have some impact on the applicability of the CTE correction equations derived above, if the observations used to derive the equations and the user’s own observations had significantly different sequences or dither strategies.

### **Long vs. Short Anomaly (non-linearity)**

Early in the WFPC2 mission there was evidence that long exposures of a given field would tend to give brighter magnitudes than short exposures of the same field. This effect was termed the “long vs. short anomaly.” The effect was first noted by Stetson, as reported in Kelson et al. (1996) and Saha et al. (1996). These authors used a 5% correction factor for the effect in their papers. A more detailed study was made by Casertano and Mutchler, as reported in [WFPC2 ISR 1998-02](#). They found that this apparent non-linearity appears to be strictly a function of total counts in each source. The errors are less than 1% for well-exposed stars (over 30,000 e<sup>-</sup>), but may be much larger for faint stars. However, subsequent studies have not been able to confirm the existence of the so called “long vs. short” anomaly (e.g., Saha, Labhart, & Prosser 2000; and Dolphin 2000).

The current prevailing wisdom is that the “long vs. short” effect is likely to be the result of inaccurately measured sky backgrounds in very crowded fields (Whitmore and Heyer, [WFPC2 ISR 2002-03](#)), where accurate sky determination becomes difficult or impossible. The effect appears to be largely a function of the photometric parameters and algorithms used for a particular study. On typical fields, where the stars are not so crowded that they overlap, the effect appears to be less than a few percent, if it exists at all. Since the effect appears to depend on factors like target crowding, and details of the analysis software, we do not provide a correction formula, but instead refer the user to [Whitmore & Heyer \(2002\)](#) for more information and possible methods of dealing with adversely affected datasets.

### Pixel Area Corrections

Geometric distortion near the edges of the chips results in a change of the surface area covered by each pixel. The flat-fielding corrects for this distortion so that surface photometry is unaffected. However, integrated point-source photometry using a fixed aperture *will* be affected by 1% to 2% near the edges, with a maximum of about 4% to 5% in the corners. A pixel area correction image, available from the [IDT Reference File Memo](#) (`f1k1552bu_r9f.fits`, a wFITS file that must be converted to the GEIS format), can be multiplied with the science image to rescale image pixel values to provide more accurate point-source photometric measurements. A small residual effect, due to the fact that the aperture radius differs from the nominal size, depends on the aperture used and is generally well below 1%. Please see [Section 5.4](#) for additional discussion on geometric distortion and astrometry. Note: this correction should not be applied to images used as input to **multidrizzle**, as well as to multidrizzled images, because geometric distortions are corrected as part of the drizzling process.

### The 34th Row Defect

Approximately every 34th row on the WFPC2 detectors possesses a reduced sensitivity (Trauger et al., 1993); these features are likely due to a manufacturing defect that resulted in the affected rows being somewhat narrower than the rest. The pipeline flat fields contain these features and produce calibrated images appropriate for surface brightness measurements. Point source photometry, however, can suffer 1% - 2% errors; and, the narrow rows have a significant effect on astrometry, causing periodic errors of up to 0.03 pixels. A paper by Anderson & King (1999) provides photometric and astrometric correction formulae for this 34th row effect, to be applied to calibrated WFPC2 images (`c0m.fits`). This correction should not be applied to input and output **multidrizzle** images because the **multidrizzle** task handles all geometric distortions.

### Gain Variation

There are slight differences in the absolute sensitivities of the four chips. These values were determined by comparing each chip in flat fields taken using `gain = 14` and normalized to 1.0 over the central image region [200:600,200:600].

The count ratios for the different chips from Holtzman (1995b) are:

- **PC1**: 1.987
- **WF2**: 2.003
- **WF3**: 2.006
- **WF4**: 1.955

However, most science observations are taken using the `gain = 7` setup. Because the gain ratio varies slightly from chip to chip, PHOTFLAM values

will be affected. These count ratios should be included in the zeropoint calculation when using values from Holtzman et al. (1995b) on gain = 7 data. Conversely, their reciprocals should be applied when using SYNPHOT zeropoints on gain = 14 data. *If you use the value of PHOTFLAM from the image header to determine your zeropoint, the different gains for the different chips will already be included.*

### **Pixel Centering**

Small, sub-pixel variations in the quantum efficiency of the detector could affect photometry. The position of a star relative to the sub-pixel structure of the chip is estimated to have an effect of less than 1% on photometry. At present there is no way to correct for this effect on a single image, but more accurate photometry may be possible by utilizing images with sub-pixel pointing dithers.

### **Possible Variation in Methane Quad Filter Transmission**

Based on results from Jupiter and Uranus archival WFPC2 data, the extended wings of the methane filter transmission curve appear to vary across the field of view (Karkoshka, priv. comm.). While this is unimportant for objects with flat spectra, it can have a major impact on photometry of objects with methane bands, where a significant fraction of photons comes from the wings. To provide data to check the methane filter, a set of nine 26 second images of Saturn, in a 3 x 3 grid around the FQCH4W3 methane quad filter aperture (one of the 9 positions falls outside of the filter) was executed as a Cycle 10 calibration program (proposal 9256). The data is available for users who wish to quantify the magnitude and direction of the effect by comparing results from the rings of Saturn (flat spectrum) to results from Saturn itself (deep methane band spectrum). Additional information can be found in a memo titled “WFPC2 Photometry for the Solar System” that’s available at:

[http://www.stsci.edu/hst/wfpc2/analysis/wfpc2\\_ss\\_phot.html](http://www.stsci.edu/hst/wfpc2/analysis/wfpc2_ss_phot.html)

### **Anomalous Rotational Offset in the Linear Ramp Filters**

For completeness, this effect is included here though we expect no impact on observations as any photometric effect is estimated to be less than 1%. Analysis of FR533N VISFLAT images has revealed an apparently randomly occurring offset of about  $0^{\circ}.5$  in the filter wheel rotation for some images, a quantity that corresponds to one filter step. The pivot point of the rotation implicates the filter wheel as the source of the inconsistency. A handful of other filters, on different filter wheels as well, appear to exhibit the same problem; at this time, the source of this anomaly, whether it is mechanical or due to a software error, is unknown. A detailed report is available in [WFPC2 ISR 02-04](#) (Gonzaga et al.).

### 5.2.3 Other Photometric Corrections

Miscellaneous corrections that must be taken into account include: aperture corrections, color terms if transforming to non-WFPC2 filters, digitization noise and its impact on the estimate of the sky background, the effect of red leaks and charge traps, and the uncertainty of exposure times on short exposures taken with serial clocks on.

#### Aperture Correction

It is difficult to directly measure the total magnitude of a point source with the WFPC2 because of the extended wings of the PSF, scattered light, and the small pixel size. One would need to use an aperture far larger than is practical.

A more accurate method is to measure the light within a smaller aperture, then apply an offset to determine the total magnitude. Typically, magnitudes measured in a small aperture well-suited to the data at hand (a radius of 2 to 4 pixels) with a background annulus of 10 to 15 pixels, have been found adequate for data without excessive crowding; the results are then corrected to the aperture for which the zeropoint is known. The aperture correction can often be determined from the data themselves, by selecting a few well-exposed, isolated stars. If these are not available, encircled energies and aperture corrections have been tabulated by Holtzman et al. (1995a). If PSF fitting is used, then the aperture correction can be evaluated directly on the PSF profile used for the fitting.

For very small apertures (1 to 2 pixels), the aperture correction can be influenced by the HST focus position at the time of the observation. The secondary mirror of HST is known to drift secularly towards the primary, and to move slightly on time scales of order of an orbit. The secular shift is corrected by biannual moves of the secondary mirror, but the net consequence of this motion is that WFPC2 can be out of focus by up to 3 to 4  $\mu\text{m}$  of secondary mirror displacement at the time of any given observation. This condition affects the encircled energy at very small radii, and thus the aperture corrections, by up to 10% in flux (for 1 pixel aperture in the PC); see [WFPC2 ISR 97-01](#) for more details. If the use of very small apertures is required—because of crowding, S/N requirements, or other reasons—users are strongly advised to determine the aperture correction from suitable stars in their images. If such are not available, an approximate aperture-focus correction can be obtained as described in [WFPC2 ISR 97-01](#).

A standard aperture radius of 0".5 has been adopted by Holtzman et al. (1995b; note that Holtzman et al. 1995a used a radius of 1".0). For historic consistency, the WFPC2 group at STScI and the **SYNPHOT** tasks in STSDAS refer all measurements to the total flux in a hypothetical infinite aperture. In order to avoid uncertain correction to such apertures, both in calibration and in science data, this infinite aperture is defined by an aperture correction of exactly 0.10 mag with respect to the standard 0".5

aperture. This value (0.10 mag) is close to the values tabulated in Holtzman et al. (1995a) as well as consistent with Whitmore (1995); only extended sources larger than  $\sim 1''$  are likely to require a more accurate aperture correction ([WFPC2 ISR 97-01](#)). Equivalently, the total flux is defined as 1.096 times the flux in the standard aperture of  $0''.5$  radius. In practice, this means that observers wishing to use the SYNPHOT zeropoints should:

1. Correct the measured flux to a  $0''.5$  radius aperture.
2. Apply an additional aperture correction of  $-0.10$  mag (equivalently, multiply the flux by 1.096).
3. Determine the magnitude using the appropriate zeropoint.

See the example in [Section 5.2.5](#).

### Color Terms

In some cases it may be necessary to transform from the WFPC2 filter set to more conventional filters (e.g., Johnson UBV or Cousins RI) in order to make comparisons with other datasets. The accuracy of these transformations is determined by how closely the WFPC2 filter matches the conventional filter and by how closely the spectral type (e.g., color, metallicity, surface gravity) of the object matches the spectral type of the calibration observations. Accuracies of 1% to 2% are typical for many cases, but much larger uncertainties are possible for certain filters (e.g., F336W, see the [Red Leaks](#) section below), and for certain spectral types (e.g., very blue stars). Transformations can be determined by using SYNPHOT, or by using the transformation coefficients in Holtzman et al. (1995b).

### Digitization Noise

The minimum gain of the WFPC2 CCDs,  $7 e^-/ADU$ , is larger than the read noise of the chip. As a result, digitization can be a source of noise in WFPC2 images. This effect is particularly pernicious when attempting to determine sky values because the measured values tend to cluster about a few integral values (dark subtraction and flat-fielding cause the values to differ by slightly non-integral amounts). As a result, using a median filter to remove objects that fall within the background annulus in crowded fields, can cause a substantial systematic error, whose magnitude will depend on the annulus being measured. It is generally safer to use the mean, though care must then be taken to remove objects in the background annulus.

A more subtle effect is that some statistics programs assume Gaussian noise characteristics when computing properties such as the median and mode. Quantized noise can have surprising effects on these programs. Based upon the analysis of a variety of possible strategies for sky determination ([WFPC2 ISR 96-03](#)), the centroid and the optimal filter (*ofilter*) of the histogram of sky pixel values were found to produce the least biased result for typical WFPC2 data with low background levels.

### Red Leaks

Several of the UV filters have substantial red leaks that can affect the photometry. For example, the U filter (F336W) has a transmission at 7500 Å that is only about a factor of 100 less than at the peak transmission at about 3500 Å. The increased sensitivity of the CCDs in the red, coupled with the fact that most sources are brighter in the red, makes this an important problem in many cases. The **synphot** tasks can be used to estimate this effect for any given source spectrum.

As part of a closeout calibration program (CAL/WFPC2 11327, PI Chiaberge), a red star and a blue star were observed with the aim of better characterizing the red leaks in the WFPC2 UV filters, and derive more accurate correction factors. Please refer to [WFPC2 ISR 09-07](#) for the most updated information.

As a result of this work, revised SYNPHOT throughput curves were derived for the F185W, F218W, and F255W filters. It is also possible that post-mission laboratory tests on the WFPC2 filters may yield new results on the filter red leaks, and readers are advised to check for any new reports on this subject.

### Charge Traps

There are about 30 macroscopic charge transfer traps, where as little as 20% of the electrons are transferred during each time step during the readout. These defects result in bad pixels, or in the worst cases, bad columns and should not be confused with microscopic charge traps which are believed to be the cause of the CTE problem. The traps result in dark tails just above the bad pixel, and bright tails for objects farther above the bad pixel that get clocked out through the defect during the readout. The tails can cause large errors in photometric and astrometric measurements. In a random field, about 1 out of 100 stars are likely to be affected. Using a program which interpolates over bad pixels or columns (e.g., **wfixup** or **fixpix**) to make a cosmetically better image can result in very large (e.g., tenths of magnitude) errors in the photometry in these rare cases. See also [Section 3.6.4](#).

### Exposure Times: Serial Clocks

The serial clocks option (i.e., the optional parameter `CLOCKS = YES` in the Phase II proposal instructions) is occasionally useful when an extremely bright star is in the field of view, in order to minimize the effects of bleeding. However, the shutter open time can have errors of up to 0.25 seconds due to the manner in which the shutters are opened when `CLOCKS = YES` is specified. If the keyword `SERIALS = ON` is in the image header, then the serial clocks were employed. Header information can be used to correct this error. The error in the exposure time depends on the `SHUTTER` keyword. If the value of this keyword is “A”, then the true exposure time is 0.125 seconds less than that given in the header. If instead

the value is “B”, then the true exposure time is 0.25 seconds less than the header value.

Users should also note that exposure times of non-integral lengths in seconds cannot be performed with the serial clocks on. Therefore, if a non-integral exposure time is specified in the proposal, it will be rounded to the nearest second. The header keywords will properly reflect this rounding, although the actual exposure time will still be short as discussed above.

### **F1042M Extended Halo**

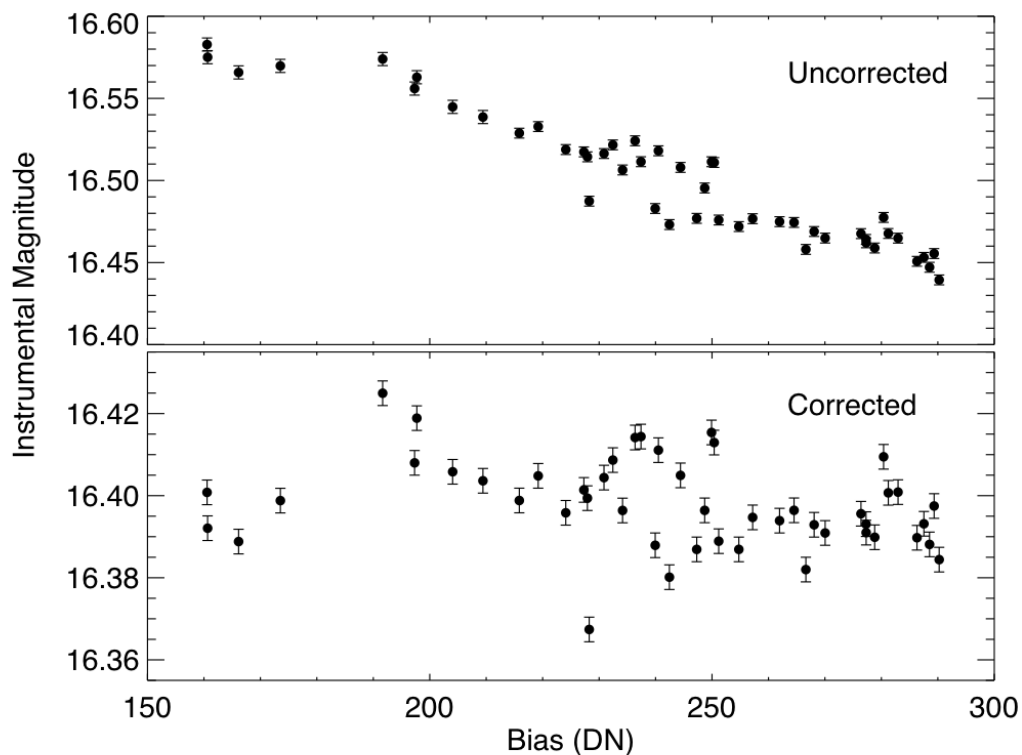
Observers using the F1042M filter should be aware that it possesses an anomalous PSF containing additional light in a broad halo component. The defocused halo is likely due to the CCD detector becoming transparent at this wavelength, so that the light is reflected and scattered by the back of the CCD. The scattering will impact photometry in the F1042M filter relative to other filters, since a greater fraction of the counts will lie outside the 1 arcsecond diameter aperture used for photometry on standard stars. The [WFPC2 Instrument Handbook](#) provides a comparison of azimuthal averages for an observed F1042M and F953N PSFs; additional PSF examples are in the [WFPC2 PSF Library](#).

### **WF4 Anomaly and Correcting Background Streaks**

Some WF4 images obtained after March 2002 show a reduction in the detector gain. Characterized by low or zero bias levels, faint horizontal streaks, and low photometry, the WF4 anomaly is thought to be caused by a failing amplifier in the WF4 signal-processing electronics. Examples of images affected by the WF4 anomaly are shown in [Figure 4.1](#) and [Figure 5.6](#)

A correction algorithm, described in [WFPC2 ISR 09-03](#) and incorporated into the calibration pipeline, rescales each pixel by a factor that depends on both the bias level of the entire image and the observed counts in the individual pixel. Photometric tests indicate that stellar magnitudes derived from corrected images are generally accurate to  $\sim 0.01$  magnitudes rms ([Figure 5.4](#)).

**Figure 5.4: Instrumental Magnitudes of the Standard Star GRW+70D5824 as Observed on the WF4 Chip (with gain 7) vs. the WF4 CCD Bias Value**



**In the upper panel, the data are processed with the WF4 gain correction turned off, and the star appears fainter in low-bias images. In the lower panel, the data are corrected for the WF4 anomaly, and the resulting magnitudes are independent of bias. The standard deviation in the corrected sample is 0.01 magnitudes. Error bars are purely statistical.**

A new Pyraf task, `wdestreak`, ([WFPC2 ISR 2008-03](#)) uses data from the entire image to model and subtract the horizontal streaks seen in WF4 images with low bias values while preserving the photometric accuracy of the image. This stand-alone task is not included in the WFPC2 calibration pipeline, as it can require manual intervention, especially for crowded fields. It should be performed after all other calibration steps have been completed.

The procedure involves creating a mask in which all pixels affected by cosmic rays or bright sources are given zero values. This is an iterative process. For a detailed discussion of this algorithm, see ([WFPC2 ISR 2008-03](#)).

For a given image, the correction for each row is the difference between the mean value of the unmasked pixels within the row and the global mean of all the unmasked pixels in the image. The correction can be either positive or negative and is applied to all pixels in the row. The algorithm thus flattens the background and gives more accurate photometry for faint

objects. A detailed discussion and comparison of photometry before and after the application of this procedure can be found in [WFPC2 ISR 2008-03](#).

**wdestreak** can be found in the **stdas.hst\_calib.wfpc** package. The graphic user interface parameter file for **wdestreak** is shown in [Figure 5.5](#). The meaning of the various parameters is explained below:

The **group** parameter specifies which image group to correct, and has a default value of 4 for WF4. This procedure can also be used to correct streaks in any of the WFPC2 chips by specifying the appropriate value (1, 2, 3, or 4). To correct streaks in multiple chips, the procedure must be run multiple times, specifying one group at a time.

The row threshold parameter **row\_thresh** sets the minimum absolute value of the allowed correction, so if a calculated correction is less than this value for a given row, no correction will be applied to that row. The default value for this parameter has been set to an arbitrary value of 0.1. It is important to have a value greater than zero and ideally equal to the mean sigma of the sky background for this parameter to avoid over smoothing of the background.

The parameter **bias\_thresh** is compared to the mean of the pixels remaining after clipping. If the bias threshold is exceeded by the image mean, no correction will be applied to the image. The default value for this parameter is  $10^5$ . As this value exceeds any image's bias value, by default the task will calculate and apply the corrections. This parameter is provided to allow the users to apply the task to multiple input files from within their higher-level script.

The parameter **input\_mask** is an optional parameter. A mask is created by the program as described above. The user can optionally supply a mask instead of having the program calculate a mask. This option allows the user to fine-tune the process, by first running the program and allowing it to create a mask, editing the mask, then running the program with the edited mask as input.

The parameter **niter** sets the number of iterations to use in the source masking step; the default is 5, and the maximum allowed value is 10. A greater (lesser) value generally results in more (fewer) pixels being masked around bright sources or cosmic rays.

A challenging example of how the results can be improved by changing the default values of **wdestreak** is illustrated in [Figure 5.6](#). This routine has been tested on several types of data (images with stars, small extended sources, large galaxies, etc.) and is seen to work satisfactorily.

**Figure 5.5: Parameter File of the Task wdestreak Within Pyraf**

PyRAF Parameter Editor: wpc.wdestreak

File Options Help

Package = WFPC  
Task = WDESTREAK

Execute Save Save As... Unlearn Cancel Task Help

input

(group)

(row\_thresh)

(bias\_thresh)

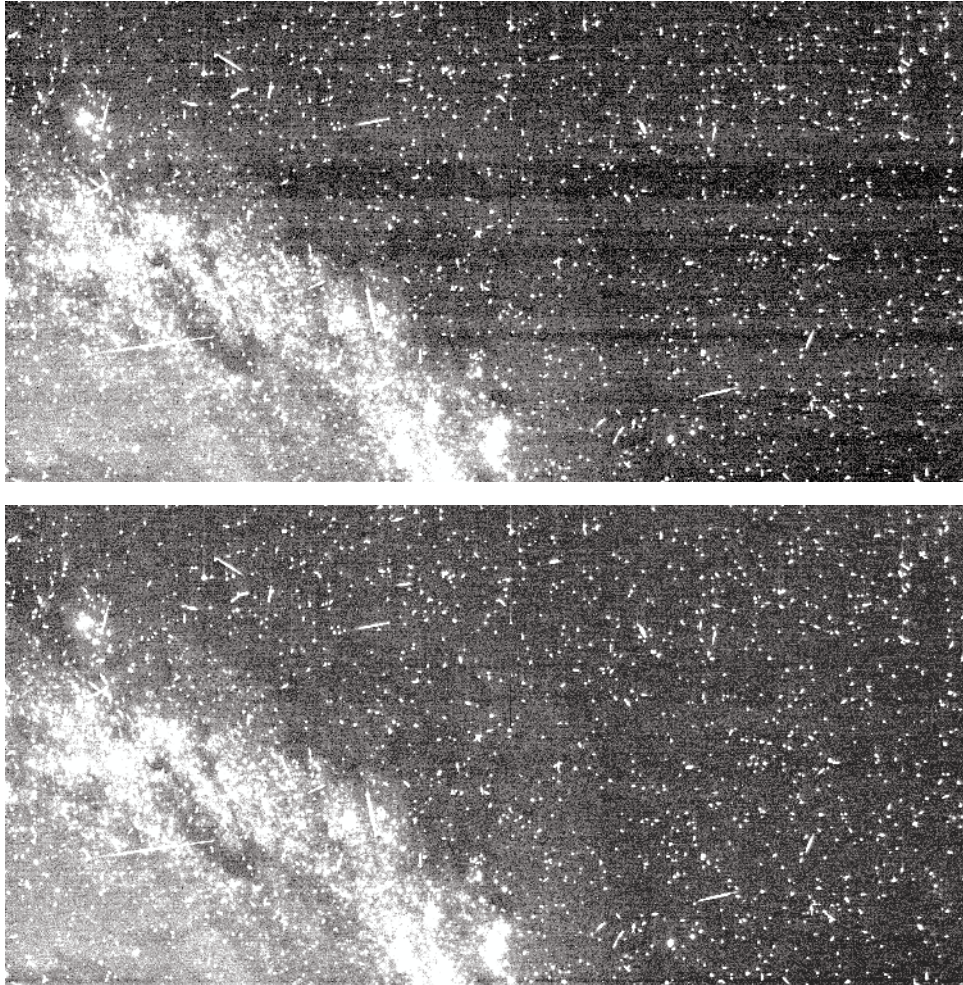
(input\_mask)

(niter)

(verbosity)  Yes  No level for diagnostic print statements

(mode)

**Figure 5.6: An Illustration of the Streak Removal Process in a Complex Case**



**Top: image of a spiral galaxy on the WF4 chip. Note the presence of several horizontal streaks on the image. Bottom: the resulting image obtained after processing with wdestreak.**

#### 5.2.4 Photometry on Saturated Stars With WFPC2.

The CCDs on STIS and ACS have been proven to remain perfectly (to test limits  $< \sim 0.1\%$ ) linear beyond saturation of the detector when a gain is used that samples beyond the detector full well depth. In the above cases, photometry of even heavily saturated sources can be accurately recovered by simply summing the counts over all of the CCD pixels that have been bled into along the columns.

For WFPC2 it is likely that the CCD itself remains linear beyond saturation, however, even at  $\text{GAIN} = 15$  (approximately  $14 \text{ e}^-/\text{DN}$ ) the analog-to-digital converter samples only some 60% of the full well depth.

Therefore to recover photometry on saturated targets two approaches are generally possible and have been applied several times in the literature.

The first approach relies on knowledge of the WFPC2 PSF and performs fits using only the unsaturated wings. The second approach is more analogous to the simple summation over all pixels that have been bled into that works very well for STIS and ACS, but with the caveat that for WFPC2, empirical estimates need to be made about the effective full well depth of the pixel count levels since these are not sampled by the electronics.

Gilliland (1994, ApJ 435, L63-66) analyzed back-to-back WFPC2 exposures in the same filter with significantly different exposure times, which provided many measurements of stars unsaturated in the short exposure and saturated in the long exposure, to establish simple algorithms for recovering photometry of saturated point sources. If the gain = 14 e<sup>-</sup>/DN option was used, it is possible to generally recover photometry to a precision of ~2% for stars up to at least 5 magnitudes brighter than saturation. This is a simple means of extending the useful dynamic range of WFPC2 photometry on the bright side in archival data.

### 5.2.5 Example: Point Source Aperture Photometry with WFPC2

This observation of Omega Cen (from proposal 11040, visit 6, exposure 2) has three sub-exposures taken at the same pointing, each 500 seconds long. The task **hselect** can be used to get some additional information about the data, like date of observation, gain, and filter.

```
-->hsel *c0m.fits[1]
$I, date-obs, atodgain, filtnam1, filtnam2 yes
ua3f0603m_c0m.fits[1] 2007-12-25 7.0 F218W
ua3f0604m_c0m.fits[1] 2007-12-25 7.0 F218W
ua3f0605m_c0m.fits[1] 2007-12-25 7.0 F218W
```

Outlined below are the steps for obtaining  $STMAG_{F218W}$  magnitudes. Note: this example is meant for calibrated WFPC2 data (`c0m.fits` or `.c0h/.c0d` files), not drizzled WFPC2 images.

1. Apply the pixel area corrections and 34th row corrections to the calibrated images (`c0m.fits`). (Never apply those corrections to drizzled images [`drz.fits`] because geometric distortion corrections are handled by the **multidrizzle** task.)
2. Combine the images using the STSDAS task **crrej**.
3. For the purposes of this exercise, manually select several stars in WF2 for photometric measurement. Then run the aperture photome-

try task, **phot**, on the stars using two aperture sizes; one will be used for CTE correction and the other for determining the aperture correction to a radius of 0".5.

4. Apply an aperture correction to convert counts in aperture radius of 2 pixels to a radius of 0".5.
5. Perform the CTE correction for the stars using aperture-corrected counts, for a 0".5 radius, from step 4.
6. Determine the contamination and long-term QE change corrections using the value of the group header keyword ZP\_CORR.
7. Use the value of the group header keyword PHOTFLAM to determine the  $STMAG_{F218W}$  zeropoint. Complete the final calculations by computing the magnitude, applying the CTE corrections (step 5), zeropoint correction (step 6), and the aperture correction from radii 0".5 to an infinite aperture (subtract 0.1 mag).

### *1. Apply the Pixel Area Corrections and 34th Row Corrections*

Retrieve the pixel area reference file (`f1k1552bu_r9f.fits`) from the [WFPC2 IDT Reference Files](#) Web page. Place it in the working directory with the science images. Since the pixel area map file is in wFITS format, convert it to GEIS.

```
-->unlearn strfits
-->strfits f1k1552bu_r9f.fits "" ""
```

Multiply the calibrated science images with the pixel area correction reference image.

```
-->imcalc "ua3f0603m_c0m.fits,f1k1552bu.r9h" ua3f0603m_c0m_a.fits "im1*im2"
-->imcalc "ua3f0604m_c0m.fits,f1k1552bu.r9h" ua3f0604m_c0m_a.fits "im1*im2"
-->imcalc "ua3f0605m_c0m.fits,f1k1552bu.r9h" ua3f0605m_c0m_a.fits "im1*im2"
```

Apply the 34th row correction. Since the arithmetic operation is a bit long, the expression can be written to a file. For instance, create the file “row34” that contains the following text:

```
if mod(y+3.95,34.1333) .le. 1.0 then im1*0.97 else im1*1.0
```

```
-->imcalc ua3f0603m_c0m_a.fits ua3f0603m_c0m_ar.fits @row34
-->imcalc ua3f0604m_c0m_a.fits ua3f0604m_c0m_ar.fits @row34
-->imcalc ua3f0605m_c0m_a.fits ua3f0605m_c0m_ar.fits @row34
```

## 2. Combine the Images

Combine the three corrected images using **crrej**. The image A-to-D gain is 7, and the read noise is  $5 e^-$  (0.72 DN). Make a list of the input images and their data quality files (the rootnames in both lists should match on each line.)

```
-->ls *c0m_ar.fits > c0m_ar.list
-->ls *c1m.fits > c1m.list
```

Restore the task parameters to default values, which are optimized for WFPC2 data, then run the **crrej** task.

```
-->unlearn crrej
-->unlearn dq # this is a pset or sub-task called by crrej
-->crrej @c0m_ar.list omegacen_f218w.fits @c1m.list "8,6,4" readnoise=0.72 atodgain=7
```

## 3. Run *phot* to Obtain Counts in Aperture Radii of 2 and 5 Pixels

Since there are just a few stars in each chip, the coordinate list has been created manually by picking 26 stars in WF2. For more crowded fields, the IRAF task **noao.digiphot.apphot.daofind** can be used to automatically detect point sources. The positions of the 26 manually-selected stars in WF2, centered using the task **imcntr**, is placed in the file `pos_wf2.list`:

```
-->!more pos_wf2.list
638.25    64.937
210.183   138.871
453.005   147.169
437.849   154.779
744.413   154.87
179.897   248.266
243.093   377.254
483.531   466.359
685.466   477.136
83.106    571.06
501.502   681.156
194.527   752.31
236.199   659.211
253.000   592.493
377.181   675.592
433.861   665.613
712.928   430.216
656.501   366.000
615.100   343.866
442.029   230.301
546.028   249.210
574.204   110.349
581.300   140.000
685.699   257.229
768.318   204.956
```

Determine the **phot** parameters for these images:

- the A-to-D gain parameter: **epadu** = 7
- the read noise, in electrons, for three combined images is  $\sqrt{(5^2 \times 3)}$ , **readnoise** = 8.66
- the sky area is an annulus that's 15 pixels away from the star's center and 5 pixels wide, **annulus** = 15, **dannulus** = 5
- for CTE corrections (Dolphin 2009), photometry for WF point sources need to be measured with an aperture radius = 2 pixels. The photometry then needs to be aperture-corrected to a radius of 0".5 or 5 WF pixels for the CTE corrections—this will be done by selecting a few well-exposed stars from the list, as outlined in step 4. Therefore, **apertures** = "2,5"

The help file for **phot** has a lot of information about setting the task parameters.

Load the **phot** package:

```
-->noao
-->digi
-->apphot
```

Reset the **phot** parameters and its psets, then run **phot** using the coordinate list `pos_wf2.list`. (The results are written to a file, using a default file-naming convention, which is the image name followed by the suffix ".mag.1.")

```
-->unlearn phot
-->unlearn datapars
-->unlearn centerpars
-->unlearn fitskypars
-->unlearn photpars
-->phot omegacen_f218w.fits[2] epadu=7 readnoise=8.66
annulus=15 dannulus=5 apertures="2,5"
coords="pos_wf2.list" exposure=exptime interactive=no
verify=no
-->ls *mag*
omegacen_f218w.fits2.mag.1
```

The photometric measurements for the 26 stars are written to the file `omegacen_f218w.fits2.mag.1`. The task **txdump** is then used to extract information from that output file, which is redirected to `mag_f218w.txt`; an excerpt is shown below.

```

-->txdump omegacen_f218w.fits2.mag.1 "xinit,yinit,msky,stdev,flux"
yes > mag_f218w.txt

-->!more mag_f218w.txt

638.250  64.937   0.2712871  1.425934  1388.22   1733.069
210.183  138.871   0.3004114  1.381436  2622.651  3146.707
453.005  147.169   0.3805611  1.563836  2015.067  2430.098
437.849  154.779   0.5881297  1.478667  2341.49   2816.261
744.413  154.870  -0.1140052  1.382533  1675.304  2101.08
179.897  248.266   0.4207503  1.453788  723.9127  873.957
243.093  377.254   0.3069543  1.461139  1485.52   1803.764
.....

```

In the file `mag_f218w.txt` listed above, each row contains measurement information for one star. The numbers in each column correspond to the following parameters<sup>7</sup>:

|          |       |   |
|----------|-------|---|
| column 1 | xinit | <i>x</i> position                           |
| column 2 | yinit | <i>y</i> position                           |
| column 3 | msky  | sky counts per pixel in units of DN         |
| column 4 | stdev | standard deviation of msky                  |
| column 5 | flux  | total counts in aperture radius = 2 pixels  |
| column 6 | flux  | total counts for aperture radius = 5 pixels |

As the calculations proceed, each successive value will be appended in a column at the end of each row.

#### 4. Aperture Correction from $r = 2$ Pixels to $r = 5$ Pixels

By convention, the magnitude in a  $0''.5$  radius aperture is converted to an infinite aperture by subtracting 0.1 mag. But first, the counts in aperture radius = 2 pixels need to be converted to counts in radius = 5 pixels ( $0''.5$ ), by applying an aperture correction.

This is done by first selecting a few well-exposed stars that were measured earlier in **phot**. In this exercise, eight stars (in file `reference_stars.txt`) were used to calculate the fractional value needed to convert counts in a 2 pixel aperture radius to that of a 5 pixel aperture radius. The median fractional value for those stars is adopted as the aperture correction.

---

7. The column definitions and **phot** parameters are recorded in the **phot** output file, `omegacen_f218w.fits2.mag.1`.

```

-->!more reference_stars.txt

210.183 138.871 0.3004114 1.381436 2622.651 3146.707
453.005 147.169 0.3805611 1.563836 2015.067 2430.098
437.849 154.779 0.5881297 1.478667 2341.49 2816.261
179.897 248.266 0.4207503 1.453788 723.9127 873.957
243.093 377.254 0.3069543 1.461139 1485.52 1803.764
483.531 466.359 0.3940198 1.319769 2173.86 2603.825
685.466 477.136 0.5255948 1.555987 2210.843 2674.164
83.106 571.06 0.3655507 1.510812 1167.822 1408.229

-->tcalc reference_stars.txt c7 "c6/c5"

210.183 138.871 0.3004114 1.381436 2622.651 3146.707 1.1998
453.005 147.169 0.3805611 1.563836 2015.067 2430.098 1.2060
437.849 154.779 0.5881297 1.478667 2341.49 2816.261 1.2028
179.897 248.266 0.4207503 1.453788 723.9127 873.957 1.2073
243.093 377.254 0.3069543 1.461139 1485.52 1803.764 1.2142
483.531 466.359 0.3940198 1.319769 2173.86 2603.825 1.1978
685.466 477.136 0.5255948 1.555987 2210.843 2674.164 1.2096
83.106 571.06 0.3655507 1.510812 1167.822 1408.229 1.2059

--> tstat reference_stars.txt c7
# reference_stars.txt c11
# nrows      mean      stddev      median      min      max
      8      1.205407791    0.0052833    1.20591    1.19779    1.21423

```

The median fractional aperture correction is  $1.2059 \pm 0.0053$ . This value, multiplied with the total counts in an aperture radius of 2 pixels, will give aperture-corrected total counts for an aperture radius =  $0''.5$ . These counts will be used in the next step for determining the CTE correction. An excerpt of `mag_f218w.txt`, below, shows column 7 with aperture-corrected counts.

```

-->tcalc mag_f218w.txt c7 "c5 * 1.2059"

-->!more mag_f218w.txt

 638.25  64.937 0.2712871 1.425934 1388.22 1733.069 1674.054
210.183 138.871 0.3004114 1.381436 2622.651 3146.707 3162.655
453.005 147.169 0.3805611 1.563836 2015.067 2430.098 2429.969
437.849 154.779 0.5881297 1.478667 2341.49 2816.261 2823.603
744.413 154.87 -0.1140052 1.382533 1675.304 2101.08 2020.249
179.897 248.266 0.4207503 1.453788 723.9127 873.957 872.9663
.....

```

### 5. Calculate CTE Loss

Determine the CTE loss using the aperture-corrected counts obtained in step 4, using the correction formulae by [Dolphin \(2009\)](#)<sup>8</sup>.

$$\text{lb}g = \ln(\sqrt{\text{background}^2 + 1}) - 1$$

“background” is the sky counts in units of electrons.

(Reminder: when operating on a text table, the column nomenclature is *c* followed by the column number. Below, *c8* is column 8, which is a new column for storing the value of *lb**g*. *c3* is the sky counts [*m*sky] in DN multiplied by the gain, 7, for conversion to electrons.)

```
-->tcalc mag_f218w.txt c8 "log(sqrt((c3*7)**2 + 1)) - 1"
```

$$\text{yr} = (\text{MJD} - 49461.9) / 365.25$$

MJD is the date of observation in Modified Julian Date. That value, stored in the image header keyword EXPSTART, is 54459.96.

```
-->tcalc mag_f218w.txt c9 "(54459.96 - 49461.9)/365.25"
```

$$\text{XCTE}(\text{mag}) = 0.0077 * \exp(-0.50 * \text{lb}g) * (1 + 0.10 * \text{yr}) * x / 800$$

```
-->tcalc mag_f218w.txt c10 "0.0077*exp(-0.50*c8)*(1+0.10*c9)*c1/800"
```

$$\text{lct} = \ln(\text{counts}) + 0.921 * \text{XCTE} - 7$$

(“counts” for aperture radius = 0".5, in electrons)

```
-->tcalc mag_f218w.txt c11 "log(c7*7) + 0.921*c10 - 7"
```

$$\text{C1} = \max(1.0 - 0.201 * \text{lb}g + 0.039 * \text{lb}g * \text{lct} + 0.002 * \text{lct}, 0.15)$$

```
-->tcalc mag_f218w.txt c12 "max(1.0-0.201*c8+0.039*c8*c11+0.002*c11, 0.15) "
```

$$\text{C2} = 0.96 * (\text{yr} - 0.0255 * \text{yr} * \text{yr}) * \exp(-0.450 * \text{lct})$$

```
-->tcalc mag_f218w.txt c13 "0.96*(c9-0.0255*c9*c9)*exp(-0.450*c11) "
```

$$\text{YCTE}(\text{mag}) = 2.41 * \ln(\exp(0.02239 * \text{C1} * \text{y} / 800) * (1 + \text{C2}) - \text{C2})$$

```
-->tcalc mag_f218w.txt c14 "2.41*log(exp(0.02239*c12*c2/800)*(1+c13)-c13) "
```

$$\text{Total CTE loss (radius = 5 pix)} = \text{XCTE} + \text{YCTE}$$

8. Please check the Dolphin CTE web page for the latest CTE correction equations and coefficients. [http://purcell.as.arizona.edu/wfpc2\\_calib/](http://purcell.as.arizona.edu/wfpc2_calib/)

XCTE and YCTE, in magnitudes, are in columns c10 and c14, respectively. The CTE correction will be applied after the aperture-corrected radius = 0".5 counts are converted to magnitudes.

### 6. Corrections for UV Contamination and Long-term QE Change

Two time-dependent corrections need to be applied to the magnitudes: changes in throughput due to UV contamination at the time of the observation and long-term QE changes (see [Section 5.2.1, UV Contamination](#)). These quantities (in magnitudes) have already been computed as part of the pipeline calibration, and are stored in the group header keyword ZP\_CORR. Therefore, to correct for UV contamination and QE change, simply add the value of ZP\_CORR from the aperture-corrected magnitude. This zeropoint correction, for F218W/WF2, can be obtained using the task **hselect**:

```
-->hsel *c0m.fits[2] $I,zp_corr yes
ua3f0603m_c0m.fits[2]    -0.06900072
ua3f0604m_c0m.fits[2]    -0.06902218
ua3f0605m_c0m.fits[2]    -0.06904125
```

### 7. Compute $STMAG_{F218W}$ with CTE Corrections, Zeropoint Corrections, and Aperture Correction to an Infinite Aperture

The  $STMAG_{F218W}$  values for the stars are computed as:

$$STMAG_{F218W} = -2.5 * \log_{10}(\text{total counts} / \text{exposure time}) + ZP_{F218W} - \text{Corrections}$$

where,

- Corrections = XCTE + YCTE + 0.1
- $ZP_{F218W} = -2.5 * \log_{10}(\text{PHOTFLAM}) - 21.1$
- “total counts” refers to total counts for aperture-corrected radius = 0".5
- exposure time<sup>9</sup>: 500 seconds x 3 = 1500 seconds

The PHOTFLAM keyword value, from group 2 of the input image headers, is 9.886809E-16. Therefore,

$$\begin{aligned} ZP_{F218W} &= -2.5 * \log_{10}(9.886809E-16) - 21.1 \\ &= 16.4124 \end{aligned}$$

---

9. The exposure time for an image combined using **crrej** is the sum of exposure times of all input images.

Calculating the  $STMAG_{F218W}$  values:

```
tcalc mag_f218w.txt c15 "-2.5 * log10(c7/1500) + 16.4124 + 0.0690 - (c10 +
c14 - + 0.1)"
```

To extract some values, such as x- and y-positions and final magnitudes (columns 1, 2, and 15, respectively), use the task **tdump**.

```
-->tdump mag_f218w.txt columns="c1,c2,c15" datafile=final_f218w_wf2_mag.txt
-->!more final_f218w_wf2_mag.txt

 638.2500000000001      64.9370000000001      16.2281600000001
 210.1830000000001           138.871      15.5358400000001
 453.0050000000001      147.1690000000001      15.8131200000001
 437.8490000000001           154.779      15.6532700000001
 744.4130000000001           154.87      15.9921000000001
 179.8970000000001           248.266      16.8848300000001
           243.093      377.2540000000001      16.0843500000001
 483.5310000000002      466.3590000000001      15.6595800000001
           685.466      477.1360000000001      15.6394100000001
 83.1060000000002      571.0600000000001      16.2904300000001
 501.5020000000001      681.1560000000001      16.0612500000001
           194.527      752.3100000000003      16.3198900000001
 236.1990000000001           659.211      15.6801300000001
           253.      592.4930000000001      16.4232300000001
 377.1810000000001      675.5920000000001      16.7855300000001
 433.8610000000001      665.6130000000002      15.8284000000001
 712.9280000000003      430.2160000000002      15.8013200000001
 656.5010000000002           366.      16.4186700000001
           615.1      343.8660000000001      16.6057800000001
 442.0290000000001           230.301      15.8076500000001
 546.0280000000001           249.21      15.7717300000001
 574.2040000000001           110.349      16.5587900000001
           581.3           140.      15.1244300000001
 685.6990000000001      257.2290000000001      15.8432100000001
 768.3180000000001           204.956      15.9086900000001
 270.9920000000001      372.2180000000001      16.3781700000001
```




---

*For higher precision photometric analysis, the CTE corrections should be run on the individual calibrated images. Objects in individual images are frequently contaminated by cosmic rays and their associated deferred charge trails, so some of the CTE-corrected values from individual images may be unsuitable for use. A statistical study of these individual CTE-corrected values can help determine the best ones to select for your final photometric measurements.*

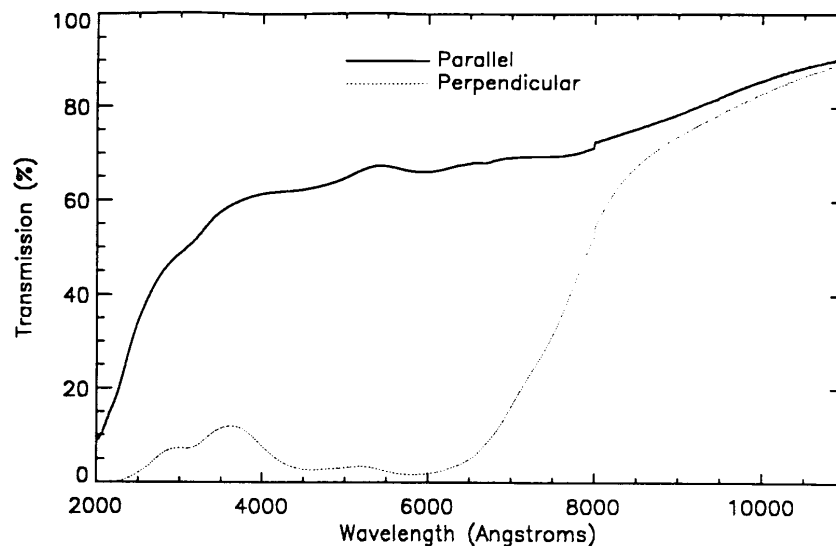
---

## 5.3 Polarimetry

WFPC2 has a polarizer filter which can be used for wide-field polarimetric imaging from about 200 nm through 700 nm. This filter is a “quad,” meaning that it consists of four panes, each with the polarization angle oriented in a different direction, in steps of  $45^\circ$ . The panes are aligned with the edges of the pyramid, thus each pane corresponds to a chip. However, because the filters are at some distance from the focal plane, there is significant vignetting and cross-talk at the edges of each chip. The area free from vignetting and cross-talk is about  $60''$  square in each WF chip, and  $15''$  square in the PC. It is also possible to use the polarizer in a partially rotated configuration, which gives additional polarization angles at the expense of more severe vignetting.

Each polarimetry observation consists of several images of the same object with different orientations of the polarizer angle. A minimum of three observations is required to obtain full polarimetry information. This can be achieved by observing the target in different chips, by rotating the filter wheel (partial rotation), or by changing the orientation of the HST field of view in the sky, using a different roll angle. In the latter case, observations must frequently occur at different times, as the solar array constraints on HST allow only a limited range of roll angles at any given time.

Accurate calibration of WFPC2 polarimetric data is rather complex, due to the design of both the polarizer filter and the instrument itself. WFPC2 has an aluminized pick-off mirror with a  $47^\circ$  angle of incidence, which rotates the polarization angle of the incoming light, as well as introducing a spurious polarization of up to 5%. Thus, both the HST roll angle and the polarization angle must be taken into account. In addition, the polarizer coating on the filter has significant transmission of the perpendicular component, with a strong wavelength dependence (see [Figure 5.7](#)).

**Figure 5.7: Parallel and Perpendicular Transmission of the WFPC2 Polarizer**

A calibration accuracy of about 2% rms for well-exposed WFPC2 polarimetry data has been achieved ([WFPC2 ISR 97-11](#)). The method uses a Mueller matrix approach to account for the orientation of both telescope and polarizer, the effect of the pick-off mirror, and the significant perpendicular transmission of the polarizer itself. A full description of the motivation behind this approach, the implementation details, and the necessary caveats are given in the ISR mentioned above. A web-based tool to aid in the calibration of polarization data has also been developed, see [WFPC2 Polarization Calibration Tools](#) Web site. With the aid of this tool, polarization properties can be derived for point sources and extended sources from an arbitrary combination of polarized images.

The procedure to obtain polarization information begins with the calibrated images, as they come out of the pipeline (plus cosmic ray and warm pixel rejection, if appropriate). The circumstances of the polarized images and the fluxes in each image are entered in the Web tool, and the calculation started. The tool then reports the values of the Stokes parameters  $I$ ,  $Q$ , and  $U$ , as well as fractional polarization and position angle. The optional **synphot** values in the first part of the tool can be used to fine-tune the results to a specific spectral energy distribution, but are in most cases not necessary.

The tool also reports expressions for  $I$ ,  $Q$ , and  $U$  as a function of fluxes in the three images. These can be used to test the sensitivity of the results to errors in the individual fluxes, or to combine images in order to obtain pixel-by-pixel values of the Stokes parameters for extended objects, resulting in  $I$ ,  $Q$ , and  $U$  images.

More details will be provided in a future ISR, as well as in the extensive help available in the Web tool itself.

## 5.4 Astrometry

It is important to distinguish three very different conditions under which observers can perform astrometric measurements with WFPC2: relative astrometry within a chip, relative astrometry among the four chips, and absolute astrometry.

### 5.4.1 Relative Astrometry Within a Chip

Relative measurements of objects in a single WFPC2 chip and single image provide the most precise astrometric measurements possible with WFPC2. With an adequate *effective PSF* model (ePSF), a well-exposed point source can be measured with respect to another in the chip with a precision of  $\sim 1$  mas.

However, if the objects are in two different WFPC2 images (e.g., taken at different epochs), additional effects come into play. The thermal “breathing” of the telescope introduces changes in the linear terms (e.g., image scale) up to  $\sim 1$  part in 4000 (or  $\sim 30$  mas across a WFC CCD).<sup>10</sup>

In order to achieve precision approaching 1 mas between two different images, it is necessary to solve for the linear transformations between the them. This can be done, provided that the field has enough well-measured point sources evenly distributed across the camera field (at least a dozen). The steps needed to achieve these high precisions are discussed below.

#### Artifacts: the 34th-row Problem

A small manufacturing defect occurs approximately every 34th row on each WFPC2 chip. This was due to an error of closure at each successive placement of the reticle used to define the CCD pixels (Shaklan, Sharman, & Pravdo 1995, *App. Opt.*, 34, 6672). The defects introduce errors in photometry at the 0.01 to 0.02 magnitude level for about 6% of stars, and periodic systematic errors in astrometry for all stars at an amplitude of 0.03 pixels (i.e.  $\sim 3$  mas for WFs, and  $\sim 1.4$  mas for PC). The best-available correction for the 34th row defect, as described in the equations below, was published by Anderson & King (1999, *PASP*, 111, 1095).

$$\begin{aligned}
 Y &= Y_{\text{raw}} + 0.06 (0.25 - p); \text{ if } p \leq 0.5 \\
 Y &= Y_{\text{raw}} + 0.0008920 (p - 17.3167); \text{ if } p > 0.5 \\
 \text{where } p &= (y + 3.70) \bmod 34.1333
 \end{aligned}$$

10. Other potential effects include velocity aberration and any long-term changes in the camera optics.

### Undersampling and the Effective PSF

The sampling parameter,  $r$ , is defined as the ratio between the FWHM of the PSF and the pixel scale ( $r = \text{FWHM}/\text{pixel-size}$ ). A value of  $r$  below 2.335 is considered an undersampled condition because there is not enough coverage of the point spread function (PSF) by CCD pixels to utilize the full-resolving power of the camera. An imperfect effective PSF (ePSF, instrumental plus the intra-pixel response function) would generate systematic offsets, known as pixel-phase errors.

The PC1 and WF detectors are undersampled; in particular WFs are severely undersampled ( $r \sim 1$ ). Anderson & King (2000, PASP, 112, 1360) developed a procedure and algorithms to remove this degeneration. The underlying assumptions are:

1. the PSF remains constant in time (this assumption, for consecutive images, is a very good approximation).
2. The light of a star never falls within a single pixel (i.e., significant light always falls on surrounding pixels). This condition is necessary so that the star's position can be located within the pixel. Though the WF is undersampled, a maximum of  $\sim 40\%$  of the light falls within the central pixel, so this condition is easily satisfied.
3. Several images with different dithers are collected, such that the same stars fell in different phases with respect to the pixel boundaries (this is possible thanks to HST relative pointing precision, which is of the order of  $\sim 0.1$  PC1 pixel).

The Anderson & King method made use of the fact that the same star at different locations with respect to the pixel boundaries introduce systematic pixel-phase errors of "random" amplitude, such that the average of these amplitudes will tend to zero, providing a better answer on the actual positions of the objects. A better knowledge of the positions of the stars, from which empirical sampling of the ePSF are extracted, will improve the model of the ePSF itself. By iterating between improved positions and improved knowledge of the ePSF shape, one can solve for both. The ePSF techniques allows precision-positioning down to  $\sim 1$  mas for a well-exposed star. This basically set the limits of the best possible astrometry with WFPC2.

### Geometric Distortion

Once the position of a target has been accurately determined on the pixel grid, it is necessary to next correct for geometric distortion in the WFPC2 and HST optics. In the case of WFPC2, most of the distortion is caused by a plano-concave Magnesium Fluoride lens located a few millimeters in front of each of the four CCDs. This lens serves both as a seal on the CCD package, and as a field-flattener, hence assuring good focus across the CCD chip. This lens contributes a geometric distortion which reaches about 6 pixels between the CCD centers and corners in all four cameras.

This lens also causes a wavelength dependence on both the image scale and distortion—this dependence is weak in the visible portion of the spectrum, but changes rapidly in the far-UV where the refractive index increases sharply (Dodge, M., *Applied Optics*, 23, 1980, 1984).

An empirical solution for the geometric distortion in each camera was derived by Anderson & King, *PASP*, 115, 113, 2003. We will give a short summary of their results. A self-calibration technique was used, wherein a star field was moved to different positions on the detector. This allowed them to simultaneously solve for the true star positions as well as the geometric distortion.

For each raw-position on the chip ( $x_{obs}, y_{obs}$ ), there corresponds a correction  $[\Delta x(\tilde{x}, \tilde{y}), \Delta y(\tilde{x}, \tilde{y})]$ <sup>11</sup>, such that the new corrected position becomes:

$$\begin{aligned} x_{corr} &= x_{obs} + \Delta x(\tilde{x}, \tilde{y}) \\ y_{corr} &= y_{obs} + \Delta y(\tilde{x}, \tilde{y}) \end{aligned}$$

The positions were normalized to use a chip center of 425 and scale factor of 375 for each axis, resulting in coordinates normalized over the range in (50:800) for x and y.

$$\begin{aligned} \tilde{x} &= (x_{obs} - 425) / 375 \\ \tilde{y} &= (y_{obs} - 425) / 375 \end{aligned}$$

The corrections are in the form of a third-order polynomial. The coefficients, from Anderson & King, 2003, are reproduced in [Table 5.5](#).

$$\begin{aligned} \Delta x &= a_2 \tilde{x} + a_3 \tilde{y} + a_4 \tilde{x}^2 + a_5 \tilde{x} \tilde{y} + a_6 \tilde{y}^2 + a_7 \tilde{x}^3 + a_8 \tilde{x}^2 \tilde{y} + a_9 \tilde{x} \tilde{y}^2 + a_{10} \tilde{y}^3 \\ \Delta y &= b_2 \tilde{x} + b_3 \tilde{y} + b_4 \tilde{x}^2 + b_5 \tilde{x} \tilde{y} + b_6 \tilde{y}^2 + b_7 \tilde{x}^3 + b_8 \tilde{x}^2 \tilde{y} + b_9 \tilde{x} \tilde{y}^2 + b_{10} \tilde{y}^3 \end{aligned}$$

---

11.  $x_{obs}$ , and  $y_{obs}$  should have already been corrected for the 34th row problem.

**Table 5.5: Geometric Distortion Coefficients from Anderson & King (2003)**

| Polynomial Term | aPC1   | bPC1   | aWF2   | bWF2   | aWF3   | bWF3   | aWF4   | bWF4   |
|-----------------|--------|--------|--------|--------|--------|--------|--------|--------|
| 2               | 0.000  | 0.418  | 0.000  | 0.051  | 0.000  | -0.028 | 0.000  | 0.070  |
| 3               | 0.000  | -0.016 | 0.000  | -0.015 | 0.000  | -0.036 | 0.000  | 0.059  |
| 4               | -0.525 | -0.280 | -0.624 | -0.038 | -0.349 | -0.027 | -0.489 | -0.050 |
| 5               | -0.268 | -0.292 | -0.411 | -0.568 | -0.353 | -0.423 | -0.391 | -0.485 |
| 6               | -0.249 | -0.470 | -0.092 | -0.444 | 0.009  | -0.373 | -0.066 | -0.406 |
| 7               | -1.902 | -0.011 | -1.762 | 0.003  | -1.791 | 0.004  | -1.821 | -0.015 |
| 8               | 0.024  | -1.907 | 0.016  | -1.832 | 0.006  | -1.848 | 0.022  | -1.890 |
| 9               | -1.890 | 0.022  | -1.825 | 0.011  | -1.841 | 0.006  | -1.875 | 0.022  |
| 10              | -0.004 | -1.923 | 0.010  | -1.730 | 0.021  | -1.788 | -0.006 | -1.821 |

This geometric distortion correction removes most of the linear geometric distortion, and essentially all the non-linear parts of the distortion. As mentioned earlier, changes can occur due to breathing of the telescope tube. This effect, however, can be absorbed by linear transformations, if there are enough well-exposed fixed point sources in the studied field (a minimum 3, few dozens at best); with this scenario, two different frames can be registered down to a few mas using the most general linear transformation (6 parameters<sup>12</sup>). Once the linear variations are removed, the solution provided by Anderson & King (2003) has proved to be stable at the level of a few mas for the filters in their study. If a user does not allow for linear transformations between different frames, the results would be at the mercy of the stability of the optical system. The Anderson & King (2003) geometric distortion solutions still represent the best solution available in literature for intra-chip astrometry with WFPC2. These solutions as utilized in the geometric distortion correction reference tables (specified by the image header keyword IDCTAB) that are used for drizzling WFPC2 data.

### Velocity Aberration

The motions of the Earth around the Sun (30 km/sec) and HST around the Earth (7 km/sec) cause aberration which can amount to tens of arcseconds depending upon the target location, time of year, and position of HST in its orbit. The differential effect of this aberration causes a change in the pixel scale which can reach a maximum of about 0.3 pixels across a

---

12. Transformation in the form

$$x_2 = ax_1 + by_1 + x_0$$

$$y_2 = cx_1 + dy_1 + y_0$$

single WFC CCD (measured corner to corner). The newly reprocessed WFPC2 images include a new header keyword called `VAFAC` which stores the average value of the scale change due to velocity aberration. This keyword is used by the Drizzle software, and these effects are automatically corrected when it geometrically rectifies and scales WFPC2 images. For additional discussion of velocity aberration effects, see Cox and Gilliland (2002).

### Avoiding the Pyramid Mirror Vertices

The first ~100 pixels in  $x$  and  $y$  should be avoided for astrometric observations because of the effect of the pyramid mirror. In these regions the pyramid mirror will divert the spherically aberrated light from the OTA into more than one CCD camera, thus corrupting the PSF and making accurate astrometry impossible. (For more accurate delineation of these regions, note the 100% illumination region in [Table 1.2](#) or [Table 2.5 in the WFPC2 Instrument Handbook](#).)

### Potential Problems due to CTE

Astrometry using the ACS/WFC are affected by CTE (Kozhurina-Platais, [ACS ISR 2007-04](#)). There are currently no studies available about the effect of CTE on WFPC2 astrometry, but given the situation for the ACS, there may be a similar degradation of WFPC2 astrometric measurements due to CTE.

### Local Transformations

For completeness, it is worth mentioning that there are techniques such as the “local-transformation” approach that, under determinate circumstances, allows for sub-mas precisions (Bedin et al., 2003, *AJ*, 126, 247; Anderson et al., 2006, *A&A*, 454, 1029).

## 5.4.2 Relative Astrometry Among the Four Chips

For cases requiring accurate positional measurements of extended targets across several chips (for example, measuring the expansion of nebulae in narrow filters where there are no point sources), it is important to know the relative positions of the four WFPC2 CCDs. This information, along with the good geometric distortion solution for each CCD, enables users to perform astrometric measurements on an accurately-constructed mosaic of the entire WFPC2 field of view. The relative positions and orientations of the CCDs were carefully studied by Anderson & King (2003); a summary of their results are provided below.

A reference point for relative positions and orientations was chosen for each chip, defined as  $(x_{corr}, y_{corr}) = (425, 425)$ . To measure the relative positions of the chip, Anderson & King used the inner calibration field of the globular cluster Omega Centauri (NGC 5139) which provided a field with many relatively isolated stars. This field was observed at several

different offsets and orientations such that measurements (corrected for geometric distortion) were obtained of stars common to different CCDs. The entire 4-CCD reference frame was normalized in scale to chip 3 using F555W. By definition, WF3 in filter F555W has a scale of 1, and relative chip scales were measured with respect to it.

Using geometric distortion-corrected positions of stars common to each CCD, the position of each star in each CCD could be derived using following transformation to a master frame ( $X, Y$ ):

$$\begin{aligned} X &= \alpha [\cos\theta (x_{\text{corr}} - 425) - \sin\theta (y_{\text{corr}} - 425)] + X_o \\ Y &= \alpha [\sin\theta (x_{\text{corr}} - 425) + \cos\theta (y_{\text{corr}} - 425)] + Y_o \end{aligned}$$

where each CCD has a set of parameters:

$\alpha$  is the scale,

$\theta$  is the rotation,

$X_o$  and  $Y_o$  are the offsets.

Anderson & King (2003) made a detailed study of the time, filter, and chip dependence of these parameters. Following up on this study, additional measurements and analysis were done (by L. Bedin) to extend their work over a larger time-scale, using existing ACS/WFC observations of the core of 47 Tuc (NGC 104). The exquisite geometric distortion solution existing for ACS/WFC (Anderson 2005, “The 2005 HST Calibration Workshop”) made it possible to avoid the uncertainties and limitations of “self-calibration” (that is, using WFPC2 data to calibrate itself).

A reference frame was derived from 205 ACS/WFC images. This field was also observed by WFPC2, which obtained about 1500 images from 1995 to 2008, and in 16 filters. This set of data provided an ideal laboratory to verify the Anderson and King 2003 study, and extend that work through the epoch 2008.

The variation of the skew terms were also investigated, using 6-parameter transformations of the individual WFPC2 CCDs to the ACS/WFC reference frame, in the form:

$$\begin{aligned} X &= A (x_{\text{corr}} - 425) + B (y_{\text{corr}} - 425) + X_o \\ Y &= C (x_{\text{corr}} - 425) + D (y_{\text{corr}} - 425) + Y_o \end{aligned}$$

The parameters  $A B C D$  can be related to scale, rotation, and shifts:

$$\begin{aligned} \text{SCALE} &= \alpha = \text{sqrt}(A * D - B * C) \\ \theta &= \text{atan2}((B - C), (A + D)) \end{aligned}$$

The two skew terms were defined as a simple functions of ABCD:

$$\begin{aligned} \text{SKEW1} &= (A - D) / 2.0 \\ \text{SKEW2} &= (B + C) / 2.0 \end{aligned}$$

If  $A = D$ , then there was no “on-axis” skew, the  $x$  and  $y$  axes have the same scale. If  $B = -C$ , then it means that the two systems have the same angle between their  $x$  and  $y$  axes.

### Relative Angles

In [Figure 5.8](#) and [Table 5.6](#), the solution for the relative angle between the axes of the chips (after distortion corrections) are shown as a function of time. Everything is in the meta-chip coordinate system, measured relative to chip WF3/WFPC2 (with filter F555W), which was chosen because WF3 is in a symmetric position with respect to the other chips. It can be clearly noted that the relative orientations of the chips remain nearly constant with time, well within  $\pm 0^{\circ}.005$ .

**Figure 5.8: Relative Angle between the Chip Axes (After Distortion Correction) as a Function of Time**

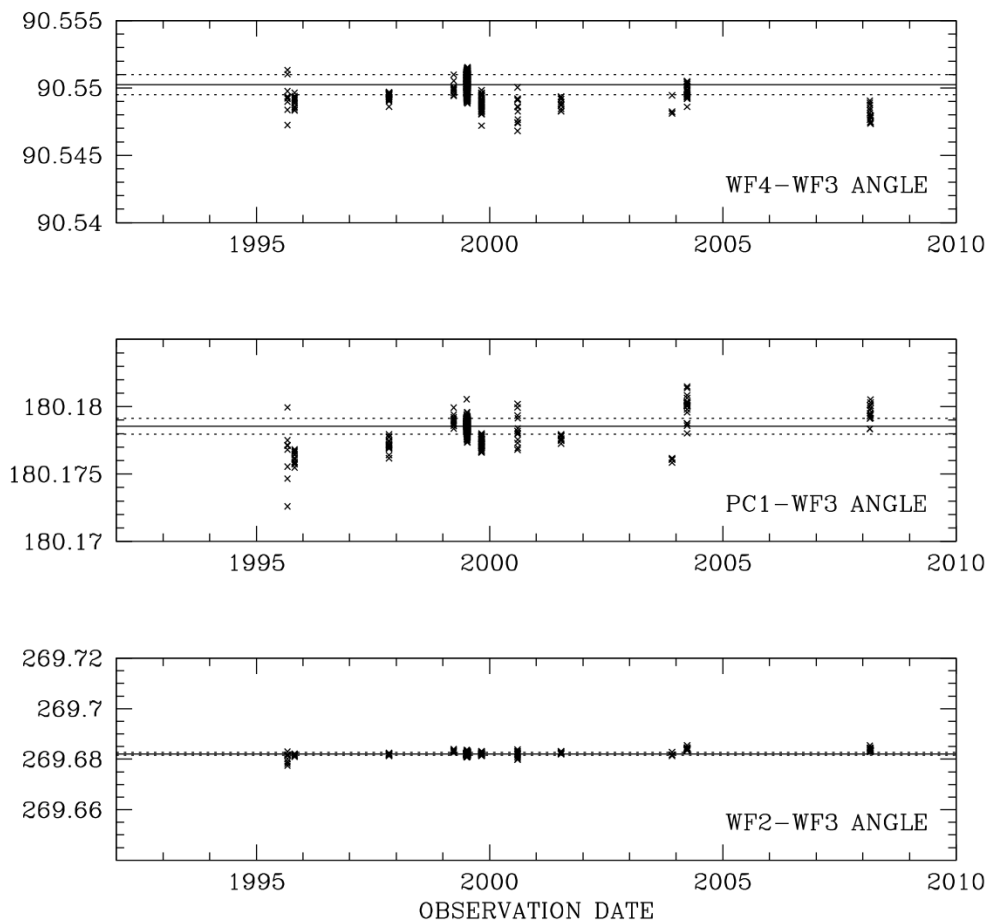


**Table 5.6: Newly-derived Relative Angles, Reference Chip 3**

|                                    | PC1      | WF2      | WF3      | WF4     |
|------------------------------------|----------|----------|----------|---------|
| <b>New Theta (deg)<sup>1</sup></b> | 180.1785 | 269.6821 | 000.0000 | 90.5502 |
| <b>Old Theta (deg)</b>             | 180.178  | 269.682  | 000.000  | 90.551  |

1. Errors are  $\sim 0.005^\circ$ . Non-significant extra digits are shown as they appeared in the computation. “Old” values are from Anderson & King, 2003, Table 3, and are in perfect agreement.

### Relative Scales

Relative scales are a function of wavelength due to chromatic aberration in the Magnesium Fluoride lens located immediately in front of each CCD (these lenses serve as both field flatteners and seals on the CCD dewars).

Using the ACS/WFC reference frame, with an assumed average pixel scale of 49.7248 mas/pixel (van der Marel et al., [ACS ISR 07-07](#)), the WFPC2 scale can be computed in arcseconds. The results, in [Figure 5.9](#), show histogram distributions of the scale measurements for each chip and 16 selected filters. For each histogram, the red line indicates a simple Gaussian fit. Within each box are indicated the number of images used to build the histogram (N), the pixel scale at the peak of the Gaussian (s), and sigma of the fitted Gaussian. While the scales for primary filters F555W and F814W are determined using a very large number of images ( $N > 500$ ), many filters have only two images ( $N = 2$ ). We further note that the measured scales are uncertain at a level of about 1 part in 4000 due to telescope OTA breathing, and other effects which may impact individual observations.

The image scale shows a gradual decrease as the wavelength decreases from the far red to the near-UV—this is due to the increasing refractive index of the Magnesium Fluoride lenses. Shortward of 300 nm the refractive index increases very sharply, and there is a corresponding sharp decrease in the image scale (see also [Section 5.4.1](#)). Several of the filters show image scales which are slightly different from other filters at nearby wavelengths (e.g., F702W), but these differences are within the range of artifacts expected from telescope OTA breathing, and hence are not significant.

Following the notation introduced by Anderson & King (2003), the camera-chip dependence of the scale ( $\alpha_k$ ) is separate from the filter dependence ( $\alpha_f$ ) of the scale, such that scale ( $\alpha$ ), is

$$\alpha = \alpha_k \alpha_f$$

In [Table 5.7](#), the scales for the different CCDs,  $\alpha_k$  are given relative to that of the WFPC2/WF3 in filter F555W, which has an assumed value of

99.6202 mas/pixels and associate uncertainty of 1/4000 (i.e.,  $\pm 0.025$  mas/pixel). The newly derived scales are in excellent agreement with Anderson and King (2003).

The values of  $\alpha_f$  are given in Table 5.8, and again there is excellent agreement with the previous work. This excellent agreement between Anderson and King (2003) and our more recent work indicates there are no sizable long-term change in the image scale.

**Table 5.7: Newly-derived Chip Scales Relative to the WF3 CCD (for filter F555W)**

|                              | PC1      | WF2      | WF3                         | WF4      |
|------------------------------|----------|----------|-----------------------------|----------|
| <b>New Alpha<sup>1</sup></b> | 0.457286 | 1.000196 | 1.000000<br>(by definition) | 1.000483 |
| <b>Old Alpha<sup>2</sup></b> | 0.45729  | 1.00020  | 1.000000                    | 1.00048  |

1. Uncertainties are 0.0003. Non-significant extra digits are from the computations.

2. “Old” values are from Anderson & King, Table 3, and are in perfect agreement with the newly-derived results.

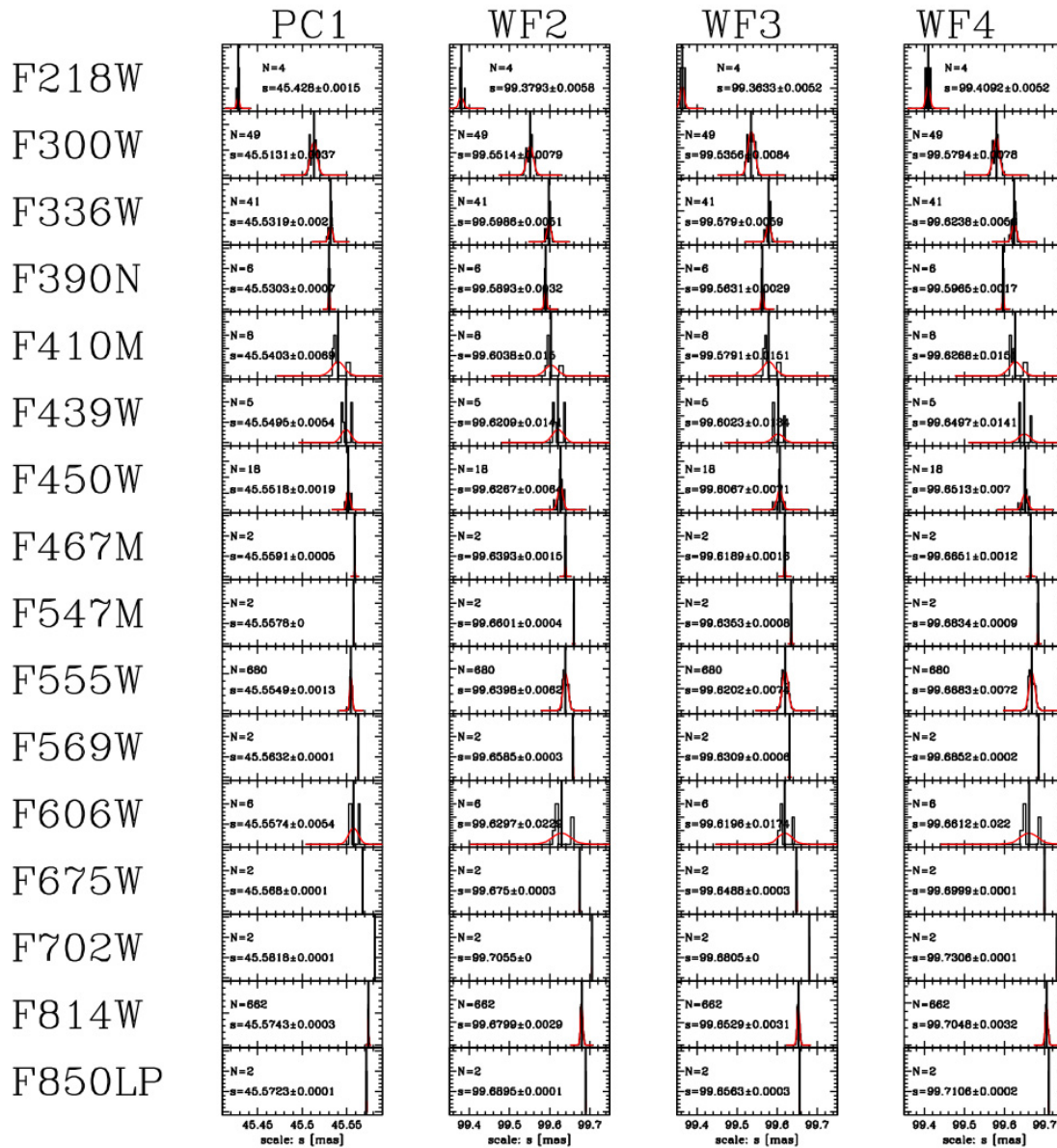
**Table 5.8: Newly-derived Filter Scales Relative to Filter F555W (for CCD WF3)**

| Filter | NEW filter scale <sup>1</sup> | OLD filter scale <sup>2</sup> |
|--------|-------------------------------|-------------------------------|
| F218W  | 0.997421                      | -                             |
| F300W  | 0.999150                      | 0.99953                       |
| F336W  | 0.999586                      | 0.99953                       |
| F390N  | 0.999427                      | -                             |
| F410M  | 0.999587                      | -                             |
| F439W  | 0.999820                      | 0.99978                       |
| F450W  | 0.999864                      | -                             |
| F467M  | 0.999987                      | -                             |
| F547M  | 1.000152                      | -                             |
| F555W  | 1.000000                      | 1.00000, by definition        |
| F569W  | 1.000108                      | -                             |
| F606W  | 0.999994                      | -                             |
| F675W  | 1.000287                      | -                             |
| F702W  | 1.000606                      | -                             |
| F814W  | 1.000328                      | 1.00036                       |
| F850LP | 1.000362                      | -                             |

1. Uncertainties are 0.0003. Non-significant extra digits are from the computations.

2. “Old” values are from Anderson & King, Table 4.

**Figure 5.9: Histogram Distributions of WFPC2 Scale Measurements for Each Chip and 16 Filters**

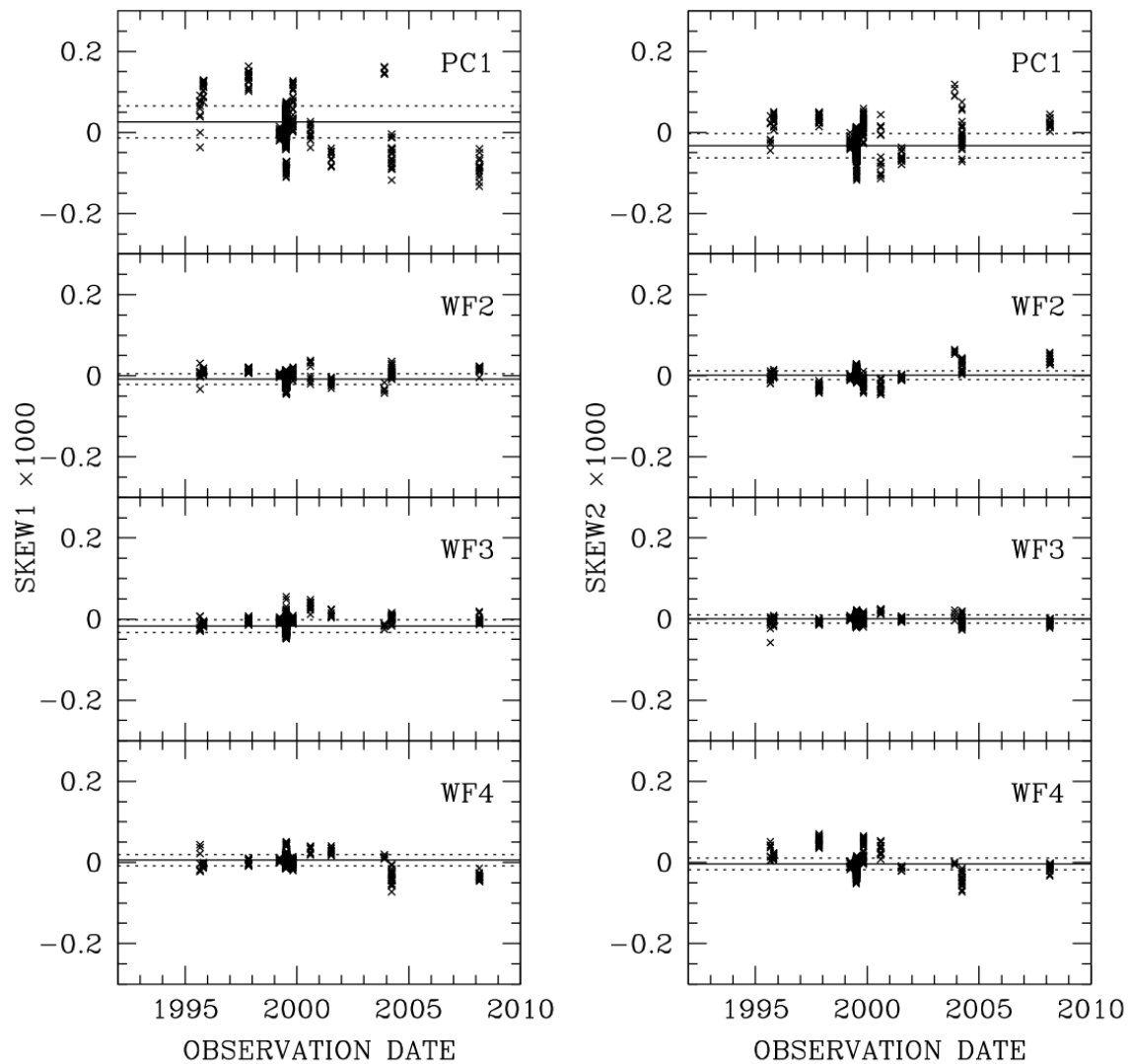


**N** is the number of images used to build that histogram (see text).

**Relative Skew Terms**

Figure 5.10 shows the two skew terms (as defined earlier) for the four chips, relative to the ACS/WFC reference frame, as a function of time. There are no sizable long-time variations for the skew terms.

**Figure 5.10: The Two Previously-defined Skew Terms for Each Chip, Relative to the ACS/WFC Reference Frame, as a Function of Epoch**



### Relative Offset $X_o, Y_o$

There is an additional complication in doing astrometry in the meta-chip system  $(X, Y)$  due to shifts in the CCD positions with respect to time. The relative positions of the four CCDs on the sky change slowly over time due to desorption of optical and detector supports within WFPC2, operating temperature changes within WFPC2 (April 1994 cool-down and late-mission temperature set-point changes, c.f. [WFPC2 ISR 2007-01](#)), and other effects.

The Anderson & King (2003) reference frame was used as a touchstone to compute the location of the CCD reference pixel (425,425) of PC1, WF2, and WF4 in the coordinate system of the WF3 chip (after distortion corrections).

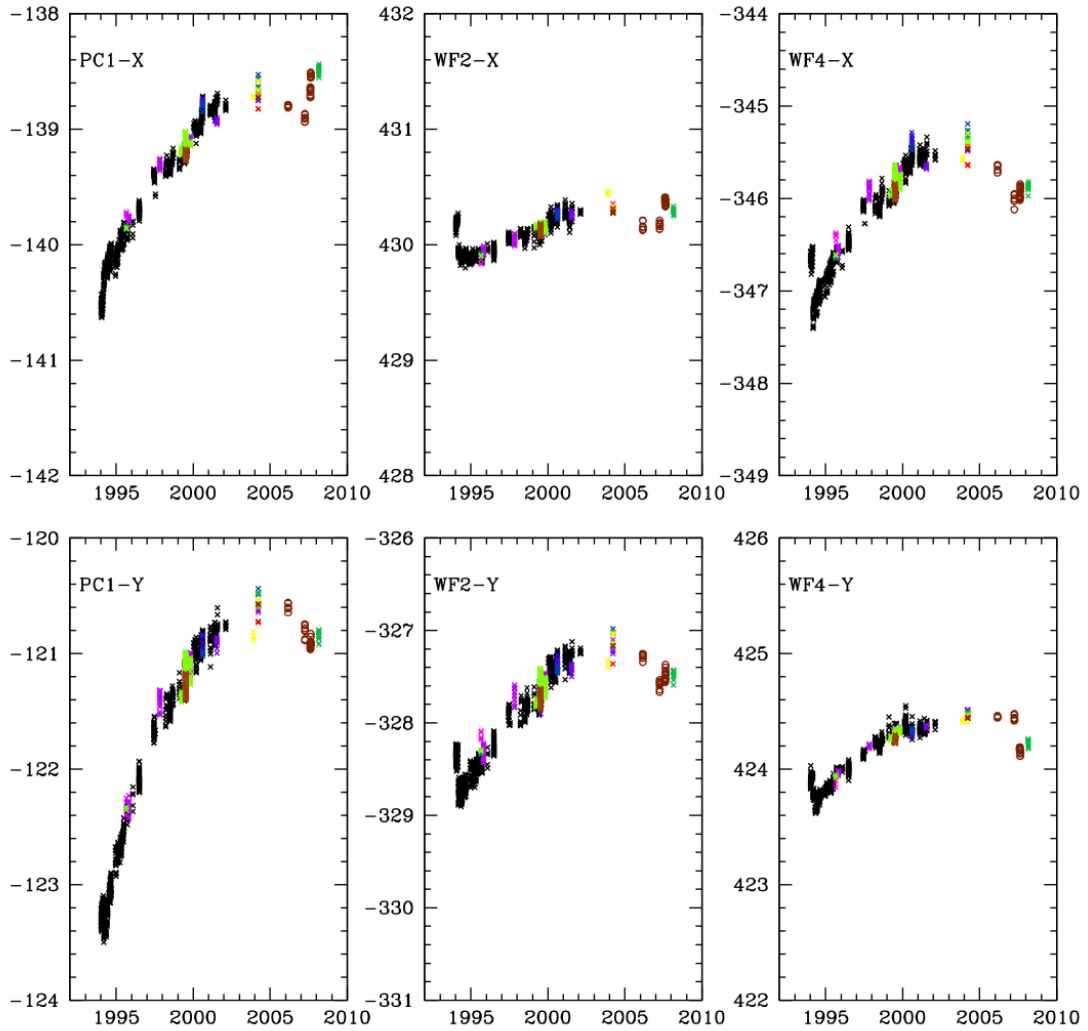
Figure 5.11 shows the observed relative offsets as a function of observation date. The black points were originally derived by Anderson & King, 2003, and primarily use the F555W filter. The colored points are additional data added by the present work, with the spectral filter indicated by the data point color. There are very tight trends over time, showing the chip movements relative to WF3. The scatter in these trends are about  $\sim 0.2$  WF3 pixels, constraining the inter-chip transformation accuracy to about 1-sigma ( $\sim 20$  mas). As noted by Casertano & Wiggs (WFPC2 ISR 2001-10) and Anderson & King (2003), there was a dramatic shift in intra-chip offsets after the WFPC2 was installed in HST in December 1993. The chips appeared to be moving monotonically until  $\sim 2005$ , after which new data points showed that the motions were slowing and later moving backwards. As expected from the camera design, the offsets are independent of filter.

Observed offsets for nine representative epochs are shown in Table 5.9. These can be interpolated to get an estimate for the offsets at any given time. For each WFPC2 image, this information is stored in the offset reference table specified by the image header keyword OFFTAB.

**Table 5.9: Offsets  $X_o$  and  $Y_o$  of the CCD Reference Centers (pixel 425,425) on the Sky Relative to the WF3 CCD Coordinates at Several Representative Epochs**

|                | PC1     | WF2     | WF3     | WF4     |
|----------------|---------|---------|---------|---------|
| $X_o(1994.07)$ | -140.51 | +430.19 | +425.00 | -346.64 |
| $X_o(1994.46)$ | -140.15 | +429.90 | +425.00 | -347.06 |
| $X_o(1995.73)$ | -139.84 | +429.92 | +425.00 | -346.61 |
| $X_o(1997.84)$ | -139.33 | +430.06 | +425.00 | -346.03 |
| $X_o(1999.52)$ | -139.12 | +430.14 | +425.00 | -345.82 |
| $X_o(2000.61)$ | -138.87 | +430.24 | +425.00 | -345.56 |
| $X_o(2004.23)$ | -138.60 | +430.32 | +425.00 | -345.32 |
| $X_o(2006.16)$ | -138.73 | +430.17 | +425.00 | -345.58 |
| $X_o(2007.63)$ | -138.54 | +430.31 | +425.00 | -345.84 |
| $Y_o(1994.07)$ | -123.27 | -328.35 | +425.00 | +423.91 |
| $Y_o(1994.46)$ | -123.17 | -328.70 | +425.00 | +423.74 |
| $Y_o(1995.73)$ | -122.38 | -328.37 | +425.00 | +423.93 |
| $Y_o(1997.84)$ | -121.52 | -327.84 | +425.00 | +424.18 |
| $Y_o(1999.52)$ | -121.18 | -327.61 | +425.00 | +424.27 |
| $Y_o(2000.61)$ | -120.89 | -327.35 | +425.00 | +424.35 |
| $Y_o(2004.23)$ | -120.54 | -327.08 | +425.00 | +424.46 |
| $Y_o(2006.16)$ | -120.52 | -327.19 | +425.00 | +424.45 |
| $Y_o(2007.63)$ | -120.80 | -327.42 | +425.00 | +424.23 |

**Figure 5.11: Offsets of the Reference Pixel (425, 425) for PC1, WF2, and WF4 in the Reference System of Chip WF3**



F218W F300W F336W F390N F410M F439W F450W F467M F547M F555W F569W F606W F675W F702W F814W F850LP

### 5.4.3 Absolute Astrometry

Absolute astrometry that can be obtained from WFPC2 images is limited by the positions of the guide stars, and by the transformation between the FGS (Fine Guidance Sensor) and the WFPC2. Until cycle 15 (mid-2006) the combination of these two errors resulted in a total positional uncertainty of between 0".5 and 1" ( $1\sigma$ ). In cycle 15 and 16, Guide Star Catalog 2's smaller errors and appropriately tighter focal plane calibrations, reduced this absolute astrometric error to between 0".2 and 0".5 ( $1\sigma$ ). For more information, please see:

[http://www.stsci.edu/institute/org/telescopes/Reports/Lallo\\_TIPS\\_19June08.pdf](http://www.stsci.edu/institute/org/telescopes/Reports/Lallo_TIPS_19June08.pdf)




---

*Relative astrometry within a chip provides precision of  $\sim 1$  mas. Absolute astrometry with WFPC2 provides accuracies of  $\sim 0".5$ .*

---



---

## 5.5 Drizzling WFPC2 Data

The MultiDrizzle software is often used to perform a wide range of actions on WFPC2 data after the pipeline calibration, such as:

- geometric distortion corrections.
- Aligning and stacking multiple images with position offsets (dithers or POS TARGs) while rejecting cosmic rays and bad detector pixels.
- Aligning and stacking sub-pixel dithered data with pixel re-sampling to improve resolution.
- Mosaicking the four CCDs into a single, geometrically-rectified image.
- Mosaicking multiple telescope pointings into a single large image.

A brief overview of the image processing steps are listed below; please refer to the [MultiDrizzle Handbook](#) for details.

- Using the CD-MATRIX positions from the image headers, **multidrizzle** determines the offset of each image with respect to a reference image. (This generally works well for images taken during the same visit. For multi-visit images, it may be necessary to improve the image alignments using a task like **tweakshifts** to generate a “shift file.”)

- A static pixel mask is made for each image, using low and negative pixel values and the image’s data quality file. ([MultiDrizzle Handbook, Section 5.4.9](#))
- The background (sky) value for each chip in each image is calculated, then stored in the header keyword MDRIZSKY. It will be used during the final **multidrizzle** step of creating a combined image. (This background determination step should be omitted for images with a variable background due to extended targets, as well as for narrow-band images.)
- Each input image is drizzled to correct for geometric distortion; they are aligned with the reference image using offsets from a user-generated “shift file” or, for observations in a single visit, using the WCS pointing information in each image header. ([MultiDrizzle Handbook, Section 5.4.10](#))
- Each single-drizzled image from the previous step is combined to create a median image that is mostly free of detector defects and cosmic rays. ([MultiDrizzle Handbook, Section 5.4.11](#))
- The median image is reverse-drizzled (blotted) to introduce the original geometric distortion and chip offsets for each input image, creating a counterpart blotted median image for each of the original input images. ([MultiDrizzle Handbook, Section 5.4.12](#))
- Each input image and its counterpart median image are used to create a mask for that input image, to be later used for removing cosmic rays and detector defects. ([MultiDrizzle Handbook, Section 5.4.13](#))
- In the final step, each of the original input images are drizzled into one final combined image, using the static pixel masks and the mask files created in the previous step. Details about setting the “drop size of the drizzle” and the grid scale of the output image can be found later in this sub-section and in the documentation referenced below. ([MultiDrizzle Handbook, Section 5.4.14](#))

Extensive documentation about the **dither** package and the **multidrizzle** task is available in [The MultiDrizzle Handbook, v. 3.0](#), at [http://www.stsci.edu/hst/HST\\_overview/documents/multidrizzle](http://www.stsci.edu/hst/HST_overview/documents/multidrizzle)

For first-time users, MultiDrizzle may appear daunting so it’s best, perhaps, to simply dive into it. For instance, one useful exercise would be to try one of the examples in the [WFPC2 Drizzling Cookbook](#), using its recommended parameter settings, then also run the same data through **multidrizzle** using the default settings. Comparing the differences between these two **multidrizzle** runs would give you a better perspective of how the parameters work. The WFPC2 Drizzling cookbook can be found at:

[http://www.stsci.edu/hst/wfpc2/analysis/WFPC2\\_drizzle.html](http://www.stsci.edu/hst/wfpc2/analysis/WFPC2_drizzle.html)

Information about the photometric and astrometric accuracy of multidrizzled images can be found in Sections 3.5 and 3.6, respectively, of the [MultiDrizzle Handbook](#).

### Running MultiDrizzle on WFPC2 images

There are several things to keep in mind when running **multidrizzle** on WFPC2 images.

Examples in the [WFPC2 Drizzling Cookbook](#) and [MultiDrizzle Handbook v.3.0](#) use the GEIS format. However, **multidrizzle** can also be run using MEF format input images (which is the default WFPC2 format from the Static Archive). Please note that the intermediate **multidrizzle** files and the final drizzle-combined image are in the MEF format.

Unlike the ACS and WFC3 pipelines, the WFPC2 pipeline does not automatically combine dithered and CR-SPLIT images (the pipeline does not create associations for WFPC2 data). Each calibrated dataset comes with a single-drizzled WFPC2 image that mosaics all four CCDs into one image. *These drizzled single images are provided as “quick-look” images and are not meant for data analysis.*

In the [MultiDrizzle Handbook](#), users will encounter references to the MDRIZTAB reference table that contains default **multidrizzle** settings for various instrument modes. This reference file is not available for WFPC2 images.

For images taken after March 2002, the WF4 chip may contain streaks that could not be removed in the pipeline gain correction software for WF4. If you wish to remove the streaks (using the task **wdestreak**), that step needs to be applied before running **multidrizzle** on the data.

### MultiDrizzle Parameters for WFPC2 Data

Default settings in **multidrizzle** were selected to work with most instruments. Information about choosing the best **multidrizzle** parameter values for each instrument are available in the [MultiDrizzle Handbook](#). For the convenience of the user, a few WFPC2-related issues are summarized here:

- the **multidrizzle** parameter *proc\_unit* allows the user to select the count unit for the final Multidrizzle output image: *native* (the default value) or *electrons*. The parameter *final\_units* can be set to either *counts* or *cps* (counts/sec, the default value) for the final Multidrizzle output image. For WFPC2, the “native” unit is counts or Data Number (DN). Setting *proc\_unit=native* and *final\_units=cps* produces an output image in counts/second<sup>13</sup> (the output image’s units are recorded in the output image header keyword BUNIT). The PHOT-FLAM<sup>14</sup> keyword value in the final drizzled image is also updated to be compatible with the units of the final image.

---

13. Multidrizzle performs all computations in units of electrons; this was done to ensure that the final products are properly processed. Therefore, the intermediate files are in units of electrons. If *proc\_unit=native*, the final drizzled image will be rescaled from electrons back to DN.

- In the latter years of operation, WFPC2 images were increasingly degraded due to declining charge transfer efficiency (CTE), creating tails of deferred charge in the anti-readout direction. The **multidrizzle** parameter, *driz\_cr\_ctegrow* can be used for making cosmic ray rejections in the direction of these CTE tails.
- For cameras with several detectors, such as WFPC2, **multidrizzle** calculates the sky value for each detector in the image, and stores it in the image's group keyword MDRIZSKY. For each input image, **multidrizzle** scales those values to units of electrons/arcsec<sup>2</sup>; it then determines the low sky value to be used for the final combined image which is then separately rescaled for the plate scale of each chip in the image. The resulting sky value is subtracted from each input image just before it's used in the final **multidrizzle** image combination step.
- If the target falls on both the PC1 and WF chips, the data should initially be drizzled using parameters that are suitable for the WF data. For data analysis purposes, the PC1 data can be later drizzled separately using the appropriate parameters for that camera. When the target of interest is only in one chip, **multidrizzle** can be run to combine the images from that one chip using the *group* parameter. For instance, to combine only the WF2 chip in the images, use *group=2*.
- Values for the *final\_pixfra* and *final\_scale* parameters depend on the number of input images and the size of the shifts. If there are enough images, sub-pixel shifts at about 0.5 pixel increments (such as 5.5, 5.5 pixels in x and y, respectively) would make it possible to recover some of the resolution lost in the undersampled input images. This can be done by drizzling the output image onto a smaller pixel scale and selecting a "drop" size that is larger than the output pixel scale so that some of the "drop" falls into adjacent output pixels (example, for WF images: *final\_scale=0.05* arcseconds, which is 0.5 WF pixels and *final\_pixfra=0.8* pixels). For offsets close to integer values, it would be difficult to recover any resolution, so a larger *final\_pixfra* value is recommended (example, for WF images: *final\_scale=0.1* arcseconds, which is 1 WF pixel, and *final\_pixfra=1* pixel).
- It's best to try different values, to see which combination of *final\_scale* and *final\_pixfra* yields the best results. Ideally the end products should have the following outcomes: for recovering resolution, the full-width at half-maximum of a PSF in the final image

---

14. For *proc\_unit=native*, the PHOTFLAM value of the PC1 is adopted for the entire 4-group mosaicked final drizzle-combined image. Even though each CCD has slightly different gain and readout values, the difference is considered small. (See Table 4.2 of the WFPC2 Instrument Handbook.)

should be around 2.5 pixels for a well-sampled output image. The rms of the final weight image should be less than 20% to 30% of the median. (Exclude measurements from areas, like the edges of the final weight image, that do not have contributions from all the input images. Statistics can be obtained using the IRAF tasks **imstat** or **imexam**.) More information about choosing the *final\_scale* and *final\_pixfra* parameter values can be found in the [MultiDrizzle Handbook](#), Sections 5.5.6.1 and 5.5.6.2, respectively.

### WFPC2 Geometric Distortion and MultiDrizzle

As outlined in [Section 5.4](#), there are three components to geometric distortion in WFPC2:

- distortion polynomial fit coefficients due to camera optics, which are stored in a reference file called the Instrument Distortion Coefficients TABLE or IDCTAB (file suffix, `idctab.fits`).
- Offsets between the CCDs that change with time, stored in a reference table called OFFTAB (file suffix, `off.fits`)
- 34th row defect corrections, in the reference image DGEODFILE (file suffix, `dxy.fits`).

At the time of this writing, Multidrizzle v.3.3.5 obtains the distortion coefficients in the following way: when *multidrizzle.coeffs=header*, **multidrizzle** will obtain the distortion correction values from the geometric distortion and time-dependent chip offsets reference files, as specified by the header keywords IDCTAB and OFFTAB, respectively. If the 34th row correction reference file, as specified in the DGEODFILE header keyword, can be accessed by **multidrizzle**, that correction will be performed as well; if not, **multidrizzle** will continue to run without applying the 34th row correction.

Future enhancements are planned for the **dither** package; please check the [WFPC2 Web page](#) (click on the Dither/Drizzle link), and the [STSDAS MultiDrizzle Web page](#) for the latest updates.

### Additional Information on the Resampling of WFPC2 images

The pixels of the PC1 undersample the point spread function (PSF) of the HST by a factor of about two, and the pixels of the WF are a factor of two coarser yet. Thus WFPC2 does not recover a substantial fraction of the spatial information that exists at the focal plane of the instrument. However, this information is not completely lost. Some of it can be recovered by *dithering* or *sub-stepping* the position of the chips by non-integral pixel amounts.

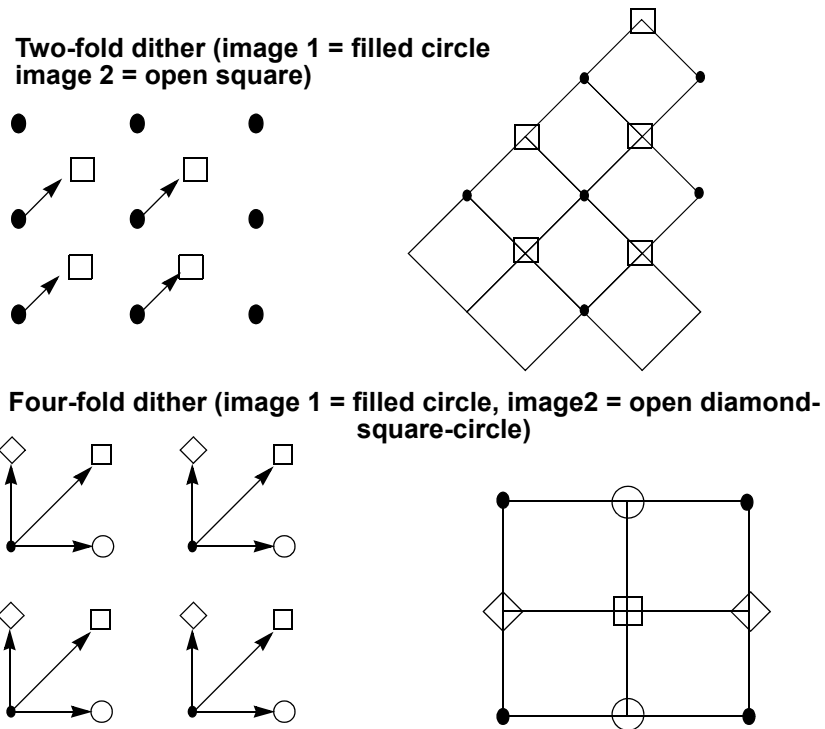
The recovery of high frequency spatial information is fundamentally limited by the pixel response function (PRF). The PRF of an ideal CCD with square pixels is simply a square boxcar function the size of the pixel. In practice, the PRF is a function not only of the physical size of the pixels,

but also of the degree to which photons and electrons are scattered into adjacent pixels, as well as smearing introduced by telescopic position wandering. The image recorded by the CCD is the “true” image (that which would be captured by an ideal detector at the focal plane) convolved with this PRF. Thus, at best, the image will be no sharper than that allowed by an ideal square pixel. In the case of WFPC2, in which at least 20% of the light falling on a given pixel is detected in adjacent pixels, the image is even less sharp.

The PRF of an ideal square pixel, that is a boxcar function, severely suppresses power on scales comparable to the size of the pixel. According to the Shannon-Nyquist theorem of information theory the sampling interval required to capture nearly all of the information passed by square pixels is  $1/2$  the size  $l$  of a pixel. This corresponds to dithering the CCD from its starting position of  $(0,0)$  to three other positions,  $(0, 1/2 l)$ ,  $(1/2 l, 0)$  and  $(1/2 l, 1/2 l)$ ; however, in practice, much of the information can be regained by a single dither to  $(1/2 l, 1/2 l)$ .

The process of retrieving high-spatial resolution information from dithered images can be thought of as having two stages. The first, reconstruction, removes the effect of sampling and restores the image to that produced by the convolution of the PSF and PRF of the telescope and detector. The more demanding stage, deconvolution (sometimes called restoration), attempts to remove much of the blurring produced by the optics and detector. In effect, deconvolution boosts the relative strength of the high-frequency components of the Fourier spectrum to undo the suppression produced by the PSF and PRF.

If your observations were taken with either of the two dither patterns discussed above, and if the positioning of the telescope was accurate to about a tenth of a pixel (this is usually true but not always the case), then you can reconstruct the image merely by interlacing the pixels of the offset images. In the case of a two-fold dither—that is images offset by a vector  $(n + 1/2, n + 1/2)$  pixels, where  $n$  is an integer—the interlaced images can be put on a square grid rotated  $45^\circ$  from the original orientation of the CCD (see [Figure 5.12](#), top diagrams). In the case of a four-fold dither, the images are interlaced on a grid twice as fine as the original CCD and coaligned with it (see [Figure 5.12](#), bottom diagrams).

**Figure 5.12: Interlacing Pixels of Offset Images**

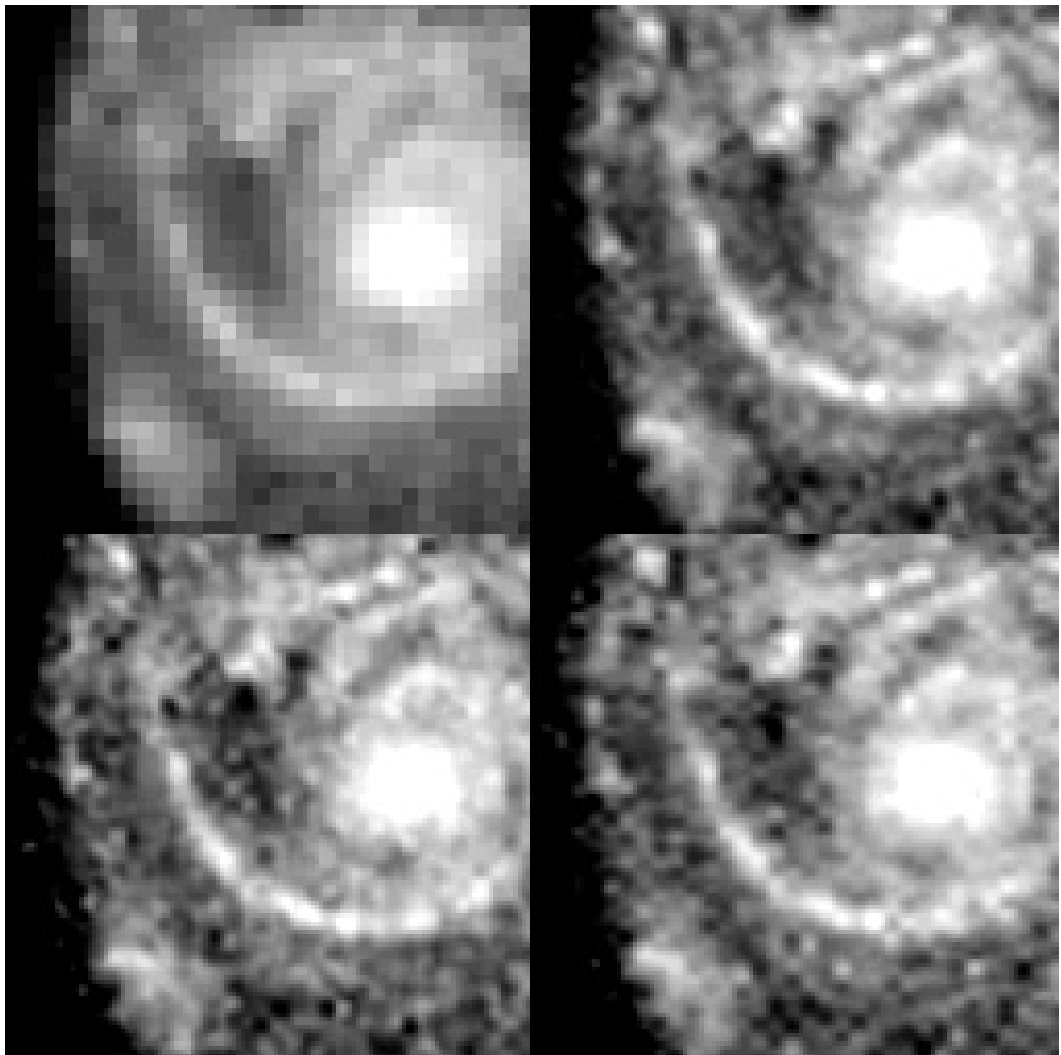
**Top diagrams, two-fold dither: filled circles and open squares represent pixels in image 1 and 2, respectively. Bottom diagrams, four-fold dither: filled circles, open squares, open diamonds, and open circles represent pixels in images 1,2,3,4, respectively.**

As part of the Hubble Deep Field project, a new method was developed to linearly reconstruct multiple offset images. This method, variable pixel linear reconstruction (also known as *drizzle*), can be thought of as shifting and adding with a variable pixel size. For poorly sampled data, the shifted pixels retain the initial pixel size—the final image combines the shifts correctly, but the gain in resolution is minimal. For a well-sampled field, such as that of the Hubble Deep Field, the size of the shifted pixels can be made quite small, and the image combination becomes equivalent to interlacing. Drizzling also corrects for the effects of the geometric distortion of WFPC2; correction of geometric distortion is important if shifts between dithered images are of order ten pixels or more.

## 5.6 Deconvolution of WFPC2 Data

Although reconstruction largely removes the effects of sampling on the image, it does not restore the information lost to the smearing of the PSF and PRF. Deconvolution of the images, however, does hold out the possibility of recapturing much of this information. [Figure 5.13](#), supplied by Richard Hook of the ST-ECF, shows the result of applying the Richardson-Lucy deconvolution scheme to HST data, used extensively in the analysis of WF/PC-1 data. The upper-left image shows one of four input images. The upper-right image shows a deconvolution of all of the data, and the lower two images show deconvolutions of independent subsets of the data. A dramatic gain in resolution is evident.

**Figure 5.13: Richardson-Lucy Deconvolution of HST Data**



A version of the Richardson-Lucy (RL) deconvolution scheme capable of handling dithered WFPC2 data is already available to STSDAS users. It is the task **acoadd** in the package **stsdas.contrib**. In order to use **acoadd**, users will need to supply the program both with a PSF (which in practice should be the convolution of the PRF with the optical PSF) and with the offsets in position between the various images. The position offset between the two images can be obtained using the task **crossdriz** in the **dither** package.

In principle, image deconvolution requires an accurate knowledge of both the instrument PSF and PRF. At present, our best models of the WFPC2 PSF come from the publicly available [Tiny Tim](#) software (Krist, 1995). The quality of the TinyTim model can be improved substantially by taking into account the exact position of the source within the pixel. Remy et al. (1997) discuss how this can be accomplished by generating multiple TinyTim images at various focus and jitter values, oversampled with respect to the camera pixels. At present, this is very labor-intensive, and the results cannot be easily integrated into the existing deconvolution software. Another limitation of the existing software is that it cannot incorporate the significant variation of the PSF across the field of view. As a result, the Richardson-Lucy approach can only be applied to limited regions of a chip at a time. Nonetheless, tests done on WFPC2 images suggest that RL deconvolution can give the WFPC2 user a substantial gain in resolution even in the presence of typical PSF and PRF errors. Users interested in more information on dithering, reconstruction, and deconvolution should consult the [MultiDrizzle Handbook](#).

---

## 5.7 Accuracy of WFPC2 Results

[Table 5.10](#) summarizes the accuracy to be expected from WFPC2 observations in several areas. The numbers in the table should be used with care, and only after reading the relevant sections of this handbook and the documents referenced therein; they are presented in tabular form here for easy reference.

**Table 5.10: Accuracy Expected in WFPC2 Observations**

| Procedure  | Estimated Accuracy   | Notes  |
|--|--|--|
| <b>Calibration (flat-fielding, bias subtraction, dark correction)</b>  |  |  |
| Bias subtraction   | 0.1 DN rms   | Unless bias jump is present.   |
| WF4 Anomaly<br>(Impacts data on<br>WF4 CCD taken<br>after March 2002.) | ~0.01 mag<br>~0.02 mag   | Gain 7 and high-bias gain 15.<br>Gain 15 with bias < 280.  |
| Dark subtraction   | 0.1 DN/hr rms  | Error larger for warm pixels; absolute error<br>uncertain because of dark glow.  |
| Flat-fielding  | < 1% rms large scale<br>0.3% rms small scale<br>~10%   | Visible, near UV.<br><br>F160BW: however, significant noise reduction<br>is achieved with use of correction flats.   |
| <b>Relative Photometry</b>   |  |  |
| Residuals in CTE<br>correction   | < 1% early in the mission (1996)<br>< 3% at mid-mission (2002)<br>< 5% at end of mission (2009)  |  |
| Long vs. short<br>anomaly (uncor-<br>rected)                           | < 5%   | Errors < 0.01 magnitude for well-exposed<br>stars. Larger errors for faint stars in crowded<br>fields. Some studies fail to confirm existence<br>of the effect, and suggest it may be an artifact<br>of analysis methods (see "Long vs Short<br>Anomaly"). |
| Aperture correction  | 4% rms focus dependence (1 pixel aperture)<br><1% focus dependence (> 5 pixel)<br>1% - 2% field dependence (1 pixel aperture)  | Can (should) be determined from data.  |
| Contamination cor-<br>rection  | 3% rms max (28 days after decon) (F160BW)<br>1% rms max (28 days after decon) (filters bluer<br>than F555W)  |  |
| Background deter-<br>mination  | 0.1 DN/pixel (background > 10 DN/pixel)  | May be difficult to exceed, regardless of<br>image S/N.  |
| Pixel centering  | < 1%   |  |
| <b>Absolute Photometry</b>   |  |  |
| Sensitivity  | < 2% rms for standard photometric filters<br>2% rms for broad and intermediate filters in visible<br>< 5% rms for narrow-band filters in visible<br>2% - 8% rms for UV filters | Red leaks are uncertain by ~10%.   |
| <b>Astrometry</b>  |  |  |
| Relative   | 0".005 rms (after geometric distortion and<br>34th-row corrections)<br>0".1 (estimated)  | Same chip<br><br>Across chips  |
| Absolute   | 1" rms (estimated)   |  |



# References

- Anderson, J. & King, I., 1999, Astrometric and Photometric Corrections for the 34th Row Error in HST's WFPC2 Camera, *PASP*, 111, 1095.
- Anderson, J., & King, I., 2000, Toward High-Precision Astrometry with WFPC2. I. Deriving an Accurate Point-Spread Function, *PASP*, 112, 1360.
- Anderson, J., & King, I., 2003, An Improved Distortion Solution for the Hubble Space Telescope's WFPC2, *PASP*, 115, 113.
- Anderson, J, et al., 2005, Empirical PSFs and Distortion in the WFC Camera, The 2005 HST Calibration Workshop, eds. Koekemoer, A., et al.
- Anderson, J., et al., 2006, Ground-Based CCD Astrometry with Wide Field Imagers, *A&A*, 454, 1029.
- Barstow, M.A., et al., 2001, Resolving Sirius-like Binaries with the Hubble Space Telescope, *MNRAS* 322, 891.
- Bedin, L. R., et al., 2003, Hubble Space Telescope Astrometry of M4 and the Galactic Constant V0/R0, *AJ*, 126, 247.
- Bernstein, R.A., Freedman, W.L., Madore, B.F, The First Detection of the Extragalactic Background Light at 3000, 5500 and 8000 Å: Results, *ApJ*. 2001.
- Bertin, E. & Arnouts, S., 1996, SExtractor: Software for source extraction, *A&A Supplement*, 117, 393.
- Bessell, M. S., 1983, VRI photometry - an addendum, *PASP*, 95, 480.
- Bohlin, R. & Gilliland, R., 2004, Hubble Space Telescope Absolute Spectrophotometry of Vega from the Far-Ultraviolet to the Infrared, *AJ* 127, 3508.
- Buser, R. & Kurucz, R. L., 1978, A systematic investigation of multi color photometric system. III. Theoretical UBV colors and the temperature scale for early-type stars, *A&A*, 70, 555.

- Cox, C. & Gilliland, R., 2002, The Effect of Velocity Aberration on ACS Image Processing, HST Calibration Workshop, eds. S. Arribas, et al.
- Dodge, M., 1984, Refractive properties of magnesium fluoride, *Applied Optics*, 23, 1980.
- Dolphin, A. E., 2000a, The Charge-Transfer Efficiency and Calibration of WFPC2, *PASP*, 112, 1397.
- Dolphin, A. E. 2000b, WFPC2 Stellar Photometry with HSTPHOT, *PASP*, 112, 1383.
- Dolphin, A. E., 2002, 2002 HST Calibration Workshop, eds. S. Arribas, et al., p. 301.
- Dolphin, A. E., 2004, Short-Period Variable Stars in the M31 Halo, *AJ*, 127, 875.
- Dolphin, A. E., 2009, A Revised Characterization of the WFPC2 CTE Loss, *PASP*, 121, 655.
- Gilliland, R., 1994, Stellar photometry including saturated images: Results on M67 with WFPC2, *ApJ*, 435, L63.
- Harris, H.C., et al., 1993, Photometric calibration of the HST wide-field/planetary camera. II - Ground-based observations of calibration fields, *AJ*, 105, 1196.
- Holtzman, J.A., et. al, 1994, The Performance and Calibration of the WFPC2, *PASP* 107, 156.
- Holtzman, J.A., et al., 1995, The Photometric Performance and Calibration of WFPC2, *PASP* 107, 1065.
- Johnson, H. L., 1965, Interstellar Extinction in the Galaxy, *ApJ*, vol. 141, 923.
- Kelson, D. D., 1996, The extragalactic distance scale key project. III. The discovery of Cepheids and a new distance to M101 using the Hubble Space Telescope, *ApJ*, 463, 26.
- Krist, J., 1995, Simulation of HST PSFs using Tiny Tim, *Astronomical Data Analysis Software and Systems IV*, ASP Conference Series, eds. Shaw, R.A., et al., 77, 349.
- Lub, J. & Pel, J. W., 1977, Properties of the Walraven VBLUW photometric system, *A&A*, 54, 137.
- Matsushima, S., 1969, On the UVBY Photometric System, *ApJ*, 158, 1137.
- Oke, J. B., 1974, Absolute Spectral Energy Distributions for White Dwarfs, *ApJ Supplement*, 27, 21.

- Remy, M., et al., 1997, WFPC2 photometry from subtraction of Tiny-Tim PSFs, The 1997 HST Calibration Workshop with a New Generation of Instruments, eds. Casertano, S., et al., 374.
- Saha, A., Labhart, L. & Prosser, C., 2000, On Deriving Distances from Cepheids Using the Hubble Space Telescope, PASP, 112, 163.
- Saha, A., et al., 1996, Cepheid Calibration of the Peak Brightness of SNe Ia. V. SN 1981B in NGC 4536, ApJ, 466, 55.
- Shaklan, S., Sharman, M. C. & Pravdo, S. H., 1995, High-precision measurement of pixel positions in a charge-coupled device, Applied Optics, 34, 6672.
- Shupe, D. L., et al., 2005, The SIP Convention for Representing Distortion in FITS, Astronomical Data Analysis Software and Systems XIV ASP Conference Series, Vol. 347, Proceedings of the Conference held 24-27 October, 2004 in Pasadena, California, USA, Astronomical Society of the Pacific, 2005., eds. Shopbell P., et al., 491.
- Surdej, J. et al., 1997, WFPC2 Photometry from Subtraction of Observed PSFs, The 1997 HST Calibration Workshop with a new generation of instruments, eds. Casertano, S., et al., 386.
- Trauger, J.T., 1994, The On-orbit Performance of WFPC2, ApJ, 435, L3.
- Whitmore, B., 1995, Photometry with the WFPC2, Calibrating Hubble Space Telescope. Post Servicing Mission. Proceedings of a Workshop held at the Space Telescope Science Institute, in Baltimore, Maryland, May 15-17, 1995, eds. Koratkar, A. et al., 269.
- Whitmore, B., Heyer, I., & Casertano, S. 1999, Charge-Transfer Efficiency of WFPC2, PASP, 111, 1559.
- Williams, R., et al., 1995, The Hubble Deep Field: Observations, Data Reduction, and Galaxy Photometry, AJ, 112, 1335.

---

## WFPC2 Instrument Science Reports (ISRs)

All ISRs (those listed below and to be added after publication of this Data Handbook) are available online at:

<http://www.stsci.edu/hst/wfpc2/documents/isrs>

- 10-02: Improved SF4 Anomaly Corrections, V. Dixon and J. Biretta.
- 10-01: WFPC2 Standard Star CTE, M. McMaster and J. Biretta.
- 09-07: Red Leak Characterization for the WFPC2 UV Filters, P. L. Lim, M. Chiaberge, J. Biretta, and D. Di Nino.

- 09-06: On-Orbit Photometric Calibration of the WFPC2 Linear Ramp Filters, J. Biretta, P.L. Lim, M. McMaster, and S. Gonzaga.
- 09-05: Bandwidth Stability of the WFPC2 Narrow Band and Linear Ramp Filters, P.L. Lim and J. Biretta.
- 09-04: Wavelength Stability of the WFPC2 Narrow Band and Linear Ramp Filters, J. Biretta and P.L. Lim.
- 09-03: Pipeline Correction of Images Impacted by the WF4 Anomaly, V. Dixon and J. Biretta.
- 09-02: WFPC2 F343N Filter Throughput Decline, S. Gonzaga and J. Biretta.
- 09-01: Rapid Pinhole Growth in the F160BW Filter, J. Biretta and K. Verner.
- 08-03: Correcting Background Streaks in WFPC2 Data, A. Maybath, D. Grumm, M. McMaster, and M. Sirianni.
- 08-02: Evolution of WFPC2 Superbiases, D. Thatte and J. Biretta.
- 08-01: Flat Fields from the Moonlit Earth, R. Bohlin, J. Mack, and J. Biretta.
- 07-01: Temperature Reductions to Mitigate the WF4 Anomaly, V. Dixon, J. Biretta, S. Gonzaga, and M. McMaster.
- 05-02: Early Assessment of the WF4 Anomaly, J. Biretta and S. Gonzaga.
- 05-01: Hot Pixels as a Probe of WFPC2 CTE Effects, J. Biretta and V. Kozhurina-Platais.
- 04-01: The Accuracy of WFPC2 Photometric Zeropoints, I. Heyer, M. Richardson, B. Whitmore, and L. Lubin.
- 03-03: WFPC2 Cycle 12 Calibration Plan, A. Koekemoer, I. Heyer, G. Brammer, V. Kozhurina-Platais, J. Rhoads, and B. Whitmore.
- 03-02: Toward a Multi-Wavelength Geometric Distortion Solution for WFPC2, V. Kozhurina-Platais, J. Anderson, A. Koekemoer.
- 03-01: WFPC2 Cycle 9 Closure Report, A. M. Koekemoer, S. Baggett, S. Casertano, S. Gonzaga, I. Heyer, and the WFPC2 Group.
- 02-07: Updated Contamination Rates for WFPC2 UV Filters, M. McMaster and B. Whitmore.
- 02-06: Results of the Observatory Verification for WFPC2 after Servicing Mission 3B, A. M. Koekemoer and the WFPC2 Group.
- 02-05: WFPC2 Cycle 11 Calibration Plan, S. Gonzaga and the WFPC2 Group.

- 02-04: An Analysis of WFPC2 Filter Positional Anomalies, S. Gonzaga, S. Baggett, J. Biretta.
- 02-03: Charge Transfer Efficiency for Very Faint Objects and a Reexamination of the Long-vs-Short Problem for the WFPC2, B. Whitmore and I. Heyer.
- 02-02: Updated WFPC2 Flatfield Reference Files for 1995 - 2001, A. Koekemoer, et al.
- 02-01: WFPC2 Clocks-ON Close Out, A. Schultz, et al.
- 01-11: Summary of WFPC2 SM3B Plans, A. Koekemoer, et al.
- 01-10: An Improved Geometric Solution for WFPC2, S. Casertano and M. Wiggs.
- 01-09: The WFPC2 Photometric CTE Monitor, I. Heyer.
- 01-08: Creating WFPC2 Dark Reference Files: Addendum, J. Mack, et al.
- 01-07: WFPC2 Flatfields with Reduced Noise, E. Karkoschka and J. Biretta.
- 01-06: WFPC2 Cycle 8 Closure Report, S. Baggett, et al.
- 01-05: WFPC2 Dark Current vs. Time, J. Mack, et al.
- 01-04: Preliminary Assessment of the FR533N Filter Anomaly, S. Gonzaga, et al.
- 01-03: WFPC2 Cycle 10 Calibration Plan, S. Baggett, et al.
- 01-02: Noiseless Preflashing of the WFPC2 CCDs, A. Schultz, et al.
- 01-01: Creating WFPC2 Dark Reference Files, J. Mack and M. Wiggs.
- 00-04: How CTE Affects Extended Sources, J. Riess.
- 00-03: Update on Charge Trapping and CTE Residual Images in WFPC2, S. Baggett, et al.
- 00-02: Results of the WFPC2 Observatory Verification after SM3a, S. Casertano, et al.
- 00-01: WFPC2 Cycle 9 Calibration Plan, S. Baggett, et al.
- 99-05: WFPC2 Cycle 7 Closure Report, S. Baggett, et al.
- 99-04: Time Dependence of CTE from Cosmic Ray Trails, A. Riess, et al.
- 99-03: Summary of WFPC2 SM3a Plans, S. Casertano, et al.
- 99-02: WFPC2 Cycle 8 Calibration Plan, S. Baggett, et al.

- 99-01: Internal Flat Field Monitoring II. Stability of the Lamps, Flats, and Gains, C. O’Dea, et al.
- 98-04: The Drizzling Cookbook, S. Gonzaga, et al.
- 98-03: WFPC2 Long-Term Photometric Stability, S. Baggett and S. Gonzaga.
- 98-02: The Long vs. Short Anomaly in WFPC2 Images, S. Casertano and M. Mutchler.
- 98-01: WFPC2 Cycle 6 Calibration Closure Report, S. Baggett, et al.
- 97-11: WFPC2 Polarization Calibration, J. Biretta and M. McMaster.
- 97-10: WFPC2 SYNPHOT Update, S. Baggett, et al.
- 97-09: Results of the WFPC2 Post-Servicing Mission-2 Calibration Program, J. Biretta, et al.
- 97-08: New Results on CTE and Constraints on Flat-Field Accuracy, B. Whitmore and I. Heyer.
- 97-07: WFPC2 Electronics Verification, M. Stiavelli and M. Mutchler.
- 97-06: WFPC2 Cycle 7 Calibration Plan, S. Casertano, et al.
- 97-05: Charge Trapping and CTE Residual Images in the WFPC2 CCDs, J. Biretta and M. Mutchler.
- 97-04: Properties of WFPC2 Bias Frames, C. O’Dea, et al.
- 97-03: Summary of WFPC2 SM97 Plans, J. Biretta, et al.
- 97-02: WFPC2 Cycle 5 Calibration Closure Report, S. Casertano and S. Baggett.
- 97-01: Impact of Focus Drift on Aperture Photometry, A. Suchkov and S. Casertano.
- 96-08: WFPC2 Cycle 6 Calibration Plan, S. Casertano, et al.
- 96-07: WFPC2 Throughput Stability in the Extreme Ultraviolet, J. MacKenty and S. Baggett.
- 96-06: Photometric Calibration of WFPC2 Linear Ramp Filter Data in SYNPHOT, J. Biretta, et al.
- 96-05: Wavelength/Aperture Calibration of the WFPC2 Linear Ramp Filters, J. Biretta, et al.
- 96-04: Effects of Contamination on WFPC2 Photometry, B. Whitmore, et al.
- 96-03: Background Subtraction in WFPC2 Frames, H. Ferguson.

- 96-02: Contamination Correction in SYNPHOT for WFPC2 and WF/PC-1, S. Baggett, et al.
- 96-01: Internal Flat Field Monitoring, M. Stiavelli and S. Baggett.
- 95-07: WFPC2 Cycle 4 Calibration Summary, S. Baggett, et al.
- 95-06: A Field Guide to WFPC2 Image Anomalies, J. Biretta, et al.
- 95-05: WFPC2 Ghosts, Scatter, and PSF Field Dependence, J. Krist.
- 95-04: A Demonstration Analysis Script for Performing Aperture Photometry, B. Whitmore and I. Heyer.
- 95-03: Charge Transfer Traps in the WFPC2, B. Whitmore and M. Wiggs.
- 95-02: The Geometric Distortion of the WFPC2 Cameras, R. Gilmozzi, et al.
- 95-01: WFPC2 Polarization Observations: Strategies, Apertures, and Calibration Plans, J. Biretta and W. Sparks.
- 94-03: WFPC2 Pipeline Calibration, C. Burrows.
- 94-02: Observed WFPC2 Bias Jumps, J. Fitch.
- 94-01: Large Angle Scattering in WFPC2 and Horizontal “Smearing” Correction, J. Krist and C. Burrows.
- 93-01: Polarizer Quad Nomenclature, M. Clampin.
- 92-06: WFPC2 CCDs, M. Clampin.
- 92-05: WFPC2 AFM and POMM Actuation Algorithm, C. Burrows.
- 92-04: Science with the Second Wide Field and Planetary Camera, J. Trauger, et al.
- 92-03: WFPC2 Science Observation and Engineering Modes, J. Trauger and D. Brown.
- 92-02: System Level Contamination Issues for WFPC2 and COSTAR, M. Clampin.
- 92-01: WFPC2 Science Capability Report, D. Brown.

---

## WFPC2 Links

WFPC2 Home Page: <http://www.stsci.edu/hst/wfpc2>

---

### Site Map of WFPC2 WWW pages

---

|   |   |
|---|---|
| Advisories                                    | <a href="http://www.stsci.edu/hst/wfpc2">http://www.stsci.edu/hst/wfpc2</a> (middle of page)  |
| Document (archive)                            | <a href="http://www.stsci.edu/hst/wfpc2/documents">http://www.stsci.edu/hst/wfpc2/documents</a>   |
| Software Tools                                | <a href="http://www.stsci.edu/hst/wfpc2/software">http://www.stsci.edu/hst/wfpc2/software</a>   |
| User Support                                  | <a href="mailto:help@stsci.edu">help@stsci.edu</a>  |
| Frequently Asked Questions                    | <a href="http://www.stsci.edu/hst/wfpc2/faqs">http://www.stsci.edu/hst/wfpc2/faqs</a>   |
| WFPC2 Instrument Handbook                     | <a href="http://www.stsci.edu/hst/wfpc2/documents/IHB_17.html">http://www.stsci.edu/hst/wfpc2/documents/IHB_17.html</a>   |
| Multidrizzle Handbook                         | <a href="http://www.stsci.edu/hst/HST_overview/documents/multidrizzle">http://www.stsci.edu/hst/HST_overview/documents/multidrizzle</a>   |
| WFPC2 Drizzling Cookbook                      | <a href="http://www.stsci.edu/hst/wfpc2/analysis/WFPC2_drizzle.html">http://www.stsci.edu/hst/wfpc2/analysis/WFPC2_drizzle.html</a>   |
| WFPC2 Exposure Time Calculators               | <a href="http://www.stsci.edu/hst/wfpc2/software/wfpc2-etc.html">http://www.stsci.edu/hst/wfpc2/software/wfpc2-etc.html</a>   |
| WFPC2 Reference Files                         | <a href="http://www.stsci.edu/hst/observatory/cdbs/SIfile-Info/WFPC2/reftablequeryindex_wfpc2">http://www.stsci.edu/hst/observatory/cdbs/SIfile-Info/WFPC2/reftablequeryindex_wfpc2</a> |
| IDT Reference Files                           | <a href="http://www.stsci.edu/hst/observatory/cdbs/SIfile-Info/WFPC2/reftablequeryindex_wfpc2">http://www.stsci.edu/hst/observatory/cdbs/SIfile-Info/WFPC2/reftablequeryindex_wfpc2</a> |
| WFPC2 PSF page                                | <a href="http://www.stsci.edu/hst/wfpc2/analysis/wfpc2_psf_page.html">http://www.stsci.edu/hst/wfpc2/analysis/wfpc2_psf_page.html</a>   |
| Warm Pixel Tables                             | <a href="http://www.stsci.edu/hst/wfpc2/analysis/warpix.html">http://www.stsci.edu/hst/wfpc2/analysis/warpix.html</a>   |
| Instrument Science Reports (ISRs)             | <a href="http://www.stsci.edu/hst/wfpc2/documents/isrs">http://www.stsci.edu/hst/wfpc2/documents/isrs</a>   |
| Polarizer Calibration Tools                   | <a href="http://www.stsci.edu/hst/wfpc2/software/wfpc2_pol_top.html">http://www.stsci.edu/hst/wfpc2/software/wfpc2_pol_top.html</a>   |
| Calibrating Linear Ramp Filter Data           | <a href="http://www.stsci.edu/hst/wfpc2/analysis/lrf_calibration.html">http://www.stsci.edu/hst/wfpc2/analysis/lrf_calibration.html</a>   |
| Linear Ramp Filter Calculator                 | <a href="http://www.stsci.edu/hst/wfpc2/software/wfpc2_lrfcalc.html">http://www.stsci.edu/hst/wfpc2/software/wfpc2_lrfcalc.html</a>   |
| Decontamination Dates                         | <a href="http://www.stsci.edu/hst/wfpc2/analysis/wfpc2_decon_dates.html">http://www.stsci.edu/hst/wfpc2/analysis/wfpc2_decon_dates.html</a>   |
| STAN, the Space Telescope Analysis Newsletter | <a href="http://www.stsci.edu/hst/wfpc2/documents/newsletters">http://www.stsci.edu/hst/wfpc2/documents/newsletters</a>   |
| Workshops and Conference Proceedings          | <a href="http://www.stsci.edu/hst/wfpc2/documents/proceedings">http://www.stsci.edu/hst/wfpc2/documents/proceedings</a>   |

---

# Index

## Numerics

34th row defect 106, 117, 127

## A

AB System 86

absolute sensitivity 50

accuracy of WFPC2 results 148

archive

    HST Archive 46

    Hubble Legacy Archive (HLA) 24

    WFPC2 Static Archive 12, 26

astrometry 127

    34th row defect 127

    absolute astrometry 140

    CCD chip relative angles 133

    CTE 131

    ePSF (effective PSF) 128

    geometric distortion 128

    header keywords 15

    local transformations 131

    pointing precision 72

    pyramid mirror vignetting 5, 131

    relative astrometry within a chip 127

    relative scales 134

    Science Instrument Aperture File 15

    shifts in CCD positions with respect to time  
    137

    time-dependent skew terms relative to  
    ACS/WFC 136

    undersampling 128

    velocity aberration 130

## C

calibrated data files 14

calibration 25

    A/D correction 36

    absolute sensitivity 50

    bias image subtraction 38

    bias level removal 37

    calibration steps 33, 35

    calwp2 31, 49

    charge traps 62

    creation of photometry keywords 39

    dark current 69

    dark image subtraction 38

    Data Quality File (DQF) flags 42

    data quality file creation 41

    flat field correction errors 66

    flat field multiplication 39

    Multi-extension FITS 49

    On-The-Fly-Calibration (OTFC) 25

    On-The-Fly-Reprocessing (OTFR) 25

    OPUS pipeline 26

    polarimetry 125

    post-calwp2 pipeline processing 44

    post-pipeline calibration 52

    recalibration 33, 45

    reference files 32, 35, 47

    reference files suffix 35

    shutter shading correction 39

    static mask application 35

    trailer file 27

    warm pixels 52, 55

    WF4 anomaly correction 37, 74, 111

    calibration steps 31, 33, 35

    calwp2 30, 45, 49

- pipeline processing not included in calwp2 44
- recalibration 33
- CCD 5
  - 34th row defect 106, 127
  - bias jumps 76
  - charge traps 62, 110
  - cosmic rays 60
  - dark current 7, 69
  - detector type 6
  - digitization noise 109
  - dimensions 6
  - field of view 5
  - gain 7
  - gain variations between chips 106
  - image pixel format 6
  - operating temperature 7
  - operating temperature cool down on April 23, 1994 99
  - permanent bad pixels 35
  - pixel scale 6
  - pixel size 6
  - read noise 6
  - readout 3
  - readout modes 6
  - relative angles 133
  - relative scales 134
  - relative shifts over time 137
  - residual image 77
  - saturated stars 115
  - Serial Clocks 110
  - warm (or hot) pixels 52
  - WF4 Anomaly 37
  - WF4 anomaly 111
- cosmic rays
  - PSF 60
  - rate of hits 60
  - South Atlantic Anomaly 60
- CTE (Charge Transfer Efficiency) 101
  - astrometry 131
  - corrections for extended sources 103
  - corrections for point-source photometry 101
  - Dolphin CTE correction formulae 101, 122
  - first exposure effect 104
  - header keywords for charge transfer loss estimates 44
- D**
  - DAOPHOT 24
  - dark current 7, 69
    - dark glow 71
  - dark reference files 70
  - data formats
    - calibrated data files 14
    - dataset 14
    - dataset suffixes 14
    - GEIS vs. MEF 13
    - Generic Edited Information Set (GEIS) 11, 13
    - Multi-extension FITS (MEF) 13
    - raw data files 14
    - recalibration 33
    - rootname 14, 23
    - waiver FITS (wFITS) 11, 13
  - Data Number (DN) 36
  - Data Quality File (DQF) flags 42
  - dataset 14
  - decontaminations 54, 93
  - deconvolution 145
    - Richardson-Lucy 147
  - Dolphin CTE corrections for point source photometry 101
- F**
  - field of view 2, 6
    - CCD 5
    - HST 2
    - WFPC2 4
  - filters
    - linear ramp filters 58
    - linear ramp filters anomalous rotational offsets 107
    - methane quad filter transmission variations 107
    - polarimetry 125
    - UV filters red leaks 110
  - first exposure CTE effect 104
  - flat fields 58

photometry 69  
focal ratio 5

**G**

gain 7  
  A/D correction 36  
  Data Number (DN) 36  
  gain variation 106  
  WF4 anomaly 74  
  WF4 anomaly pipeline correction 37  
  WF4 anomaly streak correction 111  
Generic Edited Information Set (GEIS) 11, 13  
geometric distortion 128, 144  
global header keywords 16  
group header keywords 18  
guide star catalog precision 140  
guide star guiding modes 72

**H**

header keywords 15  
  astrometry 15  
  CTE group header keywords 44  
  global 16  
  group 18  
  HISTORY 42  
  HST keyword dictionary 16  
  PHOTFLAM 50  
  UV throughput  
    ZP\_CORR 98  
header keywords for CTE loss estimates 44  
HST Archive 46  
HST focus history 100  
HST keyword dictionary 16  
Hubble Legacy Archive (HLA) 24

**I**

icons  
  used in this manual xi  
image anomalies 81  
  bias jumps 76  
    correction 76  
  bright Earth reflections 80  
  ghost images 78  
  PC1 stray light 81  
  residual image 77  
interrupted observations 72

**IRAF**

cosmicrays 55  
daofind 118  
DAOPHOT 24  
hedit 13  
hselect 13, 40  
imcntr 118  
imexamine 76  
imheader 13  
imshift 60  
imstat 76  
phot 117, 119  
txdump 119

**J**

jitter files 73

**L**

linear ramp filters 58  
  anomalous rotational offsets 107

**M**

MultiDrizzle 140  
  parameters for WFPC2 data 142  
  processing steps 140  
  running multidrizzle on WFPC2 data 142  
  undersampling 144  
  WFPC2 geometric distortion 144  
Multi-extension FITS 13  
  calibration 49

**O**

On-The-Fly Calibration (OTFC) 25  
On-The-Fly-Reprocessing (OTFR) 25  
operating temperature 7  
optical configuration 3  
OPUS Pipeline 26

**P**

permanent bad pixels 110  
PHOTFLAM 50  
photometry 116, 148  
  34th row defect 117  
  AB System 86  
  absolute sensitivity 50

- aperture correction 108
- aperture corrections and zeropoints 83
- bright Earth reflections 80
- charge traps 110
- color terms 109
- correcting background streaks in WF4 111
- cosmic rays 60
- DAOPHOT 24
- decontaminations 93
- digitization noise 109
- F1042M extended halo 111
- flat field correction errors 66
- gain variations between chips 106
- group header keywords 39
- infinite aperture 123
- magnitude definition 83
- PC1 stray light 81
- pixel area correction for point source photometry 106, 117
- point source
  - flat fields 69
- point source aperture correction 120
- point source CTE loss 122
- point source example 116
- position-dependent corrections 101, 104
  - anomalous rotational offset in linear ramp filters 107
  - CTE 101
  - Dolphin CTE correction for point sources 101
  - extended source CTE corrections 103
  - long vs. short anomaly 105
  - methane quad filter transmission variations 107
  - pixel area corrections for point source photometry 106, 117
  - pixel centering 107
- pyramid mirror vignetting 5
- saturated stars 115
- serial clocks 110
- STMAG system 86
- throughput loss due to UV contamination 97
- time-dependent corrections
  - cool down on April 23, 1994 99
  - PSF variations 100
  - UV contamination & long term QE changes 93
- transformations 84, 90, 109
- UV contamination & QE changes 123
- UV filters red leaks 110
- UV throughput 93
- warm pixels 53
- WF4 anomaly 37
  - background streaks correction 111
- WFPC2 flight system 85
- WFPC2 synthetic system 85
- WFPC2 VEGAMAG System 85
- zeropoint correction 97
- zeropoint determination 87
- zeropoints 83
  - Holtzman 88
  - PHOTFLAM 88
  - STMAG 88
  - VEGAMAG 88
- pipeline 44
  - calwp2 31
  - On-The-Fly Calibration (OTFC) 25
  - On-The-Fly-Reprocessing (OTFR) 25
  - OPUS 26, 74
  - post-calwp2 pipeline processing 44
  - post-pipeline calibration 52
  - PyDrizzle 44
  - telemetry (POD) files 25
  - trailer file 27
  - WF4 anomaly correction 74
- pixel area correction for point source photometry 106, 117
- pixel response function (PRF) 144
- pixel scale 5
- plate scale 6
- POD files 25
- point source photometry example 116
- pointing precision 72
- post-pipeline calibration 44, 52
  - correction flat fields 58
  - CTE 101
  - pixel area correction for point source photometry 106, 117
- recalibration 45

- warm pixels 52
  - WF4 anomaly streak removal 111
  - PSF
    - ePSF (effective PSF) 128
    - F1042M extended halo 111
    - pixel response function (PRF) 144
    - PSF variations 100
    - TinyTim 100, 148
    - undersampled 144
  - PyDrizzle 44
  - pyramid mirror vignetting 5, 131
- R**
- raw data files 14
  - read noise 6
  - readout modes 6
  - recalibration 33, 45
    - calibration steps 33, 35
    - calwp2 30, 45
    - changing calibration switches 48
    - custom dark reference file 57
    - histogram creation 41
    - linear ramp filters 58
    - reference files 32, 47
    - WFPC2 IDT reference files 35
  - reference files 32
    - bias reference image 38
    - calibration steps 35
    - correction flat fields 58
    - custom darks 57, 71
    - dark reference image 38
    - darks 70
    - flat fields for special observations and special purpose filters 68
    - geometric distortion 144
    - history of flat fields 66
    - linear ramp filters 58
    - naming convention 67
    - pixel area correction reference file for point source photometry 106
    - suffix 35
    - superdark 71
    - WFPC2 IDT 35
  - reprocessing
    - final
      - WFPC2 Static Archive 12, 26
      - On-The-Fly-Reprocessing (OTFR) 25
      - OPUS pipeline 26
      - telemetry (POD) files 25
    - rootname 14, 23
- S**
- Science Instrument Aperture File (SIAF) 15
  - software (also see IRAF and STSDAS)
    - SExtractor 24
    - TinyTim 100, 148
  - South Atlantic Anomaly 60
  - spherical aberration 3
    - pyramid mirror vignetting 5, 131
  - Static Archive 12, 70
  - STMAG System (photometry) 86
  - stray light 81
  - STScI ACS-WFPC2 Team vii
  - STSDAS 49
    - acoadd 148
    - bandpar 51
    - calcpht 90
    - calwp2 30, 49
    - catfits 13
    - crrej 61
    - dither package 141
    - fixpix 110
    - gcombine 60
    - imcalc 117
    - multidrizzle 140
    - plband 91
    - pydrizzle 44
    - pyraf 49
    - showfiles 98
    - strfits 46, 47
    - stwfits 13
    - tcalc 121
    - tdump 124
    - tstat 121
    - wdestreak 112
    - wfixup 36, 63, 110
    - wfpc package 113
    - wmosaic 5
  - SYNPHOT
    - bandpar 51

- calcpot 90
- PHOTFLAM 51
- photometry header keywords 39
- plband 91
- showfiles 98
- URESP 51

- WFPC2 Static Archive 12, 26
- WFPC2 Synthetic System (photometry) 85
- WFPC2 Vegamag System (photometry) 85

## T

- telemetry (POD) files 25
- TinyTim 100, 148
- trailer file 27
- typographic conventions
  - in this manual xi

## U

- undersampling 128, 144
- user support
  - help desk ii
- UV throughput 93, 123

## V

- V3 position angle 4
- velocity aberration 130

## W

- waiver FITS (wFITS) 11, 13
- warm pixels 52, 55
- warning
  - types in this document xi
- WF4 anomaly 74
  - streak removal 112
- WF4 anomaly correction 37
- WFPC2
  - camera configurations 5
  - decontamination 54
  - field of view 4, 6
  - focal ratio 5
  - instrument properties 6
  - optical configuration 3
  - spectral response 6
  - spherical aberration correction 3
- WFPC2 Flight System (photometry) 85
- WFPC2 Instrument Definition Team (IDT) vii